



City Research Online

City, University of London Institutional Repository

Citation: Baxter, J. E. (1988). Acylphosphine oxides as photoinitiators. (Unpublished Doctoral thesis, The City University)

This is the accepted version of the paper.

This version of the publication may differ from the final published version.

Permanent repository link: <https://openaccess.city.ac.uk/id/eprint/34298/>

Link to published version:

Copyright: City Research Online aims to make research outputs of City, University of London available to a wider audience. Copyright and Moral Rights remain with the author(s) and/or copyright holders. URLs from City Research Online may be freely distributed and linked to.

Reuse: Copies of full items can be used for personal research or study, educational, or not-for-profit purposes without prior permission or charge. Provided that the authors, title and full bibliographic details are credited, a hyperlink and/or URL is given for the original metadata page and the content is not changed in any way.

THE CITY UNIVERSITY, LONDON

DEPARTMENT OF CHEMISTRY

Chapter 1 An Introduction of UV Curing Chemistry

Introduction: Part 1 UV Curing. 1

The State of the Art 1

The Fundamentals of Photochemistry 5

Electronically Excited States 8

Photochemical Reactions 10

The Absorption Process 12

Photoinitiated Polymerization 14

Free Radical Polymerization 16

ACYLPHOSPHINE OXIDES

State of the Art 22

AS PHOTOINITIATORS

Photoinitiators 23

Photoinitiators for Free Radical Polymerization 25

Unimolecular Radical Generation 25

Enols and Derivatives 26

Substituted Acetophenones 27

Bimolecular Radical Generation 30

Photoinitiators for Anionic Polymerization 32

Diazonium Salts 33

Triarylsulphonium and Diaryliodonium Salts 34

Photoinitiators for Cationic Polymerization 35

Prepolymers 36

Unreacted Monomer 37

Polyester Amides 38

Acrylated Epoxy Resins 38

BY

JANE ELIZABETH BAXTER

A thesis submitted for the degree of Doctor of Philosophy in the Faculty of Science of The City University, London.

(1988)

CONTENTS

Chapter 1	An Introduction of UV Curing Chemistry	
	Introduction:Part I UV Curing.	
	The State of the Art	1
	The Fundamentals of Photochemistry	5
	Electronically Excited States	8
	Photochemical Reactions	10
	The Absorption Process	12
	Photoinitiated Polymerisation	15
	Free Radical Polymerisation	16
	Rate of Polymerisation	22
	Photoinitiators	23
	Photoinitiators for Free Radical Polymerisations	25
	Unimolecular Radical Generation	25
	Benzoin Derivatives	26
	Substituted Acetophenones	27
	Bimolecular Radical Generation	30
	Photoinitiators for Ionic Polymerisations	32
	Diazonium Salts	33
	Triarylsulphonium and Diaryliodonium Salts	34
	Photopolymerisable Resin Systems	35
	Prepolymers	35
	Unsaturated Polyesters	36
	Polyester Acrylates	38
	Polyether Acrylates	39
	Acrylated Epoxy Resins	39

	References	41
	Polyurethane Acrylates	41
	Monomers	42
Chapter 3	Vinyl Functional Monomers	43
	Monofunctional Acrylates	44
	Difunctional Acrylates	45
	Trifunctional Acrylates	46
	Characterisation of UV Networks	47
	Chemical Resistance	47
	Hardness	47
	Limitations of the UV Curing Technique	48
	Oxygen Inhibition	48
	Reactivity	50
	Adhesion	51
	Pigmentation of UV Curable Coatings	52
	Hazards in UV Curing	53
	Selection of UV Radiation Sources	54
	Applications of UV Curing	58
	Introduction:Part II	
	Acylphosphine Oxides	61
	References	65
Chapter 2	Synthesis of Photoinitiators	
	Introduction	72
	Michaelis-Arbusov Rearrangement	74
Chapter 4	Results and Discussion	76
	Experimental	89

References	116
------------	-----

Chapter 3	Photoinduced Cleavage of Acylphosphine Oxides	
	Introduction	118
	Detection of Free Radical Species	121
	Chemically Induced Dynamic Electron Polarisation (CIDEP)	124
	Results and Discussion	128
	Acknowledgements	133
	Experimental	134
	Appendix A: Trapping of Primary Radicals by a Stable Nitroxyl.	136
	Results and Discussion	136
	Acknowledgements	138
	Experimental	138
	Appendix B	141
	Results and Discussion	141
	Experimental	143
	Acknowledgements	145
	Appendix C	146
	Results and Discussion	146
	Acknowledgements	148
	Experimental	149
	References	158
Chapter 4	Methods for Screening Photoinitiators	
	Introduction	161
	Free Radical Polymerisation of Vinyl	

	Monomers	163
	Bulk Polymerisation	164
	Solution Polymerisation	165
	Results and Discussion	167
	(1) Solution Polymerisation Monitored by Laser Nephelometry	167
	(2) Bulk Polymerisation of Methyl Methacrylate and Styrene	174
	Acknowledgements	179
	Experimental	180
	Appendix A	184
	Appendix B	186
	References	191
Chapter 5	The Photopolymerisation of Non-Pigmented (Acrylate and Unsaturated Polyester)	Films
	Introduction	193
	Photoinitiator Concentration and Film Thickness	195
	Oxygen Inhibition and Autooxidation	198
	Results and Discussion	201
	Acknowledgements	218
	Experimental	219
	References	221
Chapter 6	The Photopolymerisation of Pigmented Films	
	Introduction	224

Effects of Pigmentation on the UV Curing of	
Thin Films	226
Competitive Absorption Effects	226
Effect of Scattering by Pigment	227
Titanium Dioxide as a Pigment	228
Results and Discussion	230
Acknowledgements	241
Experimental	242
References	244

Chapter 7	Using FTIR Spectroscopy to Measure the Residual	
	Unsaturation in Polymer Films	243
	Introduction	246
	Background and Principles of Fourier Transform	
	Infrared Spectroscopy	248
	Background	248
	Principles of Fourier Transform Infrared	
	Spectroscopy	249
	Attenuated Total Reflectance Spectroscopy	253
	Quantitative Analysis using ATR	256
	Results and Discussion	258
	Acknowledgements	266
	Experimental	267
	Appendix A	275
	Appendix B	281
	References	284

Chapter 8	Investigation of the Photodecomposition Products of Photoinitiators and Proposed Mechanisms for their Formation	
	Introduction	286
	Chromatography	288
	Liquid Chromatography	289
	Gas Chromatography	291
	Gas Chromatography-Mass Spectrometer Systems	292
	Results and Discussion	293
	(1) Investigation of the Photodecomposition of TMBPO and DMPA	293
	The Mechanism of Photodecomposition	302
	(2) Decomposition of a TMBPO UV Curable Formulation	302
	Conclusion	307
	Acknowledgements	308
	Experimental	309
	Appendix A	319
	Appendix B	321
	Appendix C	323
	References	326

successful.

Last but not least, I would like to thank the SERC and Akzo Research Laboratories, Arnhem for the provision of a grant.

DECLARATION

The experimental work in this Thesis has been carried out by the author in the laboratories of the Chemistry Department of The City University, London and The Corporate Research Department of Akzo Research Laboratories, Arnhem, The Netherlands between 1st October 1984 and 30th September 1987. This work has not been presented and is not being presented for any other degree.

[2] Trapping of Primary Radicals by a Stable Nitroxyl.

Makromol. Chem., Rapid Commun. 1987, 8, 311-314.

[3] Acylphosphine Oxides as Photoinitiators for Acrylate and Unsaturated Polyester Resins.

European Polymer J., accepted for publication.

[4] Acylphosphine Oxides as Photoinitiators for Titanium Dioxide Pigmented Acrylic Resins.

European Polymer J., accepted for publication.

[5] The Use of Acylphosphine Oxides and Acylphosphonates as Photoinitiators.

Polymer, accepted for publication.

Jane Baxter

May 1988

[6] The Use of Fourier Transform Infrared to Determine the Photoinitiating Efficiency of the Acylphosphine Oxides.

European Polymer J., accepted for publication.

The City University, London.

Some of the work presented in this Thesis has already been published. The relevant publications are listed below:-

Polymer, accepted for publication.

- [1] The Photo-induced Cleavage of Acylphosphine Oxides. *J. Chem. Soc., Chem Comm.*, 1987, (2), 73-75.
J. Chem. Soc. Chem Comm., accepted for publication.
- [2] The Photo-induced ~~C~~Cleavage of Acylphosphine Oxides. Trapping of Primary Radicals by a Stable Nitroxyl. *Makromol. Chem., Rapid Commun.* 1987, 8, 311-314.
- [3] Acylphosphine Oxides as Photoinitiators for Acrylate and Unsaturated Polyester Resins. *European Polymer J.*, accepted for publication.
- [4] Acylphosphine Oxides as Photoinitiators for Titanium Dioxide Pigmented Acrylic Resins. *European Polymer J.*, accepted for publication.
- [5] The Use of Acylphosphine Oxides and Acylphosphonates as Photoinitiators. *Polymer*, accepted for publication.
- [6] The Use of Fourier Transform Infrared to Determine the Photoinitiating efficiency of the Acylphosphine Oxides. *European Polymer J.*, accepted for publication.

[7] A Study of the Photodecomposition Products of an Acylphosphine Oxide and 2,2-Dimethoxy-2-phenylacetophenone. Polymer, accepted for publication.

[8] Oxidative Desulphurisation at Pentavalent Phosphorus by Photogenerated Radicals.

J. Chem. Res (S) 1988., accepted for publication.

ABSTRACT

A comparison of the photoinitiating efficiency of acylphosphine oxides, in particular 2,4,6-trimethylbenzoyldiphenylphosphine oxide, 2,2-dimethoxy-2-phenylacetophenone, acylphosphonates, 2-chlorothioxanthone and other commercial photoinitiators for the polymerisation of UV curable formulations was made. The formulations investigated included a non-pigmented epoxy-acrylate, a pigmented epoxy-acrylate and an unsaturated polyester. During these investigations it was found necessary to add tertiary amines to all the photoinitiator formulations in order to obtain efficient cure speeds. Experimental evidence is provided showing the role of amines to be that of efficient oxygen scavengers. The acylphosphine oxides were found to be more efficient photoinitiators for the curing of thin films than the acylphosphonates, but were no better than the other commercial photoinitiators. Laser nephelometry and bulk polymerisation techniques were investigated as possible photoinitiator screening methods. Their limitations are reported. The efficiency of an acylphosphine oxide and a commercial photoinitiator were compared for the polymerisation of a difunctional acrylate. The residual unsaturation in the thin polymer film was measured using Fourier transform infrared spectroscopy in conjunction with transmission and ATR measurements. The photodecomposition products of the acylphosphine oxides were characterised and mechanisms for their formation suggested. The shelf-life stability of an acylphosphine oxide and a commercial photoinitiator were investigated using a typical UV curable formulation. The photocleavage mechanism of the acylphosphine oxides was elucidated by CIDEP and chemical radical trapping techniques.

Chapter 1

An Introduction of UV Curing Chemistry

Chapter 1	An Introduction of UV Curing Chemistry	
	Introduction:Part I UV Curing.	
	The State of the Art	1
	The Fundamentals of Photochemistry	5
	Electronically Excited States	8
	Photochemical Reactions	10
	The Absorption Process	12
	Photoinitiated Polymerisation	15
	Free Radical Polymerisation	16
	Rate of Polymerisation	22
	Photoinitiators	23
	Photoinitiators for Free Radical Polymerisations	25
	Unimolecular Radical Generation	25
	Benzoin Derivatives	26
	Substituted Acetophenones	27
	Bimolecular Radical Generation	30
	Photoinitiators for Ionic Polymerisations	32
	Diazonium Salts	33
	Triarylsulphonium and Diaryliodonium Salts	34
	Photopolymerisable Resin Systems	35
	Prepolymers	35
	Unsaturated Polyesters	36
	Polyester Acrylates	38
	Polyether Acrylates	39
	Acrylated Epoxy Resins	39
	Polyurethane Acrylates	41
	Monomers	42

Vinyl Functional Monomers	43
Monofunctional Acrylates	44
Difunctional Acrylates	45
Trifunctional Acrylates	46
Characterisation of UV Networks	47
Chemical Resistance	47
Hardness	47
Limitations of the UV Curing Technique	48
Oxygen Inhibition	48
Reactivity	50
Adhesion	51
Pigmentation of UV Curable Coatings	52
Hazards in UV Curing	53
Selection of UV Radiation Sources	54
Applications of UV Curing	58
Introduction:Part II	
Acylphosphine Oxides	61
References	65

INTRODUCTION:PART I

UV CURING

The State of the Art

The rapid growth of the UV curing industry, in terms of the tonnage of formulations consumed and the increasing number of applications, is due in part to the stringent regulations concerning water and air pollution. The necessity to reduce energy consumption because of increased fuel costs and limited fuel availability, increased solvent prices and the development of higher powered UV sources with reasonable life expectancy, have provided further incentives for the development of such systems. Radiation processes involved in the inks, coatings and paint industries comprise mainly of UV, electron beam (EB), infra-red (IR), radio-frequency and microwave curing systems. Of these, UV-curing systems have been the most developed and have been widely used on a commercial scale. EB cured systems have also attained some commercial acceptance. The other curing techniques have been less exploited on a commercial scale. This is mainly due to the problems associated with the design, cost and modification of curing equipment to form the basis of on-line production units compared to those for UV [1-3].

The contributions which UV curing technology has made toward the improvements in the coatings industry are quite significant. UV-cured systems render rapid cure, so throughput can be accelerated, thus increasing productivity. The low curing temperatures required to effect the photopolymerisation of UV curable

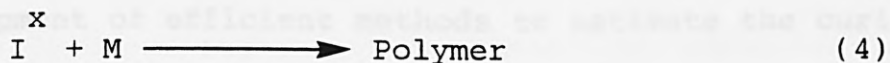
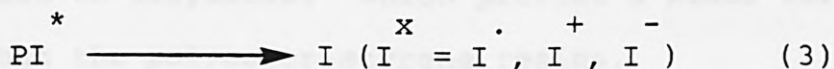
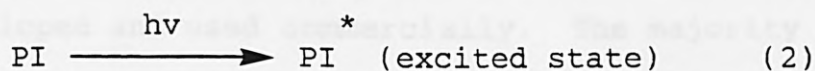
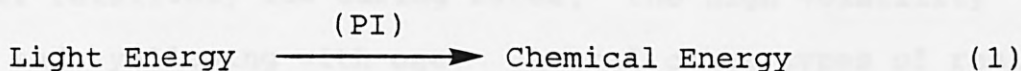
coatings widens the number of applications to include heat-sensitive substrates. UV curable formulations are solvent-free, thus eliminating the necessity for after burning and ovens. This in turn reduces air pollution and solvent wastage, thus improving cost efficiency. UV curing systems enable in-line multiprocessing (e.g., decorating, die cutting) in one machine pass. They also give improved film properties (e.g. colour) thus increasing the value of the end product. The UV curable formulations use less total energy for curing compared to conventional surface coatings, because the energy is concentrated upon the coating itself, with little or no incidental heating of the substrate, thus conserving energy. Analysis of the running-energy costs show those for UV to be about 20% of the costs of running an IR system. The equipment for UV irradiation is relatively simple and cheap compared with that required for EB curing, requiring low capital cost and minimal space for the installation and operation [1-3].

These advantages have resulted in an increase in the number of commercial applications of UV-based systems compared with conventional surface coatings. In the UK, sales of UV cured inks have trebled over the last five years and are only outpaced by the near quadruple growth of UV varnish sales [4]. The UV-curable formulations are however associated with certain disadvantages. There is the possibility of adverse toxicology problems with the UV formulations used, particularly those based on acrylates. In addition highly pigmented systems are often difficult to cure by UV radiation and pure metallic pigmented ink will reflect the incident UV thereby resisting cure. The price of UV lacquers

appears to be high, but based on the cost of a dry film per unit area of coated substrate, these costs are not extreme. Apart from these disadvantages, the UV curing technique is only really suitable for curing flat substrate surfaces and the UV curable formulations are not ideal for exterior applications.

The polymerisation of a large number of commercially available UV curable formulations is initiated by a radical or an ionic mechanism. The main steps in the photoinitiated polymerisation can be represented as shown in Scheme 1:

Scheme 1:



where PI and M represent photoinitiator and monomer molecules. UV curable formulations based on free radical chemistry consist mainly of the following components:

1. A liquid resin, usually an oligomer or a prepolymer containing double bond unsaturation.
2. A reactive diluent, usually monomer with varying degrees of unsaturation. Monomers are mainly used to fulfil a dual function, that is to reduce the viscosity of the formulation and to crosslink on curing.

3. A photoinitiator or sensitizer, capable of absorbing UV radiation and generating reactive molecules which in turn can initiate polymerisation.
4. Additives such as pigments, stabilisers, flow agents and so on.

The first commercial UV formulations of the type described were based on polyester-styrene resins. These were mainly used in particle board as paste fillers and lacquers, and are still used as wood coatings. The main disadvantages of these formulations were their relatively low curing rates, the high volatility of styrene, and yellowing with age. Several other types of resins have since been developed and used commercially. The majority of these resins are based on acrylates, which provide a wider formulation latitude than the polyester-styrene resins.

The development of efficient methods to estimate the curing rates of surface coatings and their dependence upon various experimental and photochemical parameters is important for the evaluation of UV curable coatings. Several methods have been reported in the literature, which include measuring the physical properties of the cured films [5,6], the use of specially designed differential scanning calorimeters [7,8], the use of IR analysis [9-11], and Fourier transform infrared (FTIR) spectroscopy in conjunction with photoacoustic spectroscopy [12,13] and various other experimental techniques [14].

The Fundamentals of Photochemistry

The most important steps in photochemical reactions occur initially with the absorption of light energy emitted by a particular light source, followed by the conversion of the absorbing molecules into activated species. For UV curable formulations, the light absorption is usually achieved through an additive called an initiator, or sensitizer, previously added to the binder system. It is therefore important to carefully select the additive (initiator or sensitizer) so that its absorption bands overlap with the emission spectrum of the lamps used as the source of UV radiation. The primary process of a photochemical reaction involves the interaction of a photon and a molecule, which results in the absorption of the photon and the concomitant formation of an electronically excited molecule. This electronically excited molecule may undergo photophysical processes, such as radiative (fluorescence and phosphorescence) and radiationless (internal conversion and intersystem crossing) processes, or photochemical processes in the mode of radical formation (see later). Each molecule which forms an electronically excited state by exposure to radiation absorbs one (photon) quantum of the radiation to initiate the primary process. An electronic transition will only occur if the energy difference between the two molecular orbitals in question is exactly equal to the energy of the quantum of radiation. The radiation energy of a photon or a quantum required to produce an excited state can be obtained by examination of the absorption or emission spectrum of the molecule in question, together with the application of the following

equation:

$$E_2 - E_1 = hv = \frac{hc}{\lambda} = hc\bar{\nu} \quad (5)$$

where h is Planck's constant (6.626×10^{-34} J s), ν is the frequency (sec^{-1}), λ is the wavelength of the monochromatic light (\AA , nm), c is the velocity of light ($c = 3 \times 10^{10}$ cm/sec), $\bar{\nu}$ is the wave number (cm^{-1}) (number of waves per unit length) and E_2 and E_1 are the energies of an electron in the final excited (previously unoccupied orbital) and initial ground (initially occupied orbital) states respectively [1-3,15,16]. According to the Law of the photochemical equivalent which was first proposed by Einstein, equation 5 can be rewritten as equation 6. This shows that the energy absorbed per mole of photons by the compound in question, at a given wavelength, is equal to the energy of 6.02×10^{23} photons, one einstein [15,17].

$$E_2 - E_1 \text{ (kcal/mol)} = \frac{2.86 \times 10^4}{\text{nm}} \quad (6)$$

The relationship between the extent of light absorption and the depth or thickness of the film, which is an absorbing material can be determined by the Lambert—Beer law:

$$\ln \left(\frac{I_0}{I} \right) = -alc \quad (7)$$

where I_0 is the incident radiation, I is the intensity of the transmitted radiation, a is the molar absorption coefficient ($\text{l mol}^{-1} \text{cm}^{-1}$), l is the thickness of the irradiated layer and c (mol l^{-1}) is the concentration. It follows from the Lambert-Beer law that the absorption coefficient (a) is a constant value which is

independent of the concentration, layer thickness and radiation intensity, but varies with the wavelength of the absorbed radiation [17].

In practice the Lambert-Beer law is expressed in terms of the extinction coefficient E , absorption A , or optical density OD , using the following equation:

$$A = OD = \ln \left(\frac{I_0}{I} \right) = E l c \quad (8)$$

The extinction coefficient has a cumulative property. For a mixture of two or more components, the extinction coefficient can be represented by equation 9 [1-3].

$$E = l(\epsilon_1 C_1 + \epsilon_2 C_2 + \dots + \epsilon_n C_n) \quad (9)$$

The quantitative relationship between the number of molecules which react or which are formed in a photochemical reaction and the number of photons absorbed in unit time is expressed by the Quantum yield, Q . For a given system the quantum yield can be defined as follows:

$$Q = \frac{\text{number of molecules reacting in a particular process}}{\text{number of quanta absorbed by the system}} \quad (10)$$

A knowledge of the quantum yield is important for elucidating the reaction mechanism and the course of a photochemical reaction. Thus when $Q = 1$, every absorbed quantum produces one photochemical reaction; when $Q < 1$, other chemical reactions compete with the main photochemical reaction; and when $Q > 1$, a chain reaction takes place [1,15,16].

Electronically Excited States

Photochemical reactions occur via electronically excited states. Each excited state has a definite energy, structure and lifetime. The total energy of a molecule in a particular excited state is the sum of the electronic excitation energy (E_e), the vibrational energy (E_v), and the rotational energy (E_r) as shown in equation 11;

$$E = E_e + E_v + E_r \quad (11)$$

where

$$E_e > E_v \gg E_r$$

The structure of various electronically excited states and the most important photochemical processes involved are represented in the modified Jablonsky diagram (Figure 1).

In Figure 1, S_0 represents the ground state which is the initial state of the molecule before excitation. S_1 and S_2 represent the excited singlet states which are formed after the absorption of a photon. The spins of the electrons in these excited states are paired (anti-parallel). The main photochemical reactions occur from the lowest excited singlet state S_1 . The very fast rate of internal conversions from the upper singlet states, S_2 to the lowest excited singlet state S_1 make the possibility of photochemical reactions unlikely from the upper states.

T_1 , the lowest excited triplet state, is mostly formed by radiationless transmissions involving intersystem crossing from the lowest excited singlet state S_1 . The formation of a triplet state by direct absorption of a photon is a forbidden transition. The conditions for intersystem crossing require that

the potential energy curve of the lowest excited singlet state must intersect the potential energy curve of the lowest excited

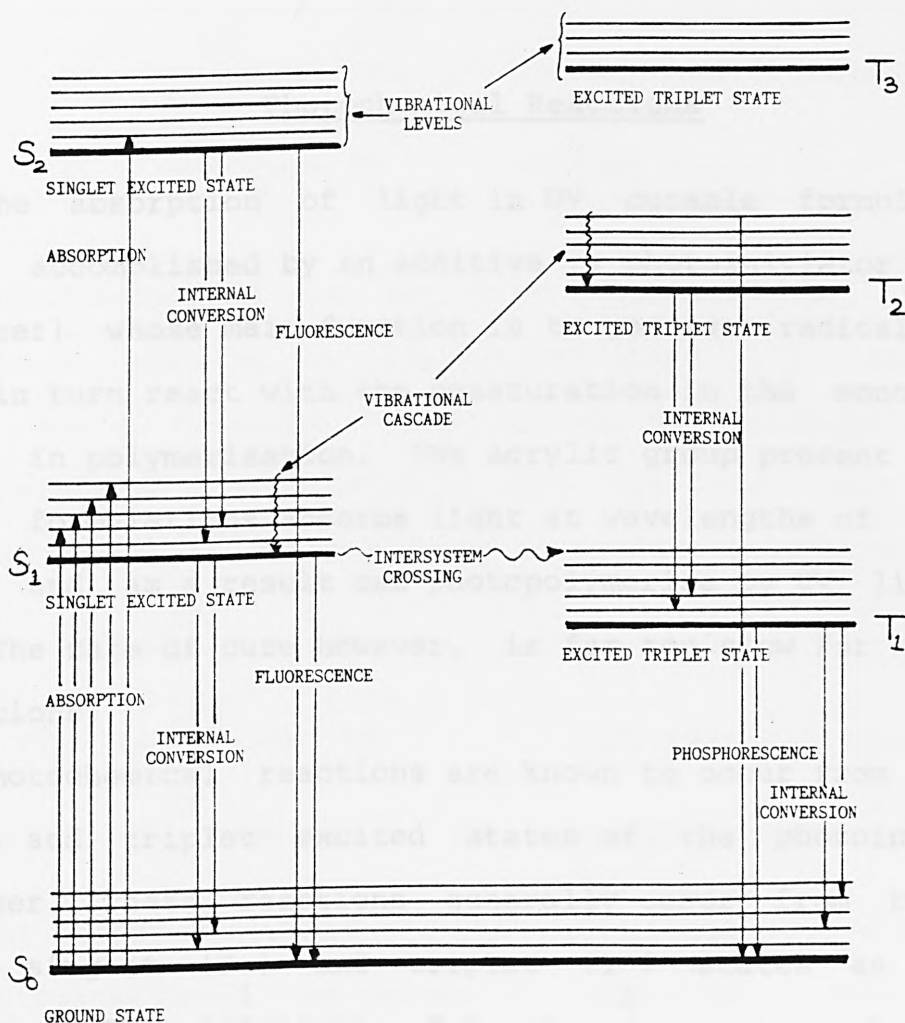


Figure 1. A Modified Jablonsky Diagram.

triplet state. If this is not the case, transition from the singlet to the triplet state cannot be attained. The spins of the electrons in the triplet state are unpaired (parallel). The higher triplet states (T_2) may be formed only when a molecule in its lowest triplet state (T_1) absorbs a new photon. Each electronic level can be further split into a series of vibrational

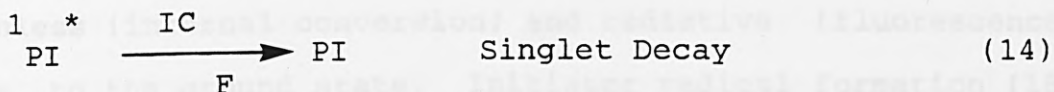
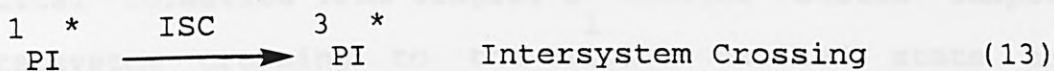
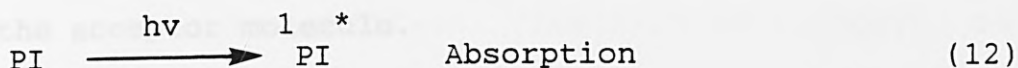
levels, and each vibrational level in itself can be split into a series of rotational levels. The various radiative and non-radiative transitions taking place are represented in Figure 1.

Photochemical Reactions

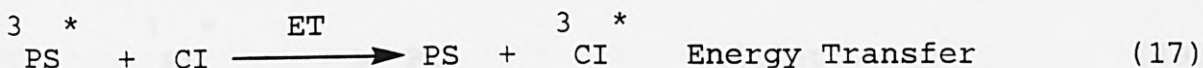
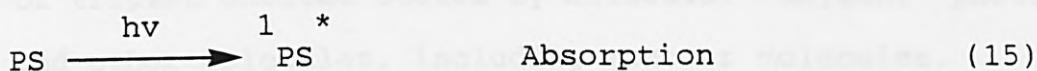
The absorption of light in UV curable formulations is usually accomplished by an additive (a photoinitiator or photosensitiser) whose main function is to generate radical species, which in turn react with the unsaturation in the monomers, resulting in polymerisation. The acrylic group present in most UV curable formulations absorbs light at wavelengths of less than 260 nm and as a result can photopolymerise by UV light alone [18]. The rate of cure however, is far too slow for commercial applications.

Photochemical reactions are known to occur from both the singlet and triplet excited states of the photoinitiator - sensitiser. These reactions generally occur from the lowest excited singlet (S_1) and triplet (T_1) states as described previously. The lifetimes of S_1 states are very short ($<10^{-8}$ secs), and as a result the many photochemical reactions which occur, particularly intermolecular processes, go via the excited triplet, T_1 states which are generally longer lived species ($>10^{-6}$ secs). The absorption of UV radiation by a photoinitiator (PI) produces an excited singlet state (12), followed by intersystem crossing to the triplet state (13). Intersystem crossing competes with singlet decay to the ground state (14), which occurs by radiative processes such as fluorescence and radiation-

less processes such as internal conversion as shown below:



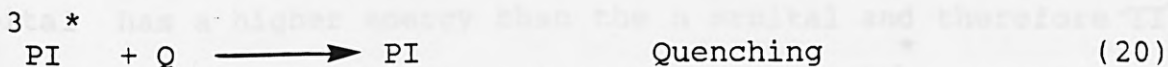
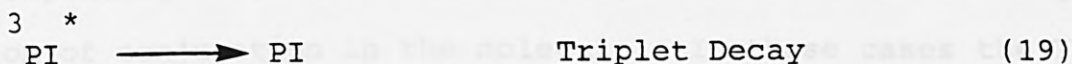
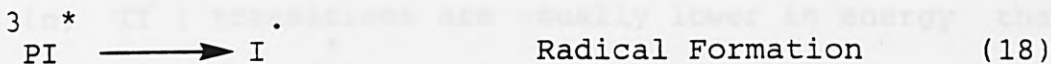
Photosensitisers will also absorb UV radiation (15), followed by intersystem crossing to the triplet state (16) and triplet-triplet energy transfer (17) to produce the chemically-reactive excited state of the coinitiator (CI). The coinitiator can undergo H-abstraction or photocleavage to produce initiator radicals.



Efficient energy transfer, via photosensitisation, will occur if the photosensitiser has strong UV absorption characteristics within the wavelength range of the UV light source. Upon the absorption of UV radiation, the photosensitiser must undergo a fast and efficient conversion to the excited triplet state. It is most important that the molar extinction coefficient of the photosensitiser at the appropriate wavelength is greater than that of the acceptor (CI) molecule so that the photosensitiser absorbs the majority of the emitted UV light. This should avoid any side reactions involving excited acceptor molecules. The photosensitiser (PS) must also have a higher triplet energy than

the acceptor molecule in order to transfer enough of its energy to excite the acceptor molecule.

Radical formation from singlet S_1 excited states compete with intersystem crossing to the triplet excited state and radiationless (internal conversion) and radiative (fluorescence) processes to the ground state. Initiator radical formation (18) from triplet T_1 excited states compete with triplet decay to the ground state (19) by radiative (phosphorescence) and radiationless (internal conversion) processes, and various bimolecular quenching (Q) processes (20), as a consequence of the longer lived triplet excited states. These latter processes include the quenching of triplet excited states by molecular oxygen, photoinitiator and other molecules, including monomer molecules.



The Absorption Process

Aromatic carbonyl compounds are generally used as initiators for the photopolymerisation of surface coatings (see later). These compounds possess absorption properties compatible with the emission spectra of most commercial UV lamps. Upon irradiation, these photoinitiators absorb UV light producing a singlet excited state from which the lowest triplet excited state can be populated. The orbitals involved in the electronic transitions are

the σ and π bonding orbitals, the n, non bonding orbitals, and the σ^* and π^* antibonding orbitals. The aromatic carbonyl compounds possess a lone pair of electrons in the non-bonding orbitals of the oxygen atom of the carbonyl functional group. The absorption of UV radiation results in the excitation of one of these electrons into a π^* or σ^* antibonding orbital i.e., transitions of the form $n-\pi^*$ or $n-\sigma^*$ [1,3,19]. The general order of bonding, antibonding and non-bonding molecular orbital energies is

$$\sigma < \pi < n < \pi^* < \sigma^*$$

which implies that the most readily observed transitions are $n-\pi^*$ and $\pi-\pi^*$ in nature [1,3,19].

The (n, π^*) transitions are usually lower in energy than the corresponding (π, π^*) transitions, unless there is a high proportion of conjugation in the molecule. In these cases the π orbital has a higher energy than the n orbital and therefore $\pi-\pi^*$ transitions will be lower in energy than $n-\pi^*$ transitions. The long wavelength absorptions (280 - 320 nm) by aldehydes and ketones are the result of a $n-\pi^*$ transition, which is mainly confined to the carbonyl group. The absorption at short wavelengths is the result of $\pi-\pi^*$ transitions. Significant differences exist in the electronic structures and the chemical reactivities of the $n-\pi^*$ and $\pi-\pi^*$ excited states. The $n-\pi^*$ transitions remove electron density from the oxygen atom with the result that the excited states (particularly the triplet $n-\pi^*$ states) display a similar reactivity to alkoxy radicals which are

known to participate in hydrogen abstraction reactions. The $\pi-\pi^*$ transitions increase the electron density at the oxygen atom, with a concomitant increase in the polar nature of the carbonyl group [1,2,19].

Changes in solvent polarity has different effects upon the transition energies of the $n-\pi^*$ and $\pi-\pi^*$ excited states, due to their different electron distributions. Increasing the polarity of the solvent causes a decrease in the energy of the $\pi-\pi^*$ transitions (red shift to longer wavelengths) and an increase in the energy of the $n-\pi^*$ transitions (blue shift to shorter wavelengths). Other differences occur in the molar extinction coefficient (E) values for each transition. Typical $n-\pi^*$ transitions have E values in the $10^2 - 10^3 \text{ M}^{-1} \text{ cm}^{-1}$ range, whereas $\pi-\pi^*$ transitions range from $10^4 - 10^5 \text{ M}^{-1} \text{ cm}^{-1}$ [1,2,19].

The most important distinction between the $n-\pi^*$ and $\pi-\pi^*$ excited states of the aromatic carbonyl compounds is the greater probability of intersystem crossing with the $n-\pi^*$ states relative to the $\pi-\pi^*$ states. The major determinants influencing this transition are:-

- 1) selection rules partly forbid the $n-\pi^*$ transition and therefore the reverse transition will be partially forbidden. As a result the lifetimes of the S_1 ($n-\pi^*$) states tend to be longer than the S_1 ($\pi-\pi^*$) states and the probability of intersystem crossing therefore, higher for the S_1 ($n-\pi^*$) states.
- 2) The energy separations between the S_1 and T_1 states of the $n-\pi^*$ type are small and are of the order 1500 -

5000 cm^{-1} whereas the corresponding $\pi^*-\pi$ states are much larger, and are of the order 10,000 - 15,000 cm^{-1} [1,3,19].

PHOTOINITIATED POLYMERISATION.

The photoinitiated polymerisation of unsaturated monomers can be controlled with much more precision than thermally initiated polymerisation reactions. This is because the generation of the initiating species, which occurs through light absorption, can be varied by controlling the intensity of the initiating light. As mentioned earlier, UV radiation of short wavelengths will initiate the polymerisation of some unsaturated monomers directly. It is however, the general practise to use photochemical initiators which decompose rapidly into active species by UV light, thus initiating the polymerisation reaction much faster [20]. The photopolymerisation of the vinyl monomers can occur by either an addition or a condensation reaction. The photocondensation reaction is the least efficient of the two mechanisms [21,22]. It occurs by a step growth mechanism where the monomers first react with each other to form dimers which react to form tetramers and so on to give high polymers [21,22]. The most efficient and widely used reaction for the photopolymerisation of unsaturated monomers [23] occurs by an addition reaction. The addition reaction functions by a chain growth mechanism, where monomer units add on to the growing end of a polymer chain. This

efficient reaction mechanism can be controlled easily, but is susceptible to retardation and inhibition. The photoinduced species which initiate and generate the propagation of the chain include free radicals, anions or cations [1,20].

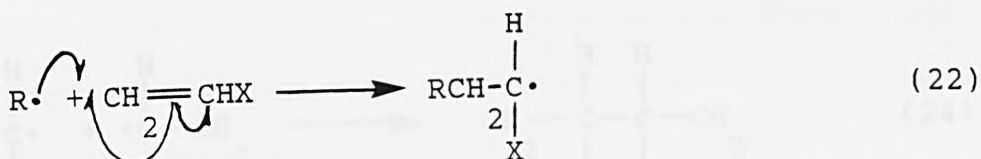
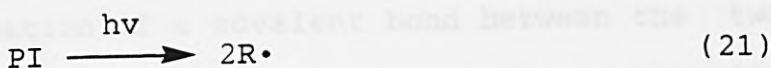
The chain-growth, or addition polymerisation mechanism is characterised by three main stages, which are the initiation, propagation and termination steps. All three steps differ significantly in rate and mechanism. Monomers will react readily with free radicals, cations and anions but relatively few other reactive species. The addition of monomers at the few active centres on the growing polymer chains result in the very rapid growth of the long chain molecules until they reach their definitive length by chain termination. Once the growth has been terminated, the macromolecules formed no longer participate in the polymerisation reaction (except where chain transfer reactions occur) [2,20].

Free Radical Polymerisation

The photoinduced free radical polymerisation reactions are used widely on a commercial scale for a number of different applications. High molecular weight polymers and copolymers are produced relatively easily with a number of different and specific properties. The final properties of the polymer film are obtained by the careful selection of specific monomers, prepolymers and oligomers from the wide variety available commercially. The three steps of a free radical polymerisation reaction are characteristic of all chain growth polymerisations [23].

Initiation

The photogeneration of free radicals in the presence of a vinyl monomer results in the addition of the radical species to the double bond of the monomer. One electron from the double bond joins with the unpaired electron of the free radical to form a carbon-radical sigma bond. The other electron from the double bond moves on to the other carbon atom to generate a new radical centre. The addition of a free radical species to an unsymmetrically substituted alkene gives the most stable radical. The order of stability of radicals is like that of a carbonium ions, i.e., tertiary > secondary > primary. If the photogenerated radical of the photoinitiator (PI) is designated by $R\cdot$, then the first step in the reaction is the formation of the secondary radical (22):

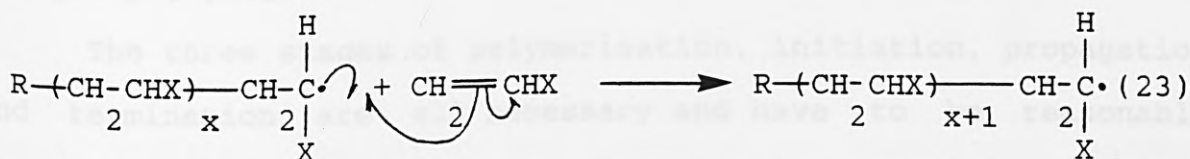


The regeneration of another radical species is characteristic of chain reactions, which result in the formation of a reactive growing end. The concentration of photoinitiator used is generally low, because only one molecule of photoinitiator is required to initiate the growth of two long polymer chains.

Propagation

The chain radical formed in the initiation step above is capable of adding successive monomers to its reactive growing end, i.e.,

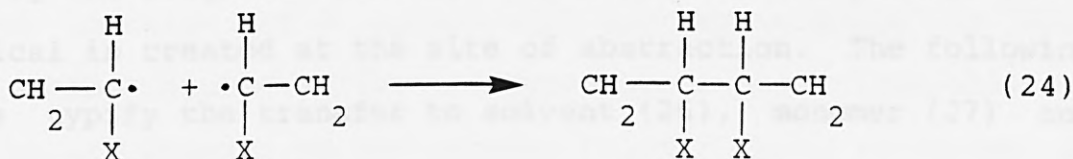
at the radical centre, thus propagating the chain growth:



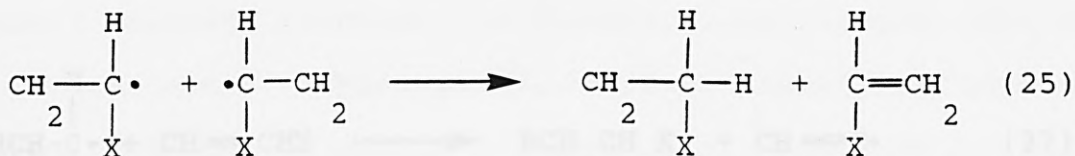
For chain addition reactions, the chain grows at the reactive growing end, the radical centre, only [2,20].

Termination

Theoretically, propagation would continue until the supply of monomer was totally exhausted. In practise however, in radical reactions, the growing chain is terminated, producing a stable polymer. The termination step can proceed via two mechanisms. Termination by the formation of a covalent bond between the two radical species coming together, a process known as recombination or coupling, is merely the reverse of the initiation



Alternatively, termination can occur by disproportionation which involves the abstraction of a hydrogen atom from one radical species by the other radical species.

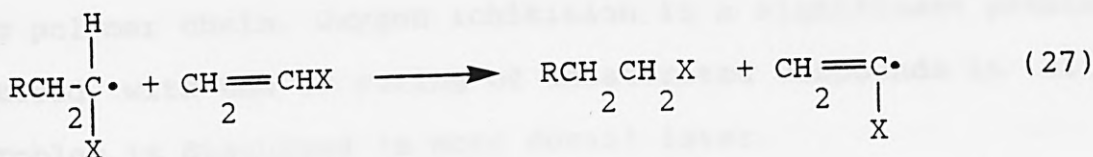
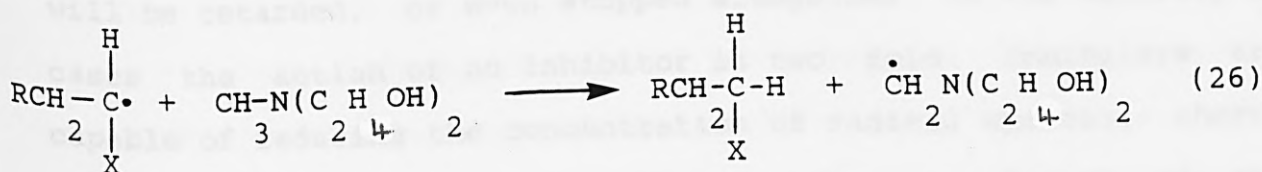


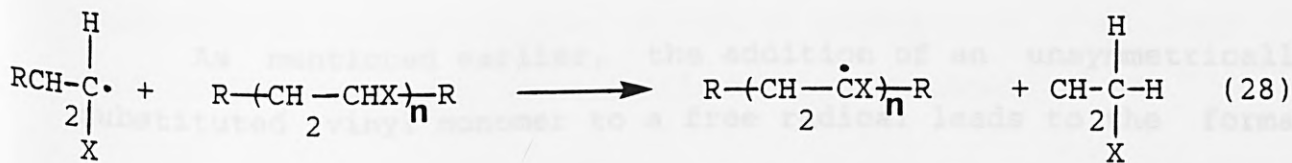
This hydrogen abstraction mechanism results in the formation of

two molecules, one with a saturated and one with an unsaturated end group [1,20].

The three stages of polymerisation, initiation, propagation and termination are all necessary and have to be reasonably efficient to maintain a chain polymerisation reaction. Competitive reactions however can take place during the polymerisation. Such competitive reactions include chain transfer reactions, which will ultimately affect the polymerisation reaction and the polymers formed, and inhibition [1,20].

The chain transfer reactions which occur during photopolymerisation, result in the transfer of the reactivity of the growing chain radical to another species capable of continuing the chain polymerisation reaction. Transfer may involve unreacted monomer or fully grown polymer, as well as solvent or 'chain transfer agent' if present. An atom (usually hydrogen) is abstracted by the original radical, which dies in the process and a new radical is created at the site of abstraction. The following examples typify the transfer to solvent (26), monomer (27) and polymer (28) respectively.





Chain transfer results in the formation of additional polymer molecules for each radical chain initiated. The transfer of radical reactivity to polymer and monomer with the subsequent polymerisation of the double bond can lead to the formation of branched molecules. The transfer does not affect the overall rate of monomer consumption, but has a pronounced effect on the molecular weight distribution of the product. The efficiency of compounds acting as chain-transfer agents and the reactivity of various polymer radicals to transfer, varies widely. The overall result of these uncontrolled reactions is the loss of the desired polymer film properties expected from the selection of specific monomers.

The reaction of a radical with another molecule or substance which results in the formation of products incapable of adding to the monomer or the growing polymer chain is known as inhibition. If the inhibitor is very effective, polymerisation will be retarded, or even stopped altogether. In the majority of cases the action of an inhibitor is two fold. Inhibitors are capable of reducing the concentration of radical species, shortening their average lifetime and therefore the length of the growing polymer chain. Oxygen inhibition is a significant problem encountered with the UV curing of unsaturated compounds in air. This problem is discussed in more detail later.

syndiotactic (alternating). A random sequence of positions is said to lead to the atactic configuration (random).

Rate of Polymerisation.

If the photoinitiator concentration does not vary much during the course of polymerisation and the photoinitiator efficiency is independent of monomer concentration, then polymerisation proceeds by first order kinetics. In this case, the overall rate of polymerisation as a function of conversion is proportional to the monomer concentration.

The overall rate of polymerisation, R_p , of vinyl monomers initiated by free radicals is given by [23] the following equation

$$R_p = (k_p / k_t)^{1/2} (R_i)^{1/2} (M) \quad (31)$$

where, k_p and k_t are the rate constants for the propagation and the termination steps respectively, R_i is the rate of initiation, and M is the concentration of monomer. The rate of initiation, R_i , is given by

$$R_i = QI_a = QI_0 [1 - \exp(-ECl)] \quad (32)$$

where I_a is the light intensity absorbed by the polymerisable monomer, I_0 is the incident light intensity, Q is the quantum yield for the initiation of radical chain polymerisation, E is the extinction coefficient of the photoinitiator at the wavelength of the incident light, and l is the path length in the

monomer [24,25].

The rate of initiation is less than the rate of primary radical formation due to competitive reactions. Such reactions include radical cage recombination, oxygen inhibition, solvent quenching of excited states and chain termination processes [24,25].

PHOTOINITIATORS

The overall efficiency of a photoinitiator is related to the efficiency of its photophysical and photochemical processes, and the radical processes resulting from its photodecomposition, which lead to the initiation and propagation processes of the growing polymer chain. Nonproductive competing processes will reduce this efficiency. Light absorption by species other than the photoinitiators, such as pigments, and the spontaneous deactivation and bimolecular quenching of the excited state of the photoinitiator are two such competing processes. Initiator radical recombination reactions, and also the reaction of initiator radicals and oxygen with the growing polymer chain adversely affect the efficiency and the film properties in UV curing [18,26].

It is important for photoinitiators used commercially that their absorption characteristics are compatible with the emission characteristics of the UV source used. Also, the efficient generation of reactive radical species capable of attacking the olefinic double bond of unsaturated monomers is most important. The

photoinitiator needs to be soluble in the UV curable formulation and have good storage stability in the dark, even at temperatures of 50 °C. The photodecomposition of the photoinitiator should not give rise to unpleasant odours or yellowing of the polymer film. It is also very important that the photoinitiators, and their decomposition products are non toxic.

Photoinitiators can be classified according to their decomposition mechanism. The more important mechanisms fall into the following categories:

1. Fragmentation reactions.
2. Hydrogen abstraction reactions.
3. Ionic initiation reactions involving electron transfer.
4. Triplet energy transfer reactions via a photosensitiser.
5. Cationic reactions.

These photoinitiating mechanisms have been covered in detail in a large number of articles [26-38] over the last 15 years. The photochemical disruption of a molecule usually proceeds via the uncoupling of an electron pair, leading in most cases to the formation of radical, rather than ionic intermediates. Therefore, it is the free radical intermediate which plays a dominant role in the chemistry of photoinitiation and any subsequent polymerisation reactions [2]. Categories 1, 2 and 5 (fragmentation, hydrogen abstraction and cationic reactions) will be the only categories discussed in any detail in the following sections.

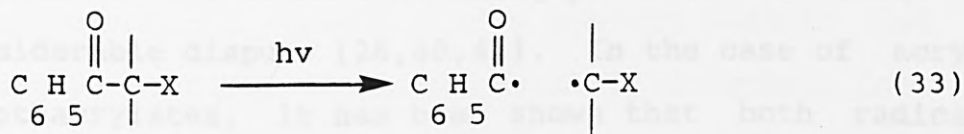
Photoinitiators for Free Radical Polymerisations.

The largest number of photoinitiators available commercially belong to the general class of aromatic carbonyl compounds. The favourable absorption characteristics of these compounds lie in the 300-400 nm range, which is compatible with the emission spectrum of most commercial UV lamps. A large number of the photoinitiators used commercially for the free radical polymerisation of UV curable formulations will undergo two major primary photoreactions. These photoreactions include intramolecular bond cleavage, leading directly to free radicals in an unimolecular process or homolytic reaction, and intermolecular H-abstraction from a H-donor, or a coinitiator, leading to free radicals by a bimolecular process [1,2,3,26,30,36]. The formation of free radicals, and their subsequent reactions, is particularly favoured in non-polar environments. These conditions are predominant in UV curable ink and coatings formulations.

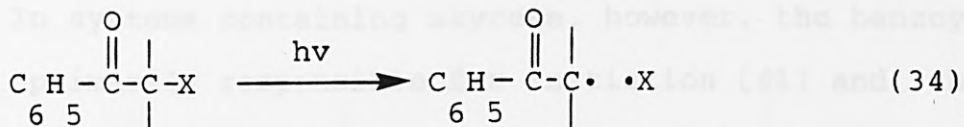
Unimolecular Radical Generation.

The formation of initiating free radicals by the fission of a covalent bond in a molecule, either via a singlet or triplet excited state, is an unimolecular processes. Excited organic carbonyl compounds will undergo this type of direct photofragmentation which can be subdivided further into two categories. The first category is the Norrish Type I Reaction where homolytic cleavage occurs in the primary process, resulting in the bond between the carbonyl group and adjacent α -carbon atom being severed [1,2,3,26,30]. This reaction is also commonly known as α

cleavage;



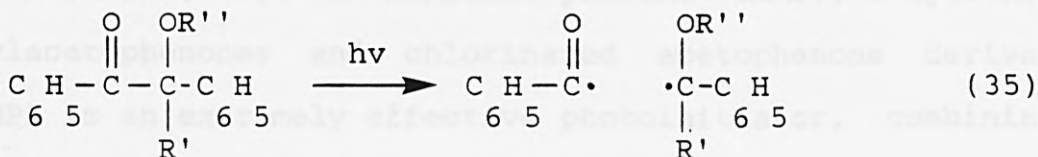
The second category is known as β -cleavage;



The mode of photofragmentation is dependent upon the nature of the functional group X. Generally, α -cleavage is the predominant fragmentation pathway, however, β -cleavage is the major fragmentation pathway when X = hal and -SR. When X = -OAr both fragmentation pathways have been observed to occur independently [26]. Aromatic carbonyl compounds which undergo direct photofragmentation can be subdivided further into categories based upon their chemical structures.

Benzoin Derivatives

Benzoin and its derivatives, particularly the benzoin ethers, were amongst the earliest patented photoinitiators for free radical polymerisation. They were, and still are predominantly used in the area of particle board finishing. These photoinitiators dissociate from the excited triplet state into free radicals according to a Norrish Type 1 cleavage mechanism, [26,30,39]



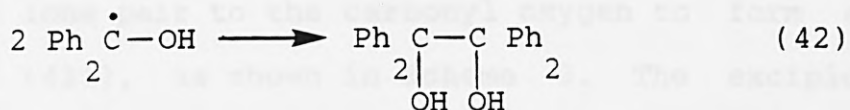
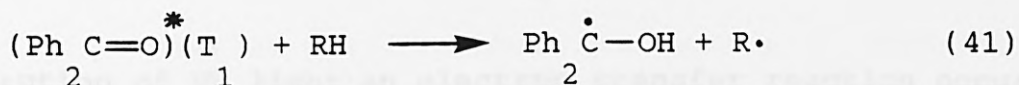
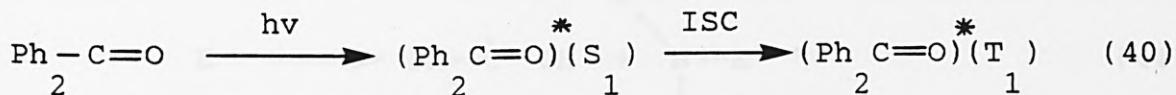
The relative efficiencies of these two radical species appears to be system specific and their initiating potential is still a matter of considerable dispute [26,40,41]. In the case of acrylates and methacrylates, it has been shown that both radical species are comparable in their efficiency to initiate polymerisation [41]. In systems containing styrene, however, the benzoyl radicals are primarily responsible for initiation [41] and the ether radicals participate predominantly as chain-terminating agents [26]. UV curable formulations containing benzoin alkyl ethers are used in a range of applications. These photoinitiators compete efficiently and effectively against the bimolecular quenching reactions of atmospheric oxygen and monomers [18]. The direct photocleavage of the benzoin alkyl ethers cannot be quenched by the usual triplet quenchers [39,42] which is indicative of an exceptionally rapid (short lived) triplet excited state of the order $< 10^{-10}$ sec [26]. Benzoin ethers are reported to exhibit relatively low storage stability in UV curable formulations [18], which may be attributed to the labile benzylic hydrogen atom.

Substituted Acetophenones

The acetophenone derivatives used as effective photoinitiators in a number of applications include 2,2-dimethoxy-2-phenylacetophenone (DMPA), 2,2-diethoxyacetophenone (DEAP), 2-hydroxy-2,2-dialkylacetophenones and chlorinated acetophenone derivatives. DMPA is an extremely effective photoinitiator, combining high initiating efficiency with high thermal stability

oxygen and monomer. The photoreduction of benzophenone and related carbonyl compounds [19,33] can be illustrated by the simplified scheme shown below:

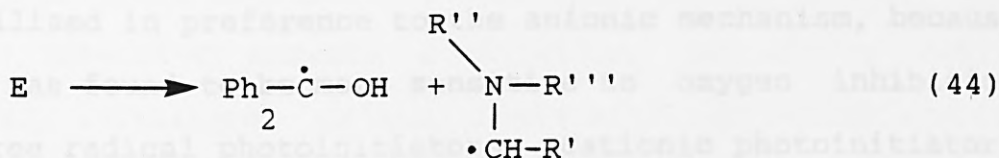
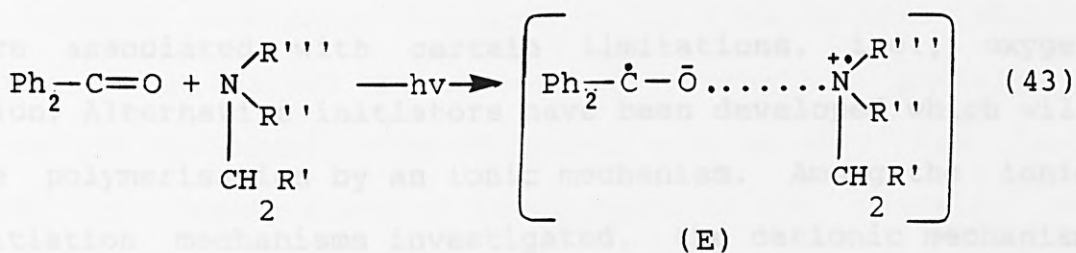
Scheme 2



The efficiency of the H-abstraction process is dependent upon the nature of the H-donor compounds. H-donors such as alcohols and ethers, when used in conjunction with aromatic ketones, have been unable to find widespread applications, although propan-2-ol and THF have been found to be extremely active H-donors [40,45].

Tertiary amines with abstractable α -H atoms are particularly effective H-donors for the UV curing of acrylate monomers and oligomers in an air atmosphere [18]. This has been attributed to the rapid formation of a complex (exciplex) between the excited state of, for example, the photoinitiator benzophenone and a tertiary amine, as shown in Scheme 3. The amine-derived radicals generated are responsible for the efficient initiation of acrylic monomers [1-3,18,26,38].

Scheme 3



Upon absorption of UV light an electron transfer reaction occurs from the nitrogen lone pair to the carbonyl oxygen to form an exciplex [(E) and (43)], as shown in Scheme 3. The exciplex either reverts back to starting materials in their ground state or proceeds to form a ketyl radical and an α -aminoalkyl radical by proton transfer, as shown in Scheme 3 (44). The radicals produced can initiate polymerisation, recombine, cross-couple and disproportionate. Evidence supporting these reaction sequences has been recorded [47-57].

Thioxanthone derivatives used in combination with tertiary amines have also been shown to be effective photoinitiators. Investigations of the photochemical reactions of several thioxanthone derivatives, including thioxanthone (TX), 2-isopropyl thioxanthone (ITX) and 2-chlorothioxanthone (CTX) in the presence of tertiary amines have been reported [54,58,59].

Photoinitiators for Ionic Polymerisation

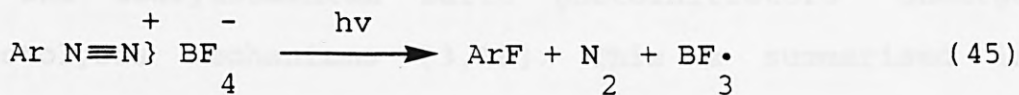
Although photoinitiators functioning by free radical mech-

anisms are widely used in a number of industrial applications, they are associated with certain limitations, i.e., oxygen inhibition. Alternative initiators have been developed which will initiate polymerisation by an ionic mechanism. Among the ionic photoinitiation mechanisms investigated, the cationic mechanism has been utilised in preference to the anionic mechanism, because the latter was found to be more sensitive to oxygen inhibition than the free radical photoinitiators. Cationic photoinitiators can be used to polymerise vinyl monomers and monomers containing lactone, epoxy, cyclic ether, sulphide and acetal groups. A wide formulation latitude is therefore possible using the cationic photoinitiators and the many different types of polymers and diluents available commercially. The various photoinitiators available for cationic polymerisation, and their different initiation mechanisms have been reviewed elsewhere [15,18,34].

Diazonium Salts

These photoinitiators belong to a general class which can be applied to a variety of cationically polymerisable formulations. The photodecomposition mechanism of the diazonium salts is represented in Scheme 4.

Scheme 4



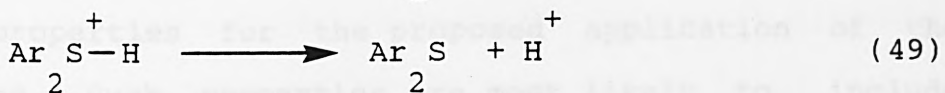
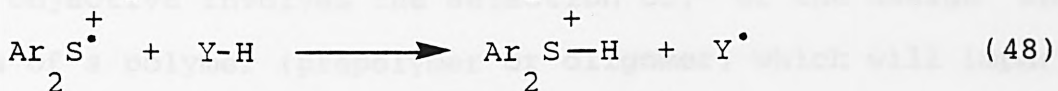
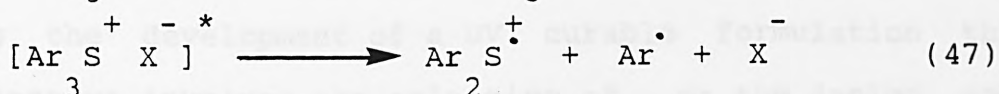
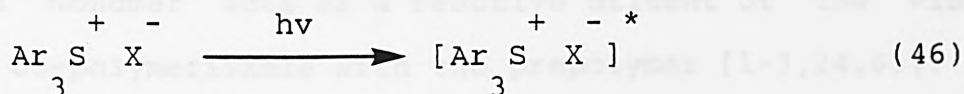
The Lewis acid BF_3 generated as a result of photolysis, initiates the polymerisation reaction. The aryldiazonium salt initiators

exhibit certain advantages compared to the free radical photoinitiators. These include the absence of termination processes, due to the low nucleophilicity of anions such as PF_6^- , AsF_6^- and SbF_6^- , and the regeneration of Lewis acids by the reaction of growing polymer chain cations (P^+) with the complex anions. The short shelf life of UV curable formulations containing aryl-diazonium salt initiators, unless Lewis acid complexing agents are added, is one of the major disadvantages encountered when using these photoinitiator systems. Other disadvantages include the sensitivity of the aryldiazonium salts to visible radiation, causing yellowing in the surface coatings upon ageing, their strong colour restricts their use in certain applications, and the evolution of nitrogen gas during photolysis leads to cratering in thicker (25 μm) films. These disadvantages have led to the development of commercial photoinitiators based on triaryl sulphonium salts and diaryliodonium salts.

Triarylsulphonium and Diaryliodonium Salts

The triarylsulphonium salts are enjoying a period of renewed interest as the search for improved surface coating characteristics continues [60-62]. The thermally stable [18] triarylsulphonium and diaryliodonium salts photoinitiators undergo similar photolysis mechanisms [3,18]. This is summarised in Scheme 5 using a triarylsulphonium salt as the example.

Scheme 5



Upon photolysis, these photoinitiators generate Brønsted acids HBF_4 , HAsF_6 , HSbF_6 and not Lewis acids as in the case of the diazonium salts [1-3]. The triarylsulphonium and diaryliodonium salts are efficient photoinitiators for a wide variety of vinyl and heterocyclic monomers. The chemistry and reactions of these cationic photoinitiators is covered in more detail in a number of publications [15,26,34].

PHOTOPOLYMERISABLE RESIN SYSTEMS

Prepolymers

Over the last 15 years or so, the surface coatings industry has seen a rapid growth in the tonnage of UV curable media used. The increase in the number of different applications has led to the development of a variety of novel UV curable resins. The solvent free, 100% solid photopolymerisable resins used in numerous industrial applications contain a substantial amount, up to 99%, of a mixture consisting of a reactive viscous prepolymer or oligomer and a mono- or polyfunctional monomer. The mono- or

polyfunctional monomer acts as a reactive diluent of low viscosity and is co-polymerisable with the prepolymer [1-3,24,63].

During the development of a UV curable formulation the primary objective involves the selection of, or the design and synthesis of a polymer (prepolymer or oligomer) which will impart the optimum properties for the proposed application of the surface coating. Such properties are most likely to include adhesion to a variety of substrates, tensile strength and flexibility. The prepolymer must also have good pigment wetting and rheological properties. Currently, the polymers found to meet these requirements include unsaturated polyesters, epoxy acrylates, polyester acrylates, urethane acrylates and polyether acrylates [1-3,24,63].

Unsaturated Polyesters

The earliest types of resins used in UV cured systems involved unsaturated polyesters dissolved in styrene and other monomers (i.e., butane-1,4-diol). These systems were mainly used, and still are, for wood finishing, as fillers, sealers and lacquers. Despite their good mechanical properties and significant cost advantage, the general properties of the unsaturated polyesters are inferior to the current systems available. Unsaturated polyesters are characterised by slow curing properties, insufficient adhesion and flexibility on metals, plastic foils and paper, and a concomitant volatile, low flash point solvent (styrene) [1-3,24,64]. These reactive prepolymers are soluble, resinous, polycondensation products of the esterification reac-

finish for furniture items.

Polyester Acrylates

Although these compounds are polymers, their characteristic low viscosity and cost enables polyester acrylates to be used as reactive diluents. The preparation of polyester acrylates involves either the synthesis of a saturated polyester backbone with residual hydroxyl groups which are then esterified with acrylic acids, or the reaction of an unsaturated primary alcohol, such as a hydroxy acrylate with residual acid groups on the polyester chain [1-3,64]. Both preparations result in acrylate groups attached to the saturated polyester backbone. Polyester acrylates exhibit a satisfactory all-round performance, although they are generally not outstanding in any particular property. The number of possible structural variations in the polyester is large, and similarly the extent to which acrylic esters can be modified is extensive [65]. As mentioned earlier, polyester acrylates, as radiation curable polymers, are characterised by their low viscosity and their relatively low cost compared with other acrylated polymers. They show good compatibility with other polymers and as a result polyester resins are used as reactive diluents in many radiation curable formulations [1-3]. The application and property advantages of these resins provides a wide range of end uses which includes overprint varnishes for polyurethanes, PVC, leather, metals, inks and so on.

Polyether Acrylates

Polyethers are another class of low molecular weight, low viscosity resins, which can be acrylated to produce relatively inexpensive polyether acrylate polymers. The polyether acrylates tend to yield very hard films with low flexibility and for this reason are not recommended for coating metals, plastics and paper. However, a new generation of low viscosity, low toxicity polyether acrylates, such as the ethoxylates and propoxylates of trimethylol propane, pentaerythritol and polyethers of butane diol are found in a large number of applications [1-3,64].

Acrylated Epoxy Resins

The mechanical and adhesive properties of epoxy-acrylate UV curable resins are much better than those of similarly cross linked polyester resins. There are a number of epoxy containing compounds which can be acrylated, including the bisphenol A diglycidyl ethers, epoxidised oils and epoxy novalacs. The preparation of epoxy resins is shown diagrammatically in Scheme 7, using bisphenol A type resins as the example. Initially, as shown in this example, bisphenol A and two moles of epichlorohydrin react via a condensation reaction to give the basic epoxy unit (Scheme 7). This is followed by an addition reaction (with two moles of acrylic acid), whereby the terminal epoxide rings open forming hydroxy groups. The double bond functionality of the epoxy resin can be increased and the characteristics of the resin improved by reacting the epoxy resin with a half-ester of fumaric

Polyurethane Acrylates

The reaction of the hydroxy group of an acrylic monomer and or polyester, polyether or polyol with di-isocyanates or polymers containing an excess of isocyanate groups will produce radiation curable acrylated polyurethanes. A wide range of final film properties can be achieved using such compounds, which vary in their molecular weight and functionality. Coatings based on these resins are capable of providing good cure speeds combined with good all round performance properties on a variety of substrates. The properties of the finishes are dependent, amongst other things on the oligomer structure, including its level of unsaturation, functionality, molecular weight and viscosity [1-3,64].

Flexible urethane acrylates can be prepared by the reaction of a di-isocyanate or half adduct of a di-isocyanate with a long chain glycol. A polyethylene glycol, or alternatively a hydroxy functional polyester or polyether will impart flexibility into the molecule [63]. Increasing the flexibility of a urethane acrylate results in the loss of its hardness properties, cure speed and solvent resistance. A hard urethane acrylate can be prepared by the reaction of di-isocyanates with tri- or higher functional polyols and unsaturated hydroxy monomers. This produces polymers which are highly viscous, with rigid branched structures capable of high levels of cross linking [1-3,64], providing very hard, inflexible but chemically resistant coatings [63].

Urethane acrylates tend to be more expensive than epoxy acrylates and for this reason their application is generally

limited to end uses which specifically require chemical resistance, hardness, toughness and adhesion to difficult substrates. Combined with other polymers however, they provide systems with various performance advantages without being too expensive. General applications include floor tiles requiring abrasion resistance, wood coatings, printing inks, adhesives and overprint varnishes.

Monomers

The implementation of environmental and safety regulations have influenced the development of UV curable formulations over the last few years. A direct result of this is shown by the replacement of the volatile monomers originally used in the early formulations by less volatile monomers. Monomers are chiefly added as diluents to control the viscosity of the UV curable formulation. They form an integral part of the film, contributing significantly to the cure speed, rheology and the final properties of the film.

The diluents used in radiation curable systems are either reactive or non reactive. Non reactive diluents are usually solvents or plasticisers added predominantly to reduce the viscosity and to impart some flexibility into the cured film. Reactive diluents can be classified as mono- or multifunctional monomers, where the former has one double bond per molecule and the latter two or more double bonds per molecule. Besides reducing the viscosity and modifying the application rheology, reactive diluents are largely responsible for determining the cure speed

of a UV curable formulation (along with the photoinitiator). They also contribute significantly towards the degree of crosslinking, modification and improvements in the properties of the cured film [1-3,64].

Monomers suitable for UV curable formulations can be mono-, di-or polyfunctional. During the selection of a suitable monomer for a UV curable formulation the monomer's reactivity towards UV, functionality, volatility, solubility, toxicity, viscosity, odour, and cost need to be considered. The present trend is towards the selection of monomers which are reactive, with low volatility, and have very low toxicological properties, in particular skin irritancy. However, the reactivity, functionality and percentage shrinkage of the monomers are also considered as these control the overall film performance (i.e., cure speeds, flexibility, hardness and adhesion to a variety of substrates) [1-3,64].

Vinyl Functional Monomers

These include styrene, vinyl acetate, N-vinyl pyrrolidone (NVP) and vinyl toluene. Styrene is used predominantly as a solvent for unsaturated polyester resins. Early UV curing systems were based upon unsaturated polyesters dissolved in styrene and used on a commercial scale for wood finishing. Styrene contributes towards the hardness of the surface coating and has good copolymerisation characteristics towards many resins and other monomers. Unfortunately, styrene is a slow curing volatile monomer and the current demands for faster-curing coatings with low

volatility to reduce atmospheric pollution have resulted in the substitution of styrene for other more suitable monomers. Despite this, styrene still forms the main monomer component in wood finishing applications, where its low price has been an outstanding advantage [1-3,64].

Vinyl acetate is a very reactive monomer, but is inflammable (low flash point) and volatile. Formulations using this diluent are liable to give cured films with a poor resistance to weathering. NVP is probably the most widely used vinyl monomer. It reduces the viscosity of the pre-polymer very efficiently and is highly reactive, particularly with multifunctional acrylate diluents. Unfortunately, it has a strong odour which restricts its use in a number of applications.

Monofunctional Acrylates

The use of straight chain alkyl acrylates in UV curable formulations is limited due to their volatility (in the case of short chain alkyl acrylates), characteristic strong odour and the tendency to produce soft films (in the case of long chain alkyl acrylates). Branched acrylates, such as 2-ethylhexylacrylate (EHA) (Figure 2), with their relatively low volatility, find applications because of their plasticising properties. The branched acrylates however, have very pungent odours thus restricting their usefulness. Monomers such as isobornyl acrylate, where the acrylic functionality is attached to a cyclic group also have strong odours, but they are less volatile than other

monofunctional monomers and have low shrinkage properties and low toxicity [1-3,64].

Difunctional Monomers

These materials, produced by the reaction of two moles of acrylic acid and one mole of a diol, have been developed over the last 15 years or so. The direction of the development has been towards low skin irritancy and other toxicological hazards. Commercially significant monomers include tripropylene glycol diacrylate (TPGDA) (Figure 2), 1,6-hexanediol diacrylate (HDDA) (Figure 2), and tetra-ethylene glycol diacrylate (TEGDA).

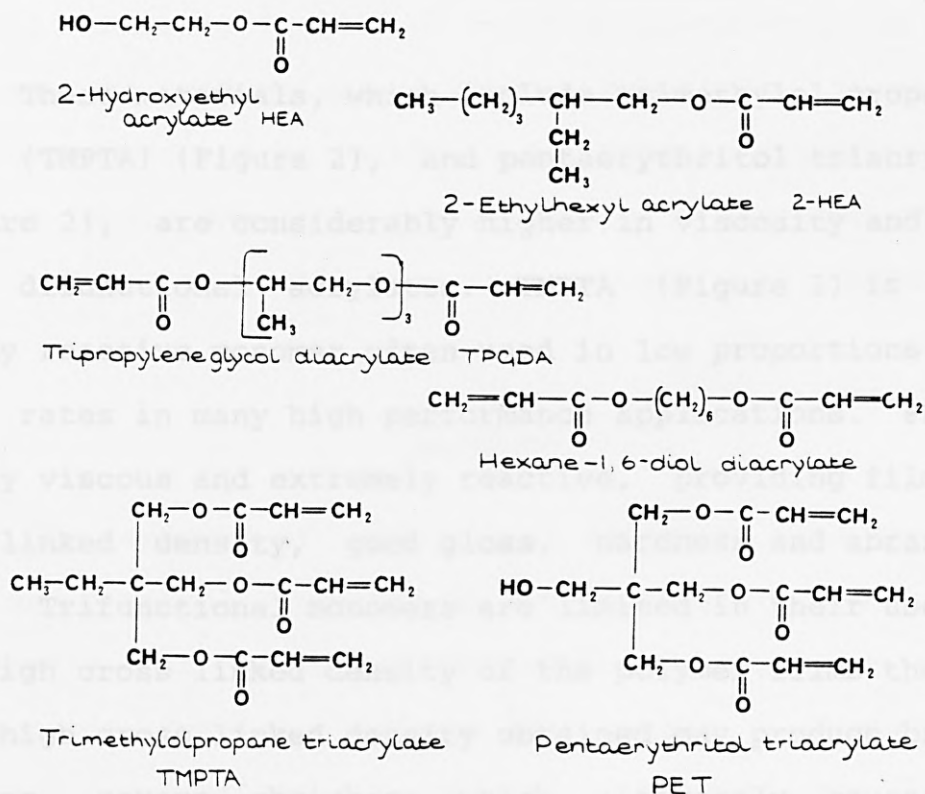


Figure 2 Examples of commercially available monomers.

TPGDA is a low viscosity diluent, highly reactive, a good solvent for most acrylated prepolymers (see Figure 2), and is one of the most widely used monomers in UV curable formulations. HDDA offers very similar characteristics to TPGDA, but with its straight carbon chain backbone, offers the best combination of flexibility, adhesion, reactivity^t and toughness available in the difunctional acrylates. HDDA (Figure 2) is included extensively in UV curable formulations used for wood coatings, floor coverings, paper and board coatings. TEGDA is used in formulations for low viscosity coatings requiring good adhesion and flexibility, such as metal decorating, floor, paper and board coatings [1-3].

Trifunctional Monomers

These materials, which include trimethylol propane triacrylate (TMPTA) (Figure 2), and pentaerythritol triacrylate (PETA) (Figure 2), are considerably higher in viscosity and reactivity than difunctional acrylates. TMPTA (Figure 2) is a viscous, highly reactive monomer often used in low proportions to improve cure rates in many high performance applications. PETA is also highly viscous and extremely reactive, providing films with high crosslinked density, good gloss, hardness and abrasion resistance. Trifunctional monomers are limited in their use because of the high cross linked density of the polymer films they produce. The high cross linked density obtained may produce brittle films showing severe shrinkage which ultimately causes adhesion failure.

CHARACTERISTICS OF UV-CURED NETWORKS

As described in the previous section the UV-cured polymer networks exhibit specific properties as a direct result of their high crosslink density.

Chemical Resistance

Generally the UV cured surface coatings are insoluble in organic solvents, as are other highly crosslinked systems, the solvent resistance being a function of the chemical structure and crosslink density. This property enables UV curable formulations to function as effective negative photo resists in the electrographic industry [1-3]. UV cured polyester-styrene coatings are resistant to both polar and aqueous solutions. Acrylic coatings however, need to be carefully selected to provide resistance to aqueous media and it is not advisable to use them for applications where they will come into contact with hydrophilic solvents.

Hardness

The hardness of a coating is dependent upon the functionality and chemical structure of the prepolymer used, as described previously. It is usually determined by measuring the pendulum (Persoz or Koenig) hardness [5], where a dampening of the pendulum oscillations are recorded in seconds (see Chapters 5 and 6). The pendulum hardness provides information about the degree of conversion which is directly related to the hardness and the

crosslinked density of the cured coating [66,67]. This method is not only influenced by the surface hardness of the coating, but also the thickness of the coating and the hardness of the coated substrate.

The ability of the cured coating to resist abrasion is an indication of the toughness of the film. The harder the cure, i.e., the greater the crosslinked density the greater the resistance to abrasion [3,64].

LIMITATIONS OF THE UV CURING TECHNIQUE

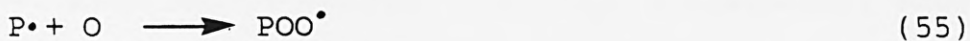
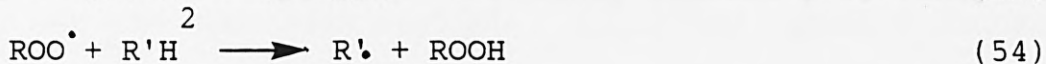
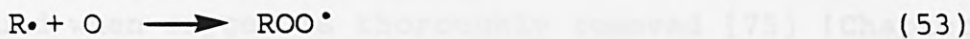
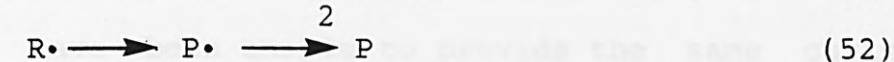
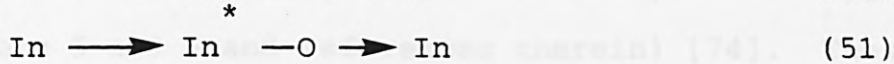
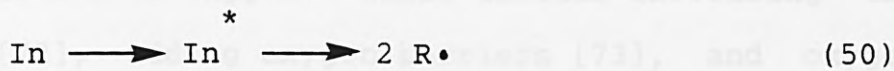
Oxygen Inhibition

Nearly all UV cured coatings are produced by free radical polymerisation reactions and are usually performed in an air atmosphere. One of the most important problems that plagues users of photopolymerisation processes arises from the deleterious effects of atmospheric oxygen which strongly inhibits radically induced polymerisation reactions [1-3,64,69,70]. Molecular oxygen exists as a bi-radical in its ground state which makes it very reactive towards both the excited states of the photoinitiator and the free radical species produced. One might therefore expect molecular oxygen to interfere in the photopolymerisation reaction by quenching the excited states of the photoinitiator, scavenging the initiating radicals and also the growing polymer radicals. This inhibiting effect results in the reduction of the rate of polymerisation, as shown by an undercured tacky surface layer requiring further irradiation to reach the desired physical prop-

erties i.e., hardness and gloss, of the end product [71].

The effect of oxygen upon the free radical polymerisation reaction is shown in Scheme 8, (where In is the initiator).

Scheme 8



As shown in Scheme 8, oxygen is capable of quenching the excited state of the photoinitiator (51), scavenging the initiating radicals R·(53) and the growing polymer radicals P·(55). The peroxy radicals formed in these scavenging reactions can abstract hydrogen atoms from a donor molecule R'H, (56). The donor molecule could be the monomer itself, or an added tertiary amine (see Chapters 5 and 6), the H-abstraction resulting in the formation of a hydroperoxide (ROOH, POOH) and a chain propagating radical (R'·) (54 and 56). The formation of hydroperoxides (54 and 56) is detrimental to both the chemical and physical resistance properties of the film. The addition of oxygen to the growing polymer chain results in the formation of peroxy radicals with relatively low reactivity. These are unable to maintain the propagation reaction and are terminated, giving short chain polymers [1-3,18,64,71]. The presence of hydroperoxides ultimately reduces

the long term stability of the cured coatings. The free radicals which escape scavenging will react with the surrounding monomer molecules, and initiate the polymerisation.

Several methods have been employed in an attempt to reduce the undesirable effects of oxygen. These include increasing the light intensity [72], adding oxygen barriers [73], and oxygen scavengers (Chapters 5 and 6 and references therein) [74]. These methods however, have been unable to provide the same curing efficiency found when oxygen is thoroughly removed [75] (Chapters 5 and 6).

Reactivity

The reactivity of some UV curable formulations, therefore the rate of polymerisation, is inherently low as a result of the type of prepolymer, monomer, and photoinitiator combination used. The reactivity of the formulation can be enhanced by selecting a more efficient photoinitiator system, i.e., a mixture of two or more photoinitiators may be used to increase the amount of UV radiation absorbed over a range of wavelengths. The selection of reactive prepolymers and diluents with greater functionality would also improve the reactivity of the UV curable formulation [66]. The photoinitiator concentration and the coating thickness will affect the penetration of UV light through both clear and pigmented thin films, which ultimately affects the rate and degree of polymerisation. These attributes are discussed in Chapters 5 and 6.

Adhesion

As the basic function of the cured coating is to protect the substrate it is applied to, it is very important that an excellent and long term adhesion exists between the film and the substrate surface. Adhesion is controlled by many factors which include interfacial contact and surface tension, curing time, shrinkage forces and coating substrate interactions [3,64,76].

It is important that the surface coating is applied to adequately wet the substrate surface, achieving intimate contact in the time available before curing, otherwise satisfactory adhesion will not be obtained. When using the UV curing technique, there is very little time between the application of the fluid medium to the formation of a solid film for the coating to diffuse into the substrate. This emphasises the importance of electrostatic and adsorption phenomena and thus the critical wetting tension to UV curing. If differences between the surface tension of the coating and substrate exist, interfacial contact between them will be lost [76,77]. The substrates surface energy will require maximising to achieve adequate adhesion or the surface tension of the coating will need to be minimised. Metal decorating presents problems, unless the substrate is pre-treated to remove the rolling oils (palm oil, sebacates) which destroy adhesion [3,64].

The polymerisation of most UV curable formulations result in a certain amount of volume shrinkage. If the surface of the film polymerises before the bulk (lower layers) the surface of the film will wrinkle and the adhesion to the substrate is sever-

ly strained. The wrinkling effect at the surface of the film arises as a result of shrinkage forces in the bulk of the film occurring upon polymerisation after the top layers have been polymerised. This effect can be observed with any type of coating, but pigmented films where the pigment scatters and absorbs the UV, and thicker films, when penetration of UV to the bottom layers of the film is proportionally lower than at the surface layers are particularly susceptible (see next section and Chapter 6 and references therein) [1-3]. The factors affecting adhesion in UV curable coatings is discussed elsewhere [77].

Pigmentation of UV Curable Coatings

UV curable formulations have found greater application for the curing of clear coatings, thin films of pigmented inks and coatings pigmented primarily with inert pigments, such as fillers for particle board. Unfortunately, UV curable formulations appear to be ineffective when cured as thick pigmented films. This presents severe limitations to the number of applications of the formulations since most surface coatings are basically applied to cover or 'hide' the substrate and consequently are applied as thick pigmented films. The ineffectual curing efficiency observed for pigmented or opaque films are the direct result of the absorption, scattering and reflection of the UV radiation caused by the pigments present in the films. This will, in turn, reduce the efficiency of the UV radiation to generate the excited states of the photoinitiator and therefore the efficiency to produce initiating radical species [1-3,18 and Chapter 6 and the references

therein].

As uniform curing throughout the film is required to avoid surface wrinkling effects light must be uniformly absorbed by the photoinitiators present at all layers in the film. Photoinitiator light screening effects can prevent through cure, which ultimately affects the adhesion of the coating to the substrate. The presence of highly absorbing pigments will drastically reduce the absorption of UV radiation by the photoinitiator in the lower layers of the film also, resulting in a poor through cure. Absorption of UV radiation by the photoinitiators in the lower film layers is drastically reduced by the presence of high-scattering pigments, especially in thicker films. The use of substrates with high reflectance properties leads to an increase in the amount of UV absorbed by the photoinitiator [1-3,64 Chapter 6 and the references therein].

Hazards in UV Curing

Although the use of acrylate monomers in UV curable formulations impart a wide range of property advantages, the associated hazards of handling these materials have probably been one of the main reasons why the growth of the UV curing industry has not been much greater. The most serious hazards include the toxicity of the monomers and photoinitiators, stray UV light from the lamps and the formation of ozone.

Acrylic monomers must be regarded as hazardous materials. Even the generation of monomers used today are considered to be skin irritants. During the handling of these materials care must be taken to avoid both skin and eye contact, as well as inhala-

tion, which could damage the respiratory tract [1-3,64].

In the case of stray UV light, the emitted radiation at wavelengths of 254 nm can severely affect the eyes and the skin. Observing an unscreened mercury arc at several meters distance is sufficient to cause painful eye conditions, such as conjunctivitis and also to cause burning to the skin. For this reason all UV sources must be adequately screened and particular attention must be paid to eye protection by using suitable goggles. The formation of ozone occurs as the short wave UV (i.e., below 220 nm) passes through air. It is important to avoid the build up of toxic ozone concentrations, hence adequate ventilation is required. However, the formation of ozone can be eliminated using quartz screens to absorb the short wave UV radiation.

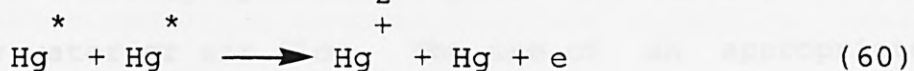
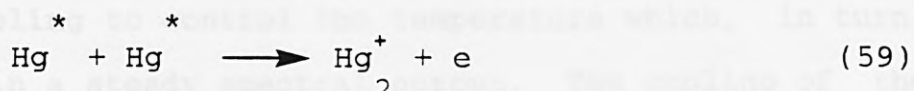
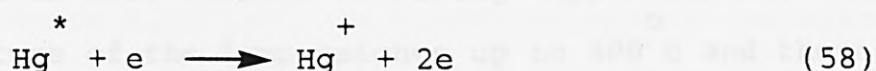
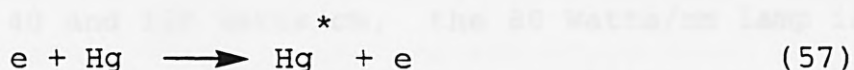
SELECTION of UV RADIATION SOURCES

During the selection of the UV light source for the photopolymerisation of UV curable formulations, certain characteristics need to be considered. These characteristics include a high intensity in the desired spectral region, long life, stability of output, ease of operation, proper physical dimensions for the process under consideration, and the minimum amount of ancillary equipment. Of the various lamps commercially available, the most commonly used source of UV for the curing of coatings and inks is the mercury vapour lamp [1-3].

Mercury vapour lamps are available at low, medium and high pressure. They usually consist of a sealed transparent quartz tube of variable length into which mercury has been introduced,

and are required to withstand operating temperatures of about 700 °C. Electrodes are located at either end of the tube (mostly tungsten), and an arc is struck by passing an electric current between the electrodes. When an electric current is passed between two electrodes separated by a gas or vapour, radiation of various wavelengths is generated. The intensity and the wavelength distribution of the light produced depends upon the gas, its pressure, the applied current and the arc tube diameter. Mercury vapour generates radiation rich in UV light, is relatively inert and does not attack either the glass or the electrode material [1-3]. The vaporisation and ionisation of mercury atoms occurs through collisions with electrons of sufficient kinetic energy, as shown below in Scheme 9.

Scheme 9



The excited mercury electrons move from one transition state to another, lower transition state. As they do so, energy is released as photons. The wavelength emitted by the photon is dependent upon the actual transition taking place [1-3].

Low pressure mercury vapour lamps are characterised by the generation of the 253.7 nm line with high efficiency, and by low heat evolution (about 40 °C) during operation. The output of this

lamp is 46% UV radiation at 254 nm, 50% infrared radiation irradiated by the quartz lamp wall, and 4 % infrared radiation which is directly irradiated by the lamp arc. The lamps operate at a rather low output and are therefore inexpensive to run. The expected lifetime of the lamps is around 7500 hours of operation. Although the UV output of these lamps is very efficient, the intensity is very low which can result in the limited penetration of the short wave UV through the surface coating, and therefore longer curing times. The low price of these lamps, however, enables multiple lamps to be used to reduce the curing time. The space requirements of a multiple lamp unit can be minimised by placing these lamps close to each other, since the lamp jackets remain close to room temperature during operation [1-3].

Medium-pressure mercury lamps operate below 1 atm and at loadings of between 40 and 120 Watts/cm, the 80 Watts/cm lamp is commonly installed in most current UV-curing applications. The operating temperature of the lamp reaches up to 800 °C and therefore requires cooling to control the temperature which, in turn, helps to maintain a steady spectral output. The cooling of the lamps can be by water or air flow. The use of an appropriate extraction unit to cool the lamps will also serve to remove any ozone produced. The higher operating temperatures and pressures present in the medium pressure mercury lamp result in many more collisions and interactions taking place. This results in a much wider spectral output, with the emission bands being broader than those of the low-pressure mercury lamps, and major peaks at 313 and 366 nm. The lifetime of these lamps is guaranteed to be

about 1000 hours, although 2000 hours may be a more realistic figure [2]. The medium-pressure mercury lamps emit 17.4% UV from the 200-400 nm region, 23.8% of visible light, 5.8% infra-red radiation, and 53% of their input power is lost as heat. The heat emitted however, is important in practical terms, since the temperature increase it confers to the coating helps to increase the polymerisation process by reducing the coating viscosity and consequently the overall rate of cure. One mercury vapour lamp can cure films faster than many low-pressure mercury lamps, mainly because of the range of UV wavelengths that the medium pressure lamp emits. The medium-pressure mercury lamps radiate energy throughout the UV spectrum which can penetrate thick films [1-3].

High-pressure mercury lamps are the source of most intense UV and visible radiations. The light output is about ten times that of a medium-pressure mercury lamp and 100 times that of a low-pressure lamp. These high pressure lamps operate in the range of 10 to 100 atmospheres with a loading of 160 Watts/cm. The lifetime of these lamps can be extended using efficient cooling devices. The higher operating temperatures and pressures result in a marked increase in the radiation bandwidths compared to those of a medium pressure mercury lamp. In addition, a large proportion of the total radiation is in the infrared range which can be utilised to accelerate the curing by a thermal mechanism. The thermal mechanism is caused by IR radiation after the UV radiation has started the initiation reaction. The lamps are usually smaller in dimension than the medium pressure mercury lamp and find applications in photolithography [1-3].

The UV initiation process is extremely rapid on account of the short lifetimes of the excited triplet states of the photo-initiator. The process is proportional to the intensity of the incident radiation, therefore the positioning of lamps and the types of reflectors used play an important role in obtaining optimum curing efficiency. Both parabolic and elliptical reflectors are used commercially, although the elliptical or semi-elliptical reflector is probably the most widely used reflector for curing coatings applied to a moving flat substrate. The parabolic reflectors provide a parallel beam of UV intensity, whereas the elliptical reflectors produce a focussed beam of radiation as an intense band onto the substrate to be cured. Parabolic reflectors are suitable for curing coated containers or other non flat applications where focussing is not required. The materials used for the reflectors must be able to withstand high temperatures as well as being resistant to the influence of ozone produced during the irradiation process. In the case of medium and high-pressure mercury lamps, which operate at temperatures over 700 °C, cooling of reflectors is required [1-3].

APPLICATIONS of UV CURING

There are many applications for which UV curable formulations provide the ideal surface coating characteristics and more to be exploited. The earliest commercial applications of UV curable formulations were in the field of paste fillers, sealers and topcoats for chipboard. These were formulated from unsaturated polyester resins in styrene, containing a very high prop-

ortion of transparent extender pigments. The compositions exhibited excellent filling power at high drying speeds, providing smooth non porous surfaces suitable for further processing. The main advantage of UV curing applications in the wood finishing industry arises from the ability to incorporate the process into compact, continuous flow production lines without large space requirements. Another significant advantage of the UV curing process lies with the production of finishes with good adhesion, solvent and scratch resistance and low shrinkage. UV curable coatings based on urethane acrylate formulations are used commercially as coatings for vinyl flooring on account of their excellent abrasion resistance [1-3,24].

UV curable formulations are also employed commercially for coating paper by roller application as overprint varnishes where high-gloss finishes similar to that of laminated film are produced, but at a much lower cost [24], in adhesives [24, 78,79], and in printing inks [24,79,80]. UV curing has been used in conjunction with lithographic, letter press and gravure and also web offset processes for sheet base colour coats and clear lacquers [79,80]. The container decorating process, where exceptionally high line speeds are involved, also uses UV curable formulations [81] showing a high degree of flexibility and chemical resistance [24].

A more recent application of UV curable formulations is that of a dental material [24]. Such formulations are used for the repair of teeth, as fillings, pit and fissure sealants and adhesives. UV curable epoxy and urethane acrylates are employed as optical fibre coatings for the telecommunication industry

[24,82-85] and provide a very efficient protective coating from mechanical damage and attack by moisture.

The acylphosphine oxides were introduced in 1963 as a novel class of photoinitiators for the photopolymerization of pigmented formulations in particular. The efficiency of these photoinitiators was reported to depend critically upon their substitution, in particular the 2,4,6-trimethylbenzoyl diphenylphosphine oxide (TMBO) being the most favoured photoinitiator [86]. The acylphosphine oxides absorb in the long-wave region of the ultraviolet spectrum at about 380 nm, and are therefore suitable for the curing of white titanium dioxide pigmented lacquers, primers and thick walled glass fibre-reinforced polyesters [87]. Compared to most other known photoinitiators, the acylphosphine oxides were reported to exhibit little yellowing and high light resistance, as well as being suitable for the polymerization of unsaturated polyester resins containing styrene [86]. These compounds were expected to extend the scope of UV curing to applications that were formerly the domain of electron beam curing.

Further investigations conducted by Sumiyoshi et al. [87] proposed that TMBO, fragmented by a Norrish Type I process to give a 2,4,6-trimethylbenzoyl radical and a diphenylphosphonyl radical. The quantum yields of radical formation were reported to be between 0.5 and 0.7 [87] which has since been substantiated by others [88].

From the laser flash photolysis investigations reported by Sumiyoshi et al. [87,88] no decision could be made as to whether

INTRODUCTION:PART II

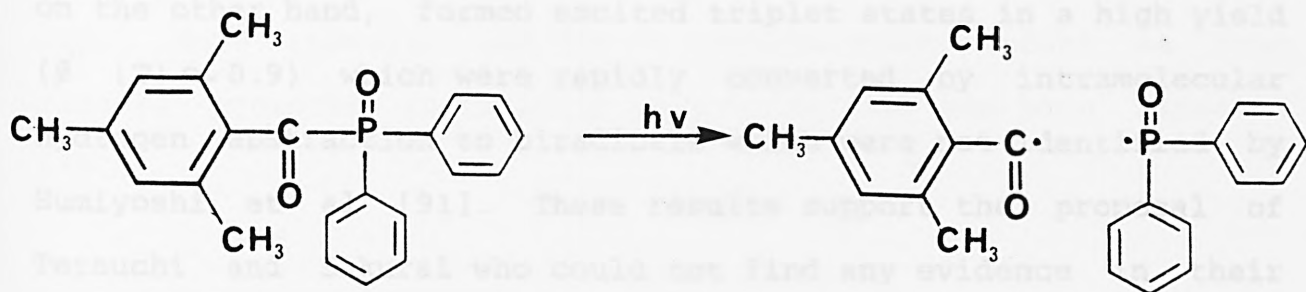
ACYLPHOSPHINE OXIDES

The acylphosphine oxides were introduced in 1983 as a novel class of photoinitiators for the photopolymerisation of pigmented formulations in particular. The efficiency of these photoinitiators was reported to depend critically upon their substitution, in particular the 2,4,6-trimethylbenzoyldiphenylphosphine oxide (TMBO) being the most favoured photoinitiator [86]. The acylphosphine oxides absorb in the long-wave region of the ultraviolet spectrum at about 380 nm, and are therefore suitable for the curing of white titanium dioxide pigmented lacquers, primers and thick walled glass fibre-reinforced polyesters [87]. Compared to most other known photoinitiators, the acylphosphine oxides were reputed to exhibit little yellowing and high light resistance, as well as being suitable for the polymerisation of unsaturated polyester resins containing styrene [86]. These compounds were expected to extend the scope of UV curing to applications that were formerly the domain of electron beam curing.

Further investigations conducted by Sumiyoshi et al [87] proposed that TMBO, fragmented by a Norrish Type 1 process to give a 2,4,6-trimethylbenzoyl radical and a diphenylphosphonyl radical. The quantum yields of radical formation were reported to be between 0.5 and 0.7 [87] which has since been substantiated by others [88].

From the laser flash photolysis investigations reported by Sumiyoshi et al [87,89] no decision could be made as to whether

the photofragmentation shown in Scheme 9 involved both singlet and triplet excited states or just triplet excited states of the Scheme 9.



photoinitiator TMBPO. Schnabel had claimed that the Norrish Type 1 cleavage occurred in less than 300 ps from singlet states [90]. Chemically induced dynamic electron polarisation studies, which are discussed in more detail in Chapter 3, have shown unequivocally by direct observation that the acylphosphine oxide TMBPO and 2,6-dimethoxybenzoyldiphenylphosphine oxide (DMBPO) dissociate through their excited triplet states to produce radicals via a Norrish Type 1 cleavage.

Trimethyl substituted benzoylphosphonates such as 2,4,6-trimethylbenzoyldimethyl and diethyl phosphonates, (TMBMP) and (TMBEP) respectively, were reported to undergo a significant amount of scission mainly (if not exclusively) via the excited singlet state [91]. A large proportion of these singlet states were found to undergo intersystem crossing, as indicated by the high quantum yield of triplets recorded during this investigation ($\phi(T) \sim 0.6$). This was believed to be followed by a sequence of intramolecular processes involving enolisation in the triplet state. TMBPO did not undergo enolisation [92]. Sumiyoshi et al concluded that this was because enolisation involved triplets and

that triplet lifetimes longer than a few nanoseconds were a prerequisite for this reaction. Benzoyldiethylphosphonate (BDEP) on the other hand, formed excited triplet states in a high yield ($\phi(T) \sim 0.9$) which were rapidly converted by intramolecular hydrogen abstraction to biradicals which were not identified by Sumiyoshi et al [91]. These results support the proposal of Terauchi and Sakurai who could not find any evidence in their photochemical studies of benzoylphosphonates undergoing photo-fragmentation via a Norrish Type 1 cleavage [93].

High rate constant values were obtained for the reaction of TMBPO with methyl methacrylate and styrene [87]. This led to the conclusion that TMBPO would be a highly appropriate photoinitiator for the polymerisation of surface coatings. TMBMP and TMBEP were also found to initiate the free radical polymerisation of methyl methacrylate [91]. In the same investigation however, BDEP was found to be ineffective as a photoinitiator for the polymerisation of methyl methacrylate.

Sumiyoshi and Schnabel generated phosphonyl radicals by the UV-photolysis of the appropriate acylphosphine oxides and acylphosphonates in the presence of a range of monomers [94]. These radicals were reputed to be effective initiators of the free radical polymerisation of olefinic compounds. All of the radical species generated were found to be very reactive toward acrylonitrile, styrene, methyl methacrylate, methyl acrylate, t-butylvinyl ether and vinyl acetate. It was proposed that the high reactivity of the radicals was due to their tetrahedral structure

[87,94,95]. It must be stressed that these reactions were performed in solutions freed from oxygen by bubbling through with purified argon, conditions not typical of the UV curing of coatings. More recently the use of acylphosphine oxides as free radical promoters in cationic polymerisations has been reported [96].

- [97] Roffey, C. G., *Photopolymerisation of Surface Coatings*, 1982, Wiley - Interscience.
- [98] Alexander, T., *Packaging Weekly*, 1987, July, 15.
- [99] Sato, K., *Prog. In. Org. Coatings*, 1986, 5 1 - 12.
- [100] Brann, B. G., *J. Rad Curing*, 1985, 11 (3) 4 - 10.
- [101] Thandavella, C. H., *J. Rad Curing*, 1985, 11 (4) 2 - 9.
- [102] (Slee) Le, D. D., *J. Rad Curing*, 1985, 11 (2) 2 - 8.
- [103] Sendaikha, T., Decker, C., *J. Rad Curing*, 1984, 11 (2) 6 - 13.
- [104] Tanny, G. B., Rav-nos, D., Lubelsky, A., Shchori, N., *Conf. Proc. Radcure FC-85-440* 1985 Basel Switz.
- [105] Chambers, S., Guthrie, G., Orterburn, M. S., Woods J., *Polym. Commun.* 1986, 27 207 - 211.
- [106] Urban, H. W., *J. Coat. Technology*, 1987, 59 (745) 29 - 34.
- [107] Chamberlain, H. S., Verbeem, R. S., *Conf. Proc. Radcure FC-86-054* 1986 Baltimore, USA.
- [108] Nguyen, T., *Prog. In Org. Coatings*, 1985, 11 1 - 34.
- [109] Turro, S. J., *Modern Molecular Photochemistry*, 1978, Benjamin/Cummings.
- [110] Neckers, D. C., *Mechanistic Organic Photochemistry*, Reinhold.
- [111] Glasstone, B., Luria, O., *Elements of Physical Chemistry*,

REFERENCES

- [1] Paul, S., Surface Coatings Science and Technology, 1986 Wiley - Interscience.
- [2] Holman, R., UV and EB Curing Formulations for Printing Inks Coatings and Paints, 1984, Sita Technology.
- [3] Roffey, C, G., Photopolymerisation of Surface Coatings, 1982, Wiley - Interscience.
- [4] Alexander, T., Packaging Weekly, 1987, July, 15.
- [5] Sato, K., Prog. in. Org. Coatings, 1980, 8 1 - 18.
- [6] Brann, B, L., J. Rad Curing, 1985, 12 (3) 4 - 10.
- [7] Thanawalla, C, H., J. Rad Curing, 1985, 12 (4) 2 - 9.
- [8] (Ziem) Le, D, D., J.Rad Curing, 1985, 12 (2) 2 - 8.
- [9] Bendaikha, T., Decker, C., J. Rad Curing, 1984, 11 (2) 6 - 13.
- [10] Tanny, G, B., Rav-noy, Z., Lubelsky, A., Shchori, E., Conf. Proc. Radcure FC-85-440 1985 Basel Switz.
- [11] Chambers, S., Guthrie, J., Otterburn, M, S., Woods J., Polym. Commun, 1986, 27 209 - 211.
- [12] Urban, M, W., J. Coat. Technology, 1987, 59 (745) 29 - 34.
- [13] Chamberlain, M, R., Davidson, R, S., Conf. Proc. Radcure FC-86-854 1986 Baltimore, USA.
- [14] Nguyen, T., Prog. in Org. Coatings, 1985, 13 1 - 34
- [15] Turro, N, J., Modern Molecular Photochemistry, 1978, Benjamin/ Cummings.
- [16] Neckers, D, C., Mechanistic Organic Photochemistry, Reinhold.
- [17] Glasstone, S., Lewis, D., Elements of Physial Chemistry,

- 2nd Edition, 1984, MacMillan.
- [18] Pappas, S, P., Ed., UV Curing: Science and Technology, Vol 1, 1978, Technology Marketing Corporation.
- [19] Hutchison, J., Ledwith, A., Adv. Polym. Sci, 1974, 14 49 - 86.
- [20] Billmeyer, F, W., Textbook of Polymer Science, 2nd Edition, Wiley - Interscience.
- [21] Flory, P, J., Chem. Rev, 1968, 39 137 - 197
- [22] Mayo, F, R., Walling, C., Chem. Rev, 1950, 46 191 - 287.
- [23] Oster, G., Yang, Nan-loh ,Chem. Rev, 1968, 68 (2) 125 - 151.
- [24] Green, G, E., Stark, B, P., Zahir, S, A., J. Macro. Sci - Revs. Macro. Chem, 1981/2 C21 (2) 187 - 273.
- [25] Eaton, D, F, in Advances in Photochemistry, Vol 13 427 - 487
- [26] Hageman, H, J., Prog in Org Coatings, 1985, 13 123 - 150.
- [27] Berner, G., Puglisi, J., Kirchmayr, R., Rist, G., J. Rad Curing, 1979, 6 (2) 2 - 9.
- [28] Green, P, N., Polym. Paint Colour J, 1985, 175 (4141) 246 - 252.
- [29] Gatechair, L, R., Wostratzky, D., J. Rad Curing, 1983, 10 (3) 4 - 18.
- [30] Berner G., Kirchmayr, R., Rist, G., J.O.C.C.A. 1978, 61 105 - 113.
- [31] Pappas, S, P., Prog Org Coatings, 1973/4, 2 333 - 347.
- [32] Ledwith, A., Pure and Applied Chem., 1977, 49 431 - 441.
- [33] Block, H., Ledwith, A., Taylor, A, R., Polymer, 1971, 12 271 - 288.

- [34] Pappas, S, P., Radiat. Phys. Chem, 1985, 25 (4 - 6) 633 - 641.
- [35] Heine, Von H, G., Rosenkranz H, J., Rudolph, H., Angew Chem., 1972, 84 (21) 1032 - 1036.
- [36] Osborn, C, L., J. Rad Curing, 1976, 3 (3) 2 - 11.
- [37] Heine, H, G., Traenckner, H, J., Prog. Org. Coatings, 1975, 3 115 - 139.
- [38] Pappas, S, P., Ed., UV Curing: Science and Technology, Vol II, 1985, Technology Marketing Corporation.
- [39] Chattopadhyay, A., Pappas, S, P., J. Am. Chem. Soc., 1980, 102 5686 - 5688.
- [40] Hutchison, J., Leadwith, A., Polym, 1973, 14 405 - 408.
- [41] Charlblom, L. H., Pappas, S, P., J. Polym Sci. Polym Chem Ed, 1977, 15 1381 - 1391
- [42] Lewis, F, D., Lauterbach, R, T., Heine, H, G., Hartmann, W., Rudolph, H., J. Am. Chem. Soc., 1975, 97 (6) 1519 - 1525.
- [43] Chattopadhyay, A., Pappas, S, P., Polym. Letts. Ed, 1975, 13 483 - 486.
- [44] Decker, C., Fizet, M., Makromol Chem., Rapid Commun, 1980, 1, 637 - 642.
- [45] Kuhlmann, R., Schnabel, W., Polymer, 1976, 17 419 - 422.
- [46] Merlin, A., Loughnot, D, J., Fouassier, J, P., Polym. Bull., 1980, 2 847 - 853.
- [47] Davidson, R, S., Lambeth, P, F., McKeller, J, F., Turner, P, H., Wilson, R., J. Chem Soc., Chem. Commun, 1969, 732 - 733.
- [48] Wamser, C, C., Hammond, G, S., Chang, C, T., Baylor, C.,

- J. Am. Chem Soc., 1970, 92 (21), 6362 - 6363.
- [49] Davidson, R, S., Orton, S, P., J. Chem. Soc., Chem. Commun, 1974, 209 - 210.
- [50] Arimitsu, S, J., J. Phys. Chem, 1975, 79 (13) 1255 - 1259.
- [51] Stone, P, G., Cohen, S., J. Am Chem Soc., 1980, 102 5686 - 5688.
- [52] Griller, D., Howard, J, A., Marriott, P, R., Sciano, J, C., J. Am Chem Soc., 1981, 103 619 - 623.
- [53] Inbar, S., Linschitz, H., Cohen, S, G., J. Am. Chem Soc., 1981, 103 1048 - 1054.
- [54] Amirzadeh, G., Schnabel, W., Makromol Chem, 1981, 182 2821 - 2835.
- [55] Davidson, R, S., Goodin, J, W., Eur Polym J, 1982, 18 597 - 606.
- [56] Stone, P, G.,Cohen, S, G., J. Am. Chem Soc., 1982, 104 3435 - 3440.
- [57] Merlin, A., Lougnot, D, J., Fouassier, J, P., Polym. Bulletin, 1980, 3 1 - 6.
- [58] Allen W, S., Catalina, F., Green, P, N., Green, W, A., Eur Polym J, 1986, 22 (1) 49 -56.
- [59] Allen W, S., Catalina, F., Green, P, N., Green, W, A., Eur Polym J, 1986, 22 (5) 347 - 350.
- [60] Sitek, F., Rembold, M., Cont. Proc. Radcure FC87-274. 1987, Munich, W. Ger.
- [61] Crivello, J, V., Lee, J, l., Macromolecules, 1981, 14, 1141-1147
- [62] Pappas, S, P., Jilek, J, H., Photograph. Sci., & Engin.,

- 1979 23 (3) 140-143.
- [63] O'Hara, K., Polymer Paint Colour Journal, 1985, 175 (4141) 254 - 270.
- [64] Young, S, E., Prog in Org. Coatings, 1976, 4 225 - 249.
- [65] Dufour, P., Conf. Proc. Radcure. FC83-261 1983 Lausanne, Switz.
- [66] Kuhl, G., Conf. Proc. Radcure. FC83-262 1983 Lausanne, Switz.
- [67] Gaube, H, G., Polym. Paint. Col. J, 1987, 177 (4197) 582 - 590.
- [68] Decker, C., J. Coatings. Tech. 1987, 59 (751) 97 - 106.
- [69] Wight, F, R., J. Polym. Sci. Polym. Letts Ed, 1978, 16 121 - 127.
- [70] Chong, J, S., J. Appl. Polym. Sci., 1969, 13 241 - 247.
- [71] Decker, C., Conf. Proc. Radcure FC85-432 1985 Basel, Switz.
- [72] Decker, C., Bendaikha, T., Eur Polym J, 1984, 20 (8) 753 - 758.
- [73] Bolon, D, A., Webb, K, K., J. Appld. Polym Sci, 1978, 22 2543 - 2551.
- [74] Bartholomew, R, F., Davidson, R, S., J. Chem Soc, (C), 1971, 2342 - 2346.
- [75] Decker, C., Jenkins, A, D., Macromolecules 1985 18 1241-1244.
- [76] Guthrie, J, T., Conf. Proc. Radcure 1985 Basel, Switz.
- [77] Brann, B, L., J. Rad. Curing, 1986, 13 (2) 12 - 16.
- [78] Woods, J., Conf. Proc. Radcure FC85-414 1985 Basel, Switz.
- [79] Roesch, K, F., Conf. Proc. Radcure FC83-259 1983 Lausanne, Switz.

- [80] Zylka, P., Conf. Proc. Radcure FC83-251 1983 Lausanne, Switz.
- [81] Turner, T, A., Conf. Proc. Radcure FC83-268 1983 Lausanne, Switz.
- [82] Lamberts, J, J, M., Meinders, H, C., Conf. Proc. Radcure FC85-411 1985 Basel, Switz.
- [83] Kitayama, S., Conf. Proc. Radcure FC85-423 1985 Basel, Switz.
- [84] Newman, H, C., Conf. Proc. Radcure FC83-267 1983 Lausanne, Switz.
- [85] Lawson, K, R., Conf. Proc. Radcure FC83-264 1983 Lausanne, Switz.
- [86] Jacobi, M., Henne, A., J. Rad Curing, 1983, 10 (4) 16 - 25.
- [87] Sumiyoshi, T., Schnabel, W., Henne, A., Lechtken, P., Polymer, 1985, 26 141 - 146.
- [88] Baxter, J, E., Davidson, R, S., Hageman, H, J., Overeem, T., Makromol Chem., Rapid Commun., 1987, 8 311 - 314.
- [89] Sumiyoshi, T., Schnabel, W., Henne, A., Lechtken, P., Z Naturforsch, 1984, 39a 434 - 436.
- [90] Schnabel, W., J. Rad Curing, 1986, 13 (1) 26 - 34.
- [91] Sumiyoshi, T., Schnabel, W., Henne, A., J. Photochem, 1985 30 63-80
- [92] Sumiyoshi, T., Schnabel, W., Henne, A., J. Photochem, 1986, 32 119-130.
- [93] Terauchi, K., Sakurai, H., Bull Chem Soc Japan, 1970, 43 883 - 890.
- [94] Sumiyoshi, T., Schnabel, W., Makromol Chem, 1985, 186 1811-1823.

- [95] Sumiyoshi, T., Schnabel, W., in New Trends in the Photochemistry of Polymers, Ed., Allen, N, S., Rabek, J. F., Elsevier Appl Sci, 1985, Chapter 4, 69 - 83.
- [96] Yagci, Y., Schnabel, W., Makromol. Chem. Rapid Commun, 1987, 8 209-213.

Synthesis
of
Photoinitiators

Chapter 2

Synthesis of Photoinitiators

Chapter 2	Synthesis of Photoinitiators	
	Introduction	72
	Michaelis-Arbusov Rearrangement	74
	Results and Discussion	76
	Experimental	89
	References	116

of a large number of compounds available UV lamps used in the surface coatings industry. The efficiency of many of these photoreactions leads to fast rates of polymerization, by a free radical mechanism. These reactions have been described previously in Chapter 1. Some of these compounds particularly suitable for the photopolymerization of UV curable formulations (1,2). The spectral properties of various compounds containing phosphorus moiety, such as the triphosphines, phosphites, phosphonates and acylphosphine oxides (3-5) show enhanced absorption characteristics in the 300-400 nm region of the UV spectrum by virtue of their absorption bands occurring between 300-400 nm. These phosphorus compounds, in addition to their high photoreactivity, would be particularly suitable for the photopolymerization of pigmented e.g., vitreous enamel formulations.

The introduction of acylphosphine oxides as a novel class of photoinitiators for the polymerization of pigmented films and unsaturated polyesters (6) has been discussed previously in Chapter 1. These compounds undergo photolysis by a very fast Norrish Type I cleavage mechanism (4,7) producing phosphinoyl radicals which are very reactive towards olefinic compounds (7,8). The phosphorus moiety extends their absorption

INTRODUCTION

Many aromatic carbonyl compounds are used commercially as photoinitiators for the free radical polymerisation of UV curable formulations. This particular class of compounds show absorption characteristics in the 300-400 nm region of the UV spectrum due to a $n \rightarrow \pi^*$ transition, which coincides with the emission spectrum of a large number of commercially available UV lamps used in the surface coatings industry. The efficiency of many of their photo-reactions leads to fast rates of polymerisation, by a free radical mechanism. These attributes and others, mentioned previously in Chapter 1, make these compounds particularly suitable for the photopolymerisation of UV curable formulations [1,2]. The spectral properties of carbonyl compounds containing a phosphorus moiety, such as the acylphosphonates, aroylphosphonates and acylphosphine oxides [3-6] also show enhanced absorption characteristics in the 300-400 nm region of the UV spectrum. By virtue of their absorption maxima occurring between 350-380 nm, these phosphorus compounds, if able to function as photoinitiators, would be particularly suitable for the photopolymerisation of pigmented e.g., titanium dioxide formulations.

The introduction of the acylphosphine oxides as a novel class of photoinitiators for the polymerisation of pigmented films and unsaturated polyesters [4] has been discussed previously in Chapter 1. These compounds undergo photofragmentation by a very fast Norrish Type 1 cleavage mechanism [4,7] producing phosphinyl radicals which are very reactive towards olefinic compounds [7,8]. The phosphorus moiety extends their absorption

characteristics towards longwave UV, which also extends their use as photoinitiators for pigmented UV curable formulations. These characteristics indicate that carbonyl compounds containing a phosphorus moiety could be an ideal class of photoinitiators for applications previously the domain of electron beam curing.

The synthesis of acylphosphine oxides, acylphosphonates and related compounds are described in the experimental section of this chapter. The objective of the synthesis was to produce compounds, which when irradiated by UV light, would cleave quickly, preferably by a Norrish Type 1 cleavage into two initiating free radical species. The nature of the initiating species derived from these compounds could only be speculated at this stage. The acyl radicals however, are well known for addition to the olefinic double bond of vinyl monomers, and phosphinyl radicals have been observed [9] to display the usual free radical reactions, e.g., addition to the carbon-carbon double bond. The enhanced absorption characteristics of these compounds in the 300-400 nm region, which is somewhat reminiscent of that exhibited by 1,2-dicarbonyl compounds, was expected to provide a more efficient and economical usage of UV radiation compared to the available commercial photoinitiators.

The yellow colour of the acylphosphine oxides, acylphosphonates and related compounds arises as a result of a moderately strong conjugation between the phosphoryl group and the carbon atom of the adjacent carbonyl group [3,5,6,10]. The interaction of a filled non-bonding orbital on oxygen (of the phosphoryl group) with the π orbital of the carbon atom (of the carbonyl

group) will be at a maximum when the phosphorus-oxygen bond is perpendicular to the plane composed of the aryl ring, carbon and phosphorus [3,5,6,10], as shown in Figure 1.

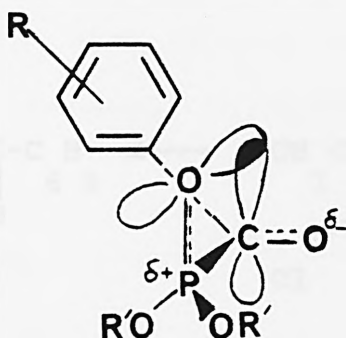


Figure 1 The orbital interactions leading to conjugation in carbonyl compounds containing a phosphorus moiety.

MICHAELIS-ARBUSOV REARRANGEMENT

The acylphosphine oxides, acylphosponates and aroylphosponates were prepared by the reaction of phosphites, or phosphines with the corresponding carboxylic acid chlorides [11,12] via a Michaelis-Arbusov rearrangement [13]. The Michaelis-Arbusov rearrangement proceeds via two successive bimolecular steps. The carboxylic acid chloride undergoes an initial substitution reaction with the trialkylphosphites, acting as a nucleophile, to give the phosphite equivalent of a phosphonium salt (i), as shown in Scheme 1. The phosphonium salt (i) however, is unstable in the presence of nucleophiles and is rapidly attacked by the chloride ion at one of the ethoxy carbon atoms to give a phosphonate (iii). The reaction of trialkyl phosphites with carboxylic acid

SCHEME 1.

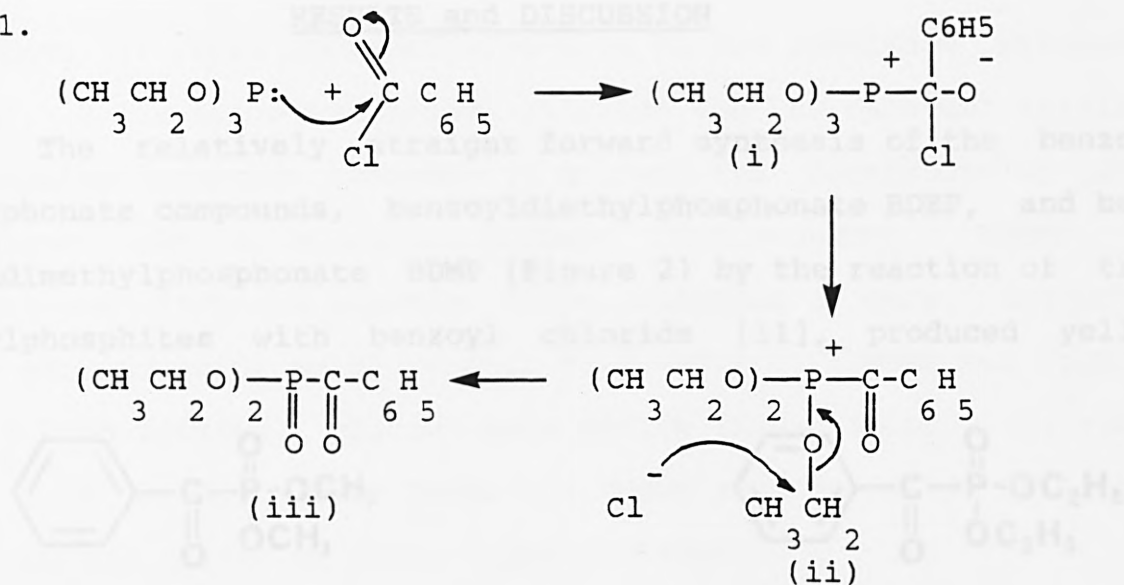
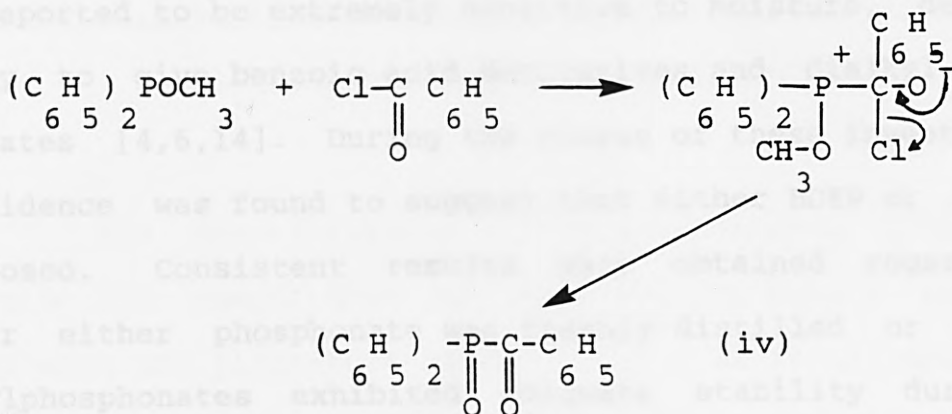


Figure 2 Benzoyl Chloride

chlorides will give the corresponding phosphonate. Phosphinites undergo identical reactions to give phosphine oxides (iv) as shown in Scheme 2.

SCHEME 2.



The driving force of the Michaelis-Arbusov rearrangement is the formation of the extremely strong phosphorus oxygen double bond (P=O).

RESULTS and DISCUSSION

The relatively straight forward synthesis of the benzoyl phosphonate compounds, benzoyldiethylphosphonate BDEP, and benzoyldimethylphosphonate BDMP (Figure 2) by the reaction of trialkylphosphites with benzoyl chloride [11], produced yellow



Figure 2 Benzoyldiethylphosphonate and benzoyldimethylphosphonate.

liquids with very high boiling points of 124 -126 °C at 0.3 mm Hg and 106 -109 °C at 0.1 mm Hg respectively. The benzoylphosphonates were reported to be extremely sensitive to moisture, decomposing readily to give benzoic acid derivatives and dialkyl hydrogen phosphates [4,6,14]. During the course of these investigations, no evidence was found to suggest that either BDEP or BDMP had decomposed. Consistent results were obtained regardless of whether either phosphonate was freshly distilled or not. The benzoylphosphonates exhibited adequate stability during the course of these investigations and were sufficiently stable towards tertiary amines, which are used as co-initiators in UV curable formulations.

The acylphosphonates 2,4,6-trimethylbenzoyldiethylphosphonate TMBEP and 2,4,6-trimethylbenzoyldimethylphosphonate

(Figure 3) were prepared according to the published procedure [12]. 2,4,6-trimethylbenzoyl chloride and the relevant trialkylphosphite reacted together to produce the corresponding phosphonate via a Michaelis-Arbusov rearrangement. TMBMP was distilled from the reaction flask producing a pure, colourless low melting point solid (m.pt., 47.7^o -49.2^o C). TMBEP was found to be a high boiling, viscous pale yellow liquid (b.pt., 204^o -206^o C at 0.35 mm Hg). Both TMBEP and TMBMP were found to be stable during the course of these investigations.

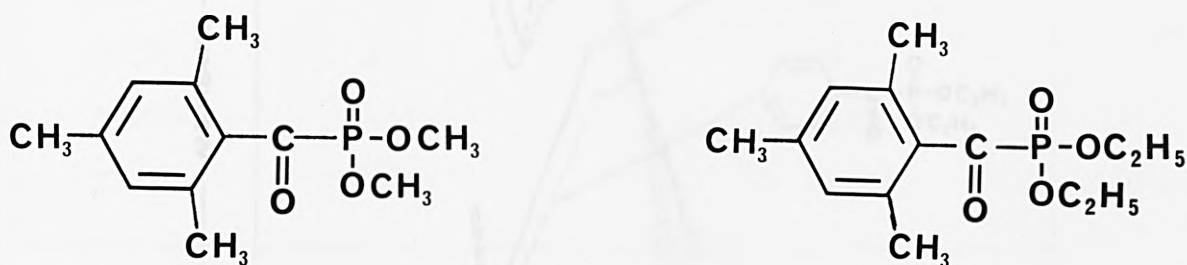


Figure 3 2,4,6-trimethylbenzoyldimethylphosphonate and 2,4,6-trimethylbenzoyldiethylphosphonate.

The identification of the phosphonates from spectral analysis and comparisons of their boiling points and melting points with the literature values [4,7,11,12,14,15] are presented in the experimental section. There was a striking similarity between the UV absorbance spectra of the phosphonate compounds, as shown in Figure 4 and Table 1, when they were compared under similar conditions.

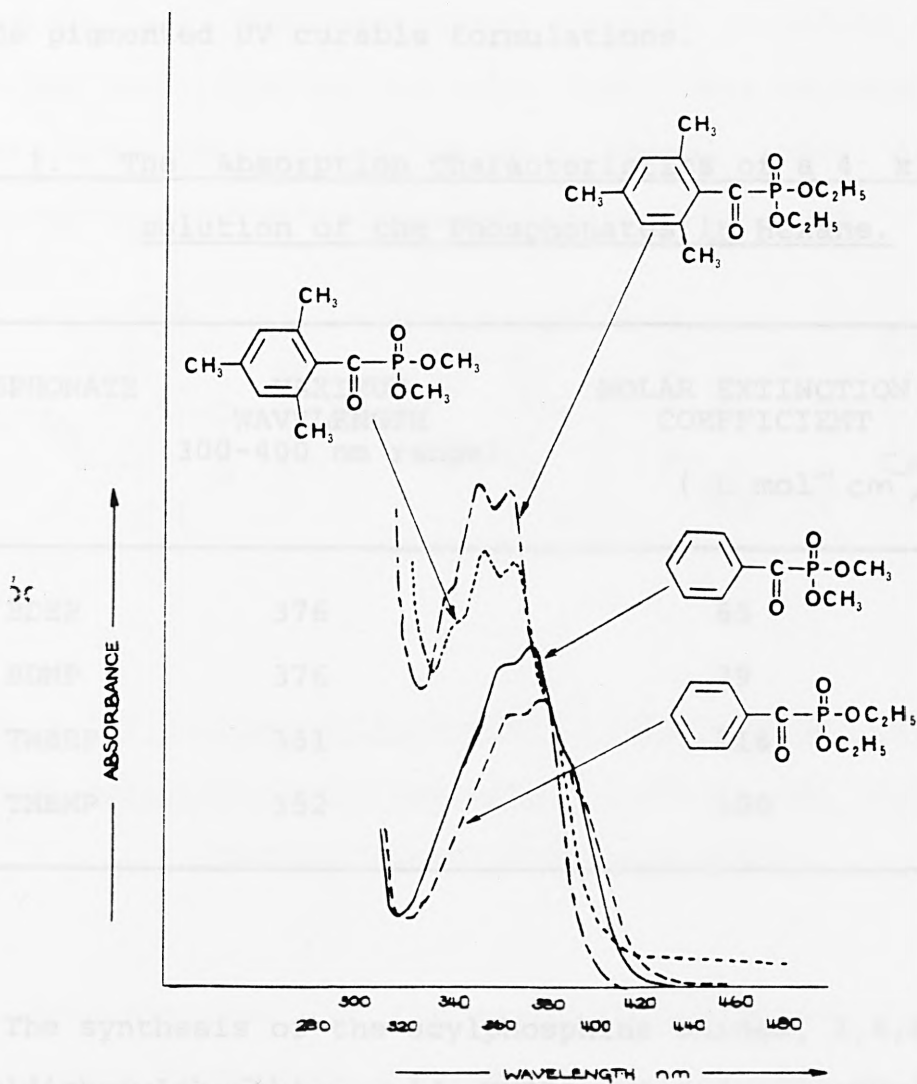


Figure 4 The absorption spectra of the benzoylphosphonates BDEP and BDMP, and the acylphosphonates TMBP and TBEP in hexane.

The UV absorption maximum of the benzoylphosphonates lies at longer wavelengths than the absorption maximum of the corresponding acylphosphonates. Despite the lower molar extinction coefficient values of the benzoylphosphonate compounds, their absorption characteristics in the 380-420 nm region extends their use as potential photoinitiators for the polymerisation of titanium

dioxide pigmented UV curable formulations.

Table 1. The Absorption Characteristics of a 4×10^{-3} mole solution of the Phosphonates in Hexane.

PHOSPHONATE	MAXIMUM WAVELENGTH (300-400 nm range)	MOLAR EXTINCTION COEFFICIENT ($\text{L mol}^{-1} \text{cm}^{-1}$)
BDEP	376	65
BDMP	376	79
TMBEP	351	116
TMBMP	352	100

The synthesis of the acylphosphine oxides, 2,4,6-trimethylbenzoyldiphenylphosphine oxide TMBPO, 2,4,6-trimethylpivaloyldiphenylphosphine oxide PDPO, and 2,6-dimethoxybenzoyldiphenylphosphine oxide, DMBPO (Figure 5) by the reaction of carboxylic acid chlorides with diphenylmethylphosphinite, produced low melting point solids via a Michaelis-Arbusov rearrangement. The phosphine oxides TMBPO and DMBPO are pale yellow crystalline solids with melting points of $79.3^{\circ} - 80.8^{\circ} \text{C}$ and $127.5^{\circ} - 127.9^{\circ} \text{C}$ respectively, and PDPO a colourless waxy solid (m.pt., $112.5^{\circ} - 114.9^{\circ} \text{C}$) [12]. The preparation of the acylphosphine oxides was relatively straight forward, although the crystallisation of TMBPO from the very viscous waxy oil of its unpurified state was often tedious.

Both TMBPO and DMBPO exhibited adequate stability during the investigations. PDPO on the other hand, was extremely sensitive to moisture and air and had to be stored under dry nitrogen conditions and recrystallised each time before use.

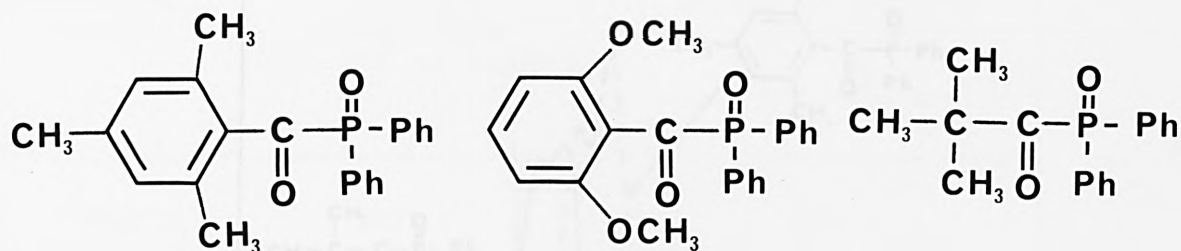


Figure 5.2,4,6-trimethylbenzoyldiphenylphosphine oxide, 2,4,6-trimethylpivaloyldiphenylphosphine oxide, and 2,6-dimethoxybenzoyldiphenylphosphine oxide.

Identification of the acylphosphine oxides by the usual spectroscopic techniques and comparisons of their melting points against those published in the literature [12] are presented in the experimental section. The UV absorption spectra for TMBPO and PDPO are shown in Figure 6. TMBPO absorbs UV radiation at longer wavelengths than PDPO, and therefore should be more suitable as a photoinitiator for the polymerisation of titanium dioxide pigmented systems. TMBPO also absorbs a more substantial amount of UV radiation than PDPO and the phosphonates, as shown by its much higher molar extinction coefficient (Table 2). The superior absorption characteristics of TMBPO compared to the phosphonates and the other phosphine oxides can be seen from a comparison of

Figures 4 and 6, and Tables 1 and 2.

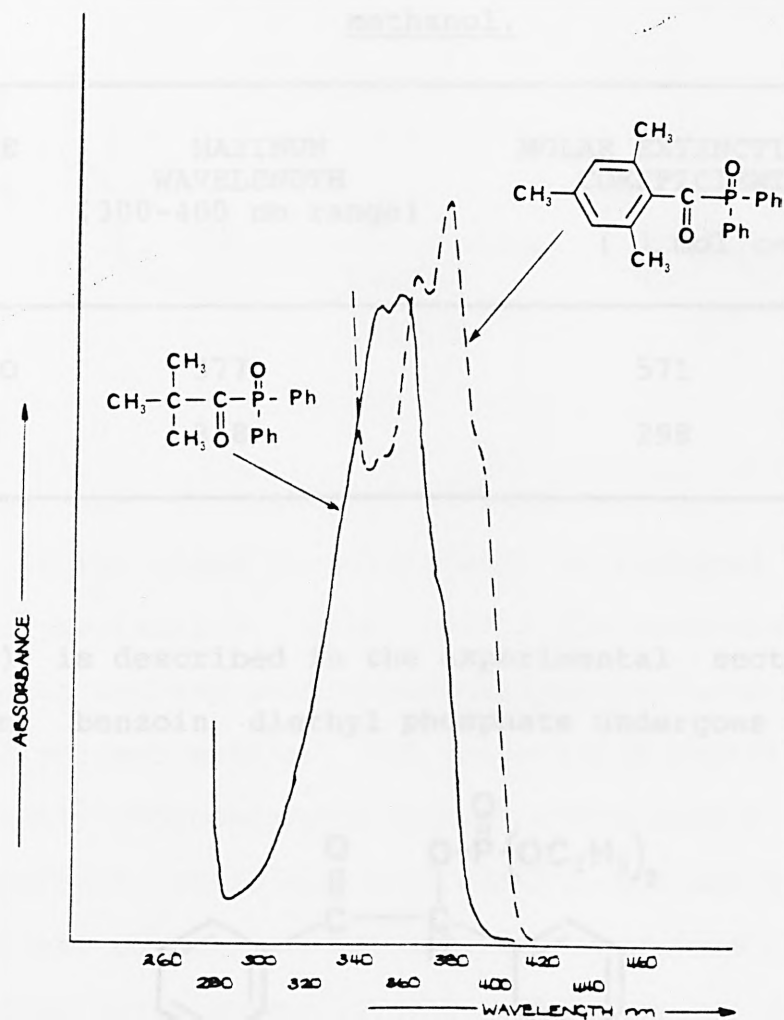


Figure 6 The absorption spectra of TMBPO and PDPO in methanol.

Benzoin and its derivatives, as discussed previously in Chapter 1, were amongst the early patented commercial photoinitiators. The preparation of a benzoin derivative containing a phosphorus moiety was therefore an obvious choice for a new novel photoinitiator. The preparation of benzoin diethyl phosphate [16]

Table 2. The Absorption Characteristics of a 1.2×10^{-3} mole solution of TMBPO and a 2.0×10^{-3} mole solution of PDPO in methanol.

PHOSPHINE OXIDE	MAXIMUM WAVELENGTH (300-400 nm range)	MOLAR EXTINCTION COEFFICIENT ($\text{L mol}^{-1} \text{cm}^{-1}$)
TMBPO	377	571
PDPO	358	298

(Figure 7) is described in the experimental section. Upon UV irradiation, benzoin diethyl phosphate undergoes intramolecular

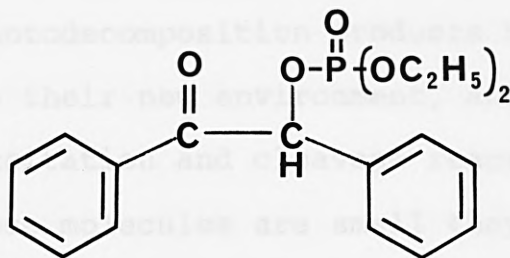
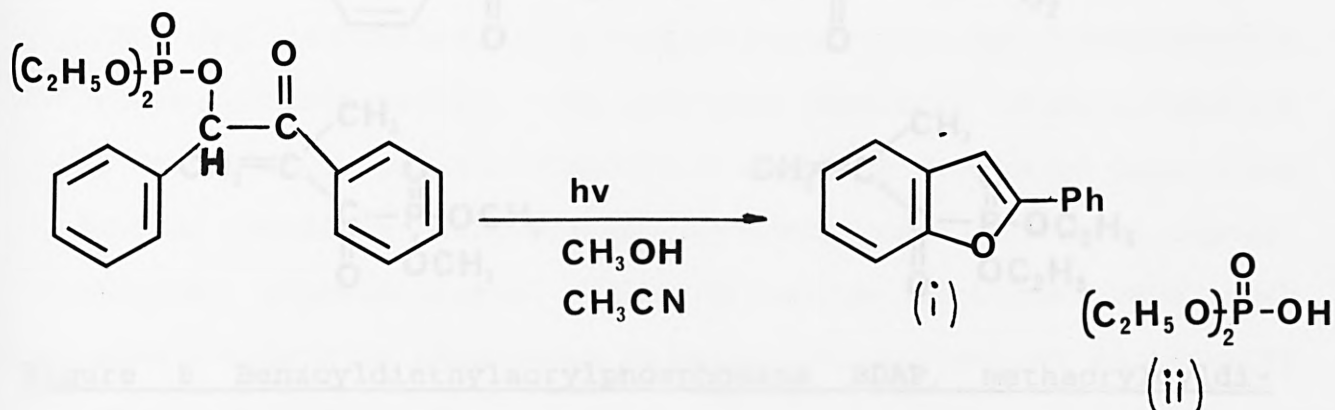


Figure 7 Benzoin diethyl phosphate.

rearrangement to give exclusively 2-phenylbenzo[b]furan (i) via an excited triplet state [17] and diethyl phosphate (ii), see Scheme 3. The absence of free radical species to initiate the polymerisation of UV curable formulations terminated further investigation of this compound.

SCHEME 3.



During the UV curing of surface coatings, only a small proportion of the added photoinitiator is consumed in the course of photopolymerisation. This leaves the remaining unconverted photoinitiator and any photodecomposition products trapped in the crosslinked polymer matrix. The unconverted photoinitiator molecules and their photodecomposition products have a low molecular weight compared to their new environment, and are also susceptible to further excitation and cleavage reactions upon UV radiation. Because these molecules are small they can diffuse through the polymer matrix towards the film surface. Migrated photoinitiator molecules and their photodecomposition products accumulated at the film surface will affect the surface coating properties, which can lead to a reduction in the coating's surface appearance. With this problem in mind, unsaturated carbonyl compounds containing a phosphorus moiety were prepared as potential copolymerisable photoinitiators. Three photoinitiators were synthesised, these were benzoyldiethylacrylphosphonate BDAP, methacryloyldimethylphosphonate MADMP, and methacryloyl-

diethylphosphonate MADEP (Figure 8).

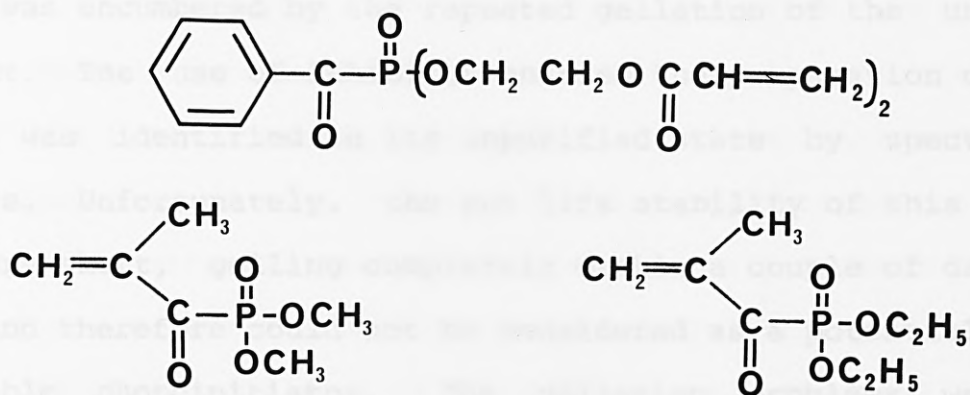


Figure 8 Benzoyldiethylacrylphosphonate BDAP, methacryloyldimethylphosphonate MADMP, and methacryloyldiethylphosphonate MADEP.

The expected advantages of this type of compound would be little, if no, migration of small molecules, either photoinitiator or decomposition products to the film surface. On account of the reactivity of free radical species towards chromophores, the probability of radical attack and combination reactions, therefore crosslinking reactions, is more likely than migration of the free radical species and small molecules to the film surface. The overall result expected would be a stabilisation of the small molecules, thus greatly retarding their migration to the film surface. These unsaturated phosphonates were prepared by the Michaelis-Arbusov reaction of trialkylphosphites with unsaturated acid chlorides, such as methacryloyl chloride [11,18].

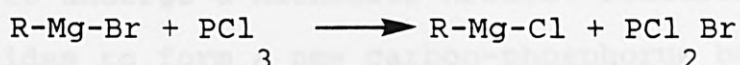
The synthesis of the copolymerisable phosphonate compounds was not entirely successful. The preparation of tris(2-acryloyloxyethyl)phosphite as a starting material for the synthesis of

BDAP was encumbered by the repeated gellation of the unpurified product. The use of inhibitor enabled the preparation of BDAP, which was identified in its unpurified state by spectroscopic methods. Unfortunately, the pot life stability of this compound was very short, gelling completely within a couple of days. This compound therefore could not be considered as a potential copolymerisable photoinitiator. The gellation problems were most probably caused by phosphorus trichloride, present as an impurity from the synthesis of tris(2-acryloyloxyethyl)phosphite, (purification of BDAP had not been perfected). Phosphorus trichloride can add to unactivated olefins by a free radical process analogous to the addition of phosphinyl radicals [9,13]. Thus the phosphorus trichloride impurities present in the product mixture most probably led to the gellation of BDAP.

During the synthesis of MADMP and MADEP [11] a large number of products were formed. Alternative preparation procedures did not reduce this number. Size exclusion chromatography techniques identified the products as low molecular weight monomeric materials. The results of subsequent HPLC analysis showed that the large number of products formed would make separation and purification very difficult, if not impossible. On this basis, further preparations and investigations were shelved. The large number of products formed most probably occurred as a result of nucleophilic attack by the phosphite at a number of possible sites, including the electron deficient centres on methacryloyl chloride. Nucleophilic attack at different sites would lead inevitably to a number of different products.

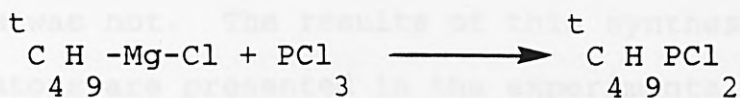
The sensitivity of the acylphosphine oxides and phosphonates to moisture and air [4,6,14], undergoing decomposition to the benzoic acid and phosphinic acid derivatives, led to the preparation of a di-tertiary-butyl-methylphosphinite moiety as a starting material for the synthesis of a new phosphine oxide photoinitiator. The presence of two tertiary butyl groups attached to the phosphorus atom of phosphate esters produced profound steric hindrance towards nucleophilic attack at the phosphorus atom [19,20]. Thus the presence of tertiary butyl groups as part of the phosphorus moiety of a photoinitiator might be expected to reduce the possibility of nucleophilic attack on the phosphorus atom by water and other small nucleophiles.

The new carbon-phosphorus bond was generated via a Michaelis-Arbusov reaction. Chloro-di-tertiary-butyl phosphine was prepared via a Grignard reaction [21-24] and then reacted with either alkoxides [19] or with alcohol and an excess of tertiary amine [20], to produce the phosphinites. The di-tertiary-butylphosphinites are reactive compounds despite their bulky tertiary-butyl groups [20]. A good yield of pure product was expected because of the tertiary alkyl group and the Grignard reagent used (R-Mg-Cl) which would prevent an exchange reaction occurring in competition.

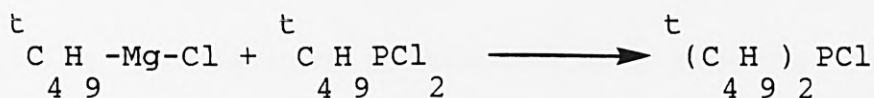


Carrying out the reaction at low temperatures of -25° to -30° C with a mole ratio of 2:1, Grignard to PCl_3 respectively was

expected to produce yields greater than 70%. With tertiary butyl groups, the reaction proceeds as follows:



Substitution of the second chloride atom occurs at room temperature.



Steric factors play an important role by lowering the substitution rate of the second chlorine, and their influence upon the substitution of the third chlorine is so great that the reaction stops under these conditions at the chloro-di-tertiarybutylphosphine stage. The preparation of these compounds, presented in the experimental section, was abandoned after several attempts to produce adequate yields of pure product for the synthesis of photoinitiator molecules.

Cyclic phosphites [25] were prepared as possible starting materials for the synthesis of new novel photoinitiators. Cyclic phosphites, of the alkoxy-dioxaphospholane type, exhibit properties typical of trialkylphosphites, therefore they could be expected to undergo a Michaelis-Arbusov reaction with carboxylic acid chlorides to form a new carbon-phosphorus bond. Glycol alkyl phosphites were prepared by the reaction of phosphorus trichloride on ethylene glycol forming 2-chloro-1,3,2-

dioxaphospholane, followed by alcoholysis in the presence of N-ethylmorpholine [25-27]. The synthesis of 2-chloro-1,3,2-dioxaphospholane was completed successfully, but unfortunately the alcoholysis was not. The results of this synthesis and the other photoinitiators are presented in the experimental section.

The mass spectra were recorded on a Finnegan MAT 312 (EI) and MAT (CI), respectively.

Melting points were determined on a melting point microscope (Zeiss, equipped with a Mettler 30 Hot Stage and PF 80 Processor) and are corrected.

HPLC analysis was performed on a Waters Modular Liquid Chromatography System equipped with Model 5000 A pumps and the Wisp 710 B Automatic Sample Processor. System control, quantification, and reporting was carried out by the Waters 845 Chromatography Station. A Kratos Spectroflow 757 UV absorbance detector (variable wavelength) was used. All separations were carried out on a Chrompack RP-S column, particle size 10 μ m, 250 x 4 mm.

8) Synthesis

Benzoyldiethylphosphonate, 90EP [11]

Method

38.21g (0.23 moles) of triethylphosphite was slowly added dropwise over a period of 30 minutes to a solution of 30.92g (0.22 moles) of benzoyl chloride in 70 cm³ of dry ether under nitrogen at 0 C. Following the addition of the phosphite, the

EXPERIMENTAL

A) Instrumentation

The ¹H NMR spectra were recorded on a Bruker WH-270 spectrometer using tetramethylsilane as internal standard.

The mass spectra were recorded on a Finnegan MAT 212 (EI) and MAT (CI), respectively.

Melting points were determined on a melting point microscope (Zeiss, equipped with a Mettler FP Hot Stage and FP 80 processor) and are corrected.

HPLC analysis was performed on a Waters Modular Liquid Chromatography System equipped with Model 6000 A pumps and the Wisp 710 B Automatic Sample Processor. System control, quantification, and reporting was carried out by the Waters 840 Chromatography Station. A Kratos Spectroflow 757 UV absorbance detector (variable wavelength) was used. All separations were carried out on a Chrompack RP-8 column, particle size 10 μ m, 250 x 4 mm.

B) Synthesis

Benzoyldiethylphosphonate, BDEP [11]

Method

38.21g (0.23 moles) of triethylphosphite was slowly added dropwise over a period of 60 minutes to a solution of 30.92g (0.22moles) of benzoyl chloride in 70 cm³ of dry ether under nitrogen at 0 C. Following the addition of the phosphite, the

reaction mixture was allowed to warm up to room temperature with continuous stirring. The mixture was stirred overnight under a stream of nitrogen. The excess solvent was removed over a steam bath under a stream of nitrogen and the product residue was fractionally distilled. The distilled product was a pale green liquid with a boiling point of 124 °C - 126 °C at 0.3mm Hg.

Theoretical yield	52.29g
Product yield	38.24g
Percentage yield	73.13%

Spectral Analysis

NMR

1.46	t (6H)	CH ₂ CH ₃
4.47	d of q (4H)	CH ₂ CH ₃
7.84	m (2H)	of phenyl
8.59	m (3H)	of phenyl

IR

1760 cm ⁻¹	C = O stretch
1250 cm ⁻¹	P = O stretch
1025 cm ⁻¹	P - O - alkyl

Absorbance Spectra

Hexane

$$\begin{aligned} \max (\pi-\pi^*) &= 253 \text{ nm} \\ \max (n-\pi^*) &= 376 - 380 \text{ nm} \\ E (n, \pi^*) &= 85 \text{ cm}^2 \text{ mol}^{-1} \end{aligned}$$

Methanol

$$\begin{aligned} \max (\pi-\pi^*) &= 226 \text{ nm} \\ \max (n-\pi^*) &= 360 - 364 \text{ nm} \\ E (n, \pi^*) &= 67.81 \text{ cm}^2 \text{ mol}^{-1} \end{aligned}$$

CHN Elemental Analysis

	Found	Theory	Difference
%C	53.64	54.54	-0.90
%H	6.50	6.24	0.24

Benzoyldimethylphosphonate, BDMP [11]

Method

35.97g (0.29 moles) of trimethylphosphite was added slowly dropwise over a period of 60 minutes to a solution of 36.55g (0.26 moles) of benzoyl chloride in 70 cm³ of dry ether under nitrogen at 0 C. Following the addition of the phosphite, the reaction mixture was allowed to warm up to room temperature, with continuous stirring. The mixture was stirred overnight under a stream of nitrogen, and the excess solvent removed over a steam bath under a stream of nitrogen. The product residue was fractionally distilled, producing a pale yellow liquid with a boiling point of 106 C - 109 C at 0.1mm Hg.

Theoretical yield 55.68g

Product yield 48.15g

Percentage yield 86.48%

Spectral analysis

NMR

4.04	d (6H)	-OCH ₃
7.81	m (3H)	of phenyl
8.52	m (2H)	of phenyl

IR

1760	cm ⁻¹	C = O stretch
1250	cm ⁻¹	P = O stretch
1025 - 1050	cm ⁻¹	P - O - alkyl

Absorbance Spectra

Hexane

max ($\pi-\pi^*$)	=	255 nm
max (n- π^*)	=	375 - 378 nm
E (n, π^*)	=	81 cm ² mol

Methanol

max ($\pi-\pi^*$)	=	226 nm
max (n- π^*)	=	358 - 363 nm
E (n, π^*)	=	53.6 cm ² mol

2,4,6-Trimethylbenzoyldimethylphosphonate, TMBMP [12]

Method

10.6g (0.085 moles) of trimethylphosphite was slowly added dropwise to 14.8g (0.081 moles) of 2,4,6-trimethylbenzoyl chloride stirring continuously under nitrogen at 20 °C. The mixture was heated over an oil bath for about one hour between 70 -

80 °C with continuous stirring under nitrogen.

The colourless product was vacuum distilled using an air condenser, and had a boiling point of 116 - 120 °C at 0.15 mm Hg, and a melting point of 47.7 - 49.2 °C.

Product Yield	13.59g
Theoretical Yield	20.75g
Percentage Yield	65.5%

Absorbance Spectra

Methanol

$$\begin{aligned} \max (n-\overline{\nu}) &= 350 \text{ nm} \\ E (n, \overline{\nu}) &= 125 \text{ cm}^2 \text{ mol}^{-1} \end{aligned}$$

The Mass Spectrum is shown below in Figure 9.

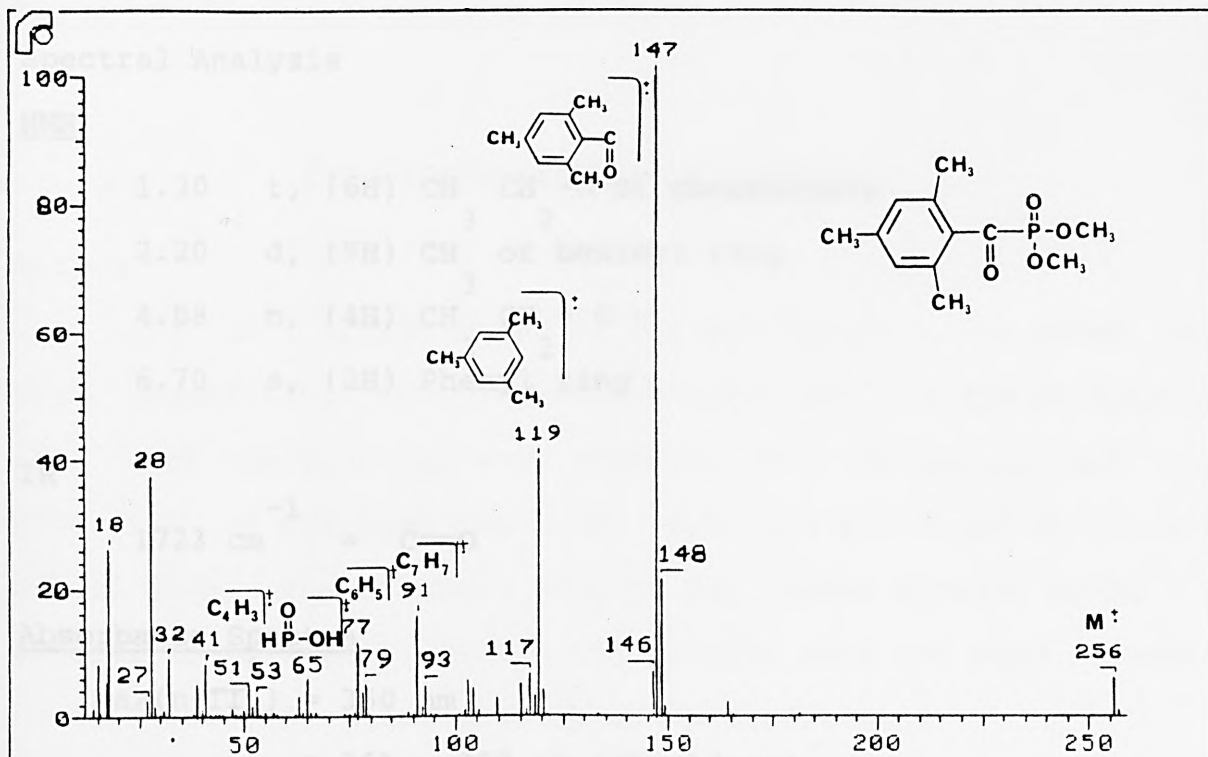


Figure 9 The mass spectrum of TMBMP

2,4,6-Trimethylbenzoyldiethylphosphonate, TMBEP [12]

Method

11.5g (0.069 moles) of triethylphosphite was slowly added dropwise over a period of about 20 minutes to 12g (0.065 moles) of 2,4,6-trimethylbenzoyl chloride stirring continuously under nitrogen. The mixture was heated to an oil bath temperature of 80 °C for about 1 hour. The faint green coloured product was distilled under vacuum and had a boiling point of 204 - 206 °C at 0.35 mmHg.

Product Yield	15.33g
Theoretical Yield	18.48g
Percentage Yield	82.95%

Spectral Analysis

NMR

1.30	t, (6H)	CH ₃	CH ₂	-O of phosphonate
2.20	d, (9H)	CH ₃		of benzoyl ring
4.08	m, (4H)	CH ₃	CH ₂	- O -
6.70	s, (2H)			Phenyl ring

IR

$$1723 \text{ cm}^{-1} = \text{C}=\text{O}$$

Absorbance Spectra

$$\max(n-\overline{\pi})^* = 350 \text{ nm}$$

$$= 361 - 363 \text{ nm (shoulders)}$$

$$(n-\overline{\pi})^* = 90.91 \text{ cm}^2 \text{ mol}^{-1}$$

The absorption spectrum of this compound is shown in Figure 4.

The Mass Spectrum is shown below in Figure 10.

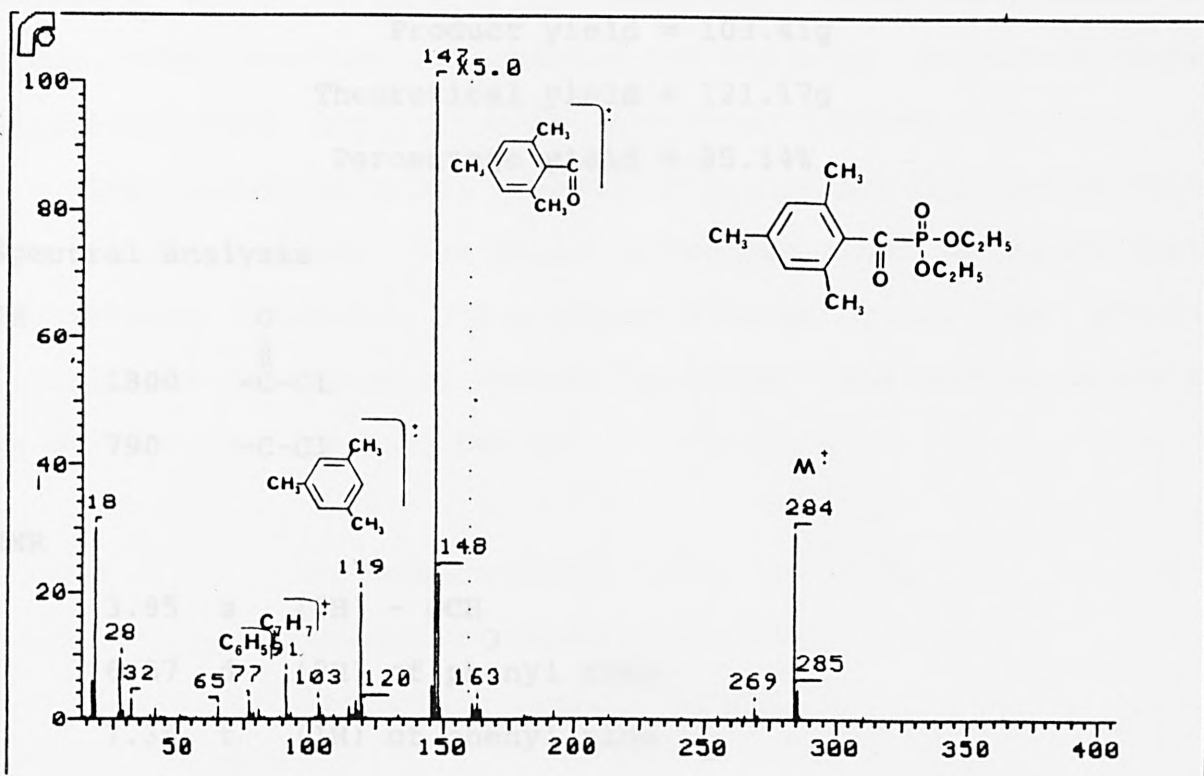


Figure 10 The mass spectrum of TMBEP

2,6-Dimethoxybenzoyl chloride

Method

The synthesis of diethyl 2,6-dimethoxybenzoyl phosphite was performed in 3
 175 cm³ (2.399 mols) of thionyl chloride was added drop-
 wise, carefully, to 110g (0.604 mols) of 2,6-dimethoxybenzoic
 acid. The reaction was very vigorous with the concomitant rapid
 evolution of hydrogen chloride. When the evolution of fumes had
 slowed down, the reaction mixture was heated between 80-85 c for
 several hours, until all of the benzoic acid had been converted
 to acid chloride (monitored by IR spectroscopy).

The product was carefully distilled under high vacuum using
 an air condenser. The boiling point of the product was between

111-114 °C at 0.5mm Hg.

Product yield = 103.41g

Theoretical yield = 121.17g

Percentage yield = 85.34%

Spectral analysis

IR

1800	$\begin{array}{c} \text{O} \\ \\ -\text{C}-\text{Cl} \end{array}$
790	$-\text{C}-\text{Cl}$

NMR

3.85	s	(6H) - OCH ₃
6.57	d	(2H) of phenyl ring
7.35	t	(1H) of phenyl ring

Diphenylmethylphosphinite

Method

The synthesis of diphenylmethylphosphinite was performed in a 3 necked flask fitted with a magnetic stirrer, thermometer, reflux condenser and dropping funnel, under dry nitrogen conditions. 180 cm³ (1.1 moles) of N,N-diethylaniline, 67 cm³ (2.0 moles) of methanol and 1350 cm³ petroleum ether (boiling range 40-60 °C) were stirred continuously under dry nitrogen conditions between 0 ° and -4 °C for about 15 minutes.

To this mixture, 225g (1.02 moles) of chlorodiphenylphosphine dissolved in 220 cm³ of petroleum ether (boiling range 40-60 °C) was added dropwise over a period of 70 minutes) with continuous stirring. This addition was carried out under nitrogen and

between 0° and -4° C. During this addition a white precipitate was formed. The ice bath was removed and stirring continued under nitrogen at room temperature for a further 2 hours.

The precipitate was removed by filtration and washed with more petroleum ether. The excess petroleum ether in the filtrate was removed carefully on a rotary evaporator and the residue obtained was subsequently vacuum distilled. The boiling point of the product was 149° C at 6mm Hg.

Product Yield = 152.35g

Theoretical Yield = 201.29g

Percentage Yield = 75.69%

NMR

3.2 - 3.35 (s) split into a doublet by ³¹P, (3H) of OCH₃
6.68 - 6.98 (m) (10H) of phenyl rings

2,6-Dimethoxybenzoyldiphenylphosphine oxide, DMBPO [12]

Method

32.4g (0.15 moles) of diphenylmethylphosphinite was added dropwise over a period of about 50 minutes to a solution of 2,6-dimethoxybenzoyl chloride in toluene (30ml) stirring continuously between 50-55° C. Stirring at 50° was continued for 3 hours after the addition of the diphenylmethylphosphinite. The reaction mixture almost completely solidified. The reaction mixture was cooled, and the solid product filtered, washed with a little cold

toluene followed by pentane.

Drying under vacuum afforded 49.8 g (m.pt., 118.5 - 120 ° C) of the product. The product was recrystallised from toluene (160 cm³)/cyclohexane (100 cm³) and gave pale yellow crystals, with a melting point of 119.7 - 120.3 ° C. Cooling and remelting gave a melting point of 127.5 - 127.9 ° C.

Product Yield = 47.30g

Theoretical Yield = 54.96g

Percentage Yield = 86.06%

Spectral analysis

NMR

- 3.70 s (6H) o,o-OCH₃
- 6.63 d (2H) m, H on 2,6-dimethoxybenzoyl
- 7.50 t (1H) p, H on 2,6-dimethoxybenzoyl
- 7.68 m (6H) o,p of phenyl,
- 8.05 m (4H) o,p of phenyl

IR

- 2855 -OCH₃
- 1685 C = O
- 1600 AR, Ph
- 1445 P - Ph
- 1265 P = O

2,4,6-Trimethylbenzoyl chloride

Method

74g (0.622 moles) of thionyl chloride, was added dropwise with care and continuous stirring, to 26g (0.155 moles) 2,4,6-trimethylbenzoic acid, with the vigorous evolution of hydrogen chloride. When the effervescence had stopped, the reaction mixture was heated over an oil bath between 70 - 80 °C until complete conversion of the benzoic acid to the acid chloride had occurred (monitored by IR spectroscopy), and all of the hydrogen chloride had been driven off. The brown residue was distilled affording a product at 115 °C and 15 mm Hg.

Product Yield 27.40g at 15 mm Hg (115 °C)

Theoretical Yield 28.31g

Percentage Yield 96.78%

2,4,6-Trimethylbenzoyldiphenylphosphine Oxide, TMBPO [12]

Method

18.4g (0.085 moles) of diphenylmethylphosphinite was added dropwise over a period of 20 minutes to 15.5g (0.085 moles) of 2,4,6-trimethylbenzoyl chloride stirring continuously between 50 - 55 °C under nitrogen. Following the addition of the phosphine, stirring at 50 °C was continued for 5 hours. The reaction mixture was cooled to 30 °C and dissolved in ether. Pentane was then added until the first visible turbidity.

Cooling afforded 20.9 g of product, with a melting point of 78.5 - 81 °C. This was dissolved in boiling ether (75 cm³) and

pentane (80 cm³) was added. Seeding and cooling slowly afforded 18 g (61% yield), with a melting point of 79.3 - 80.8 °C.

NMR

8.05 - 7.97 m (5H) phenyl

7.60 - 7.46 m (5H) phenyl

6.82 s (2H) m, m-H in 2,4,6-trimethylbenzoyl

2.25 s (3H) p - CH₃ in 2,4,6-trimethylbenzoyl

2.04 s (3H) o,o - CH₃ in 2,4,6-trimethylbenzoyl

IR

1655 C = O

1445 P - Ph

1305 P = O

Absorption Spectra

Hexane

max (n- π^*) = 380 nm

= 365, 395 nm (shoulders)

E (n, π^*) = 547.5 cm² mol

Methanol

max (n- π^*) = 377 nm

= 363 (shoulders)

E (n, π^*) = 570.8 cm² mol

Elemental (CHN) analysis

	Found	Theory	Difference
%C	74.82	74.98	-0.16
%H	6.17	6.29	-0.12

Pivaloyldiphenylphosphine Oxide [12]

Method

21.6g (0.1 moles) of freshly distilled diphenylmethylphosphinite was slowly added with continuous stirring to 12.03g (0.1 moles) of freshly distilled pivaloyl chloride under a continuous flow of nitrogen and ice bath conditions.

After 1 hour the mixture had completely solidified. The ice bath was removed, and the white crystalline product was filtered. The product was recrystallised in cyclohexane, seeded and left to cool slowly at room temperature. The recrystallised product had a melting point of 112.5 - 114.9 °C.

Product Yield	26.83g
Theoretical Yield	28.63g
Percentage Yield	93.71%

Absorbance Spectra

Methanol

$$\max(n-\pi^*) = 358 \text{ nm}$$

348 nm shoulder

$$E(n, \pi^*) = 298 \text{ cm}^2 \text{ mol}^{-1}$$

The Mass spectrum is shown in Figure 11.

NOTE

This product was found to be hygroscopic and decomposed over a period of 3 months.

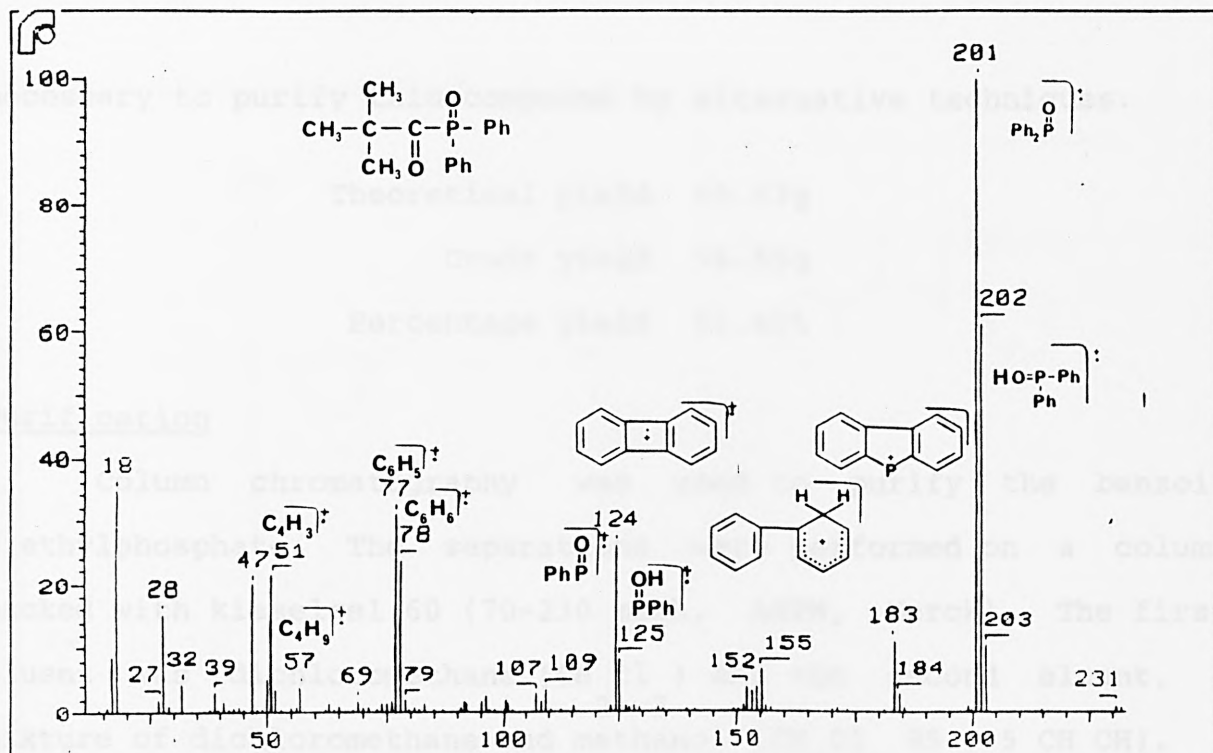


Figure 11 The mass spectrum of PDPO

Benzoin diethyl phosphate [16,17]

Method

33.6g (0.2 moles) of diethylchlorophosphate was slowly added dropwise, over a period of 2 hours to a mechanically stirred, cooled (0 C) solution of 42.46g (0.2 moles) of benzoin in 34.52g (0.4 moles) of pyridine. Following 4 additional hours of stirring at 0 C, 50 cm³ of water was added and the product extracted with 3 x 50 cm³ portions of ether. The ether layer was washed with two 50 cm³ portions of 0.5M H₂SO₄, 1 x 50 cm³ portion of 5% sodium bicarbonate, 3 x 50cm³ portions of water, 1 x 50 cm³ portion of saturated sodium chloride and then dried over MgSO₄. The ether was removed on a rotary evaporator and gave 56.85g of crude product. Distillation of the crude product under reduced pressure did not yield the pure compound. It was therefore

necessary to purify this compound by alternative techniques.

Theoretical yield 69.67g

Crude yield 56.85g

Percentage yield 81.60%

Purification

Column chromatography was used to purify the benzoin diethylphosphate. The separations were performed on a column packed with kieselgel 60 (70-230 mesh, ASTM, Merck). The first eluent was dichloromethane (CH_2Cl_2) and the second eluent, a mixture of dichloromethane and methanol (CH_2Cl_2 95 : 5 CH_3OH).

10.04g of benzoin diethylphosphate was separated on the column. 8.34g of product was obtained, but TLC analysis showed this to contain a slight impurity i.e., 2 spots, one for product one for impurity. The 8.34g of "purified" product was subjected to HPLC purification techniques. The eluent was a mixture of hexane and acetone (60:40). The removal of the impurity afforded 7g of "pure" compound.

Spectral Analysis

NMR

1.15, t, (3H) $-\text{CH}_3$ of $\text{P}-\text{O}-\text{CH}_2\text{CH}_3$

1.31, t, (3H) $-\text{CH}_3$ of $\text{P}-\text{O}-\text{CH}_2\text{CH}_3$

3.91 q split by P (2H) $-\text{CH}_2-$ of $\text{P}-\text{OCH}_2\text{CH}_3$

4.20 q split by P (2H) $-\text{CH}_2-$ of $\text{P}-\text{OCH}_2\text{CH}_3$

6.65 d (1H) $-\text{CH}-$ adjacent to phenyl ring

7.27 - 7.55 m (8H) o,m,-H of phenyl rings

7.91 d (2H) -p H of phenyl rings

The Mass spectrum is shown in Figure 12.

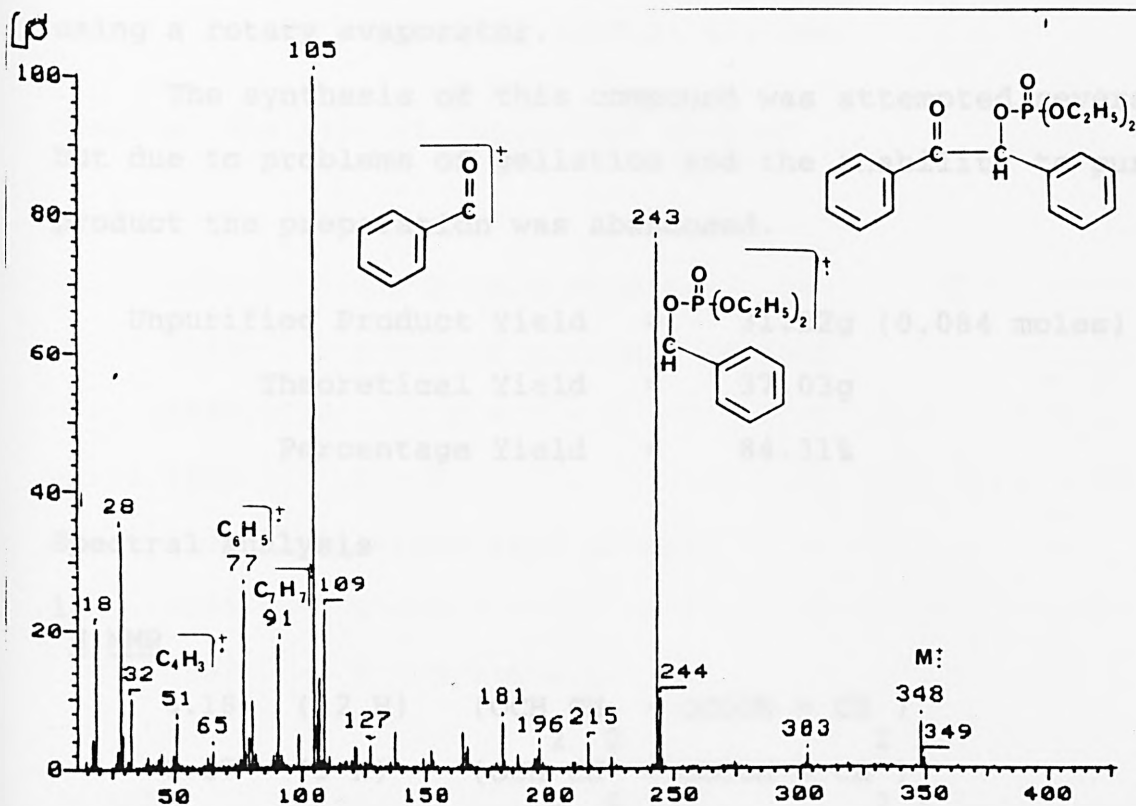


Figure 12 The mass spectrum of Benzoin diethyl phosphonate

Tris(2-acryloylethyl)phosphite

Method

To a mixture of 34.84g (0.3 moles) of 2-hydroxyethylacrylate and 30.36g (0.3 moles) of triethylamine, stirring continuously in an excess of dry diethylether between 0° and -4° c was slowly added 13.74g (0.1 moles) of phosphorus trichloride in about 50 cm³ of dry ether, over a period of about two hours. The precipitation of triethylaminehydrochloride was immediate.

The mixture was refluxed gently for 2 hours and then the precipitate was filtered off under vacuum using a sintered glass

funnel. The excess ether and triethylamine were carefully removed using a rotary evaporator.

The synthesis of this compound was attempted several times, but due to problems of gellation and the inability to purify the product the preparation was abandoned.

Unpurified Product Yield	=	31.22g (0.084 moles)
Theoretical Yield	=	37.03g
Percentage Yield	=	84.31%

Spectral analysis

1 H NMR

4.18	(12 H)	(OCH ₂ CH ₂ - OCOCH = CH ₂)
6.17	(9 H)	(OCH ₂ CH ₂ - OCOCH = CH ₂)

Benzoyldiethylacrylphosphonate [11,18]

Method

To a solution of 11.25g (0.080 moles) of benzoyl chloride in 30 cm³ of dry ether, stirring continuously under nitrogen at 0 C, was slowly added 31.22g (0.084 moles) of tris(2-acryloyl-ethylphosphite over a period of 60 minutes. The reaction mixture was stirred overnight at room temperature and the excess ether removed on a steam bath under a stream of nitrogen the following morning.

Unpurified Product Yield = 40.30 g

Theoretical Yield = 30.58 g

The yield indicates that unreacted starting materials are still present in the unpurified product mixture.

Spectral Analysis of Unpurified Product

IR

1774	C = O acid chloride
1728	C = O of carbonyl stretch
1655,1636	C = C - C = O
1620	C = C
1596, 1582, 1504	aryl(phenyl)
1298	P = O
1033	P - O - alkyl

¹H

NMR

4.46	(8H)	(OCH ₂ CH ₂ - OCOCH = CH ₂)
6.38	(6H)	(OCH ₂ CH ₂ - OCOCH = CH ₂)
7.85	(3H)	of phenyl ring
8.49	(2H)	of phenyl ring

This product and the starting material were synthesised several times, but even with inhibitor present, the reaction mixture gelled completely within 48 hours. It was therefore not possible to purify this product for further evaluation.

Methacryloyldimethylphosphonate[11,18]

Method

13.02g (0.105 moles) of trimethylphosphite was slowly added dropwise over a period of 20 minutes to a solution of 10.45g (0.1 moles) of methacryloyl chloride in 30 cm³ of sodium dried ether, stirring continuously under nitrogen at 0 °C. The reaction mixture was allowed to warm up to room temperature and was stirred overnight. The excess solvent was removed on a steam bath under a stream of nitrogen.

The reaction mixture was initially green, turning yellow on completion of the reaction.

Total crude yield = 21.00g (excess unreacted starting materials)

Theoretical yield = 17.81g

Spectral analysis on crude compound

IR

2854	-OCH ₃
1737	-CO - Cl
1695,1646	-CO - C = C
1453	-CH ₃
1268	P = O
1039	p - o - CH ₃

(see the following synthetic procedure).

Methacryloyldiethylphosphonate [11,18]

Method

15.76g (0.105 moles) of triethylphosphite was slowly added dropwise over a period of 20 minutes to a solution of 10.45g (0.1 moles) of methacryloyl chloride in 30 cm³ of sodium dried ether stirring continuously under nitrogen at 0 °C. The reaction mixture was stirred overnight at room temperature and the excess solvent removed on a steam bath under a stream of nitrogen.

The excess solvent detected on preliminary spectral analysis was removed under high vacuum, however the excess phosphite could not be removed without heating. The thermal stability of this compound was unknown so alternative purification techniques were tried.

Chromatographic purification methods were used to separate the product from unreacted starting materials. Initial TLC runs showed a large number of spots representing the different components in the mixture. Investigatory HPLC showed the reaction mixture to be composed of a number of products. Size exclusion HPLC techniques showed these products to be of low molecular weight. The number of peaks and their overlapping retention times made the separation of components a very difficult task. It was for this reason that the synthesis was postponed, pending the search for an alternative synthetic route.

Chloro-di-t-butyl phosphine [19-24]

Grignard reaction

About 10 cm³, from a total of 166.63g (1.8 moles), of 2-chloro-2-methylpropane was slowly added dropwise to a reaction flask containing 36.47g (1.5 moles) of magnesium and 375cm³ of sodium dried diethyl ether. The remaining 2-chloro-2-methylpropane was diluted in about 875cm³ of dry ether. The flask was warmed with hot water to promote the start of the reaction. The solution became cloudy after some considerable heating, finally turning a cloudy grey with gentle effervescence, which was an indication that the reaction had started. The heat was removed and the exothermic reaction was allowed to drive its own reflux. The remaining 2-chloro-2-methylpropane-ether solution was added dropwise at the same rate as the reflux, in order to maintain a gentle reaction. Following the addition of all the starting material (1.5 - 2 hours) the mixture was refluxed with stirring over a hot bath at approximately 40 °C for 2 hours, when all the magnesium had disappeared.

When the Grignard reaction mixture had been refluxed so that all of the magnesium had disappeared, 68.7g (0.5 moles) of phosphorus trichloride, diluted in dry ether, was slowly added to maintain the reaction mixture in a state of reflux, i.e., the rate of addition of the phosphorus trichloride - ether solution was equal to the rate of reflux. When all the phosphorus trichloride had been added, the reaction mixture was warmed and refluxed for 2 hours, and then left to cool slowly overnight.

The mixture was filtered several times until the filtrate obtained was clear and colourless. The clear filtrate and washings were combined and the excess ether was removed carefully on a rotary evaporator to give the product in an unpurified form.

Theoretical yield	90.48g
Unpurified yield	70.54g
Percentage yield	77.97%

To reduce problems during purification, the unpurified product was used for subsequent synthesis. 72.20g (0.4 moles) of this crude product was used to synthesise methyl-di-t-butylphosphinite directly.

Methyl-di-t-butylphosphinite [19-24]

Method

9.4g (0.4 moles) of sodium was added in small portions to 200 cm³ of methanol, to give a solution of sodium methoxide in methanol. To this solution, stirring continuously, the tertiary butylchlorophosphine synthesised previously was added slowly dropwise, over about 20 minutes, with the evolution of heat energy (temperature rose from 20 °C to 45 °C). The reaction mixture was heated under reflux for 1 hour and fractionally distilled using a 15 cm Vigreux column. The fractional distillation resulted in the total decomposition of the reaction mixture. The

synthesis was repeated several times before an alternative procedure was attempted.

Methyl-di-t-butylphosphinite [19-24] Second Preparation.

Method

13.71g (0.564 moles) of magnesium was weighed out and added to the reaction flask with 150 cm³ of sodium dried ether. About 10 cm³ of the 62.69g (0.677 moles) of freshly distilled 2-chloro-2-methylpropane was slowly added dropwise to the reaction flask. The flask was warmed with hot water to promote the start of the reaction. The solution turned a cloudy grey colour before effervescing. The heat was removed and the exothermic reaction allowed to drive its own reflux. The remaining 2-chloro-2-methylpropane in about 350 cm³ of dry ether was added. The rate of addition was such as to maintain a steady rate of reflux.

After all the reactants had been added (3/4 - 1 hour) the mixture was refluxed, with stirring, over a hot bath at approx 40 C for 2 hours, when all the magnesium had disappeared. When the Grignard synthesis was complete, 25g (0.188 moles) of methoxydichlorophosphine (Cl POCH₃) diluted in 100 cm³ of dry ether was added, so that the reaction mixture remained in a steady state of reflux. This reaction was very violent and the ether boiled off continually and had to be replaced throughout the synthesis. Once the addition of starting materials was complete, the reaction mixture was refluxed for a further 2

hours. The mixture was allowed to cool slowly to room temperature and stand under nitrogen overnight.

The mixture was filtered the following morning, until the filtrate was clear and colourless. The excess ether was removed by distillation. The remainder was distilled under reduced pressure. Fractional distillation was performed twice, resulting in the third and final fraction being retained as product. The product boiling point was 48 - 50 °C at 8 mb pressure and the yield was 27.69g.

NMR

2 peaks at 1.12 Hz and 1.24 Hz (12 Hz separation) were recorded. To determine whether the two peaks belong to a doublet or two singlets the coupling constants were measured using both the 100 MHz and 60 MHz NMR spectrometers. To improve the accuracy, each spectrum was expanded and the coupling constants remeasured.

60 MHz	Normal 12 Hz;	Expanded 12.4 Hz.
100 MHz	Normal 12 Hz;	Expanded 11.6 Hz

Therefore the phosphorus atom has coupled to a H atom and split the expected singlet for CH into a doublet. The sample was submitted for elemental analysis.

CHN Elemental Analysis

	Found	Theory	Difference
%C	49.18	53.11	-4.0
%H	9.57	10.04	-0.47

2-Chloro-1,3,2-dioxaphospholane [11,25-27]

Method

500 cm³ of dichloromethane and 220 cm³ (2.5 moles) of phosphorous trichloride were added to 139 cm³ (2.5 moles) of ethylene glycol with continuous stirring at such a rate that gentle refluxing took place with the concomitant evolution of hydrogen chloride.

The dichloromethane was distilled off over a steam bath and the residue distilled under reduced pressure.

Theoretical yield = 104.4g

Actual yield = 90.55g

Percentage yield = 85.03%

Boiling point = 46^o C at 12 mm Hg.

Theoretical boiling point = 45.5 - 47^o C at 15 mm Hg

[11,25-27].

The mass spectrum of this compound is shown in Figure 13.

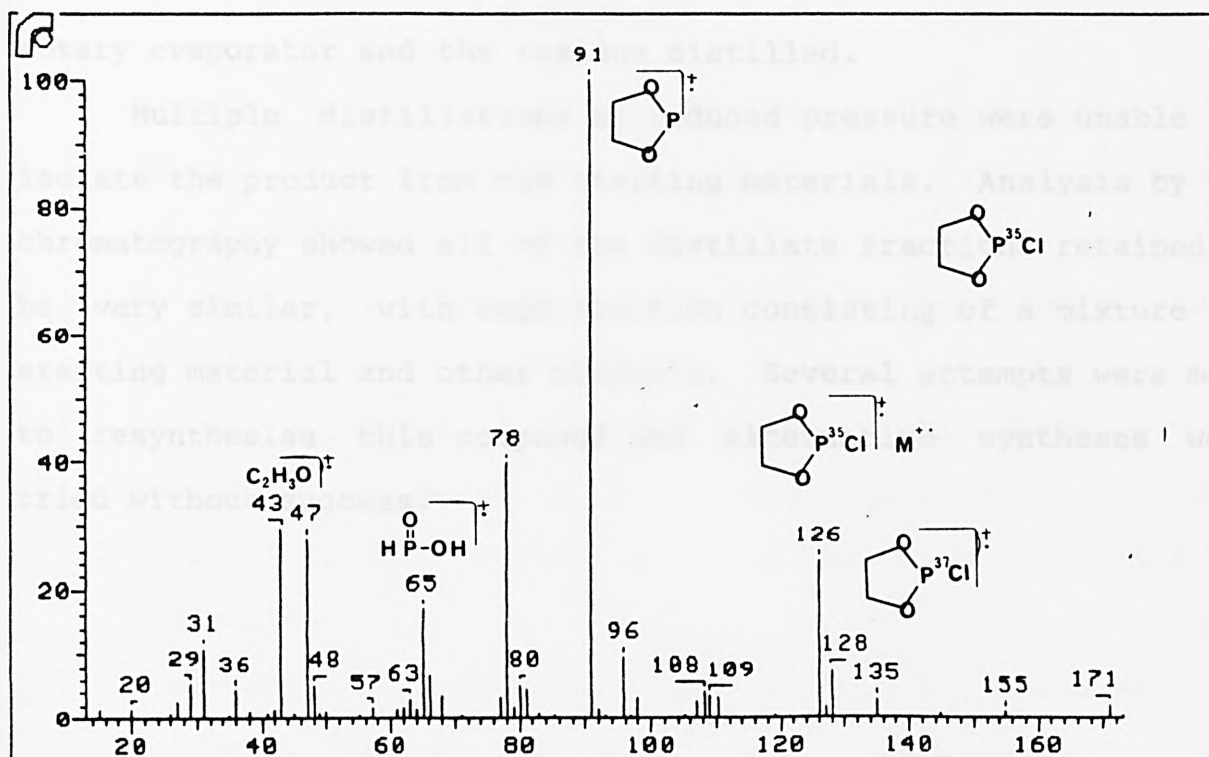


Figure 13 The mass spectrum of 2-chloro-1,3,2-dioxaphospholane.

2-Methoxy-[1,3,2]-dioxaphospholane [11,25-27]

Method

18 cm³ (0.11 moles) of N,N-diethylaniline, 7 cm³ (0.165 moles) of methanol and 150 cm³ of petroleum ether (boiling range 40-60 °C) were mixed together and stirred over an ice bath under a flow of nitrogen at a temperature between -4 °C and 0 °C.

13g (0.1 mole) of 2-chloro-1,3,2-dioxaphospholane in 50 cm³ of petroleum ether was added dropwise to this stirring mixture with the immediate formation of a precipitate. The ice bath was removed and stirring continued for another two hours at room temperature. The precipitate was removed by filtration and washed with more pet ether. The excess petroleum ether was removed on a

REFERENCES

rotary evaporator and the residue distilled.

Multiple distillations at reduced pressure were unable to isolate the product from the starting materials. Analysis by GLC chromatography showed all of the distillate fractions retained to be very similar, with each fraction consisting of a mixture of starting material and other products. Several attempts were made to resynthesise this compound and alternative syntheses were tried without success.

[66] G. W. G. Wilson, *J. Org. Chem.*, 1966, 3304-3305.

[67] Berlin, R. D., Taylor, R. A., *J. Am. Chem. Soc.*, 1964, 86, 3863-3866.

[71] Sumiyoshi, T., Schnabel, W., Henne, A., Lechtken, F., *Polymer*, 1985, 26, 141-146.

[81] Sumiyoshi, T., Schnabel, W., *Makromol. Chem.*, 1985, 186, 1811-1823.

[91] Benfrode, W. G., *Free Radicals*, Vol. 12, P. 8., 1973, Chapter 23 395-663, J. Wiley New York, Edited by Fieser.

[101] Ackerman, B., Jordan, T. A., Eddy, C. W., *Trans. R. Soc. Lond. Chem. Soc.*, 1956, 78, 6025-6027.

[111] Harner, R. S., Snyder, D., *J. Org. Chem.*, 1971, 36(1), 128-138.

[121] DOS 2830927, (1980) (BASF AG), Lechtken, F., Bueche, I., Henne, A. DOS 2909994 (1980) (BASF AG), Lechtken, F., Bueche, I., Jacobi, W., Trimmann, W. DOS 3023886 (1980) (Bayer AG), Heine, H. G., Koblenz, H. J., Rudolph, H.

[131] Sosnovsky, G., *Free Radical Reactions in Preparative Organic Chemistry*, 1964, Chapter 5, Macmillan, New York.

[141] Sekine, M., Satoh, M., Yamada, H., Hata, T., *J. Org.*

REFERENCES

- [1] Hageman, H, J., Prog in Org Coatings., 1985, 13 123-150.
- [2] Berner, G., Kirchmayr, R., Rist, G., J. Oil Col. Chem. Assoc., 1978, 61 105-113.
- [3] Terauchi, K., Sakurai, H., Bull. Chem. Soc. Japan., 1969, 42 821-823.
- [4] Jacobi, M., Henne, A., J. Rad Curing., 1983, 16-25.
- [5] Berlin, K, D., Burpo, D, H., J. Org Chem., 1966, 1304-1306.
- [6] Berlin, K, D., Taylor, H, A., J. Am. Chem. Soc., 1964, 86 3862-3866.
- [7] Sumiyoshi, T., Schnabel, W., Henne, A., Lechtken, P., Polymer., 1985, 26 141-146.
- [8] Sumiyoshi, T., Schnabel, W., Makromol. Chem., 1985, 186 1811-1823.
- [9] Bentrude, W, G., Free Radicals, Vol. II, J, K., 1973, Chapter 22 595-663, J. Wiley New York, Edited by Kochi.
- [10] Ackerman, B., Jordan, T, A., Eddy, C, R., Swern, D., J. Am. Chem. Soc., 1956, 78 6025-6027.
- [11] Marmor, R, S., Seyferth, D., J. Org. Chem., 1971, 36(1) 128-136.
- [12] DOS 2830927, (1980) (BASF AG), Lechtken, P., Buethe, I., Hesse, A. DOS 2909994 (1980) (BASF AG), Lechtken, P., Buethe, I., Jacobi, M., Trimborn, W. DOS 3023486 (1980) (Bayer AG), Heine, H, G., Rotenkranz, H, J., Rudolph, H.
- [13] Sosnovsky, G., Free Radical Reactions in Preparative Organic Chemistry, 1964, Chapter 5, MacMillan, New York.
- [14] Sekine, M., Satoh, M., Yamagata, H., Hata, T., J. Org.

Chem., 1980, 45 4162-4167.

- [15] Terauchi, K., Sakurai, H., Bull. Chem. Soc. Japan., 1970, 43 883-890.
- [16] Givens, R, S., Personal Communication.
- [17] Givens, R,S., Matuszewski, B., J. Am. Chem. Soc., 1984, 106 6860-6861.
- [18] Szpala, A., Tebby, J, C., Griffiths, D, V., J. Chem. Soc., Perkin Trans. I., 1981, 1363-1366.
- [19] Stewart, A, P., Trippett, S., J. Chem. soc., 1970, 1263-1266.
- [20] Dahl, O., J. Chem. Soc., Perkin Trans. I., 1978, 947-954.
- [21] Voskuil, W., Arens, J, F., Recueil, 1963, 82 302-304.
- [22] Scherer, O, J., Schieder, G., Chem. Ber., 1968, 101 4184-4198.
- [23] Dombek, B, D., J. Organometal. Chem., 1979, 169 315-325.
- [24] Fild M., Inorg. Synth., 1973, 14 6-9.
- [25] Lucas, H, J., Mitchell, F, W., Scully, C, N., J. Am. Chem. Soc., 1984, 106 6860-6861.
- [26] Schenck, G, O., Koltzenburg, G., Grossmann, H., Angew. Chem., 1957, 69(5) 177-178.
- [27] Anschutz, L., Broecker, W., Chem. Ber., 1928, 61 1264-1265.

Chapter 3

Photoinduced Cleavage of Acylphosphine Oxides

Chapter 3	Photoinduced Cleavage of Acylphosphine Oxides	
	Introduction	118
	Detection of Free Radical Species	121
	Chemically Induced Dynamic Electron Polarisation (CIDEP)	124
	Results and Discussion	128
	Acknowledgements	133
	Experimental	134
	Appendix A: Trapping of Primary Radicals by a Stable Nitroxyl.	136
	Results and Discussion	136
	Acknowledgements	138
	Experimental	138
	Appendix B	141
	Results and Discussion	141
	Experimental	143
	Acknowledgements	145
	Appendix C	146
	Results and Discussion	146
	Acknowledgements	148
	Experimental	149
	References	158

INTRODUCTION

During recent years a new novel class of photoinitiators were launched onto a commercial market which had an opening for compounds capable of initiating the free radical polymerisation of pigmented UV curable resins. These photoinitiators, the acylphosphine oxides and their related compounds, were claimed as effective photoinitiators for various unsaturated systems [1]. The acylphosphine oxides have a relatively strong absorption in the 300--400 nm (molar extinction coefficient value of about $600 \text{ cm}^2 \text{ mol}^{-1}$) region, which enables them to absorb UV light at the point where pigments, such as titanium dioxide, are relatively transparent. It has been claimed that the acylphosphine oxides [2, 3] and related compounds [4] readily undergo a Norrish Type I cleavage reaction in less than 300 ps from singlet states [5]. Evidence that the radicals were formed, at least to some extent, from triplet states of an estimated lifetime of $< 1 \text{ ns}$, has been deduced from studies using the technique of laser flash photolysis [2, 3, 6]. The unequivocal identification of the radicals is difficult using this technique because the absorption spectrum of the phosphorus radical is broad, relatively featureless, and is in the region of wavelength for laser excitation.

As the nature of the excited state of the photoinitiator responsible for reaction could not be identified with any degree of certainty, an attempt to record the fluorescent spectra of the acylphosphine oxides and related compounds was made. The inability to record or detect any fluorescence, coupled with the fact that during preliminary investigations in UV curable formulations

it was found necessary to add tertiary amines to effect efficient cure speeds when the experiments were performed in an air atmosphere, (Chapters 5 and 6, and [7, 8]) led to an element of scepticism about the previously reported claims. Using the technique of laser flash photolysis the acylphosphine oxides and related compounds were recently shown to produce radicals highly reactive towards acrylates, styrene and other vinyl monomers [2]. The necessity to add tertiary amines to the UV curing formulations containing these photoinitiators (Chapters 5 and 6) was an unexpected result, considering the reported high reactivity of the diphenylphosphinyl radical towards the double bonds of vinyl monomers [2, 3]. It does however, clearly demonstrate that data obtained under ideal conditions, such as rigorously degassed solutions as in the case of laser flash photolysis and electron spin resonance (esr) experiments, do not necessarily correlate to those results obtained under the conditions normally employed for UV curing. The conflicting results indicated the need to establish the nature of the excited state of the photoinitiator involved in the cleavage process, the mechanism of radical generation and the role of tertiary amine (see also Chapters 5 and 6).

Recently, a new esr method was reported [9] that could identify highly transient free radicals and the spin multiplicity of the excited state of the precursor. E.s.r is a much more powerful technique for identifying radicals than laser flash photolysis. The flash photolysis e.s.r method reported [9] together with chemically induced dynamic electron polarisation (CIDEP) has been used previously to sort out the mechanisms of

photochemical reactions leading to radical production [10-13]. The technique proved to be invaluable in those instances and was therefore employed to identify the radicals generated upon the photolysis of the acylphosphine oxides. The esr method, together with CIDEP demonstrated that the generated free radicals were produced predominantly from the triplet state.

Chemical trapping techniques using 2,2,6,6-tetramethylpiperidin-1-oxyl (TMPO) [14-16] and a non-polymerising model substrate for vinyl monomers [16, 17] have been shown recently to be extremely useful for elucidating the mechanism of photo-induced radical generating reactions. Using these techniques, chemical evidence was obtained by TMPO trapping that the acylphosphine oxides undergo a solvent-independent photo-induced Norrish Type 1 cleavage into acyl and phosphinyl radicals (Appendix A). Identification of the species which initiates polymerisation using a model substrate was and still is less clear, although results presented in Appendix C provide an indication that both radical species are involved to some extent.

Recent reports have shown [18-20] that compounds such as benzoin, which also undergoes a Norrish Type 1 cleavage [21] can lead to oxidative desulphurisation at pentavalent phosphorus in the presence of oxygen. The ability of the acylphosphine oxides and related compounds to perform in a similar way to benzoin was investigated. The results, presented in Appendix B, provide an indication of the efficiency with which each compound investigated undergoes a Norrish Type 1 cleavage.

DETECTION OF FREE RADICAL SPECIES

Over the last twenty years or so, flash-photolysis methods have been used to observe free radicals in solution, including those involved in radical-initiated polymerisations [9,22]. Unfortunately, these techniques which use UV optical spectroscopy as the method of detection, are severely limited by the low resolution associated with UV spectra in solution. Although this detection method is widely used, and is indeed essential to the fastest laser photolysis experiments, only the radical containing chromophore can be identified, and not the actual radical itself. As a result, the structure of the radical remains uncertain.

A high resolution technique which enables the direct observation and characterisation of free radicals in solution, is electron spin resonance (esr). The radical species are identified from their own characteristic esr spectrum, g-value, and hyperfine structure which is due to through-bond coupling to nearby nuclei. In the operating fields of most esr spectrometers the transitions largely satisfy the equation shown below in Figure 1.

$$\begin{array}{ccc} \text{-----} & 1/2 & \\ & & \\ hv = g\mu_B B & & B \quad (1) \\ & & \\ \text{-----} & -1/2 & \end{array}$$

Figure 1. The basic esr experiment (μ_B is the Bohr magneton).

Almost all esr spectrometers operate with the frequency of the radiation kept constant at approximately 9.6 GHz, in the micro-

wave region, whilst changing the magnetic field of the spectrometer to display the spectrum [9, 22, 23]. In this basic esr experiment (Figure 1), the electrons align themselves in the energy levels with their spins parallel and antiparallel to the direction of the magnetic field, B. Applying radiation at the correct frequency results in esr transitions between these energy levels.

The field of the spectrometer is generated by the use of electromagnets. The spectrum of the free radicals is displayed by varying the current through the coils of the electromagnet, or by using separate sweep coils. The inductive nature of the electromagnetic coils however, prevents the current passing through them being changed quickly and it is not possible to sweep through even one line in the spectrum in a time comparable with a microsecond. This makes direct observation of highly transient radicals impossible. It is for this reason that esr studies have been limited to stable radicals, or those created continuously to yield steady-state concentrations with radical lifetimes of 1 ms or greater. Shorter-lived transient species have been studied indirectly by trapping methods whereby the primary radicals react rapidly to form stable radicals. This poses problems however, in the identification of the primary radical due to the possibility of selective scavenging.

More recently, new flash photolysis methods have been developed which can be used to provide complete spectra for radical identification at times to within 20 nanoseconds (ns) of radical creation. Despite the fact that this time period is

slower than that of the fastest optical methods, it is the most favoured time period to observe free radicals rather than their precursors, although the nature of the precursors may also be deduced. When the new methods were employed, the radicals observed within a few microseconds of their creation almost always exhibited esr spectra of an unusual appearance. The line positions i.e., the g values, appeared exactly where they were expected, however the intensities and often the phases deviated from those expected for thermally equilibrated radicals. In some cases, whole spectra appeared in enhanced absorption (A) or in emission (E), whilst in other cases some of the hyperfine lines appeared in each phase. This spectral pattern, whereby the hyperfine lines appeared in each phase, had been observed previously from steady-state studies on hydrogen (H) atoms [23]. These observations implied that the relative populations of the electron energy levels involved in the transitions differed from those predicted from the Maxwell Boltzmann distribution law and the system was said to be spin polarised, a phenomenon known as chemically induced dynamic electron polarisation, CIDEP [9,23]. CIDEP provides unique information which enhances the use of flash photolysis esr techniques, providing a direct link between the photophysics of a molecule and its photochemistry.

There are two important advantages associated with the CIDEP phenomenon. The first advantage relates to the increase in the absolute intensities of the lines compared with those from similar concentrations of thermally equilibrated radicals. This increase in line intensity enables radicals to be detected at the low concentrations commonly associated with radical generation

under normal conditions (the old techniques required the radical concentrations to be unusually high in order to be detected). The second advantage associated with CIDEP is that the phases of the polarised signals allow the multiplicity of the radical precursor to be deduced directly from the spectrum without the need for further experimentation. The derivation of molecular information from the analysis of the spectra depends upon an understanding of the origins of CIDEP and their effects.

CHEMICALLY-INDUCED DYNAMIC ELECTRON POLARISATION (CIDEP)

The phenomenon of CIDEP produces esr spectra with an unusual appearance, where many different spectral behaviours are observed. The spectrum may appear normal in the relative intensities of the hyperfine components but possess non-Boltzmann absolute intensities and be either in absorption (A) or emission (E). Alternatively, half of the hyperfine lines may be in absorption and the other half, with equal overall intensity, in emission. Frequently spectra are observed which exhibit some lines in absorption and some in emission, with an excess of one phase over the other. Spectra have been observed with all their lines in a single phase but with their relative hyperfine intensities distorted. It is not possible to rationalise these phenomena in terms of a single polarisation-producing mechanism. Two main mechanisms arise however, which are independent processes producing characteristic patterns in the observed spectra. Together they can be used to explain the different spectral patterns

obtained [9, 22]. As both processes may affect the spectra observed initially, they require careful analysis to differentiate between them.

The triplet mechanism (TM) may arise if the radicals are produced by the reaction of a molecule in an excited triplet state. The resultant spectra will be entirely in a single phase, with no distortions to the relative intensities of the lines. The phase observed, either absorptive or emissive depends upon the specific molecule involved. The radical pair mechanism (RPM) occurs as a result of the fact that radicals are created, or react, in pairs. Although the origins of the RPM are quite complex, the interpretation of the spectra showing the RPM effect are relatively straightforward. Generally the RPM produces a spectrum whereby half the spectral intensity occurs in absorption and half in emission. If the pattern observed is first in emission (low field is in emission) and then in absorption (high field is in absorption) as shown in Figures 2a and 2b (both spectra are included as examples of E/A pattern only), the radicals originated from the reaction of a triplet state. Alternatively, if an A/E pattern (absorption in low field, emission in high field) is observed, then the radicals will have originated from a singlet state. The polarisation, P , which is generated as long as reactive radicals exist in solution, is hyperfine-dependent and changes sign about the mid-point of the spectrum, if the radicals are produced as an identical pair. If however the radicals are not identical, then neither are the amounts of emission and absorption in the spectrum. One radical will have more emissive

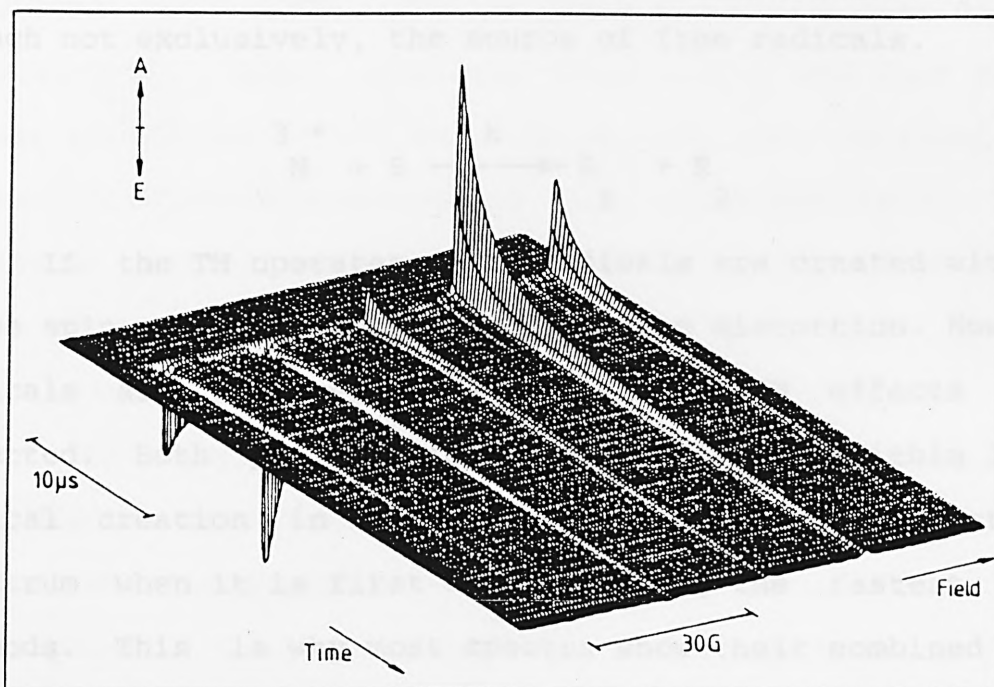
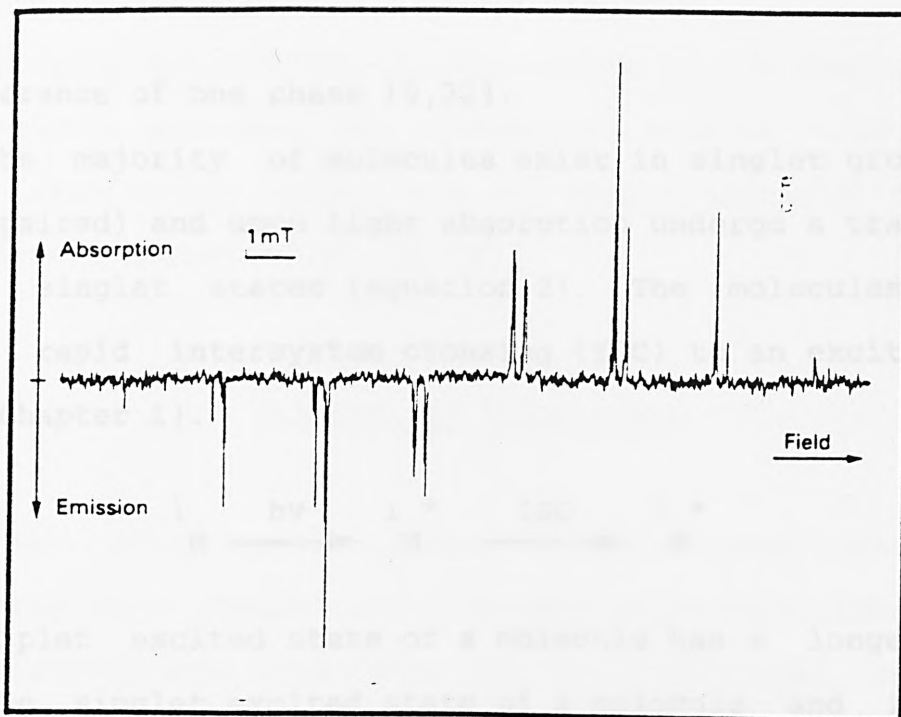


Figure 2 a) The TIS spectrum of $(\text{CH}_3)_2\text{CH}$ radicals and b) a two dimensional spectrum of cycloheptan-3-yl radicals provided as examples only to illustrate the basis of the E/A technique [23].

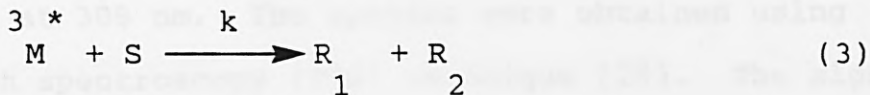
character and the other more absorptive character. These are generally designated E^*/A and E/A^* , where the asterisk denotes a

preponderance of one phase [9,22].

The majority of molecules exist in singlet ground states (spin paired) and upon light absorption undergo a transition to excited singlet states (equation 2). The molecules can then undergo rapid intersystem crossing (ISC) to an excited triplet state (Chapter 1).



The triplet excited state of a molecule has a longer lifetime than the singlet excited state of a molecule and is usually, though not exclusively, the source of free radicals.



If the TM operates, the radicals are created with single phase spin polarisation and no hyperfine distortion. However, the radicals are produced as a pair and so RPM effects are also expected. Both polarisation mechanisms occur within 10 ns of radical creation in organic systems and so both affect the esr spectrum when it is first observed using the fastest transient methods. This is why most spectra show their combined effects. Even in a symmetric radical pair the spectrum may exhibit more intensity in one phase than the other.

This very brief explanation of the detection of transient free radical species using the flash photolysis esr method together with CIDEP has been over simplified for the purpose of

interpreting and identifying the nature of the excited states and the radicals produced. The fundamental role of CIDEP in chemistry is a fascinating subject and has been eloquently described in more detail elsewhere [9, 22-24].

RESULTS AND DISCUSSION

Two acylphosphine oxides, 2,4,6-trimethylbenzoyldiphenylphosphine oxide (TMBPO) and 2,6-dimethoxybenzoyldiphenylphosphine oxide (DMBPO) were studied by the flash photolysis esr technique together with CIDEP. The two photoinitiators were dissolved in propan-2-ol, their solutions deoxygenated and then subjected to laser photolysis at 308 nm. The spectra were obtained using the time integration spectroscopy (TIS) technique [25]. The signals detected varied rapidly in time and unusually short sample periods were used. The experiments were carried out at room temperature using flow methods on the deoxygenated samples.

The spectrum of the radicals produced upon the photolysis of TMBPO consisted of three lines, and is shown in Figure 3. The signal was integrated between 0.12 and 0.24 us after the photolysis pulse. The outer two lines of the spectrum are due to the phosphorus-centred radical, and the central line is from the carbon-centred radical. The spectrum shows that the phosphorus-centred radical had been split by a phosphorus coupling of 372.7 gauss (1 G = 10⁻⁴ T), and that the small couplings of the carbon-centred radical were not resolved on the wide sweep used to construct the spectrum. The spectrum shows conclusively that the

radicals were produced as a result of a Norrish Type I cleavage.

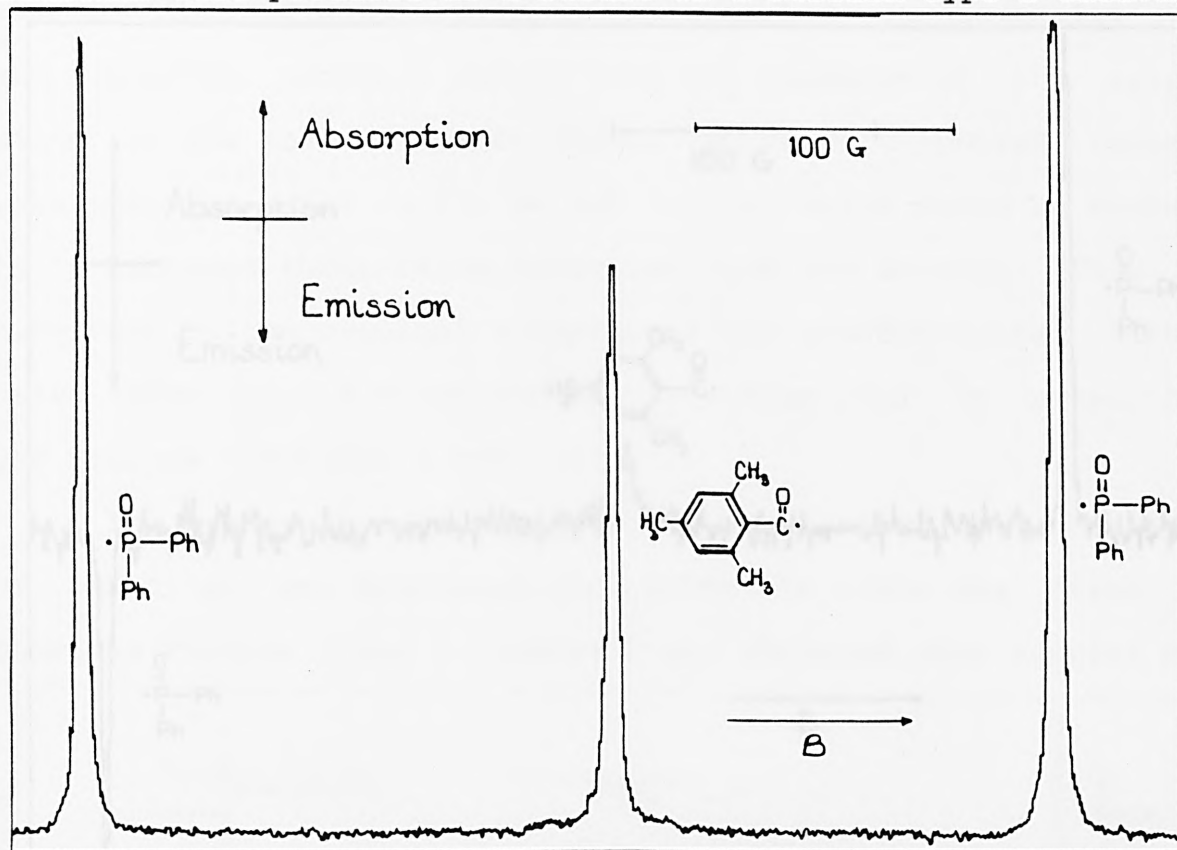


Figure 3 The TIS spectrum of radicals produced by the photolysis of TMBPO, exhibiting absorptive TM electron spin polarisation.

The spectrum obtained, at this early time was highly spin-polarised, and in enhanced absorption due to the triplet mechanism (TM) of CIDEP. The intensities of the low and high field lines (outer two lines) are almost identical and show only a very slight distortion (low field line is slightly less intense) due to emission/absorption (E/A) radical pair mechanism (RPM) polarisation. As the sample time evolved, E/A RPM polarisation distortions quickly affected the spectrum, as shown in Figure 4. Sampling between 0.5 and 2.5 us after the photolysis flash, the basic three line pattern was observed again, but not in the same phases

this time. The outer lines, as before, are due to the phosphorus

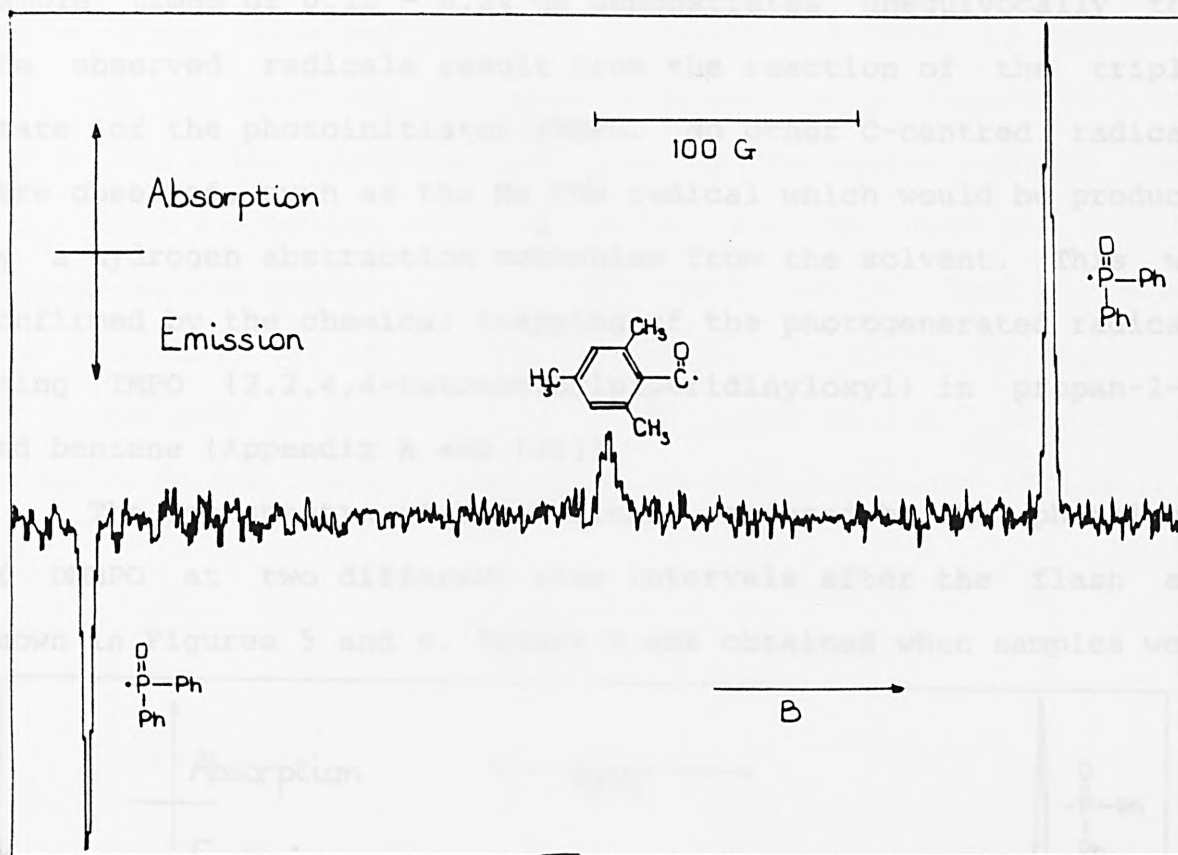


Figure 4 The TIS spectrum of radicals produced by the photolysis of TMBPO, showing how the E/A RPM spin polarisation dominates the spectrum at later sampling times.

centered radical, split by a coupling of 372.7 gauss, and the inner lines are due to the carbon-centred radical. This confirms that a Norrish Type I cleavage has occurred. However, at this later stage of sampling, which has possibly allowed a proportion of spin relaxation to occur, the spectrum is dominated by RPM polarisation. The spectrum shows the emission at low field, absorption at high field and strong (E/A) characteristics of geminate radicals formed from the excited triplet state of their precursor. The observation of the TM polarisation at such short

sample times of 0.12 - 0.24 us demonstrates unequivocally that the observed radicals result from the reaction of the triplet state of the photoinitiator TMBPO. No other C-centred radicals were observed, such as the Me COH radical which would be produced by a hydrogen abstraction mechanism from the solvent. This was confirmed by the chemical trapping of the photogenerated radicals using TMPO (2,2,4,4-tetramethylpiperidinyloxy) in propan-2-ol and benzene (Appendix A and [26]).

The esr spectra of the radicals produced by the photolysis of DMBPO at two different time intervals after the flash are shown in Figures 5 and 6. Figure 5 was obtained when samples were

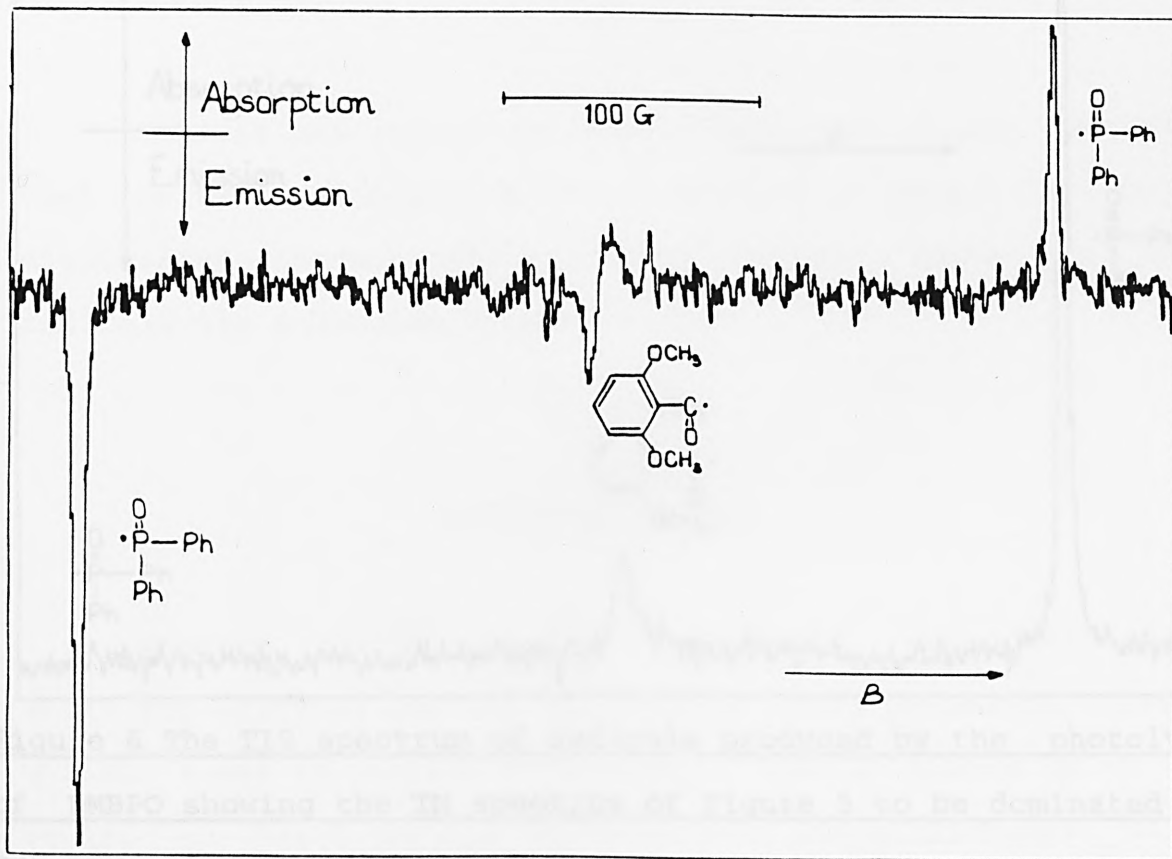


Figure 5 The TIS spectrum of radicals produced by the photolysis of DMBPO showing an absorptive TM contribution with distortion due to simultaneous geminate RPM spectrum.

recorded between 0.5 and 1.0 us after the photolysis flash. The basic three line pattern, as observed with TMBPO is apparent, although the lines are in opposite phases (as in Figure 4). Once again the outer lines emanate from the phosphorus centred radical, with a coupling of 372.7 gauss, and the inner one from the carbon-centred radical. This shows that a Norrish Type I cleavage has occurred, as in the case of TMBPO. As shown by Figure 4, this spectrum is dominated by a RPM polarisation, showing the emission at low field, absorption at high field and strong (E/A)

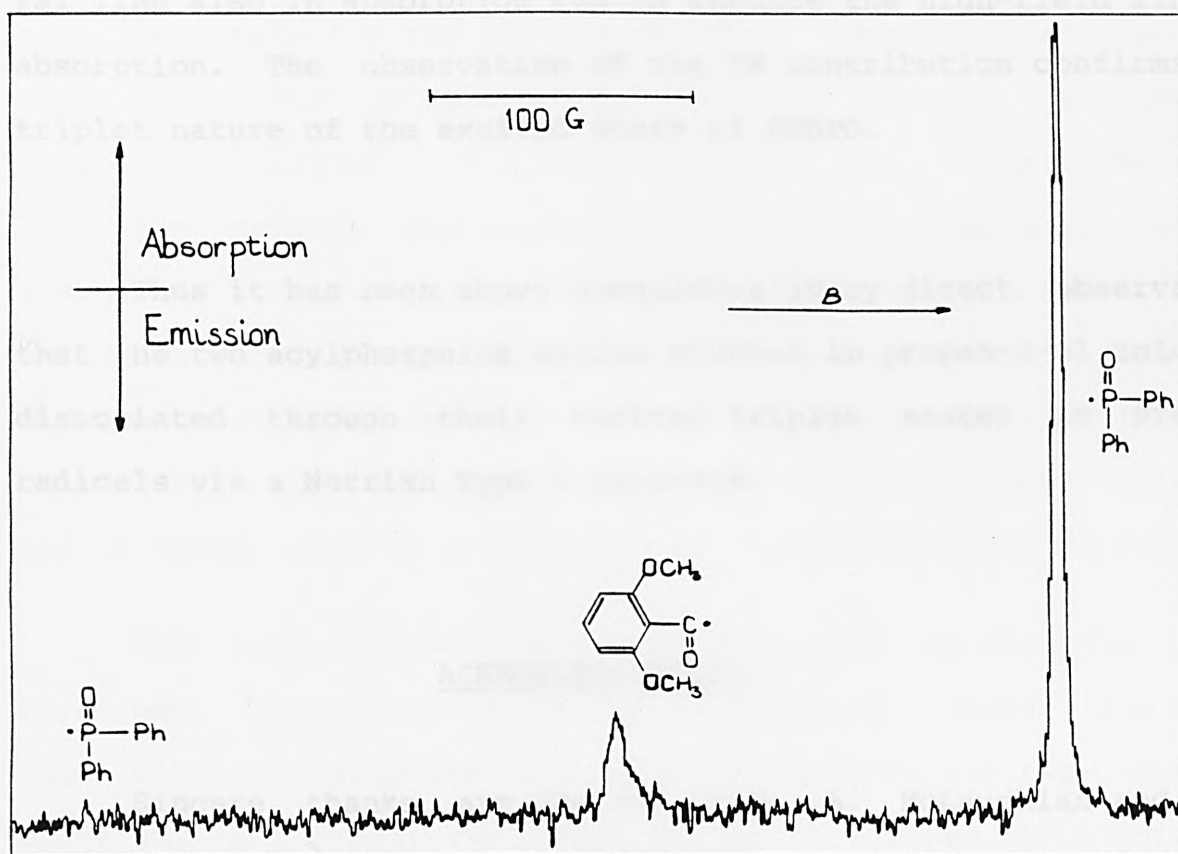


Figure 6 The TIS spectrum of radicals produced by the photolysis of DMBPO showing the TM spectrum of Figure 5 to be dominated by E/A RPM spin polarisation.

characteristics of geminate radicals which are formed from the excited triplet state of their precursor. The spectrum shows

little evidence of a TM contribution. The TM polarisation is either much weaker in this system, or spin relaxation is much faster. In Figure 6 however, the spectrum obtained with a longer integration period, between 0.1 and 0.3 μ s after the flash, shows a TM contribution similar to that obtained for TMBPO (Figure 4) adding on to an E/A RPM contribution (as recorded in Figure 5). The contribution of the TM is sufficient at this early time to just make the lowest field line visible in absorption, the central line also in absorption and to enhance the high-field line in absorption. The observation of the TM contribution confirms the triplet nature of the excited state of DMBPO.

Thus it has been shown unequivocally by direct observation that the two acylphosphine oxides studied in propan-2-ol solution dissociated through their excited triplet states to produce radicals via a Norrish Type I cleavage.

ACKNOWLEDGEMENTS

Sincere thanks are due for Dr K. A. McLauchlan and his staff for carrying out the CIDEP experiments at Oxford University whilst I was in passive attendance. Special thanks go in particular to Keith for his encouragement and willingness to help with this project when he was extremely busy with many of his own, and also for providing as much information as he thought would prove useful for the presentation of this Chapter.

EXPERIMENTAL

To obtain an esr spectrum of a highly transient free radical, and therefore to identify the radical from its hyperfine structure, requires instrumentation capable of resolving the hyperfine couplings. To achieve this the spectrometer has to respond to a fast sample time and a very short photolysis flash for radical generation. A short duration of 10-20 ns output from an excimer laser was considered instantaneous on the microsecond (us) timescale for the purpose of this investigation, without great error. The esr spectrometer detected directly the signal in a broad band system with a short response time. Pulse correlation detection methods and signal averaging techniques were used to deduce the signal to noise (S/N) ratio. The radicals were created inside a resonant microwave cavity (in the TE₁₀₂ mode) and the microwave signals were rectified with a detector crystal whose output was applied to a wide band pre-amplifier and amplifier before being input to a digital fast recording device [9,23]

The fast esr techniques used displayed the spectrum in a novel way. This involved the use of sampling methods. The radicals were not produced once in a single flash for the recorded spectrum, but repetitively in a number of flashes which occurred at different values of the magnetic field. After each flash, the signal was sampled for a specific period using the time-integration spectroscopy (TIS) method. The spectrum, at any time after the flash, was reconstructed from the data obtained from several thousand separate creations of the radical. Random pulse-to-pulse

variations were largely eliminated by signal averaging the effects of several pulses at the same magnetic field position, and the lasers were run at 20 Hz.

In TIS the decay curve is stored in a transient recorder and transferred between photolysis flashes into a dedicated microcomputer. Under control of the software, a period is chosen over which the signal is summed digitally before this integrand is output to a store location corresponding to a given magnetic field value. The decay curve is then destroyed before the magnetic field is changed and the process repeated. The esr spectrum consists of a plot of integrand against field position. The TIS method is fast in operation and requires little computer memory, however the entire field sweep with its associated thousands of laser pulses has to be repeated in order to obtain the spectrum at a different time after the photolysis flash.

On irradiation in the presence of TMPO, the acylphosphine oxides did indeed yield the products seen (as shown by GC-evidence). In both cases it is evident that the same products were formed, suggesting a solvent-independent photochemical process. The products formed during the cleavage of each photoinitiator were the corresponding 2,2,6,6-tetramethylpiperidino carboxylate compounds (where the benzoyl radical had been trapped by TMPO) and in all cases 2,2,6,6-tetramethylpiperidino diphenylphosphinate (where the diphenylphosphinoyl radical had been trapped by TMPO). The products formed were most probably the result

APPENDIX A

Trapping of Primary Radicals by a Stable Nitroxyl.

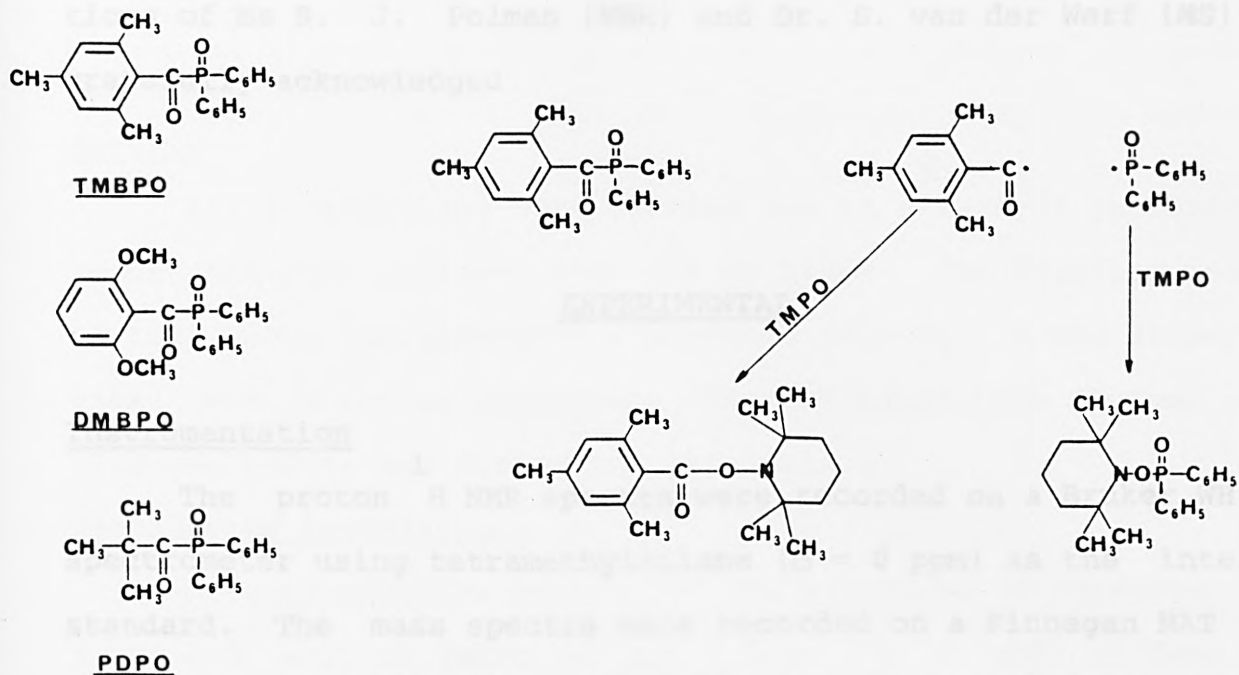
Chemical trapping of radicals using 2,2,6,6-tetramethylpiperidin-1-oxyl (TMPO) have been shown previously to be extremely useful for elucidating the mechanism of photo-induced radical-generation [14-16, 24]. Results from the photolysis of some representative acylphosphine oxides using TMPO-trapping are presented in this Appendix.

RESULTS and DISCUSSION

The photo-induced Norrish Type I cleavage of the acylphosphine oxides TMBPO (A), DMBPO (B), and pivaloyldiphenylphosphine oxide (PDPO, C) were expected to generate acyl radicals and diphenylphosphinyl radicals capable of being trapped chemically by TMPO as shown in Scheme 1, using the photoinitiator TMBPO as the example.

On irradiation in the presence of TMPO, the acylphosphine oxides did in fact yield two products each (as shown by TLC-evidence). In both benzene and in propan-2-ol the same products were formed, suggesting a solvent-independent photochemical process. The products formed during the cleavage of each photoinitiator were the corresponding 2,2,6,6-tetramethylpiperidino carboxylate compounds (where the benzoyl radical had been trapped by TMPO) and in all cases 2,2,6,6-tetramethylpiperidino diphenylphosphinate (where the diphenylphosphinyl radical had been trapped by TMPO). The products formed were most probably the result

of efficient trapping by TMPO of the photogenerated radicals formed as a result of a Norrish Type I cleavage (Scheme 1).



While acyl radicals have been previously reported [14-16, 26] to be rapidly trapped by stable nitroxyl radicals, such as TMPO, giving isolable products, the trapping of phosphorus centered radicals by stable nitroxyl radicals is relatively unknown [26].

Therefore one can conclude from the chemical evidence obtained during the TMPO-trapping experiments that the acylphosphine oxides undergo a solvent-independent photo-induced Norrish Type I cleavage into acyl and phosphinyl radicals.

ACKNOWLEDGEMENTS

I thank Prof. H. J. Hageman and Ton Overeem for the bulk of the experimental work presented in this Appendix. The contributions of Ms R. J. Polman (NMR) and Dr. S. van der Werf (MS) are gratefully acknowledged.

EXPERIMENTAL

Instrumentation

The ¹H NMR spectra were recorded on a Bruker WH-270 spectrometer using tetramethylsilane ($\delta = 0$ ppm) as the internal standard. The mass spectra were recorded on a Finnegan MAT 212 (EI) and a MAT 112 (CI), respectively. The melting points were determined on a melting point microscope (Zeiss), which was equipped with a FP Hot Stage and FP 80 Processor (Mettler). These were all corrected.

Materials

2,4,6-Trimethylbenzoic acid, 2,6-dimethoxybenzoic acid, chlorodiphenylphosphine, trimethylacetyl chloride and 2,2,6,6-tetramethylpiperidin-1-oxyl (TMPO) (all from Janssen Chimica) were used as received.

Syntheses

2,4,6-Trimethylbenzoyl chloride (b.p. 107-108 °C at 18 mbar), 2,6-dimethoxybenzoyl chloride (b.p. 111-114 °C at 0,8 mbar), methyl diphenylphosphinite (b.p. 86-87 °C at 0,11 mbar), 2,4,6-Trimethylbenzoyldiphenylphosphine oxide, (A) m.p. 80.3-80.8 °C,

2,6-dimethoxybenzoyldiphenylphosphine oxide, (B) m.p. 119.7-120.3 C, and trimethylacetyldiphenylphosphine oxide, (C) m.p. 114.3-115.8 C, were synthesised as described previously in Chapter 2.

Irradiation procedures

General

All irradiations were carried out in a Rayonet photoreactor (model RPR-208) equipped with 350 nm lamps. The reaction vessels (Pyrex) were equipped with a magnetic stirrer, a gas dispersion tube, and a reflux condenser. The solutions were flushed with nitrogen before and during the irradiation.

Preparative irradiations

A representative example of the procedure is presented. 3.48g (10^{-2} mol) of TMBPO (A) and 3.12g (2×10^{-2} mol) of TMPO were dissolved in 500 cm³ of benzene. The solution was irradiated until it was colourless (about 2 hours). The benzene was removed on a rotary evaporator (50 C at 20 mbar) and the solid residue (6.60g) was dissolved in boiling hexane. On cooling to room temperature, 2.30g of fine colourless needles with a melting point range of 126.5-127.0 C (dec.) were precipitated. The product was identified as 2,2,6,6-tetramethylpiperidino diphenylphosphinate (2), The spectroscopic properties are presented in Table 1.

The filtrate was evaporated. 4.30g of the solid residue obtained was separated on a chromatography column using silica gel (70-230 mesh; from Merck), and a solvent mixture of dichloromethane/methanol (98:2). 2.80g of a colourless material was obtained with a melting point range of 72.2-72.6 C. This was ident-

ified to be 2,2,6,6-tetramethypiperdino-2,4,6-trimethylbenzoate, (1A). The spectroscopic results are presented in Table 1.

Similarly, the acylphosphine oxides DMBPO (B) and PDPO (C) gave products 1B and 2, and 1C and 2 respectively (see Table 1). Irradiations in propan-2-ol gave the same products (as judged by TLC).

Table 1. Spectroscopic Properties of New Products

Product	¹ H NMR(CDCl ₃), in ppm	MS(70eV), m/z
1A	6,88(s; 2H, m,m'-H in benzoyl), 2,45(s;6H,o,o'-CH ₃ in benzoyl), 2,30(s;3H,p-CH ₃ in benzoyl), 1,90-1,30(m;6H,3--CH ₂ --), 1,25(s;6H, 2eq. CH ₃), 1,18(s;6H,2 ax. CH ₃)	+ 303(0,4,M), 281(0,3), 256(0,2), 185(0,1), 164(3), 148(11), 147(100,R1-CO+), 126(7), 119(7), 97(2), 91(2), 69(5)
1B	7,28(m;1H,p-H in benzoyl), 6,80(m;2H,m,m'-H in benzoyl), 3,80(s;6H,2 OCH ₃), 1,90--1,40(m;6H,3--CH ₂ --), 1,28(s;6H,2 eq. CH ₃), 1,15(s;6H,2 ax. CH ₃)	+ 321(0,M), 312(0,2), 285(0,8), 267(0,5), 257(0,4), 239(0,2), 217(0,1), 199(0,1), 185(0,2), 182(0,5), 166(10), 165(100) 150(3), 107(2), 83(0,7), 69(0,3)
1C	1,60-1,30(m;6H,3--CH ₂ --), 1,28(s;9H,--C(CH ₃) ₃), 1,18(s;6H,2 eq. CH ₃) 1,05(s;6H,2ax.CH ₃)	+ 241(2,M), 226(11), 157(5) 143(6), 142(57), 124(6), 109(5), 85(10,R1-CO+), 83(9), 69(10), 58(12), 57(100, (CH ₃) ₃ C) 56(14), 55(22), 43(5)
2	7,90--7,80(m;4H,2o,o'-H in phenyl) 7,50--7,20(m;6H,2m'm'-- and p-H in phenyl), 1,85--1,00(m;18H,2 eq. CH ₃ and 2 ex. CH ₃ super- imposed on 3__CH ₂ --)	+ 357(14,M), 342(27), 274(2), 219(22), 201(23, (C ₆ H ₅) ₂ PO+), 199(8), 139(34), 124(100) 84(18), 83(81), 77(27, C ₆ H ₅), 71(36), 70(29), 58(27), 56(79), 55(59)

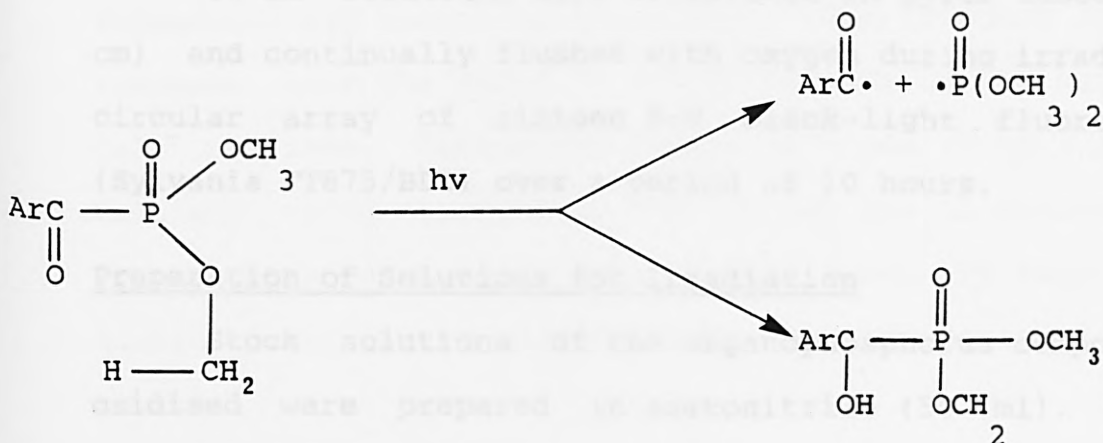
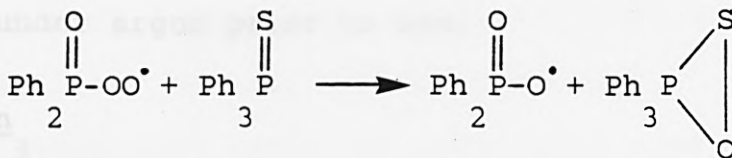
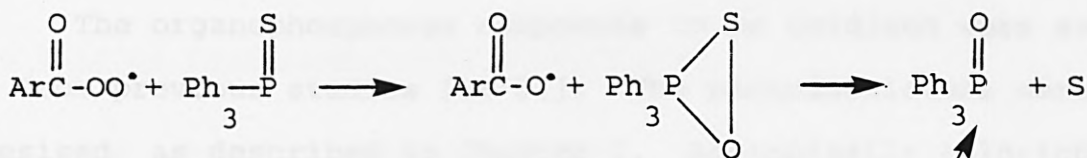
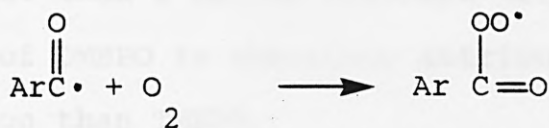
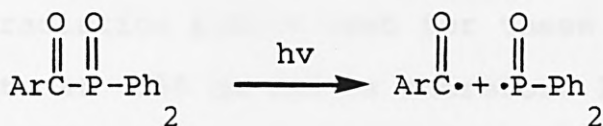
APPENDIX B

The ability of the acylphosphine oxides and acylphosphates to desulphurise a range of phosphorus sulphides by an oxidation reaction at pentacovalent phosphorus was investigated. The photoinitiators investigated were benzoyldimethylphosphonate (BDMP) I, benzoyldiethylphosphonate (BDEP) II, TMBPO III and, DMBPO IV. The organophosphorus compounds oxidised were triphenylphosphine sulphide, O-ethyl diphenylphosphinothioate, O,O-diethyl phenylphosphonothioate and O,O,O-triethylthiophosphate.

RESULTS and DISCUSSION

The ease of oxidation of the organophosphorus compounds (shown in Table 2) by the photoinitiators BDEP II, TMBPO III, and DMBPO IV, decreases as the number of alkoxy groups attached to phosphorus is increased [18-20]. BDMP (I), did not discriminate between the reactivity of triphenylphosphine sulphide and O-ethyl diphenylphosphinothioate or the reactivity of O,O-diethyl phenylphosphonothioate and O,O,O-triethylthiophosphate. The oxidative desulphurisation of the organophosphorus compounds at pentacovalent phosphorus by the acylphosphine oxides and acylphosphonates show a similar trend to that observed when benzoin was used as the photoinitiator [18-20]. BDMP (I) and BDEP (II), show similar photoreactivity, as expected from their similar structures, and are far less photoreactive than TMBPO (see Chapters 4 and 5). The greater efficiency of TMBPO can be attributed to the high efficiency with which it undergoes the Norrish Type I process

[27]. BDMP and BDEP can, in addition to undergoing the Norrish Type I process, undergo the Norrish Type II process [28, 29] which does not lead to initiating radicals, thereby decreasing the efficiency with which these compounds will initiate oxidation reactions.



DMBPO (IV) appears to be a less efficient initiator than

TMBPO for the oxidative desulphurisation reactions, although it displays similar reactivity to TMBPO during the polymerisation of vinyl monomers using a medium pressure mercury lamp (Chapter 4 and [30]). The absorption spectrum of DMBPO (IV) exhibits a much weaker absorption in the 300-400 nm region compared to TMBPO. Since the irradiation source used for these experiments had a maximum output at 350 nm and is therefore less rich in lower wavelength UV than a medium pressure mercury lamp, the lack of reactivity of DMBPO is therefore attributed to it absorbing far less radiation than TMBPO.

EXPERIMENTAL

Materials

The organophosphorus compounds to be oxidised were available from previous studies [18-20]. The photoinitiators were synthesised as described in Chapter 2. Acetonitrile (Aldrich) was distilled under argon prior to use.

Irradiation

³
10 cm solutions were irradiated in pyrex tubes (26.0 x 1.9 cm) and continually flushed with oxygen during irradiation by a circular array of sixteen 8-W black-light fluorescent lamps (Sylvania FT875/BLB) over a period of 10 hours.

Preparation of Solutions for Irradiation

Stock solutions of the organophosphorus compounds to be oxidised were prepared in acetonitrile (50 ml). An internal standard was added to each solution for the g.l.c analysis of the

3

reaction products (as shown below). To a 10 cm³ sample of each reaction mixture a 2 molar equivalent amount of the photoinitiator was added, based on the amount of organophosphorus compound used.

Details of Stock Solutions

Organophosphorus Compound (Weight in grams)	Internal Standard (Weight in grams)
Triphenylphosphine sulphide (0.6g)	Diphenylsulphone (0.4g)
O-Ethyl diphenylphosphinothiate (0.55g)	Diphenylsulphone (0.4g)
O,O-Diethyl phenyl phosphonothioate (0.47g)	Di n-butylsulphone (0.4g)
O,O,O-Triethyl phosphorothioate (0.40g)	Dimethylsulphone (0.5g)

Analysis of solutions after irradiation

The reaction mixtures were analysed by g.l.c using a Shimadzu G.C Mini 2 chromatograph fitted with a 30m x 0.31mm SE30 Flexsil capillary column and equipped with a flame ionisation detector. Retention times and peak areas were obtained using a Shimadzu C-RIB computing integrator. The detector gave a linear response over the range of concentrations of the various materials utilised. Reasonable retention times (3 to 7 minutes) were obtained using nitrogen as the carrier gas (1 ml/min) and oven temperatures between 110-250. In all cases the internal standard eluted prior to the organophosphorus compound and its oxidation product.

TABLE 2 Yields of Oxidised Organophosphorus Compound Produced by Oxidative Desulphurisation via Photoinitiated Oxidation using BDMP, BDEP, TMBPO and DMBPO.

Organophosphorus Compound	Photoinitiating Species	Unchanged Starting Material(%)	Yield of Oxidised Product(%)
Triphenylphosphine Sulphide	Benzoyldimethyl phosphonate (I)	40	47
	Benzoyldimethyl phosphonate (II)	56	32
	2,4,6-Trimethylbenzoyl-diphenyl phosphine oxide (III)	0	81
	2,6-Dimethoxybenzoyl-diphenylphosphine oxide (IV)	12	77
O-Ethyl diphenyl phosphinothioate	(I)	36	64
	(II)	67	32
	(III)	0	97
	(IV)	37	63
O,O-Diethyl phenyl phosphonothioate	(I)	69	31
	(II)	68	28
	(III)	23	64
	(IV)	67	28
O,O,O-Triethyl phosphorothioate	(I)	69	31
	(II)	75	22
	(III)	40	58
	(IV)	78	22

ACKNOWLEDGEMENTS

The contributions of J M Abrahams and M D Walker are gratefully acknowledged.

APPENDIX C

Chemical trapping using a non-polymerising model substrate to simulate vinyl monomers was previously shown to be useful for establishing the identity of the initiating radicals generated from a variety of photoinitiators [16,17, 31]. Therefore it was decided to study the photolysis of 2,4,6-trimethylbenzoyldi-phenylphosphine oxide [1] in the presence of 1,1-di(p-tolyl)ethylene (DTE) as a model substrate. The experiments were performed in the presence and absence of a tertiary amine, both in solution and in thin films in an attempt to identify the nature of the initiating radicals.

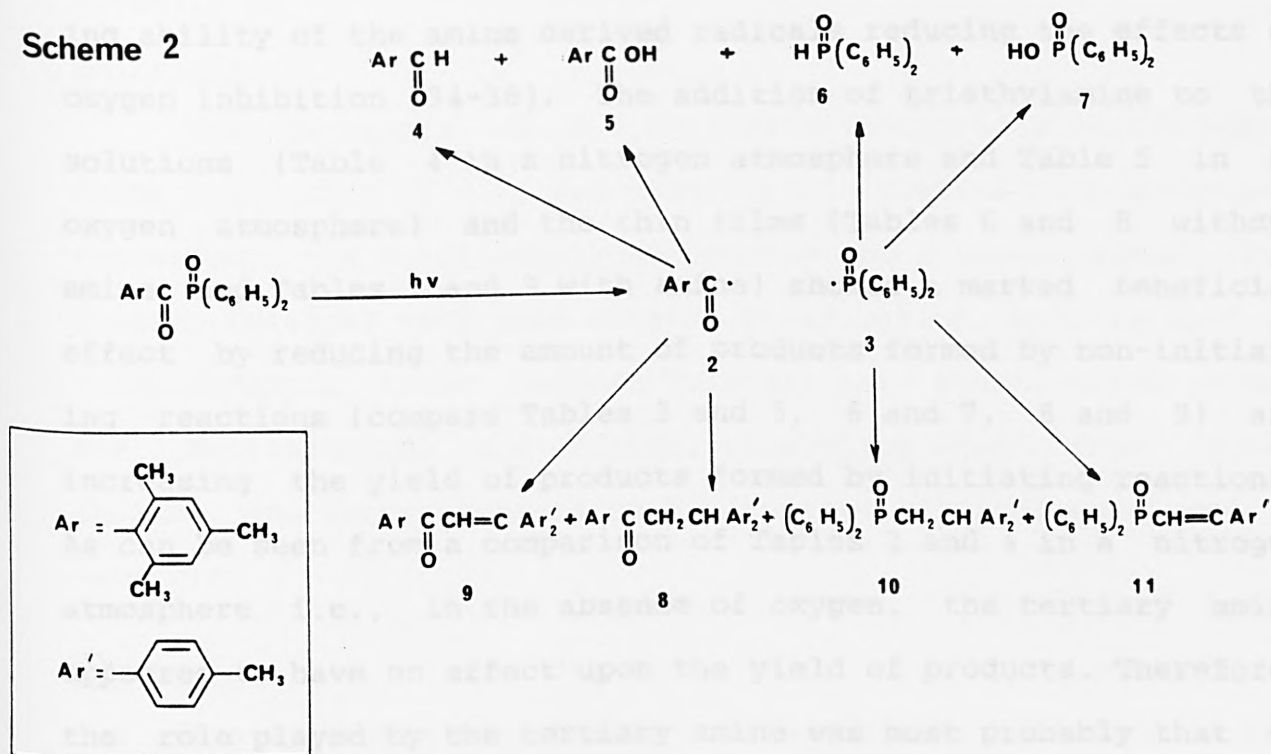
1,1-Di(p-tolyl)ethylene was selected as the model substrate rather than the 1,1-diphenylethylene (DPE) used in the previous experiments. The change of model substrate was made to avoid unnecessary complications which arose from the "anomalous" termination behaviour displayed by DPE involving the free para-rotation of its phenyl groups [16, 31].

RESULTS and DISCUSSION

The results presented in Tables 2 to 9 and in Scheme 2 show that the primary radicals formed (2 and 3 of Scheme 2) upon the photodecomposition of TMBPO result from a Norrish Type 1 cleavage. In the presence of DTE, both primary radicals were capable of adding to the olefinic double bond of the model substrate (products 8 - 11 in Scheme 2). In the absence of oxygen (in a nitrogen atmosphere) products were formed by a non-initiating reaction of the primary radicals (products 4, 5, 6 and 7 of

Scheme 2) and an initiating reaction of the primary radicals (products 8, 9, 10 and 11 of Scheme 2) as shown in Table 2. In an air atmosphere, the same products were

Scheme 2



formed, but in different proportions. There was a very marked increase in the yield of products 4 and 6 (Table 3) and a decrease in the yield of products 8 to 11. These results show clearly the inhibiting effect of oxygen upon the free radical polymerisation reaction, even with TMBPO which undergoes a Norrish Type 1 cleavage from a short lived triplet excited state to produce the primary radical species 2 and 3 shown in Scheme 2 [2,27].

The investigation of the photodecomposition of TMBPO in the presence of DTE with and without added tertiary amine was made to elucidate the role of the amine in UV curable formulations. It

has been known for some time that tertiary amines will increase the cure rate and lower the surface tackiness of UV cured films when Type 1 photoinitiators are employed [32,33]. The beneficial effect of tertiary amine has been ascribed to the oxygen scavenging ability of the amine derived radicals reducing the effects of oxygen inhibition [34-36]. The addition of triethylamine to the solutions (Table 4 in a nitrogen atmosphere and Table 5 in an oxygen atmosphere) and the thin films (Tables 6 and 8 without amine and Tables 7 and 9 with amine) showed a marked beneficial effect by reducing the amount of products formed by non-initiating reactions (compare Tables 3 and 5, 6 and 7, 8 and 9) and increasing the yield of products formed by initiating reactions. As can be seen from a comparison of Tables 2 and 4 in a nitrogen atmosphere i.e., in the absence of oxygen, the tertiary amine appeared to have no effect upon the yield of products. Therefore, the role played by the tertiary amine was most probably that of an oxygen scavenger only. This assumption is supported by the fact that no amine derived radicals were detected attached to the model substrate (see Chapters 5 and 6).

ACKNOWLEDGEMENTS

Thanks go to Professor H. J. Hageman and Ton Overeem for the photolysis, thin film irradiations and the analysis of the products which are the main subject of this Appendix. The contributions of Ms R. J. Polman (NMR) and Dr S. van der Werf (MS) are also gratefully acknowledged.

EXPERIMENTAL PART

Instrumentation

The instrumentation used was described previously in Appendix A.

Materials

The synthesis of 2,4,6-trimethylbenzoyldiphenylphosphine oxide m.p. 80.3-80.8 C, was described in Chapter 2. p-Methylacetophenone, 2,4,6-trimethylacetophenone and p-bromotoluene (from Janssen Chimica) were used without purification. Pyruvic acid and p-tolualdehyde (from Janssen Chimica) were fractionated before use. Mesitaldehyde and diphenylphosphinic acid (from Janssen Chimica) and diphenylphosphine oxide (from Aldrich) were used as received.

Syntheses

The synthesis of 1,1-di(p-tolyl)ethylene, obtained as colourless crystals, m.p. 59.5-60.0 C, 2-(p-Tolyl)vinyl 2,4,6-trimethylphenyl ketone, m.p. 106.5-107.5 C, 2,2-di(p-tolyl)ethyl 2,4,6-trimethylphenyl ketone, m.p. 65.1-66.0 C and 2,2-di(p-tolyl)vinyl 2,4,6-trimethylphenyl ketone m.p. 74.5-75.5 has been described [37].

Irradiation procedures

General

The irradiations were carried out as described in Appendix A except in this case the solutions were flushed with nitrogen and air respectively before and during the irradiations. The reactions were monitored by TLC analysis by withdrawing samples

at regular intervals.

Preparative irradiations

A representative example of the irradiation procedure is presented.

TMBPO (10^{-2} M) and 1,1-di(p-tolyl)ethylene (4.10^{-2} M) were dissolved in benzene and irradiated for 2 hours under nitrogen. The benzene was removed on a rotary evaporator (50°C at 20 mbar). The products were isolated by column chromatography on silica gel (70-230 mesh, from Merck) using dichloromethane and dichloromethane/methanol (98:2) as eluents in that order.

The products identified by spectroscopic methods (^1H NMR and MS, [37]), and in some cases by comparison with authentic samples (obtained through independent synthesis), were 1,1-di(p-tolyl)ethylene, 2,2-di(p-tolyl)ethyl 2,4,6-trimethylphenyl ketone, 2,2-di(p-tolyl)vinyl 2,4,6-trimethylphenyl ketone, diphenyl 2,2-di(p-tolyl)-3-(2,4,6-trimethylphenyl)-3-oxopropyl phosphine oxide m.p. $173.5-174.5^{\circ}\text{C}$, diphenyl 2,2-di(p-tolyl)ethyl phosphine oxide m.p. $225.5-226.5^{\circ}\text{C}$, and diphenyl 2,2-di(p-tolyl)-vinyl phosphine oxide m.p. $189.3-189.8^{\circ}\text{C}$

2,2-Di(p-tolyl)-3-(2,4,6-trimethylphenyl)-3-oxopropyldiphenyl-phosphine oxide m.p. $173.5 - 174.5^{\circ}\text{C}$,

Calculated for $\text{C}_{38}\text{H}_{37}\text{O}_2\text{P}$: C 81.98%, H 6.70%,
found : C 81.82%, H 6.78%,

^1H NMR(CDCl_3) : = 7.50 (m; 4H, 2.o,o'-H in C_6H_5),
7.37-7.25 (m; 6 H, 2.(p + m,m')-H in C_6H_5),

7.21 and 6.75 (AB, J=8 Hz; 8 H, 2.(o,o'+m,m) -H in Ar'),

6.57 (s; 2 H, m,m'-H in Ar),

3.75 (d, J=10 Hz; 2 H, P-CH₂),

2.15 (s; 9 H, (o,o'+p)-CH₃ in Ar),

1.66 (s; 6 H, 2.p-CH₃ in Ar')

MS: m/z (int.) 556 (10; M⁺), 409 (9, M⁺-147), 202 (9, (C₆H₅)₂POH⁺), 201 (57, (C₆H₅)₂PO⁺), 147 (100, ArCO⁺), 119 (7, Ar⁺), 91 (3, Ar'⁺), 77 (5, C₆H₅⁺).

2,2-Di(p-tolyl)ethyldiphenylphosphine oxide m.p. 225.5-226.5 °C,

Calculated for C₂₈H₂₇OP : C 81.93%, H 6.63%,
Found : C 80.97%, H 6.77%,

¹H NMR(CDCl₃): = 7.55 (m; 4 H, 2.o,o'-H in C₆H₅),
7.45-6.90 (m; 14 H, 2.(p-m,m')-H in C₆H₅ and 2.(o,o'+m,m')-H in Ar'),
4.55 (m; 1 H, -CHAr'₂),
3.05 (dd, 2 H, P-CH₂),
2.20 (s; 6 H, 2.p-CH₃ in Ar')

MS: m/z (int.) 410 (26, M⁺), 209 (23, M⁺-201), 202 (100, (C₆H₅)₂POH⁺), 201 (12, (C₆H₅)₂PO⁺), 183 (3, (C₆H₅)₂P⁺), 155 (10, (C₆H₅)₂POH⁺-47), 91 (3, Ar'⁺), 77 (6, C₆H₅⁺).

2,2-Di(p-tolyl)vinylidiphenylphosphine oxide m.p. 189.3-189.8 °C,

Calculated for C₂₈H₂₅OP : C 82.33%, H 6.17%,
Found : C 81.75%, H 6.22%,

¹H NMR(CDCl₃): = 7.70 (m; 4 H, 2.o.o'-H in C₆H₅),
 7.40-6.85 (m; 14 H, 2.(p+m,m')-H in C₆H₅ and
 2.(o,o'+m,m')-H in Ar'),
 6.70 (d,J=18 Hz; 1 H P-CH),
 2.36 (s; 3 H, p-CH₃ in Ar'),
 2.23 (s; 3 H, p-CH₃ in Ar')

MS: m/z (int.) 408 (100, M⁺), 393 (4, M⁺-15), 331 (69, M⁺-77),
 202 (82, (C₆H₅)₂POH⁺), 201 (35, (C₆H₅)₂PO⁺), 183 (13,
 (C₆H₅)₂P⁺), 155 (10, (C₆H₅)₂POH⁺-47), 91 (9, Ar'⁺), 77 (17,
 C₆H₅⁺).

Quantitative irradiations

In solution

1,1-di(p-tolyl) ethylene (4 x 10⁻² M) and TMBPO (10⁻² M) were
 dissolved in benzene. The solutions were irradiated in the pres-
 ence and absence of triethylamine (7 x 10⁻² M) for 2 hours under
 nitrogen and air saturated conditions respectively. The HPLC
 analysis of the irradiated solutions were performed on a modular
 system which was interfaced with the Waters 840 chromatography
 station. The system comprised of a M600-E pump and a Wisp 710B
 sample processor (both from Waters), and a Kratos spectration 757
 UV-absorbance detector ($\lambda = 240$ nm). All separations were per-
 formed on a Superspher RP - 8 column (3 μ m particle size, 25 cm
 long; from Merck). The eluent was a mixture of acetonitrile,
 water and phosphoric acid (vol ratios 75:25:0.1). The flow rate
 was 1 cm min⁻¹. Identification and quantification of the samples

was achieved by comparison with authentic samples of a known concentration. The results are presented in Tables 2 - 5.

In thin films

TMBPO (8.5×10^{-2} m) and 1,1-di(p-tolyl)ethylene (1.7×10^{-1} m) were dissolved in 1,5-pentanediol. Samples, with or without added triethylamine (5.9×10^{-1} m), were applied to satinised paper to provide a wet film thickness of 20 μ m (using an Erichsen rod). The coated sheets were irradiated (as described in Chapter 5) at 2 m.min⁻¹ and 10 m.min⁻¹, the irradiated films removed, weighed and dissolved in methanol (see Chapter 8 for more details of the procedure). These were analysed by HPLC, as described previously and the results are presented in Tables 6 to 9.

Table 2 Reaction Products from the Photodecomposition of TMBPO in the presence of DTE in a Nitrogen Atmosphere

Product	Amount of product in 10 ⁻⁵ mol	Corresponding amount in 10 ⁻⁵ mol of		
		2	3	DTE
4	3.70	3.70	--	--
5	0.67	0.67	--	--
7	1.84	--	1.84	--
8	26.30	26.30	--	26.30
9	14.00	14.00	--	14.00
10	29.70	--	29.70	29.70
11	39.50	--	39.50	39.50

Table 3 Reaction Products from the Photodecomposition of TMBPO in the presence of DTE in an Oxygen Atmosphere

Product	Amount of product in 10 ⁻⁵ mol	Corresponding amount in 10 ⁻⁵ mol of		
		2	3	DTE
4	40.40	40.40	--	--
5	3.17	3.17	--	--
6	30.10	--	30.10	--
7	4.70	--	4.70	--
8	14.55	14.55	--	14.55
9	7.43	7.43	--	7.43
10	24.04	--	24.04	24.04
11	31.57	--	31.57	31.57

Table 4 Reaction Products from the Photodecomposition of TMBPO in the presence of DTE and TEA in a Nitrogen Atmosphere

Product	Amount of product in 10 ⁻⁵ mol	Corresponding amount in 10 ⁻⁵ mol of		
		2	3	DTE
5	4.40	4.40	--	--
6	2.20	--	2.20	--
7	5.00	--	5.00	--
8	27.10	27.10	--	14.55
9	13.70	13.70	--	13.70
10	27.40	--	27.40	27.40
11	39.00	--	39.00	39.00

Table 5 Reaction Products from the Photodecomposition of TMBPO in the presence of DTE and TEA in an Oxygen Atmosphere

Product	Amount of product in 10 ⁻⁵ mol	Corresponding amount in 10 ⁻⁵ mol of		
		2	3	DTE
4	3.24	3.24	--	--
5	21.95	21.95	--	--
6	7.91	--	7.91	--
7	8.43	--	8.43	--
8	30.20	30.20	--	30.20
9	7.40	7.40	--	7.40
10	19.54	--	19.54	19.54
11	26.83	--	26.83	26.83

Table 6 Reaction Products from the Photodecomposition of TMBPO in the presence of DTE in a Thin Film of Pentane-1,5-diol at 2m.min⁻¹

Product	Amount of product in 10 ⁻⁵ mol	Corresponding amount in 10 ⁻⁵ mol of		
		2	3	DTE
4	6.08	6.08	--	--
5	4.27	4.27	--	--
6	1.99	--	1.99	--
7	2.77	--	2.77	--
8	2.53	2.53	--	2.53
9	2.26	2.26	--	2.26
10	4.89	--	4.89	4.89
11	5.16	--	5.16	5.16

Table 7 Reaction Products from the Photodecomposition of TMBPO in the presence of DTE and TEA in Thin Films of Pentane-1,5-diol at 2m.min⁻¹

Product	Amount of product in 10 ⁻⁵ mol	Corresponding amount in 10 ⁻⁵ mol of		
		2	3	DTE
5	4.88	4.88	--	--
6	1.99	--	1.99	--
7	1.84	--	1.84	--
8	3.09	3.09	--	3.09
9	2.54	2.54	--	2.54
10	5.13	--	5.13	5.13
11	5.65	--	5.65	5.65

Table 8 Reaction Products from the Photodecomposition of TMBPO in the presence of DTE in Thin Films of Pentane-1,5-diol at 10mmin⁻¹

Product	Amount of product in 10 ⁻⁵ mol	Corresponding amount in 10 ⁻⁵ mol of		
		2	3	DTE
5	2.44	2.44	--	--
7	2.76	--	2.76	--
8	1.97	1.97	--	1.97
9	1.69	1.69	--	1.69
10	3.42	--	3.42	3.42
11	3.44	--	3.44	3.44

Table 9 Reaction Products from the Photodecomposition of TMBPO in the presence of DTE and TEA in Thin Films of Pentane-1,5-diol at 10 mmin⁻¹

Product	Amount of product in 10-5mol	Corresponding amount in 10 ⁻⁵ mol of PTE		
		2	3	
5	3.05	3.05	--	--
6	1.49	--	1.49	--
7	1.84	--	1.84	--
8	1.69	1.69	--	1.69
9	1.41	1.41	--	1.41
10	2.44	--	2.44	2.44
11	3.19	--	3.19	3.19

[7] Baxter, J. E., Davidson, A. G., *Journal of Photochemistry*, 1985, 10, 1-10.

[8] Baxter, J. E., Davidson, A. G., *Journal of Photochemistry*, 1985, 10, 11-20.

[9] McLauchlan, R. M., *Chem. Phys. Lett.*, 1985, 11(9), 825-832.

[10] Basu, S., McLauchlan, R. M., Knight, A. J. D., *Chem. Phys.*, 1985, 79, 95-103.

[11] Buckley, C. D., McLauchlan, R. M., *Chem. Phys.*, 1984, 86, 323-328.

[12] Buckley, C. D., McLauchlan, R. M., *J. Photochem.*, 1984, 27, 311-316.

[13] Buckley, C. D., McLauchlan, R. M., *Mol. Phys.*, 1985, 54(11)

REFERENCES

- [1] Ger. Offen. 2830927 (1980), BASF AG; invs.: Lechtken, P., Buethe, I., Hesse, A. Chem. Abstr. 93, 46823u (1980); Ger. Offen. 2909994 (1980), BASF AG; invs.: Lechtken, P., Buethe, I., Jacobi, M., Trimborn, W., Chem. Abstr. 94, 103560c (1981).
- [2] Sumiyoshi, T., Henne, A., Lechtken, P., Schnabel, W., Polymer, 1985, 26, 141-146.
- [3] Sumiyoshi, T., Schnabel, W., Makromol. Chem., 1985, 186, 1811-1823.
- [4] Sumiyoshi, T., Schnabel, W., Henne, A., J. Photochem., 1985, 30, 63-80.
- [5] Schnabel, W., J. Rad. Curing, 1986, 13(1) 26-34.
- [6] Sumiyoshi, T., Weber, W., Schnabel, W., Z. Naturforsch., 1985, 40a, 541-543.
- [7] Baxter, J, E., Davidson, R, S., Hageman, H, J., accepted for publication in Eur. Polym., J.
- [8] Baxter, J, E., Davidson, R, S., Hageman, H, J., accepted for publication in Eur. Polym., J.
- [9] McLauchlan, K, M., Chem. in Brit., 1985, 21(9), 825-832.
- [10] Basu, S., McLauchlan, K, A., Ritche, A, J, D., Chem. Phys., 1983, 79, 95-103.
- [11] Buckley, C, D., McLauchlan, K, A., Chem. Phys., 1984, 86, 323-329.
- [12] Buckley, C, D., McLauchlan, K, A., J. Photochem., 1984, 27, 311-316.
- [13] Buckley, C, D., McLauchlan, K, A., Mol. Phys., 1985, 54, (1)

1-22.

- [14] Robbins, W, K., Eastman, R, H., J. Am. Chem. Soc., 1980, 92, 6077-6079.
- [15] Hageman, H, J., Overeem, T., Makromol. Chem., Rapid Commun., 1981 2, 719-724.
- [16] Angad Gaur, H., Groenenboom, C, J., Hageman, H, J., Hakvoort, G, T, M., Oosterhoff, P., Overeem, T., Polman, R, J., v.d. Werf, S., Makromol. Chem., 1984, 185, 1795-1808.
- [17] Groenenboom, G., Hageman, H, J., Overeem, T., Weber, A, J, M., Makromol. Chem., 1982, 183, 281-292.
- [18] Buckland S, J., Davidson R, S., J. Photochem., 1987 36 39-49.
- [19] Buckland, S, J., Davidson, R, S., Pesticide science 1987 19 61-66.
- [20] Davidson, R, S., Walker, M, D., Phosphorus and sulfur, 1987 30 305-310.
- [21] Hageman, H, J., Prog. in Org. Coatings 1985 13, 123-150.
- [22] Hore, P, J., Joslin, C, G., McLauchlan, K, A., Chem. Soc., Rev., 1979, 8, 29-61.
- [23] McLauchlan, K, A., Applications of Laws in Polymer Science and Technology, Ed., Fouassier, J, P., and Rabek, J, F., to be published by CRC press this year.
- [24] Hore, P, J., Joslin, C, G., McLauchlan, K, A., Special Periodical Report, Electron Spin Resonance, 1979, Vol 5, 1-45.
- [25] Basu, S., McLauchlan, K, A., Sealy, G, R., J. Phys. E, 1983, 16, 767-773.
- [26] Baxter, J, E., Davidson, R, S., Hageman, H, J., Overeem,

- T., Makromol. Chemie Rapid Commun., 1987, 8, 311-314.
- [27] Baxter, J, E., Davidson, R, S., Hageman, H, J., McLauchlan, K, A., Stevens, D, G., J. Chem., Soc., Chem., Commun., 1987, 73-75.
- [28] Terauchi, K., Sakurai, H., Bull. Chem. Soc., Japan 1970 43, 883-890.
- [29] Ogata, Y., Tomioka, H., J. Org.Chem. 1970 35 596-600.
- [30] Baxter, J, E., Davidson, R, S., Hageman, H, J., Accepted for publication in Polymer.
- [31] Angad Gaur, H., Groenboom, C, J., Hageman, H, J., Oosterhoff, P., Overeem, T., Polman, R, J., v.d. Werf, S., Makromol. Chem., to be published.
- [32] Osborn, C, L., J. Rad Curing 1976, 3 (3), 2 - 11
- [33] Berner, G., Kirchmayr, R., Rist, G., J. Oil Col. chem. assoc., 1978, 61, 105 - 113
- [34] Hoyle, C, E., Kim, K, J., J. Rad. curing, 1985, 12 (4) 9 - 15.
- [35] Hoyle, C, E., Kim, K, J., J. Appl. Polym. sci., 1987, 33 2985 - 2996.
- [36] Hoyle, C, E., Keel, M., Kim, K, J., 1988, Polymer, 29 (1) 18 - 23.
- [37] Baxter, J, E., Davidson, R, S., Hageman, H, J., Overeem, T., Makromol. Chem., to be published.

Chapter 4

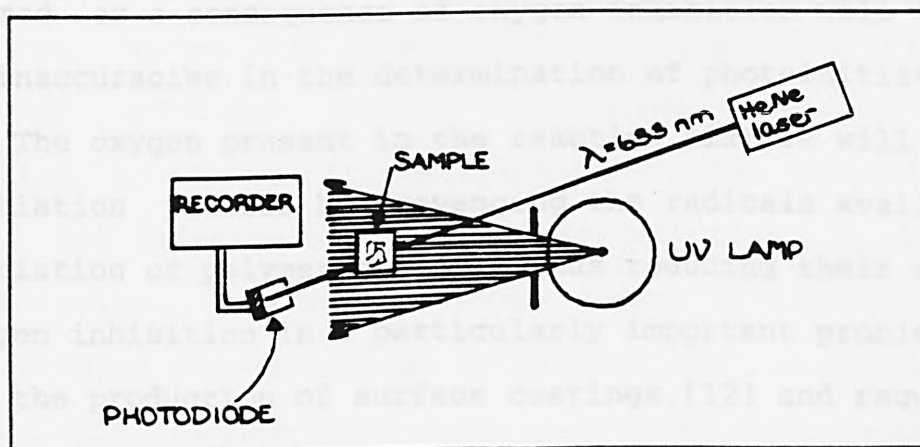
Methods for Screening Photoinitiators

Chapter 4	Methods for Screening Photoinitiators	
	Introduction	161
	Free Radical Polymerisation of Vinyl	
	Monomers	163
	Bulk Polymerisation	164
	Solution Polymerisation	165
	Results and Discussion	167
	(1) Solution Polymerisation Monitored by	
	Laser Nephelometry	167
	(2) Bulk Polymerisation of Methyl	
	Methacrylate and Styrene	174
	Acknowledgements	179
	Experimental	180
	Appendix A	184
	Appendix B	186
	References	191

INTRODUCTION

Photoinitiators suitable for the free radical polymerisation of vinyl monomers can be classified into two main categories [1-3], as described previously in Chapter 1. The two main categories include those undergoing a Norrish Type 1 photocleavage and others which undergo a bimolecular process that leads to the formation of radicals capable of initiating polymerisation.

Photoinitiator efficiency can be assessed in a number of ways, examples of which include solution polymerisation, as monitored by the laser nephelometry technique [4], and bulk polymerisation techniques [5-8]. The results obtained using these methods do not always provide a true indication of how the photoinitiator systems will perform in UV curable coatings [5]. Results obtained from the UV curing of thin films are rarely analogous to those obtained from solution or bulk polymerisation methods [5,9]. In the case of solution polymerisation, as monitored by the laser nephelometry technique, (shown diagrammatically below) the rate of polymerisation can be estimated. This is



Diagrammatic representation of the laser nephelometry apparatus used during these investigations.

achieved by measuring the rate of precipitation of polymer. The most suitable monomer for this technique has been established as trimethylolpropane triacrylate (TMPTA). TMPTA exposes the effects of oxygen inhibition [10], and forms a highly crosslinked polymer. Therefore, the amount of precipitation obtained after irradiation closely reflects the extent to which polymerisation has occurred. Bulk polymerisation techniques which employ the amount of precipitable polymer to show the extent of polymerisation can give a false indication of photoinitiator efficiency. If the photoinitiating system leads to low molecular weight oligomers because of various competitive reactions, such as efficient chain transfer, and if these low molecular weight oligomers are soluble in the solvents employed for precipitation, a true impression of the photoinitiating efficiency will not be observed.

The percentage of oxygen present in the TMPTA solution or bulk monomer, plus a contribution from atmospheric oxygen which diffuses into the mixture during irradiation, leads to the reactions exhibiting induction periods [4,11]. The induction periods formed as a consequence of oxygen inhibition will therefore lead to inaccuracies in the determination of photoinitiator efficiency. The oxygen present in the reaction mixture will slow down the initiation process by scavenging the radicals available for the initiation of polymerisation, thus reducing their concentration. Oxygen inhibition is a particularly important problem encountered in the production of surface coatings [12] and requires special precautions to be taken in order to reduce its overall effect. Both laser nephelometry and bulk polymerisation examinations can be carried out with the exclusion of oxygen. Thus the rate of

polymerisation will primarily reflect the rate of chain propagation which can be influenced by photoinitiator efficiency. The efficiency of the photoinitiator system is related to the time taken to reach the normal rate of polymerisation. This time in deoxygenated systems however, is often extremely short and difficult to determine with any degree of accuracy. Nevertheless, despite the limitations of both techniques they can be very useful for screening photoinitiators for efficiency.

Free Radical Polymerisation of Vinyl Monomers

The polymerisation of unsaturated monomers by free radicals typically involves a chain reaction. The polymerisation proceeds by a complex mechanism of initiation, propagation, and termination typical of chain reactions in low molecular weight species (see Chapter 1). When free radicals are formed in the presence of vinyl monomer, the radical adds onto the carbon-carbon double bond with the regeneration of another radical species. The chain radical formed will propagate by reacting with the surrounding monomer molecules to form long chains, the active site being shifted to the end of the chain when a new monomer is added [13-15]. The lifetime of a growing polymer chain is short, and long-chain polymer is formed at every degree of conversion. The overall rate of polymerisation is proportional to monomer concentration and follows first order kinetics. The polymerisation of certain monomers, either in solution or bulk concentrations, is accompanied by a marked deviation from first order kinetics. This

is shown by an increase in the reaction rate and molecular weight, and is known as autoacceleration or the gel effect [16]. This effect is particularly pronounced in the case of methyl methacrylate (MMA).

The gel effect occurs when the rate at which the polymer molecules diffuse through the viscous medium decreases. This is coupled with the subsequent lowering of the ability of two long chain radicals to come together and terminate. The dependence of diffusion rate on the viscosity of the medium (termination is in fact diffusion controlled for most liquid phase polymerisations) leads to the gel effect at high polymer concentrations and with high molecular weight polymers. The decrease in the rate of termination leads to an overall increase in the concentration of radicals, the rate of polymerisation, the molecular weight and the average polymer chain length because the lifetime of the growing chains has increased. This leads to still larger reductions in the termination rate until high conversions of 70 - 90%. Here the rate of polymerisation drops to a very low value as the system becomes glassy and monomer diffusion to the growing chain ends becomes severely inhibited [13-16].

Bulk Polymerisation

Bulk polymerisation involves the direct conversion of liquid monomer to polymer in a reaction system whereby the polymer remains soluble in its own monomer. The bulk polymerisation of acrylic monomers is characterised by a rapid acceleration

in the rate (in the case of MMA, an autoacceleration is observed between 20 - 40% [13]) and the formation of a crosslinked insoluble polymer network at low conversion [14] (which leads to a narrow molecular weight distribution). The formation of the polymer network is thought to occur by a chain-transfer mechanism. The abstraction of a hydrogen atom from a neighbouring polymer chain, or oligomer, by the original radical (which dies in the process) generates a new radical at the site of abstraction (see Chapter 1). The subsequent growth of a branch or new chain radical at this point occurs as more monomer molecules are added. Termination can occur by the combination of any two of these branched or chain radicals [15,16].

Solution Polymerisation

Polymerisation of vinyl monomers in solution is very dependent upon the solvent used. The solvent must be capable of dissolving the monomer, photoinitiator and in some cases the resultant polymer. The primary considerations in the selection of a suitable solvent include its reactivity with the active species of the polymerisation and its activity as a potential chain transfer agent. The chain transfer to solvent during solution polymerisation is a disadvantage of this technique which creates difficulties in the control of the polymer's molecular weight.

The type of initiator used for solution polymerisation depends on several factors, including its solubility and its rate of decomposition. During precipitation polymer techniques (e.g.,

the laser nephelometry method), the formation of a polymer which is insoluble in its monomer solution may give rise to deviations from the kinetics of homogeneous radical polymerisation. Normal bimolecular termination reactions are no longer effective due to the trapping of radicals in the unswollen, tightly coiled precipitating polymer. The laser nephelometry method however, measured the initial rate of polymerisation of a dilute monomer solution, therefore the assumption that the rate follows first order kinetics still applies [14-16].

Bulk and solution polymerisation techniques were used to study the potential of acylphosphine oxides and acylphosphonates as photoinitiators for the polymerisation of methyl methacrylate and trimethylol propane triacrylate, together with a preliminary study of a styrene system. Comparisons were drawn in a few cases with conventional photoinitiators, such as benzoin methylether (BME), benzil and 2,2-dimethoxy-2-phenylacetophenone (DMPA). The photoinitiators investigated using these techniques are shown in Figure 1.

(1) Solution Polymerisation Monitored by Laser Nephelometry

The laser nephelometry technique was set up as a preliminary screening method to determine the initiating efficiency of various photoinitiator systems. Comparisons were made initially between the photoinitiating efficiency of the acylphosphine oxides, acylphosphonates and the commercial photoinitiators benzoin methylether (BME), benzoin isopropyl ether (BIE), and

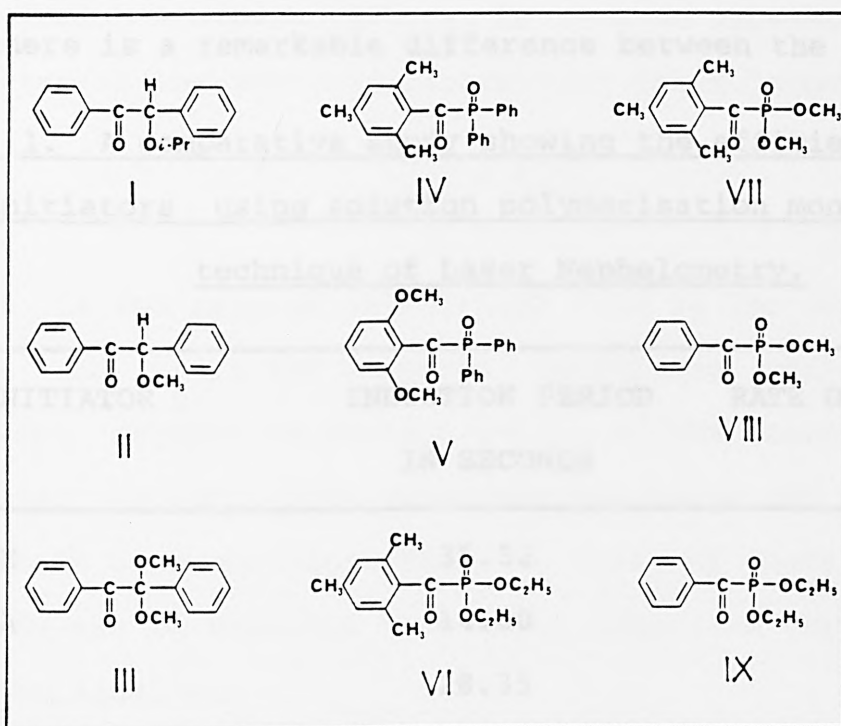


Figure 1. The photoinitiators under investigation.

I = BIPE, II = BME, III = DMPA, IV = TMBPO, V = DMBPO,
VI = TMBEP, VII = TMBMP, VIII = BDMP, IX = BDEP.

RESULTS AND DISCUSSION.

(1) Solution Polymerisation Monitored by Laser Nephelometry.

The laser nephelometry technique was set up as a preliminary screening method to determine the initiating efficiency of various photoinitiator systems. Comparisons were made initially between the photoinitiating efficiency of the acylphosphine oxides, acylphosphonates and the commercial photoinitiators benzoin methylether (BME), benzoin isopropylether (BIPE), and

2,2-dimethoxy-2-phenylaceto phenone (DMPA). The results obtained are shown in Table 1. It can be clearly seen from these results that there is a remarkable difference between the initiating

Table 1. A comparative study showing the efficiency of various photoinitiators using solution polymerisation monitored by the technique of Laser Nephelometry.

PHOTOINITIATOR	INDUCTION PERIOD IN SECONDS	RATE OF POLYMERISATN 10^{-3} S^{-1}
1) BIPE	35.52	3.48
2) DMPA	14.00	4.18
3) BME	28.35	4.10
4) TMBPO	2.01	4.65
5) DMBPO	2.02	4.24
6) BDMP	39.80	3.16
7) BDEP	114.00	0.87
8) TMBEP	54.40	4.31
9) TMBMP	51.70	2.53

efficiency of the acylphosphine oxides and the acylphosphonates with the latter exhibiting very large induction periods (Table 1 entries 6, 7, 8 and 9) compared to the acylphosphine oxides. The difference observed cannot be explained solely on the basis of differences in the absorption properties between the two types of photoinitiator [17]. The photoinitiators absorb UV radiation in a similar wavelength region, although the molar extinction coefficients for each type varies between about $80 \text{ cm}^2 \text{ mol}^{-1}$ for the

benzoylphosphonates and 600 cm² mol for the acylphosphine oxides. The following equation [18] can be used to determine the order of reactivity of the photoinitiators from their induction periods:-

$$RI = \frac{[In]}{t_i} \quad (1)$$

where R_I is the rate of initiation, $[In]$ is the inhibitor concentration and t_i is the measured inhibition period. Since the inhibitor, oxygen, is present in all of the reaction mixtures to a similar extent, its concentration value can be considered constant in each solution. Thus, an order of reactivity for these compounds can be obtained from their induction periods using the following equation:-

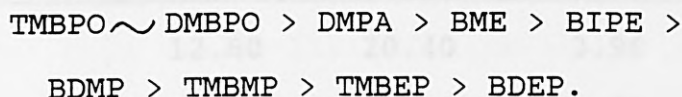
$$R_I \propto 1/t_i \quad (2)$$

It must be stressed that this order of reactivity was derived upon the assumption that each photoinitiator absorbed the same amount of UV light, which in fact was not the case [17]. The purpose of this investigation using the laser nephelometry technique however, was to establish the efficiency of the photoinitiators with respect to each other, under conditions closely associated to those employed in the UV curing process. Under UV curing conditions, the same weight percentage of each photoinitiator would be used regardless of its absorbance characteristics. Similarly, a polychromatic light source (which is also a mercury arc lamp) is used and the UV curable materials are also susceptible to the inhibiting effect of oxygen. Thus, the measurement of induction periods can be considered useful. From the

values obtained, despite assumptions leading to a tolerable level of inaccuracy, the order of reactivity of the organophosphorus type photoinitiators can be expressed as follows:-



Including the other photoinitiators, the order of reactivity becomes:



The synergistic properties of N-methyldiethanolamine and triphenylphosphine sulphide were also investigated, the results are shown in Table 2. The addition of amine appeared to have little perceptible effect upon the induction period or rate of polymerisation initiated by the acylphosphine oxides TMBPO and DMBPO (Table 1 entries 4 and 5, and Table 2 entries 3 and 4), whereas in the case of the benzoylphosphonates BDMP and BDEP (Table 1 entries 6 and 7, and Table 2 entries 5 and 6) the effect of amines was unpredictable. The addition of amine to the substituted acylphosphonates TMBEP and TMBMP resulted in a reduction of the induction period, as anticipated from the oxygen scavenging capabilities of amines, but the rate of polymerisation, especially in the case of TMBEP, was surprisingly reduced also (Table 1 entries 8 and 9, and Table 2 entries 7 and 8). The reduction in the rate of polymerisation may be a result of the amine participating in a chain transfer process, thereby leading to low molecular weight polymers which are soluble in the solvent

Table 2. A comparative study showing the efficiency of various photoinitiators in the presence of N-methyldiethanolamine, and triphenylphosphine sulphide using solution polymerisation monitored by the technique of Laser Nephelometry.

PHOTOINITIATOR	INDUCTION PERIOD		RATE OF POLYMERISATION	
	IN SECONDS		$\times 10^3 \text{ s}^{-1}$	
	N-MDEA	TPPS	N-MDEA	TPPS
1) DMPA	12.60	20.40	3.96	3.59
2) BME	23.60	34.60	4.92	2.57
3) TMBPO	2.10	1.12	6.13	3.96
4) DMBPO	1.26	2.20	5.16	3.03
5) BDMP	89.00	43.90	2.24	1.37
6) BDEP	0	0	0	0
7) TMBEP	18.6	57.30	0.98	2.89
8) TMBMP	36.00	---	2.32	---

Photoinitiator concentration $10^{-2} \text{ mol l}^{-1}$, N-methyldiethanolamine (N-MDEA) concentration $(2 \times 10^{-2} \text{ mol l}^{-1})$, triphenylphosphine sulphide concentration $(1 \times 10^{-1} \text{ mol l}^{-1})$ in TMPTA solution (10g TMPTA in 1 dm³ propan-2-ol).

used for the precipitation of polymer. In the case of the benzoylphosphonate BDEP, the addition of amine inhibited the polymerisation for the duration of the experiment (Table 2 entry 6). The laser nephelometry technique is limited because it does not allow one to assess if any polymerisation occurred during this period to give low molecular weight oligomers which are soluble in the

propan-2-ol.

The conventional photoinitiators, 2,2-dimethoxy-2-phenylacetophenone (DMPA) and benzoin methylether (BME) showed that the addition of amine did not produce particularly dramatic results. This was in agreement with their initiation by the Norrish Type 1 process (Table 1 entries 2 and 3, and Table 2 entries 1 and 2). The effect of added triphenylphosphine sulphide was also investigated. Triphenylphosphine sulphide is known to react with peroxy radicals and for this reason its addition to the reaction mixture should result in a more rapid depletion of oxygen than in the case of amines. Surprisingly, the addition of sulphide to the samples provided had no beneficial effect, but rather the reverse. It is conceivable that the sulphide was acting as a trap for photoinitiating radicals although the precise mechanism for this process is unclear [19,20].

Following the initial screening experiments, attempts were made to elucidate if the observed induction periods were due to the trapping of the photoproduct radicals. The investigations entailed the addition of increasing concentrations of conventional radical scavengers such as ditolyethylene (DTE), diphenylethylene (DPE) and 2,2,6,6-tetramethylpiperidin-1-oxyl (TMPO) to the monomer solution containing TMBPO photoinitiator (Figure 2). The results are shown in Table 3, and in Figures 3a and 3b. Increasing the concentration of these radical scavengers in the TMBPO/monomer solution led to an increase in the induction period, with the rates of polymerisation showing similar values regardless of scavenger concentration. The amount of polymer

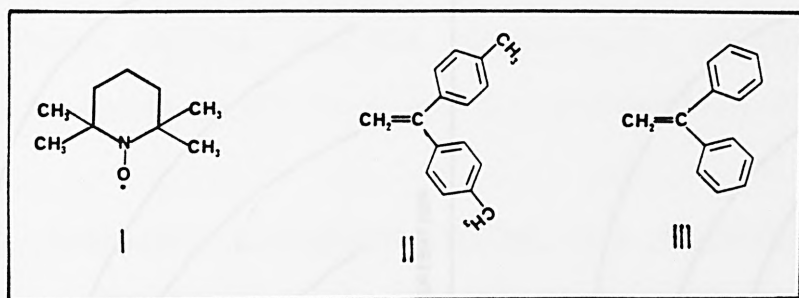


Figure 2. Conventional radical scavengers, I = TMPO, II = DTE, III = DPE.

precipitated decreased with an increase in the concentration of added scavenger. This result (Figures 3a and 3b) was expected. If, under the experimental conditions, the initiator was almost completely consumed by radical scavengers, this would lead to fewer radicals being produced which could initiate polymerisation. Considering the relative concentrations of the scavengers

Table 3. Examination of the effect of radical scavengers upon the photopolymerisation induced by TMBPO using the technique of Laser Nephelometry.

RADICAL SCAVENGER		INDUCTION PERIOD	RATE OF POLYMERISATION
3	-1		3 -1
CONC. x10	MOL L	IN SECONDS	x10 S .
DPE	1	2.70	4.32
	2	4.43	3.59
	3	5.93	2.72
	3.6	6.68	2.04
DTE	1	3.36	3.45
	2	5.05	2.84
	3	6.90	2.43
	4	9.24	2.00
TMPO	1	3.36	3.36
	2	4.32	3.10
	3	6.00	2.49
	4	6.60	2.39

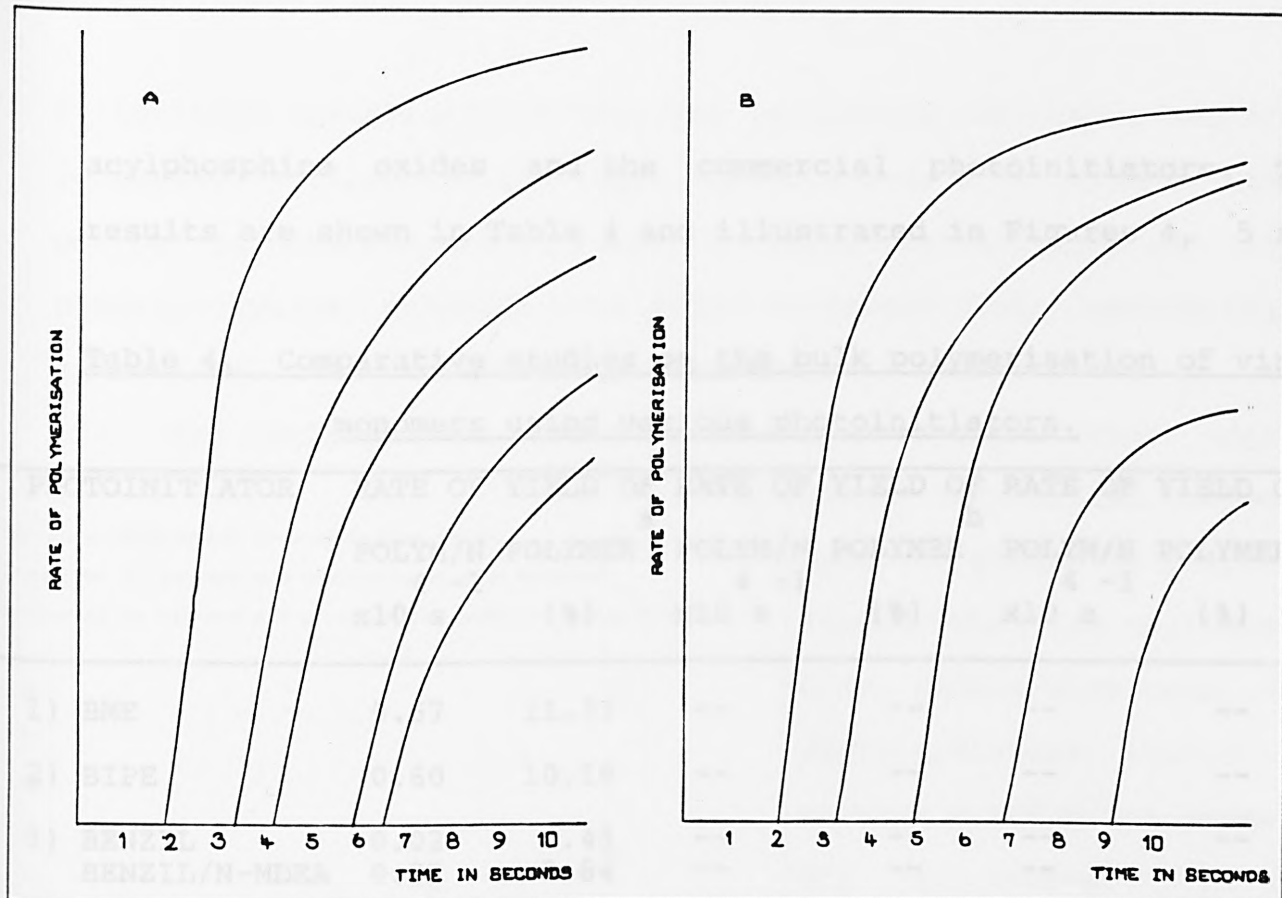


Figure 3 Effect of radical scavengers a) 2,2,6,6,-tetramethylpiperidinoxyl and b) ditolyethylene upon the photopolymerisation induced by TMBPO using the technique of Laser Nephelometry.

compared with TMPTA, it was concluded that the photogenerated radicals reacted with the scavengers far more efficiently than with the TMPTA monomer. It was interesting to note during this investigation that DPE was slightly less efficient as a radical scavenger than DTE. This was attributed to the ability of DPE to form a radical adduct which can react via the free para position of the phenyl groups with other radicals e.g., growing radical chains [21].

2) Bulk polymerisation of Methyl Methacrylate (MMA) and Styrene.

Following the solution polymerisation experiments, a second series of comparisons were made between the acylphosphonates,

acylphosphine oxides and the commercial photoinitiators. The results are shown in Table 4 and illustrated in Figures 4, 5 and

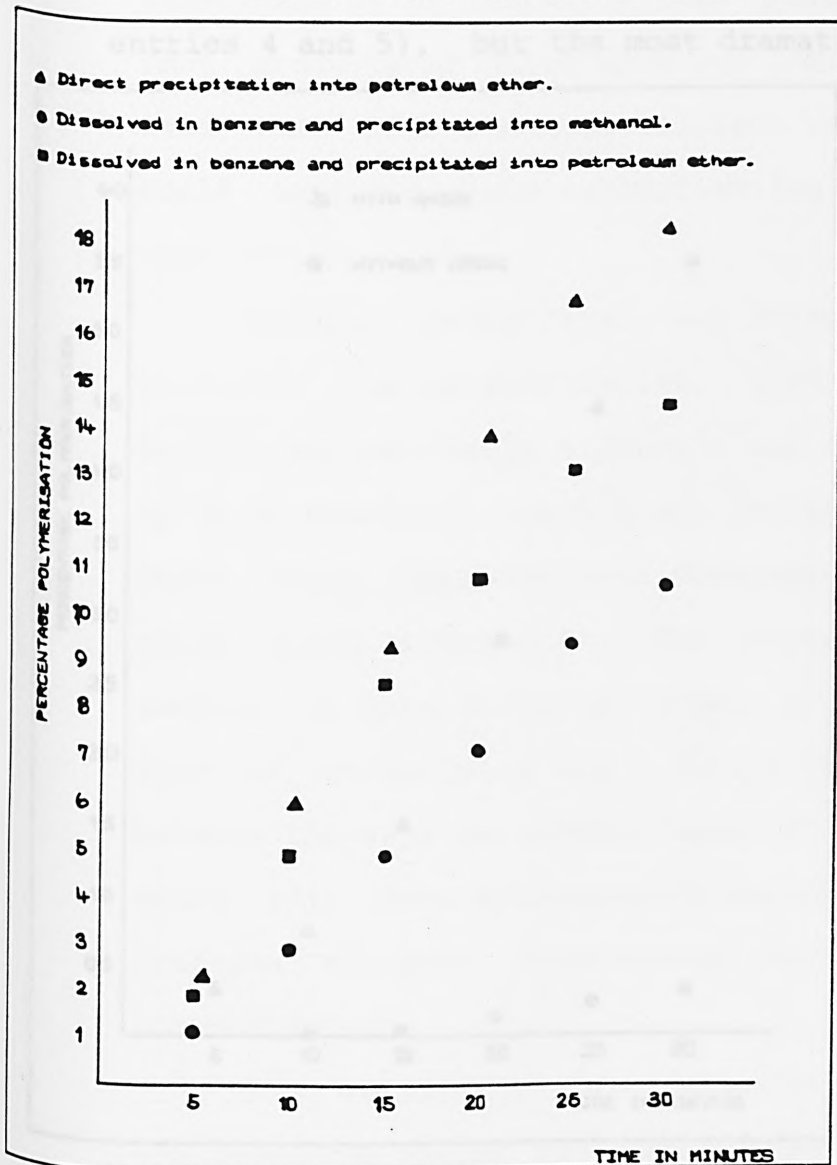
Table 4. Comparative studies on the bulk polymerisation of vinyl monomers using various photoinitiators.

PHOTOINITIATOR	RATE OF YIELD OF ^a		RATE OF YIELD OF ^b		RATE OF YIELD OF ^c	
	POLYM/N ^{4 -1} x10 s	POLYMER (%)	POLYM/N ^{4 -1} x10 s	POLYMER (%)	POLYM/N ^{4 -1} x10 s	POLYMER (%)
1) BME	0.67	11.37	--	--	--	--
2) BIPE	0.60	10.19	--	--	--	--
3) BENZIL	0.02	0.43	--	--	--	--
BENZIL/N-MDEA	0.22	3.84	--	--	--	--
4) TMBPO	1.22	19.66	0.62	10.65	0.87	14.51
TMBPO/N-MDEA	1.34	21.50	--	--	--	--
TMBPO/TPPS	1.15	18.74	--	--	--	--
5) DMBPO	1.18	19.17	0.86	14.27	0.96	15.85
DMBPO/N-MDEA	1.31	20.96	--	--	--	--
DMBPO/TPPS	1.28	20.57	--	--	--	--
6) BDEP	0.01	0.27	0.0	0.0	--	--
BDEP/N-MDEA	0.33	5.82	0.27	4.73	--	--
7) BDMP	0.02	0.38	0.00	0.00	0.02	0.32
BDMP/N-MDEA	0.37	6.38	0.41	7.19	0.32	5.51
8) TMBEP	0.53	9.12	--	--	--	--
TMBEP/N-MDEA	0.43	7.47	--	--	--	--
9) DMPA #	--	--	0.05	0.98	0.08	1.44
10) TMBPO #	--	--	0.20	3.52	0.21	3.65

Concentrations, photoinitiator = 2.5×10^{-4} mol l⁻¹; N-methyldiethanolamine (N-MDEA) = 1.25×10^{-1} mol l⁻¹; triphenylphosphine sulphide (TPPS) = 5×10^{-4} mol l⁻¹. # Styrene used instead of methyl methacrylate; a = method A; b = method B and c = method C.

6. In these investigations both the initiating efficiency and the percentage polymerisation were measured over a 30 minute time period in both MMA and styrene. N-methyldiethanolamine and tri-phenylphosphine sulphide were added to assess their synergistic value under these experimental conditions.

The bulk polymerisation results also revealed that added

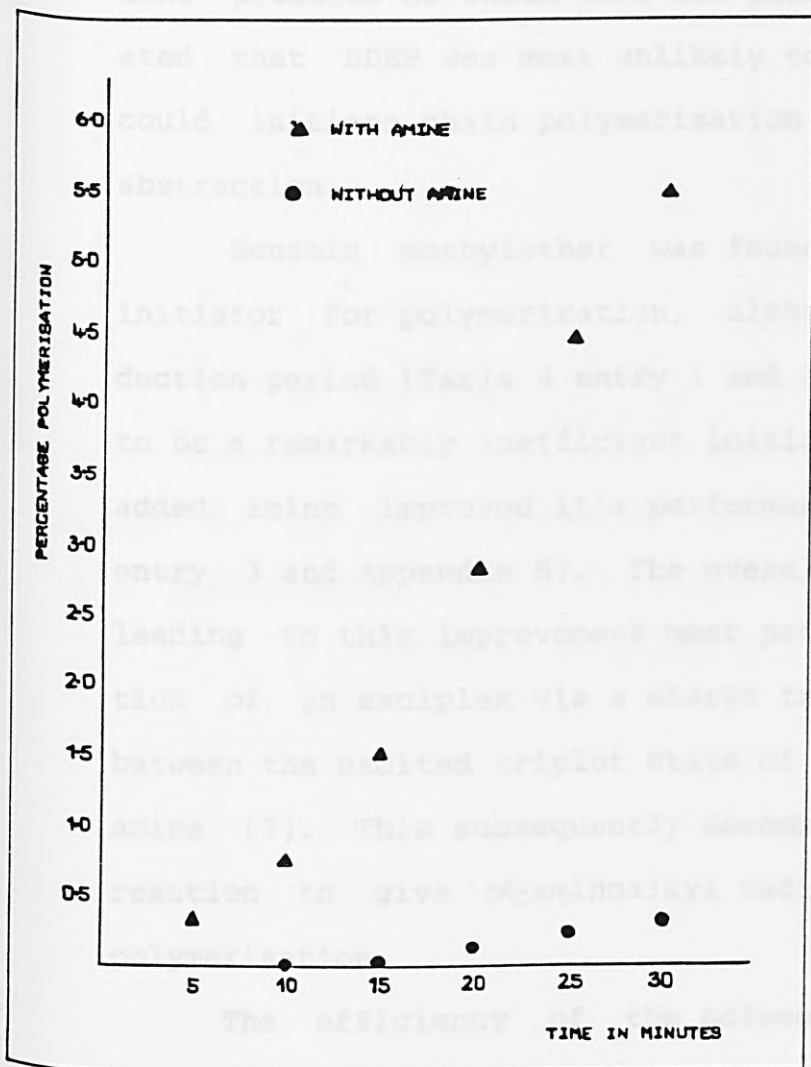


amine had little effect upon the amount of polymer formed when the acylphosphine oxides were used as photoinitiators (Table 4 entries 4 and 5 and Appendix B). However, the amount of measurable polymer formed was dependent upon the precipitating solvent used (Table 4 and Figure 4). The plot and the results show that in all cases the amount of precipitate formed in methanol was much less than that formed in petroleum ether. This result probably stems from a greater

Figure 4. The percentage methyl methacrylate polymer precipitated using 3 different precipitation methods, following bulk polymerisation induced by TMBPO.

solubility of the lower molecular weight oligomers in methanol compared with petroleum ether.

Under the conditions used for the bulk polymerisation investigations, the effect of added amine was more marked in the case of the substituted acylphosphonates (Table 4 entry 8 and Appendix B) compared with the acylphosphine oxides (Table 4 entries 4 and 5), but the most dramatic effect occurred with the



benzoylphosphonates (Table 4 entries 6 and 7, and Figure 5). The amount of precipitated polymer was vastly increased when amine was added to the photoinitiators BDEP and BDMP in MMA. This result may be due to the excited triplet states of the benzoylphosphonate abstracting hydrogen from the amine present to give an α -aminoalkyl radical which is capable of initiating polymerisation, in preference to intramolecular

Figure 5. The percentage of methyl methacrylate polymer precipitated (method C) following bulk polymerisation induced by benzoyldiethylphosphonate in the presence and absence of N-methyldiethanolamine.

hydrogen abstraction [22]. The result obtained was in direct contradiction of a recent report [23] whereby BDEP was found to be incapable of initiating the polymerisation of MMA. This claim was based upon the observation that the BDEP triplets, which did not undergo an α -cleavage reaction, were rapidly converted to biradicals by an intramolecular hydrogen abstraction, the subsequent products of which were not identified. It was also postulated that BDEP was most unlikely to form ketyl radicals which could initiate chain polymerisation by intermolecular hydrogen abstraction.

Benzoin methylether was found to be an efficient photoinitiator for polymerisation, although it had a discernable induction period (Table 4 entry 1 and Appendix B). Benzil was found to be a remarkably inefficient initiator, although the effect of added amine improved its performance substantially (Table 4 entry 3 and Appendix B). The overall radical generation process leading to this improvement most probably stems from the formation of an exciplex via a charge transfer type of interaction between the excited triplet state of benzil with the ground state amine [7]. This subsequently decomposes via a proton transfer reaction to give α -aminoalkyl radicals capable of initiating polymerisation.

The efficiency of the polymerisation of styrene by an acylphosphine oxide was also studied and it can be seen from the results that the efficiency is similar to that obtained with 2,2-dimethoxy-2-phenylacetophenone (Table 4 entries 9 and 10, and Figure 6).

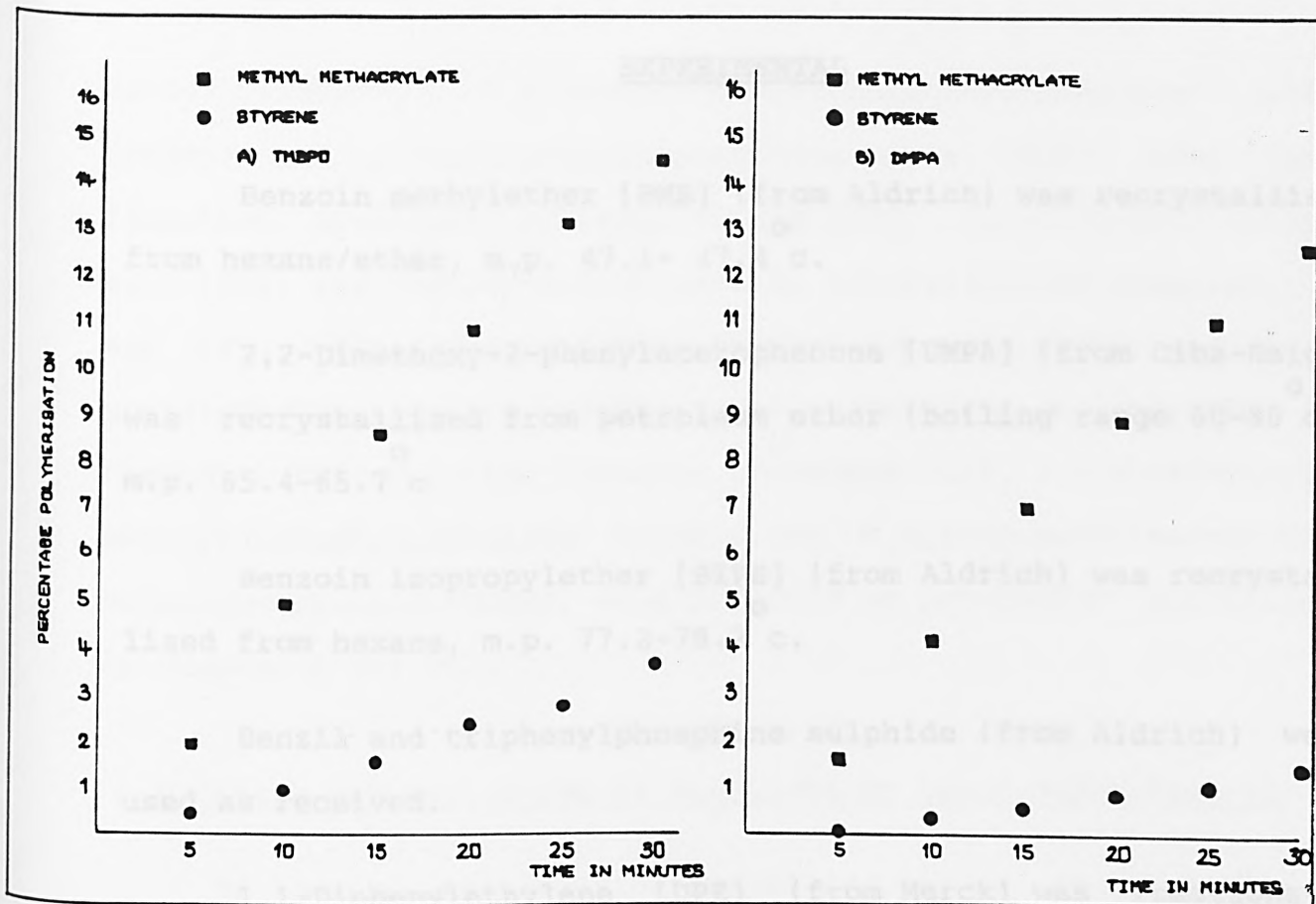


Figure 6. The percentage methyl methacrylate and styrene polymers precipitated (method C) following bulk polymerisation induced by a) TMBPO and b) DMPA.

ACKNOWLEDGEMENTS

The contribution of Gerard Hakvoort is most gratefully acknowledged for setting up and maintaining the laser nephelometry apparatus in good working order.

EXPERIMENTAL

Benzoin methylether [BME] (from Aldrich) was recrystallised from hexane/ether, m.p. 47.1- 47.4 °C.

2,2-Dimethoxy-2-phenylacetophenone [DMPA] (from Ciba-Geigy) was recrystallised from petroleum ether (boiling range 60-80 °C), m.p. 65.4-65.7 °C.

Benzoin isopropylether [BIPE] (from Aldrich) was recrystallised from hexane, m.p. 77.2-78.2 °C.

Benzil and triphenylphosphine sulphide (from Aldrich) were used as received.

1,1-Diphenylethylene [DPE] (from Merck) was fractionated prior to use; the middle fraction, b.p. 79-80 °C (at 0.3 m.bar) was used in these experiments.

2,2,6,6-Tetramethylpiperidinoxyl [TMPO] and N-Methyldiethanolamine [N-MDEA] (from Aldrich) were used as received.

Methyl methacrylate [MMA] and styrene [STY] (from Aldrich), and trimethylolpropane triacrylate [TMPTA] (Synthese b.v.) were used as received without further purification (the amount of inhibitor in the monomers is substantially less than the amount of photoinitiator employed).

Benzene, methanol and petroleum ether (boiling range 60-80 °C) (from BDH) and propan-2-ol (Baker) were used as received.

The synthesis of 2,4,6-trimethylbenzoyldiphenylphosphine

oxide (TMBPO), 2,6-dimethoxybenzoyldiphenylphosphine oxide (DMBPO) and pivaloyldiphenylphosphine oxide (PDPO) have been described previously (Chapter 2) and [24]. 1,1-di(p-tolyl)ethylene (DTE) was available from earlier investigations (Chapter 3) and [25]. Similarly benzoyldimethylphosphonate (BDMP) and benzoyldiethylphosphonate (BDEP) were synthesised as described in Chapter 2 following the reported procedure [26]. 2,4,6-trimethylbenzoyldiethylphosphonate (TMBEP) and 2,4,6-trimethylbenzoyldimethylphosphonate (TMBMP) were prepared as previously described in Chapter 2 [25,26].

Solution Polymerisation as Monitored by Laser Nephelometry.

To monitor the solution polymerisation of trimethylolpropane triacrylate (TMPTA), a trifunctional monomer, the apparatus was assembled as previously described [4]. During these experiments the laser beam passed through a 4 x 1 cm² polystyrene cuvette (from Witeg) which contained the monomer solution under investigation. The He-Ne laser (632.8 nm) had been adjusted previously to obtain a linear response of the photodiode when the intensity of the laser beam was decreased by interposing neutral density filters. Upon the exposure to UV radiation from a high pressure mercury lamp (90 Watts) encased in a spectral lamphouse (supplied by Ealing), the TMPTA solution containing photoinitiator formed a translucent white gel. The appearance of the gel was due to the formation of a crosslinked polymer which was insoluble in propan-2-ol. As the turbidity of the irradiated sample increased the laser beam became attenuated, causing the intensity

of the transmitted light detected by the photodiode to drop rapidly. Thus the curves recorded by this device directly reflect the kinetics of the polymerisation process [4].

The photopolymerisation of the monomer solution, prepared by dissolving 10g of TMPTA in 1 litre of propan-2-ol, by the photoinitiators was usually completed within a few seconds. The rate of polymerisation, R_p , was estimated from the slope of the curves plotted on the chart recorder. A calibration curve was used to standardise each series of results so that comparisons of photoinitiator efficiency could be drawn with some confidence. The instrument had been calibrated by plotting the amount of polymer formed (as determined by gravimetry) against time (measured in seconds) for a standard photoinitiator system (see Appendix A).

A variety of conditions were used to determine the photoinitiating efficiency of each photoinitiator. Initial investigations were performed using photoinitiator concentrations of 10^{-2} mol l⁻¹ in monomer solution. In other reactions the effect of adding tertiary amine (2×10^{-2} mol l⁻¹) and triphenylphosphine sulphide (1×10^{-1} mol l⁻¹) was investigated. To investigate inhibition effects, radical scavengers ditolyethylene (DTE), diphenylethylene (DPE) and 2,2,6,6-tetramethylpiperidin-1-oxyl (TMPO) were used as possible inhibitors of the polymerisation process. The solutions investigated were prepared maintaining a constant photoinitiator concentration of 10^{-2} mol l⁻¹ and an increasing radical scavenger concentration from 1×10^{-3} mol l⁻¹ to 4×10^{-1} mol l⁻¹.

Bulk Polymerisation of Methyl Methacrylate and Styrene.

A general procedure was established and then followed for each photoinitiator, photoinitiator-amine system. The photoinitiator ($2.5 \times 10^{-4} \text{ mol l}^{-1}$) was dissolved in MMA (20g). When the effect of amine was investigated, triethanolamine ($1.25 \times 10^{-3} \text{ mol l}^{-1}$) was added to the mixture and thoroughly mixed. The solution was irradiated in a stoppered pyrex tube (280 x 13 mm) in duplicate and the tube was rotated around a water-cooled medium pressure mercury lamp (Applied Photophysics Ltd., 450 Watts) over a timed period. Immediately following irradiation the solution was syringed into a flask containing 100 cm³ petroleum ether (boiling range 60-80 °C) which was vigorously agitated with a mechanical stirring device throughout the addition. The precipitated polymer was collected on a pre-weighed sinter, washed with petroleum ether and dried in a vacuum desiccator until a constant weight was obtained.

To establish the efficiency of the method used, variations of the precipitation technique were tried. Method A was assigned to the procedure described above. Method B was assigned to a procedure whereby the irradiated solution was dissolved in benzene before being syringed into a flask containing methanol at -5 °C. This was to ensure that the monomer/polymer solution, now of an increased viscosity, was totally removed from the tube prior to precipitation. For method C, the irradiated solution was also dissolved in benzene, but in this instance the solution was syringed into petroleum ether at -5 °C.

APPENDIX A

The Calibration of the Laser Nephelometry Apparatus.

From the tangent of the slope for each plot recorded during the laser nephelometry experiments, the rate of polymerisation R_{est} was estimated by a comparison with a calibration curve of the instrument. In a previous report [4], R_{est} was measured using a calibration curve obtained by plotting the transmitted laser light against the amount of polymer formed, which had been determined by gravimetric methods. The calibration curve for the instrumentation used in these investigations was determined by plotting the amount of polymer (TMPTA) precipitated (as determined by gravimetry) against time, (t in seconds).

To calibrate the instrument, a standard solution was prepared. The standard used was a 10^{-2} mol solution of BIPE which had been dissolved in the monomer solution (10g of TMPTA in 1 litre of propan-2-ol). Initially 5×3.5 cm³ samples were irradiated (as described previously) to establish an average value for the induction period, and also the time required to reach the point of maximum deflection on the resultant rate curve. From the recorded data the average value for the induction period was found to be 39.84 seconds and the maximum point of deflection of the plotted curve occurred at 58.2 seconds. Using this information, 10×3.5 cm³ samples were irradiated from and including 40 to 58 seconds at 2 second intervals, so that 10 points along the curve would be sampled. The 10 samples of polymer precipitated for each specific irradiation time were collectively filtered

through a pre-weighed sintered glass crucible and washed with about 10 cm³ of methanol before being dried in a vacuum desiccator until a constant weight was obtained.

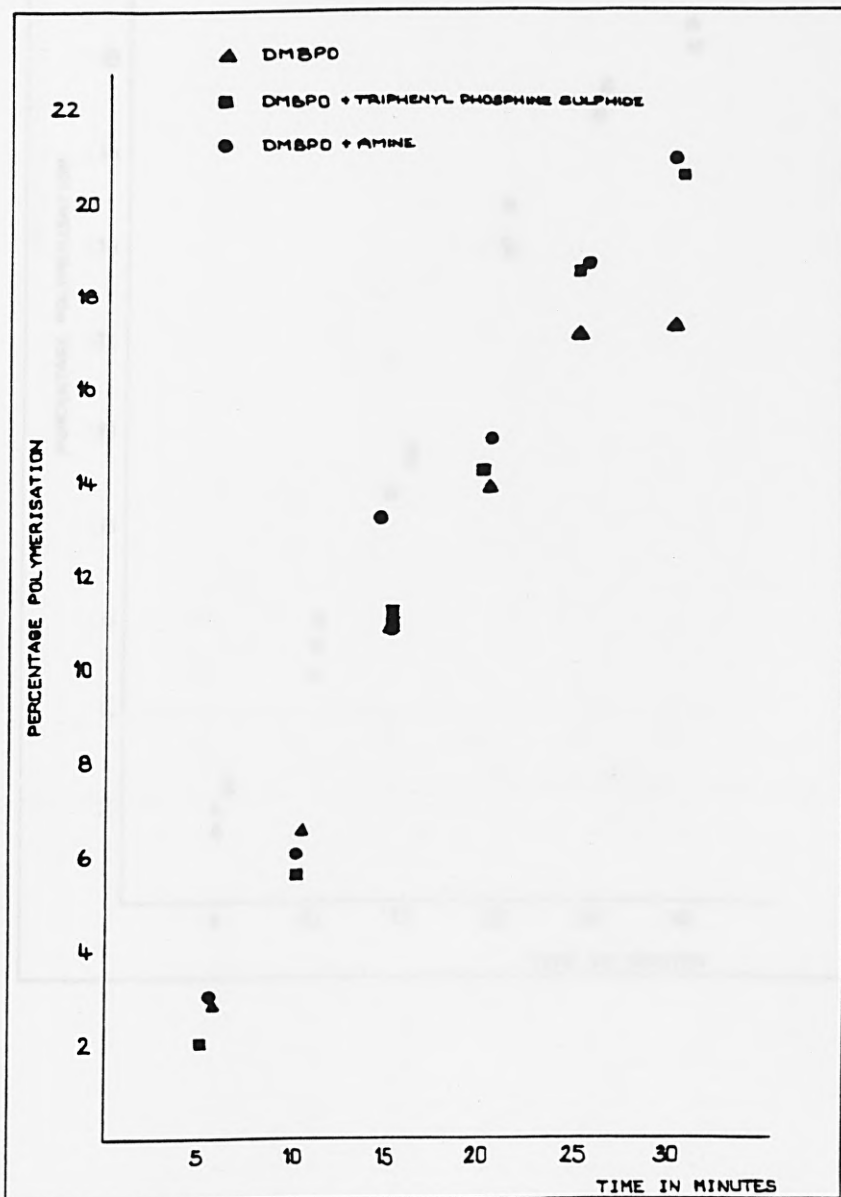
As the molecular weight of TMPTA is not known precisely, the actual concentration of the TMPTA solution could not be determined with any degree of accuracy, thus an equivalent concentration value was calculated and used for the calibration curve. First order kinetics were applied to the treatment of the data. From the plot of $\ln C$ (where C is the equivalent concentration of the TMPTA solution) against time t (in seconds) the first order rate constant was calculated to be $3.4778 \times 10^{-3} \text{ sec}^{-1}$.



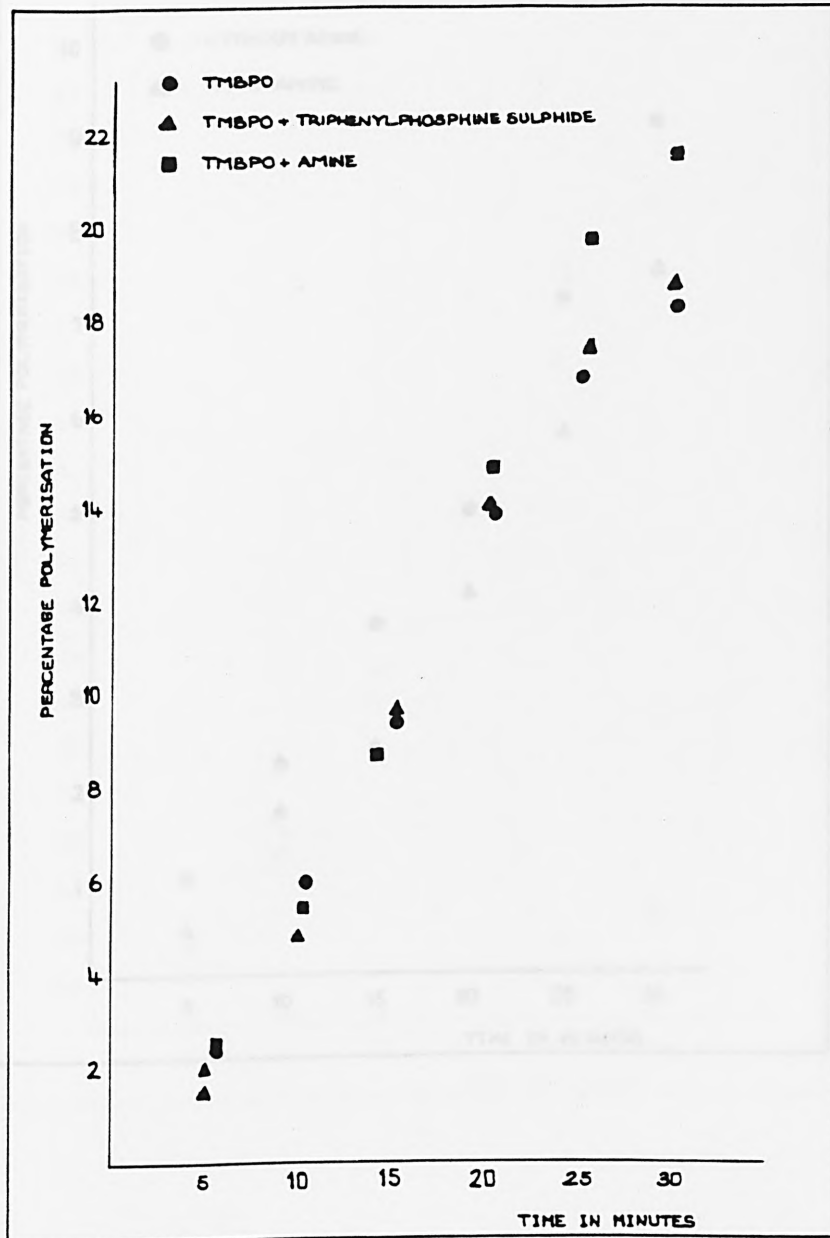
APPENDIX B

A selection of bulk polymerisation results are illustrated to show the effect of added synergist upon the percentage polymerisation of MMA.

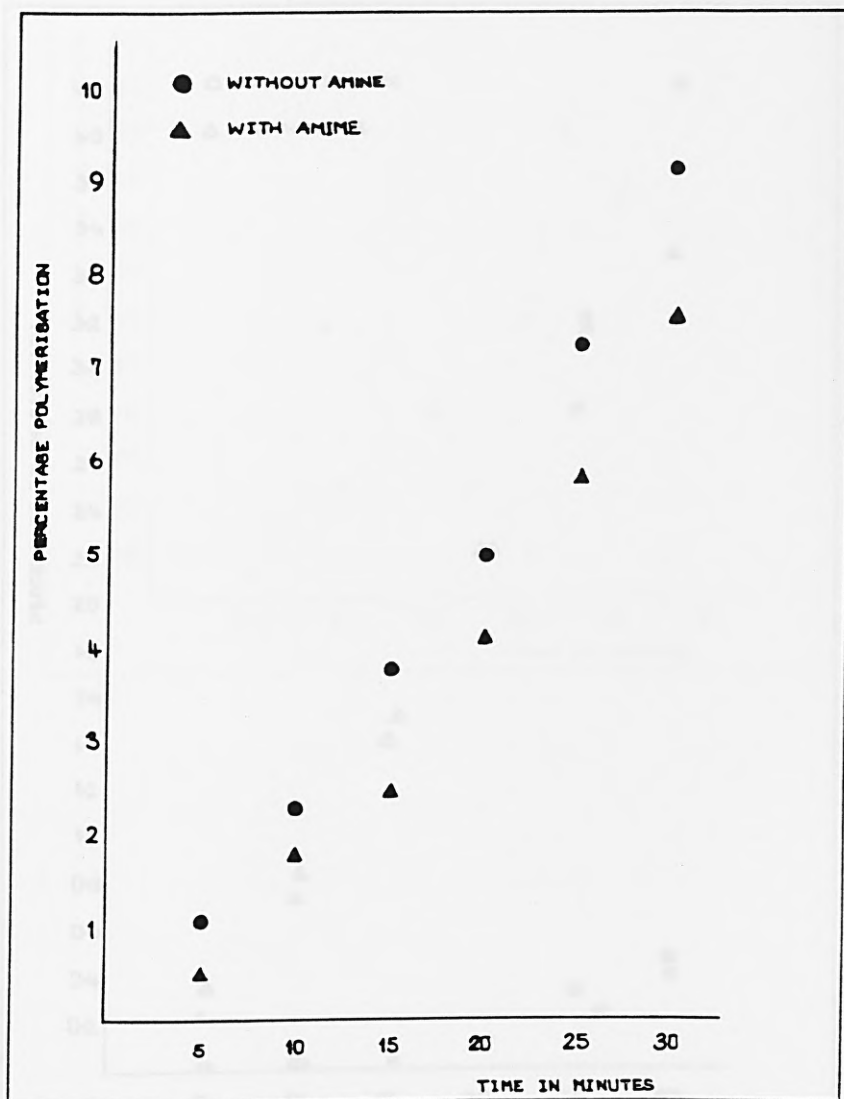
The percentage of methyl methacrylate polymer precipitated following bulk polymerisation induced by DMBPO in the presence and absence of N-methyldiethanolamine and triphenylphosphine sulphide.



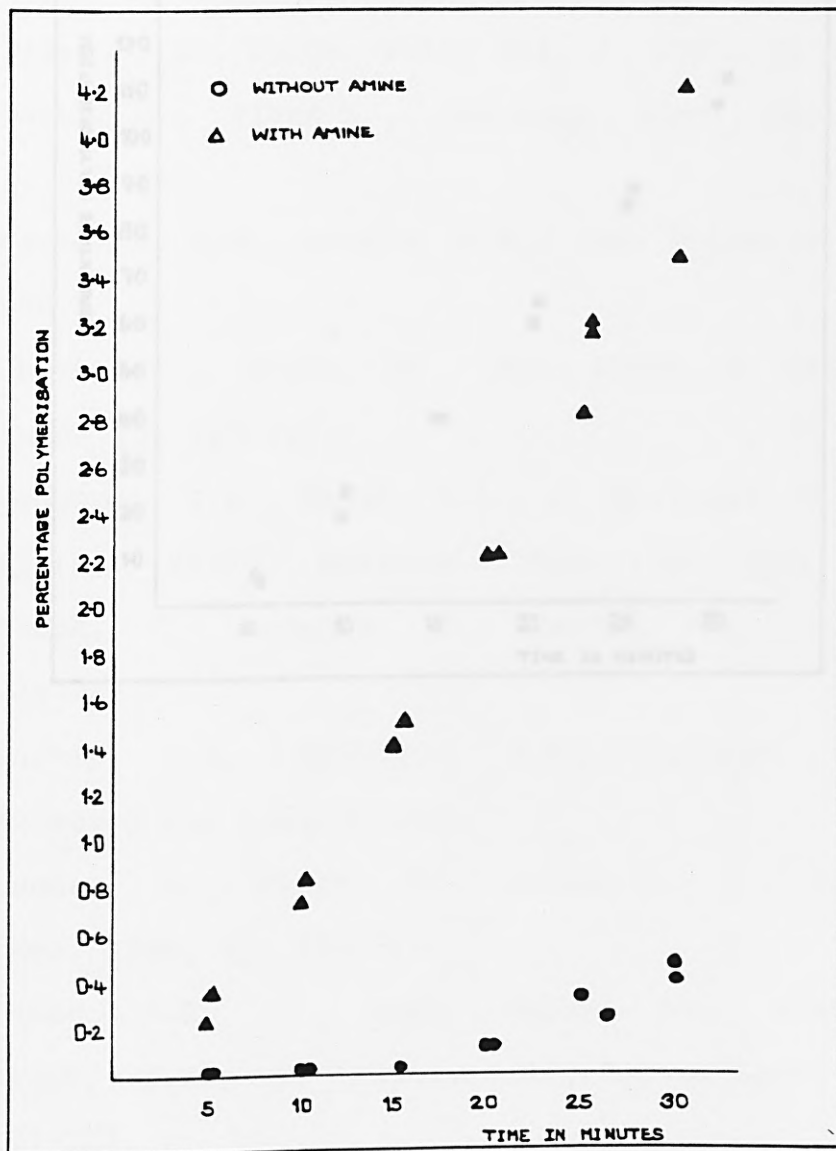
The percentage of methyl methacrylate polymer precipitated following bulk polymerisation induced by TMBPO in the presence and absence of N-methyldiethanolamine and triphenylphosphine sulphide.



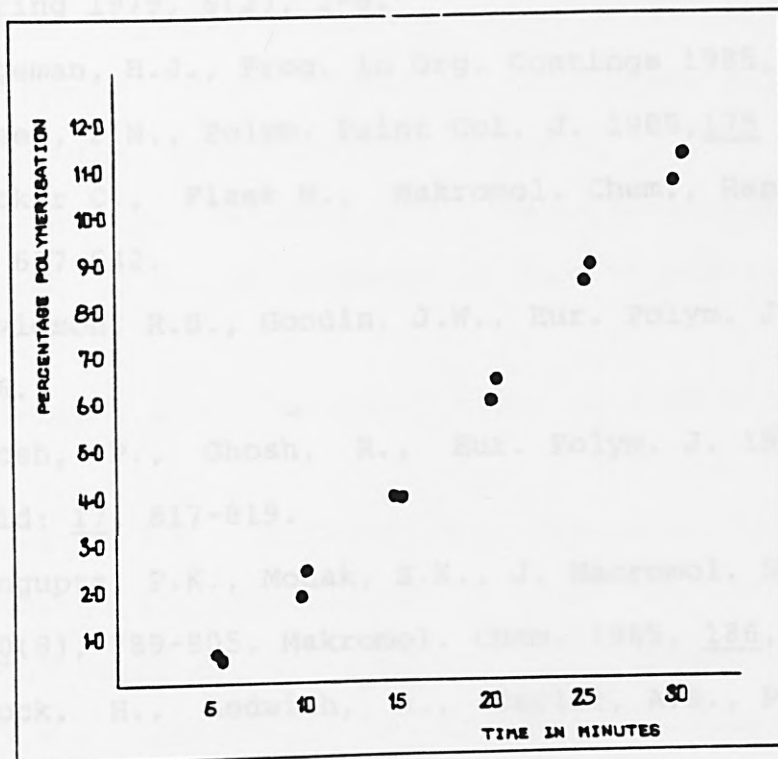
The percentage of methyl methacrylate polymer precipitated following bulk polymerisation induced by TMBEP in the presence and absence of N-methyldiethanolamine.



The percentage of methyl methacrylate polymer precipitated following bulk polymerisation induced by Benzil in the presence and absence of N-methyldiethanolamine.



The percentage of methyl methacrylate polymer precipitated following bulk polymerisation induced by BME.



[1] Berner, G., Pogliani, J., Kirchmayr, R., Plast. K., J. Appl. Polym. Sci., 1978, 23(1), 209.

[2] Reisman, R.J., Prog. in Org. Coatings 1985, 11, 123-150.

[3] Gruber, H., Polym. Paint Col. J. 1985, 112, 141, 148-150.

[4] Decker, C., Plast. K., Makromol. Chem., Rapid Commun. 1980, 1, 1-4.

[5] Decker, C., Hoadin, J.W., Eur. Polym. J. 1982, 18, 107-110.

[6] Ghosh, R., Eur. Polym. J. 1984, 20, 543-549.

[7] Sengupta, P.K., Novak, S.K., J. Macromol. Sci.-Chem., 1983, 17(9), 1619-1625.

[8] Blok, H., Eur. Polym. J. 1971, 7, 271-280.

[9] Baxter, J.E., Davidson, S.A., Reisman, R.J., Polymer, accepted for publication.

[10] Decker, C., Plast. K., Faure, J., J. Org. Coat. Plast. Chem. 1980, 12, 710-715.

[11] Chong, J.S., J. Appl. Polym. Sci., 1983, 11, 241-247.

[12] Wight, F.S., J. Polym. Sci., Polym. Lett. Ed., 1973, 11, 121-127.

[13] Decker, C., Sengupta, P., Plast. K., Faure, J., Conference Report, Recharge VI, Vol. 4-6, (1985), Basel, Switzerland.

[14] Louis, S.M., Sengupta, P., Seng, D.P., J. Appl. Polym. Sci., 1983, 19, 1985-1992.

[14] Novak, S. W., Kline, E. S., Encyclopedia of Polymer Science

REFERENCES

- [1] Berner, G., Puglisi, J., Kirchmayr, R., Rist, G., J. Rad. Curing 1979, 6(2), 2-9.
- [2] Hageman, H.J., Prog. in Org. Coatings 1985, 13, 123-150.
- [3] Green, P.N., Polym. Paint Col. J. 1985, 175 4141, 246-252.
- [4] Decker C., Fizet M., Makromol. Chem., Rapid Commun. 1980, 1, 637-642.
- [5] Davidson, R.S., Goodin, J.W., Eur. Polym. J. 1982, 18, 597-606.
- [6] Ghosh, P., Ghosh, R., Eur. Polym. J. 1981, 17, 545-549, *ibid*; 17, 817-819.
- [7] Sengupta, P.K., Modak, S.K., J. Macromol. Sci.-Chem., 1983, A20(8), 789-805. Makromol. Chem. 1985, 186, 1593-1604.
- [8] Block, H., Ledwith, A., Taylor, A.R., Polymer 1971, 12, 271-288.
- [9] Baxter, J.E., Davidson, R.S., Hageman, H.J., Polymer, accepted for publication.
- [10] Decker, C., Fizet, M., Faure, J., J., Org. Coat. Plast. Chem. 1980, 42, 710-715.
- [11] Chong, J.S., J., Appl. Polym. Sci., 1969, 13, 241-247. Wight, F.R., J. Polym. Sci., Polym. Lett. Ed., 1978, 16, 121-127.
- [12] Decker, C., Bendaikha, T., Fizet, M., Faure, J., Conference Report, Radcure 85, May 6-8, (1985), Basel, Switzerland.
- [13] Louie, B.M., Carratt, G.M., Soong, D.S., J. Appl. Polym. Sci., 1985, 30, 3985-4012.
- [14] Novak, R. W., Kine, R. B., Encyclopedia of Polymer Science

- and Technology. Vol 1, 265-272 and Tate, D. P., Bethea, T. W., Vol 2, 500-506, Wiley Int.
- [15] Lenz, R. W., Encyclopedia of Chemical Technology, Kirk-Othmer, Vol 18, Chapter 5, 740-741, Wiley Inter.
- [16] Billmeyer, F.W., Textbook of Polymer Science, 3rd Edn., Wiley-Int, 1984, Chapters 3 and 5.
- [17] Baxter J.E., Davidson R.S., to be published.
- [18] Eaton, D.F., in Advances in Photochemistry Vol 13, pp 427-487.
- [19] Buckland, S.J., Davidson, R.S., J. Photochem. 1987, 36, 39-49.
- [20] Baxter, J.E., Davidson, R.S., Hageman, H.J., Walker, M.D., Accepted for publication, J. Chem. Res (S) 1988.
- [21] Angad Gaur, H., Groenenboom, C.J., Hageman, H.J., Hakvoort, G.T.M., Oosteroff, P., Overeem, T., Polman, R.J., van der Werf, S., Makromol Chem, 1984, 185 1795-1808. Kice, J.L., Taymoorian, F., J. Amer. Chem Soc., 1959, 81 3405-
- [22] Terauchi, K., Sakurai, H., Bull. Chem Soc Japan, 1970, 43 883-890.
- [23] Sumiyoshi T., Schnabel W., Henne A., J. Photochem. 1985, 30 63-80: *ibid*, J. Photochem. 1986, 32, 119-130.
- [24] Baxter J.E., Davidson R.S., Hageman H.J., Overeem, T., Makromol. Chem., Rapid Commun. 1987, 8, 311-314.
- [25] Baxter, J.E., Davidson, R.S., Hageman, H.J., Overeem, T., to be published.
- [26] Marmor, R.S., Seyferth, D., J. Org. Chem. 1971, 36(1) 128-136.

Chapter 5

The Photopolymerisation of Non-Pigmented Films (Acrylate and Unsatutated Polyester)

Chapter 5	The Photopolymerisation of Non-Pigmented Films (Acrylate and Unsaturated Polyester)	
	Introduction	193
	Photoinitiator Concentration and Film Thickness	195
	Oxygen Inhibition and Autooxidation	198
	Results and Discussion	201
	Acknowledgements	218
	Experimental	219
	References	221

INTRODUCTION

UV curing is widely recognised as an efficient method which can be used to improve the performance of surface coatings with the additional benefits of reduced energy consumption, increased production speed and lower volatile organic components. Thus the production of surface coatings by the polymerisation of low molecular weight materials using UV light is a growing industry. The utility and improvement of this technique depends upon many integrating factors, one of the most important being the development of efficient photoinitiators. Many efforts have been directed towards gaining an understanding of the mechanistic action of photoinitiators under various conditions to achieve this aim [1,2].

In this chapter, the photoinitiating efficiency of an established commercial photoinitiator was compared with a "new, novel class of photoinitiators" [3]. At this stage it is important to point out that the performance of a photoinitiator appears to vary from formulation to formulation [4], i.e., a photoinitiator can be most efficient in one system but not in another, so direct comparisons cannot always be drawn.

The optimal photoinitiator and tertiary amine concentrations required to effect efficient curing were determined during this investigation. That an optimal concentration of photoinitiator exists in free radical polymerisations has been reported [5,6] and attributed to screening (inner filter) effects at higher photoinitiator concentrations, thereby preventing a complete through cure. This effect was found to be very marked for

film thickness greater than 1mm [5,7-9].

The "new, novel class of photoinitiators", the acylphosphine oxides have been described as " particularly suitable for photocuring compositions based on acrylates of styrene-containing UP resins and,for the initiation of polymerisation in TiO₂ pigmented coatings and of thick-walled glass fibre-reinforced polyesters" [10], and also to ..."embrace applications that were formerly the domain of electron beam curing" [3]. The performance of these photoinitiators and a series of acylphosphonates were compared with a standard photoinitiator, 2,2-dimethoxy-2-phenyl

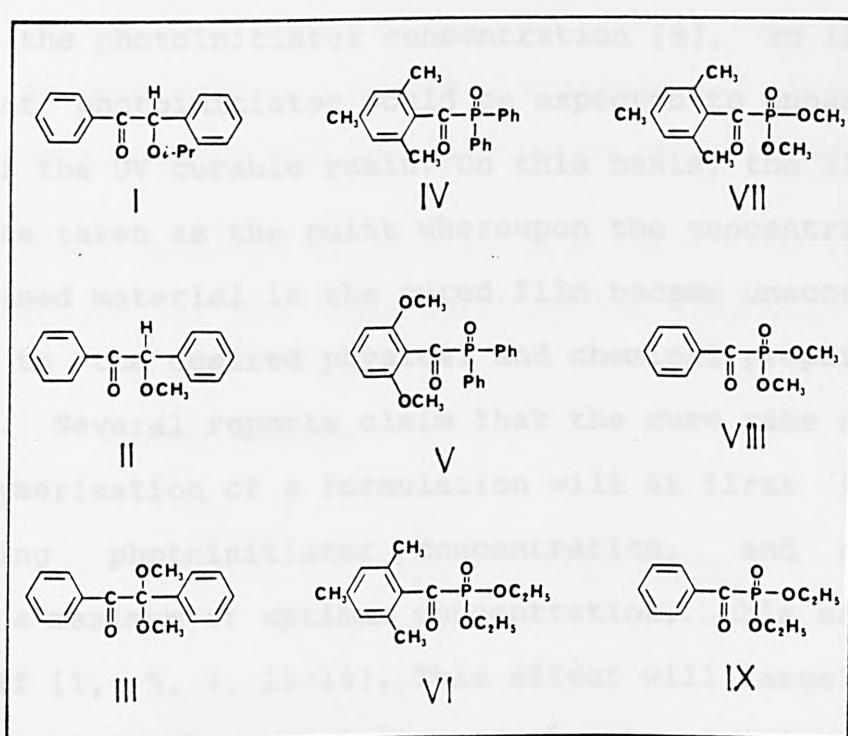


Figure 1. The photoinitiators to be compared

I = BIPE, II = BME, III = DMPA, IV = TMBPO, V = DMBPO

VI = TMBEP, VII = TMBMP, VIII = BDMP, IX = BDEP.

acetophenone (Figure 1). Comparisons were conducted both in the presence and absence of tertiary amines, and also in an acrylate

and an unsaturated polyester formulation. The factors which affect the efficiency and properties of thin clear polymer films are manifold, and include the thickness of the film, photoinitiator and amine concentrations, oxygen inhibition and autooxidation effects, as discussed below.

PHOTOINITIATOR CONCENTRATION AND FILM THICKNESS

From the rate equations presented in Chapter 1, where the rate of photoinitiation is directly proportional to the square root of the photoinitiator concentration [9], an increase in the level of photoinitiator would be expected to enhance the cure speed of the UV curable resin. On this basis, the limiting factor would be taken as the point whereupon the concentration of non-polymerised material in the cured film became unacceptably detrimental to the desired physical and chemical properties of the coating. Several reports claim that the cure rate and the degree of polymerisation of a formulation will at first increase with increasing photoinitiator concentration, and after passing through a maximum or optimum concentration, this effect rapidly falls off [1, 5, 7, 11-14]. This effect will largely depend upon the absorbance characteristics of the photoinitiator and the UV curable formulation. For this reason it is important to differentiate between surface and through cure and also to take into consideration the thickness of the film.

Significant changes in the rate of cure and the overall film properties are often observed for extremely thick or thin

films [13]. Increasing the photoinitiator concentration in such films will lead to a fast attainment of a tack free state, but will also be counterproductive for the overall polymerisation, resulting in

1. a high level of undercure at the coating/substrate interface, depending to an extent on the molar extinction coefficient of the photoinitiator. This effect will weaken the physical and chemical properties of the film (i.e., loss of adhesion to the substrate).
2. an increase in the ratio of the rate of surface polymerisation compared to the rate of bulk crosslinking polymerisation, causing differential stresses to be developed within the film which leads to wrinkling.

For thin clear coatings (Figure 2) on a reflective substrate, a high proportion of the light entering the film will reach the

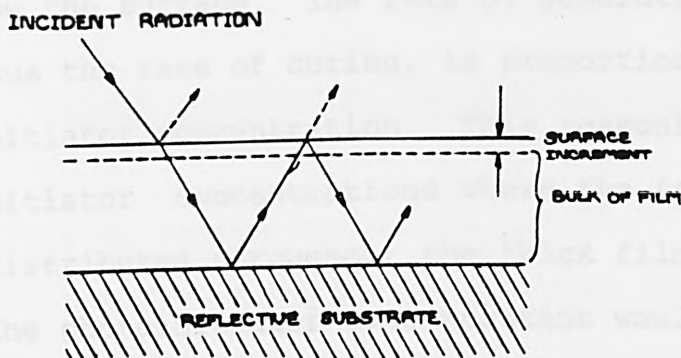


Figure 2. Reflection Situation for Thin Clear Films.

substrate and will most probably cause multiple internal reflec-

tions within the film. The surface layer of the film will therefore receive a substantial amount of radiation which has been reflected from the substrate. Consequently, the rate of surface cure is no longer a simple function of initiator concentration. Other factors, such as the film thickness, the substrate reflectivity and the refractive index of the vehicle are involved. In a thick clear film the rate of cure at any depth away from the surface can be predicted with reasonable accuracy by the application of the Lambert-Beer law:-

$$I_l = I_0 e^{-kcl}$$

where I_0 = the intensity of radiation at the surface, c = the concentration of light absorbing species, l = the path length (i.e., depth from the surface), k = the absorbance coefficient of the vehicle and I_l = the intensity of the radiation at the distance l below the surface. The rate of generation of free radicals, and thus the rate of curing, is proportional to both I_0 and the photoinitiator concentration. This reasoning holds well at low photoinitiator concentrations where the free radicals are generally distributed throughout the thick film. Thus, an increase in the photoinitiator concentration would be expected to produce an increase in the number of free radicals with a concomitant increase in the photopolymerisation reaction. The relationship between the degree of polymerisation and the chemical nature of the photoinitiator/monomer system however, is more complicated and depends upon a variety of factors which include the quantum

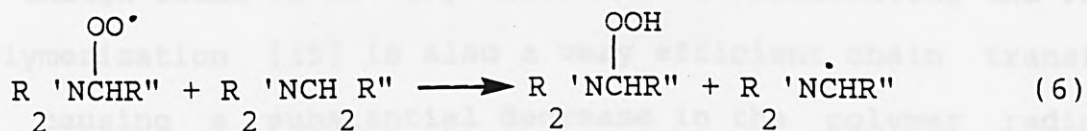
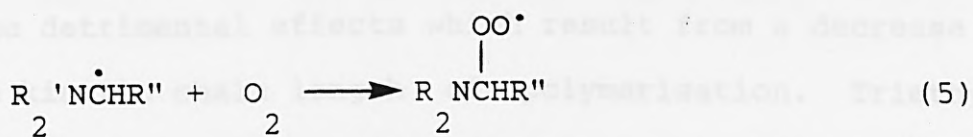
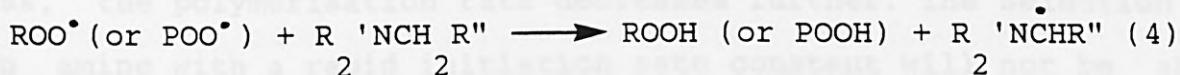
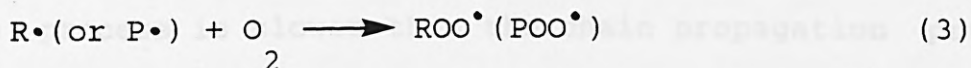
efficiency and the extinction coefficient of the monomer and photoinitiator side reactions. At higher photoinitiator concentrations the absorbance of UV light appears to generate a higher concentration of free radicals near the surface of the film. This higher concentration of photoinitiator, and therefore free radicals at the surface is thought to block sufficient energy from penetrating the film, preventing photoactivation below a given film thickness. Below this level an insufficient number of free radicals are generated in order to initiate and sustain the polymerisation process, and therefore the rate of polymerisation decreases. Photoinitiators which have a high molar extinction coefficient would be expected to give rise to this uneven distribution more readily than photoinitiators which have a low extinction coefficient and do not absorb UV light so strongly [7, 13]. Increasing the photoinitiator concentration may result in a point being reached at which so much light is absorbed in the upper regions of the film that through cure ceases to take place.

OXYGEN INHIBITION AND AUTOOXIDATION

The ability of oxygen to inhibit photoinitiation and photopolymerisation has been described previously in Chapter 1. This effect, where polymerisable surface coatings are concerned, can be very dramatic, requiring up to 20 times more energy to effect the same level of cure in the top 1 μm of a clear film exposed to air compared to the 1 μm layer 5 μm below the surface [11]. The ability of oxygen to quench the excited states of the photoinitiator and to scavenge the active radical sites on the growing

polymer chain reduces the overall rate of polymerisation. Furthermore, the formation of hydroperoxide is detrimental to the chemical and physical properties of the cured film [11, 13].

While it has long been recognised that amines are effective synergists when used with benzophenone type photoinitiators, it has been shown [1, 17] that certain amines can be used with cleavage type photoinitiators to accelerate the cure rate in an air atmosphere. This presumably occurs as a result of the generation of a radical species capable of efficient oxygen scavenging by a radical chain process, as shown in Scheme 1.



Where PI is the photoinitiator, $R\cdot$ is the primary radical and $P\cdot$ is the polymer radical. The amine radical generated in this chain process can serve either to initiate polymerisation or to combine with additional molecules of oxygen. Tertiary alkyl amines [15], aromatic amines [16] and functionalised amines [17] have recently

been reported to be effective in accelerating the photopolymerisation of an air saturated diacrylate formulation. The degree by which the rate of polymerisation increases is dependent upon the structure of the amine, as well as its concentration. As amines act both as oxygen scavengers and chain transfer agents [1], the amine concentration required to maximise the photopolymerisation rate is critical.

The main problems encountered when simple aromatic and aliphatic amines are employed^d as oxygen scavengers are the chain transfer and/or inhibition step which involves the transfer of the polymer radical to the amine by a standard hydrogen abstraction mechanism. If the amine concentration is large, the hydrogen abstraction process dominates and the kinetic chain length of the average growing polymer chain decreases. If, in addition, the reinitiation process is slower than the chain propagation process, the polymerisation rate decreases further. The selection of an amine with a rapid initiation rate constant will not be able to solve the detrimental effects which result from a decrease in the average kinetic chain length of polymerisation. Triethylamine, though found to be very effective in accelerating the rate of polymerisation [15] is also a very efficient chain transfer agent, causing a substantial decrease in the polymer radical chain length and ultimately reducing the physical properties of the film. The detrimental effect of chain transfer to amines can be avoided by incorporating the amine functional groups into monomers which themselves are capable of participating in the polymerisation process [17].

While the addition of amine serves to increase the cure

rate of polymerisation and lower the substantial differences between through cure and surface cure (caused by oxygen inhibition), the hydroperoxides (POOH) that accumulate during propagation (Scheme 1, equations 3,4) will sensitise the photodegradation of the coating. The autooxidation of the growing polymer chain ultimately leads to chain depolymerisation (chain scission) [18] which will occur at the "weak link" of the chain, i.e., a peroxide or ether link. The changes in the polymer structure arising by this mechanism, with concomitant crosslinking, will cause changes in the physical properties of the polymer such as embrittlement, colour, flexibility, hardness and so on. This chain scission can be reduced by the addition of hindered amines (derivatives of 2,2,6,6-tetramethylpiperidine) as light stabilizers [19-22]. The hindered amines show efficient radical trapping ability towards alkoxy and hydroxy radicals produced during the chain scission of the hydroperoxides, and towards the hydroperoxides themselves if the polymer is essentially non-polar [19].

RESULTS and DISCUSSION

Previous reports have shown [3] that 2,4,6-trimethylbenzoyldiphenylphosphine oxide (TMDPO) was a less efficient photoinitiator than 2,2-dimethoxy-2-phenyl acetophenone (DMPA) in clear coatings, when the photoinitiators were used at a two percent concentration. In order to achieve an efficient cure, it was found necessary to add three percent amine as a coinitiator

or synergist. The addition of amine increased the cure speed from 3.5 m.min⁻¹ to 30 m.min⁻¹ in the formulations investigated [3].

Initially, the effectiveness of the various photoinitiators (Figure 1) were compared in an epoxy-acrylate formulation in the presence and absence of triethylamine (TEA) and N-methyldiethanol amine (NMDEA). As the cure speed of most of the photoinitiators was so slow, only comparisons of the photoinitiators DMPA and TMBPO were made. These were performed in an epoxy-acrylate and unsaturated polyester formulation with various amines, in order to assess the synergistic value of the individual amines. The results of these investigations (Tables 1 and 2) clearly show the synergistic effect of the amines investigated. This advantageous effect can be attributed to the known ability of amines to act as efficient oxygen scavengers [1, 7, 15-17, 20, 21], thus counter-

TABLE 1 The Effectiveness Of Various Tertiary Amines as Synergists for the UV Curing of an Epoxy Acrylate Resin.

TERTIARY AMINE	TMBPO		DMPA	
	mm ⁻¹	secs	mm ⁻¹	secs.
No amine	2 x 2	9.60	2 x 2	9.60
N-Methyldiethanol amine	16	0.60	14	0.68
Blik	14	0.68	12	0.80
Glass	8	1.20	6	1.60
Tribenzylamine	3 x 2	14.40	3 x 2	14.40
N-Vinylcarbazole	4 x 2	19.20	2 x 2	9.60
Ethyl-4-dimethylaminobenzoate	3 x 2	14.40	5 x 2	24.00
1,3-dimopholinopropane	8	1.20	8	1.20

acting the oxygen inhibition of the chain propagation reaction. Photoinitiators such as diarylketones and thioxanthenes are used in conjunction with tertiary amines [23] because they generate free radicals by a hydrogen abstraction mechanism upon the irradiation of UV light [1, 2, 24, 25]. The excited carbonyl group abstracts hydrogen from the amine to give an α -aminoalkyl radical, which is responsible for initiating polymerisation [1,2,26]. DMPA and TMBPO on the other hand are photoinitiators which undergo a Norrish Type 1 photocleavage producing radicals which possess initiating properties [1, 2, 10, 27]. These photoinitiators generate radicals by an extremely fast photocleavage mechanism [2, 10, 28 (Chapter3)] and it is therefore very unlikely that

TABLE 2 The Effectiveness of Various Tertiary Amines as Synergists for the UV Curing of an Unsaturated Polyester.

TERTIARY AMINE	TMBPO		DMPA	
	⁻¹ mm	secs	⁻¹ mm	secs.
No amine	3 x 2	14.40	2 x 2	9.60
N-Methyldiethanol amine	2 x 2	9.60	4	2.40
Tribenzylamine	6 x 2	28.80	3 x 2	14.40
N-Vinylcarbazole	3 x 2	14.40	2 x 2	14.40
Ethyl-4-dimethylaminobenzoate	3 x 2	14.40	2 x 2	9.60
1,3- Dimopholinopropane	4	2.40	4	2.40
Blik	2 x 2	9.60	2 x 2	9.60
Glass	2 x 2	9.60	2 x 2	9.60

oxygen could quench their excited states. Hence these photo-

initiators should not need added synergist, such as tertiary amines, to produce initiating free radicals. Thus, the beneficial effect of amine under these experimental conditions is most probably that of an efficient oxygen scavenger.

Following the determination of the most efficient amine synergist, attempts were made to optimise the most rapid cure speed for the epoxy-acrylate formulation (with added N-methyldiethanolamine) and the unsaturated polyester formulation (with added 1,3-dimorpholinopropane). This required the variation of both photoinitiator and amine concentrations, the results of which are shown in Tables 3 and 4. An interesting observation from the results is that the efficiency of the amine synergist appears to be concentration dependent. The optimal concentration of amine for each formulation can be determined from Tables 3 and 4. From this it would appear that at higher amine concentrations the plasticising effect of amines or their ability to act as chain transfer agents [1], leads to the formation of lower molecular weight polymers and a consequent reduction in the apparent degree of cure.

The performance of a photoinitiator appears to vary from formulation to formulation [4] and for this reason direct comparisons cannot be drawn between the results obtained in these investigations with those of others [3]. However the claim that the acylphosphine oxide photoinitiators are suitable for the UV curing of unsaturated polyester resins containing styrene was made previously [3]. In these investigations, DMPA was found to be a more efficient photoinitiator in the unsaturated polyester

TABLE 3. Effect of Varying the Photoinitiator and N-methyldiethanol amine (Synergist) Concentration upon the Rate of Cure of the Epoxy Acrylate Resin.

<u>TMBPO CONCENTRATION PROFILES</u>							
% concn. TMBPO	% concn. AMINE	CURE SPEED -1 mm	secs.	% concn. TMBPO	% concn. AMINE	CURE SPEED -1 mm	secs.
1	2	6 x 2	28.80	3	2	12	0.80
2	2	2 x 2	9.60	3	4	20	0.48
3	2	12	0.80	3	6	16	0.60
4	2	22	0.45	3	8	2 x 2	9.60
5	2	28	0.36	3	10	3 x 2	14.40

<u>DMPA CONCENTRATION PROFILES</u>							
% concn. DMPA	% concn. AMINE	CURE SPEED -1 mm	secs.	% concn. DMPA	% concn. AMINE	CURE SPEED -1 mm	secs.
1	2	6 x 2	28.80	3	2	10	0.96
2	2	3 x 2	14.40	3	4	14	0.68
3	2	12	0.80	3	6	12	0.80
4	2	18	0.54	3	8	2	4.80
5	2	22	0.45	3	10	2 x 2	9.60

system than TMBPO, regardless of the amine concentration (Table 4).

Another interesting observation made during these investigations was the absence of an optimum photoinitiator concentration (Tables 3 and 4). This result apparently conflicts with that of previous workers who claim that there is an optimum concentration for photoinitiators in free radical polymerisations. There will be an optimal photoinitiator concentration for the systems under investigation, however this was not realised during these

experiments. Optimal photoinitiator concentration is dependent upon the absorption characteristics of the photoinitiator, spectral output from the lamp and the film thickness. Increasing the photoinitiator concentration from 1% to 5% of the weight of resin, increased the cure speed of the epoxy-acrylate markedly. A 3 fold increase in cure speed was also observed in the unsaturated polyester when the photoinitiator concentration was increased from 1% to 5% of the weight of resin.

TABLE 4 Effect of Varying the Photoinitiator and 1,3-Dimorpholinopropane (Synergist) Concentration upon the Rate of Cure of an Unsaturated Polyester Resin.

TMBPO CONCENTRATION PROFILES

% concn. TMBPO	% concn. AMINE	CURE SPEED -1 mm	secs.	% concn. TMBPO	% concn. AMINE	CURE SPEED -1 mm	secs.
3	2	2 x 2	9.60	1	6	2	4.80
3	4	2	4.60	2	6	2	4.80
3	6	4	2.40	3	6	4	2.40
3	8	4	2.40	4	6	4	2.40
3	10	4	2.40	5	6	4	2.40

DMPA CONCENTRATION PROFILES

% concn. DMPA	% concn. AMINE	CURE SPEED -1 mm	secs.	% concn. DMPA	% concn. AMINE	CURE SPEED -1 mm	secs.
3	2	2 x 2	9.60	1	6	2	4.80
3	4	2	4.80	2	6	4	2.40
3	6	4	2.40	3	6	4	2.40
3	8	4	2.40	4	6	4	2.40
3	10	4	2.40	5	6	6	1.60

A comparison was made as to the effectiveness of the acylphosphonates, acylphosphine oxides and the commercial photoinitiators (with added synergist) for the UV curing of epoxy-acrylate and unsaturated polyester thin films. The results (Table 5) show the optimal curing efficiency obtained using the amine synergists N-methyldiethanolamine (NMDEA) and 1,3-dimorpholinopropane (DMOP). The UV curing tests proved to be particularly

TABLE 5. The effectiveness of various photoinitiators for the UV curing of oligomeric mixes.

PHOTOINITIATOR	EPOXY-ACRYLATE*		UNSAT. POLYESTER**	
	M/MIN	SECONDS	M/MIN	SECONDS
1) TMBPO	16	0.60	1	9.60
2) DMBPO	12	0.80	4	2.40
3) BDMP	0.4	24.00	1	9.60
4) BDEP	0.4	24.00	2	4.80
5) TMBEP	2	4.80	2	4.80
6) TMBMP	0.4	24.00	2	4.80
7) DMPA	14	0.68	2	4.80
8) DMPA #	1	9.60	1	9.60
9) TMBPO #	1	9.60	0.6	14.40

* Epoxy-acrylate resin contains 3% photoinitiator and 6% N-methyldiethanol amine. ** Unsaturated polyester resin contains 4% dimorpholinopropane and 3% photoinitiator. # 3% Photoinitiator samples in the absence of amine.

informative. The three categories of organophosphorous compounds initiated the polymerisation of acrylate films with varying degrees of efficiency. The acylphosphine oxides led to cure at speeds of approximately 1 m.min^{-1} or 9.6 seconds in the absence of amine (Table 5 entry 9). The efficiency of the acylphosphine oxides however, was increased with the addition of amine (Table 5 entries 1 and 2). In the preceding chapter it was shown that added amine had little effect upon the bulk polymerisation initiated by the acylphosphine oxides, and upon the solution polymerisation monitored by laser nephelometry. From those results and the results shown in Table 5 the beneficial effect of added amine in the UV curing tests must be due to the amines acting as efficient oxygen scavengers.

The acylphosphonates proved to be inefficient photoinitiators compared to the acylphosphine oxides, curing at speeds of less than 0.5 m.min^{-1} or 19.2 seconds in the absence of amine synergists. The results of this investigation however, showed the performance of these photoinitiators to be improved by the addition of amines (Table 5 entries 5 and 6). This improved efficiency can be ascribed to the amines reducing the effects of oxygen inhibition and also increasing the efficiency of production of initiator radicals.

The benzoylphosphonates were also found to be inefficient photoinitiators compared to the acylphosphine oxides, with cure speeds of less than 0.2 m.min^{-1} or 48.0 seconds in the absence of amine synergists. This result, although very poor, is in direct contradiction to a report published by Schnabel et al [27] who claimed that benzoyldiethylphosphonate (BDEP) was ineffective as

a photoinitiator for the polymerisation of methyl methacrylate. It was also claimed by these authors that BDEP was most unlikely to form ketyl radicals which could initiate radical chain reactions by intermolecular hydrogen abstraction, because the excited state of BDEP rapidly converted to biradicals via intramolecular hydrogen abstraction (Norrish Type II reaction). The performance of these photoinitiators was improved by the addition of amines (Table 5 entries 3 and 4), which suggests that the amine derived radicals are most probably functioning as the polymerising radicals.

A study of the UV curing efficiency of an unsaturated polyester in styrene was performed using various organophosphorus compounds as photoinitiators. From the results in Table 5 it can be seen that the unsaturated polyester system cures slowly by comparison with the epoxy-acrylate formulation. The acylphosphonates TMBEP and TMBMP (Table 5, entries 5 and 6), and the benzoylphosphonate BDEP (Table 5, entry 4) gave cure rates comparable to the acylphosphine oxide TMBPO (Table 5, entry 1). One would assume that this is due to the propagation reaction determining the cure speed, rather than the efficiency of the photoinitiator.

The high gloss epoxy-acrylate films produced were all very coloured. The films cured using the acylphosphine oxides were a lighter brown/yellow colour than those cured by the acylphosphonates and benzoylphosphonates. The latter were most probably darker in colour due to their longer exposure to UV light. It was not possible to distinguish clearly between the unsaturated poly-

ester films cured using an acylphosphine oxide, an acylphosphonate or a benzoylphosphonate. All of the polyester films produced by these organophosphorus compounds were of high gloss, clear and only very slightly coloured.

The effect of the substrate (paper, blik, glass) upon the rate of cure and the quality of the film formed were assessed using the photoinitiators TMBPO and DMPA and two different formulations. The degree of cure was measured by the Persoz (pendulum) hardness test [29]. The pendulum hardness is related primarily to a better cure response and a higher crosslink density within the film [30]. There is generally a good correlation between pendulum hardness and residual unsaturation in a polymer film [1], as determined by infrared techniques. The measurements of the pendulum hardness, as shown in Tables 6 and 7, provide an approximate parameter for determining the level of cure within each film.

The application of the coatings to different substrates resulted in a difference in the rate of cure being observed, as shown in Tables 6 and 7. The substrates each possess different reflective properties and thermal capacities and will therefore affect the degree of internal reflection and thermal cure to different extents. Clearly, as the extent of internal reflection increases, so too will the efficiency of the photoinitiator to absorb the incident radiation. The thermal capacities of the substrates vary and this difference will affect the degree of thermal cure which occurs as a result of the exothermic nature of the photoinitiated reaction. The hardness of the film is also affected by the nature of the substrate, although this could be

due in part to a contribution to the hardness by the substrate.

TABLE 6 A Comparative Study Showing the Effect of Substrate on the Rate of Cure of an Epoxy Acrylate Resin.

PHOTOINITIATOR	SUBSTRATE	CURE SPEED		HARDNESS $x \pm \sigma$	APPROX. % CURE
		⁻¹ mm	secs.		
TMBPO	Paper	18	0.54		
	Blik	16	0.60	48.33 \pm 1.25	84.20
	Glass	12	0.80	64.33 \pm 3.30	77.56
DMPA	Paper	16	0.60		
	Blik	16	0.60	49.67 \pm 4.50	86.53
	Glass	14	0.68	59.33 \pm 6.60	71.53

TABLE 7 A Comparative Study Showing the Effect of Substrate on the Rate of Cure of an Unsaturated Polyester Resin.

PHOTOINITIATOR	SUBSTRATE	CURE SPEED		HARDNESS $x \pm \sigma$	APPROX. % CURE
		⁻¹ mm	secs.		
TMBPO	Paper	4	2.40		
	Blik	2 x 2	9.60	304.70 \pm 2.49	100.00
	Glass	2	4.80	383.30 \pm 3.30	100.00
DMPA	Paper	4	2.40		
	Blik	2 x 2	9.60	284.30 \pm 6.02	94.30
	Glass	2 x 2	9.60	367.00 \pm 2.16	95.93

A claimed advantage of the acylphosphine oxides is their

ability to cure thick films [3]. A comparison was made of the effectiveness of the photoinitiators TMBPO and DMPA to cure

TABLE 8. Effect of Varying the Thickness of Films upon Curing Efficiency and Film Properties (Epoxydiacrylate Resin).

RATE OF CURE.

PHOTOINITIATOR	THICKNESS uM	CURE SPEEDS IN m.min ⁻¹ and SECONDS					
		PAPER		BLIK		GLASS	
TMBPO	20	18	0.54	16	0.60	12	0.80
	40	18	0.54	16	0.60	14	0.68
	80	16	0.60	16	0.60	16	0.60
	120	14	0.68	16	0.60	18	0.54
DMPA	20	16	0.60	16	0.60	14	0.68
	40	14	0.68	14	0.68	16	0.60
	80	12	0.80	12	0.80	14	0.68
	120	10	0.96	14	0.68	16	0.60

CURING EFFICIENCY AS MEASURED BY THE PERSOZ HARDNESS TEST.

THICKNESS uM	TMBPO HARDNESS		DMPA HARDNESS	
	BLIK	GLASS	BLIK	GLASS
20	48.33 ± 1.25	64.33 ± 3.30	49.67 ± 4.50	59.33 ± 6.60
40	38.67 ± 2.49	40.00 ± 0.82	38.67 ± 1.25	40.67 ± 1.25
80	29.00 ± 0.82	33.67 ± 0.47	33.33 ± 0.94	31.33 ± 0.47
120	28.33 ± 1.25	27.67 ± 1.25	28.67 ± 0.47	33.00 ± 0.00

different thicknesses of epoxy-acrylate and unsaturated polyester films. The results are shown in Tables 8 and 9. Investigation of these effects upon the rate of cure was particularly instructive. It can be seen that the acylphosphine oxide TMBPO, despite previous claims, [10] performs no better than DMPA and that the observed general trends are not consistent with those described

by others [5-9].

TABLE 9. Effect of Varying the Thickness of Films upon the Curing Efficiency and Film Properties (Unsaturated Polyester Resin).

RATE OF CURE.

PHOTOINITIATOR	THICKNESS μM	CURE SPEEDS IN m.min-1 and SECONDS					
		PAPER		BLIK		GLASS	
TMBPO	20	4	2.4	1	9.6	2	4.8
	40	4	2.4	1	9.6	2	4.8
	80	4	2.4	2	4.8	2	4.8
	120	4	2.4	1	9.6	1	9.6
DMPA	20	4	2.4	1	9.6	1	9.6
	40	4	2.4	1	9.6	1	9.6
	80	4	2.4	1	9.6	1	9.6
	120	4	2.4	1	9.6	1	9.6

CURING EFFICIENCY AS MEASURED BY THE PERSOZ HARDNESS TEST.

THICKNESS μM	TMBPO HARDNESS		DMPA HARDNESS	
	BLIK	GLASS	BLIK	GLASS
20	304.7 ± 2.49	383.3 ± 3.30	284.3 ± 6.02	367.0 ± 2.16
40	290.0 ± 2.94	366.3 ± 5.44	263.0 ± 2.16	369.7 ± 0.47
80	250.3 ± 2.49	351.3 ± 2.62	247.3 ± 5.79	347.7 ± 2.05
120	171.3 ± 9.84	342.0 ± 4.24	241.0 ± 4.90	339.7 ± 3.86

It is obviously necessary to excite as many photoinitiator molecules as possible in the coating to achieve efficient radical generation and therefore efficient polymerisation. For this to occur in thick films, the light has to penetrate the full depth of the film. If the concentration of the photoinitiator is not

carefully controlled, it is very easy to obtain the situation where most of the light is absorbed near the surface of the film, as described earlier in this Chapter. The photoinitiating efficiency of both DMPA and TMBPO is similar when they are both used at the same percentage concentration level. If the cure rates are considered on the basis of molar concentrations, then TMBPO is more efficient. This however, is most likely due to the better light absorption characteristics of TMBPO compared to DMPA, as shown in Figure 3 and Table 10. The absorption spectrum (Figure

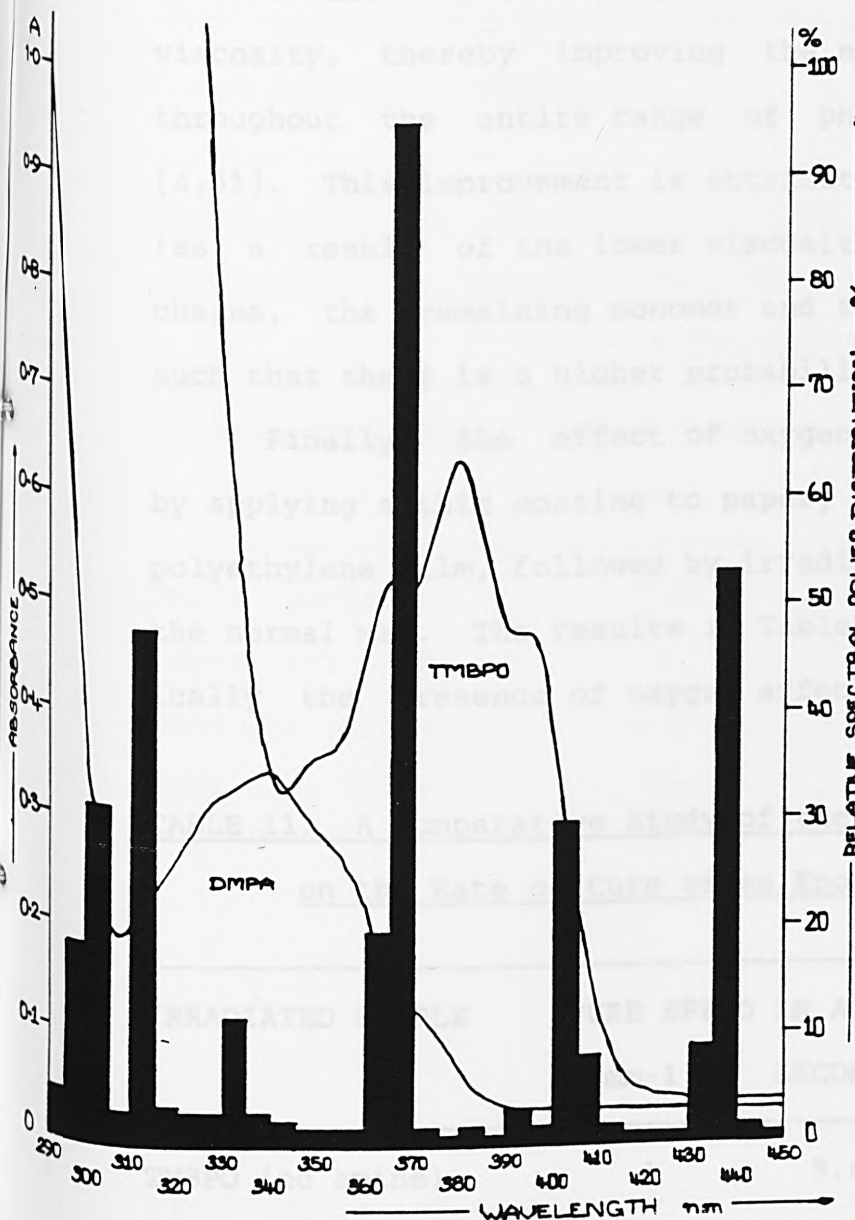
TABLE 10. Absorption Characteristics of TMBPO and DMPA in Methanol and Acetonitrile.

PHOTOINITIATOR	MAXIMUM WAVELENGTH (nm)	EXTINCTION COEFFICIENT ($\text{L mol}^{-1} \text{cm}^{-1}$)	SOLVENT
TMBPO	377	563	METHANOL
TMBPO	378	530	ACETONITRILE
DMPA	339	295	METHANOL
DMPA	332	281	ACETONITRILE

3) of the acylphosphine oxide indicates that it should have a superior photoinitiating performance compared to DMPA.

The absorbance spectra of the photoinitiators TMBPO and DMPA were recorded at fixed concentrations and compared with a histogram showing the relative spectral power distribution, as a percentage of the lamp output, for the lamps used in the UV curing experiments. The results shown in Table 10 were calc-

ulated from the spectra. It can be clearly seen from Figure 3



that the acylphosphine oxide absorbs strongly in the wavelength region where the UV lamp has a particularly strong emission line, at 365-370nm. This suggests that the acylphosphine oxide could be used at a much lower concentration than the DMPA, which possesses a much lower extinction coefficient in this region, and still provide a similar efficiency. In practise this was not found to be the case.

Figure 3. The absorption spectra of TMBPO and DMPA in acetonitrile.

It was noted during the experiments that increasing the film thickness led to a considerable increase in the amount of heat retained in the film immediately following irradiation. As film thickness increased, so too did the length of time the heat was retained in the film, particularly on blik and glass. A temp-

erature increase in a polymer film is known to reduce the film viscosity, thereby improving the extent of cure by up to 15%, throughout the entire range of photoinitiator concentrations [4,31]. This improvement is attributed to the increased mobility (as a result of the lower viscosity) of the growing polymer chains, the remaining monomer and the photoinitiator radicals, such that there is a higher probability for collision.

Finally, the effect of oxygen inhibition was investigated by applying a thin coating to paper, covering the coating with a polyethylene film, followed by irradiation of the coated paper in the normal way. The results in Tables 11 and 12 show how dramatically the presence of oxygen affects the performance of the

TABLE 11. A Comparative Study of the Effect of Oxygen Inhibition on the Rate of Cure of an Epoxydiacrylate Resin.

IRRADIATED SAMPLE	CURE SPEED IN AIR		CURE SPEED NO AIR	
	mm-1	SECONDS	mm-1	SECONDS
TMBPO (no amine)	1	9.6	>60	<0.16
TMBPO with amine	8	1.2	>60	<0.16
DMPA (no amine)	0.5	19.2	>60	<0.16
DMPA with amine	8	1.2	>60	<0.16

photoinitiator. In the absence of oxygen, both TMBPO and DMPA were able to effect cure without amine synergists. Remarkably, the cure under these conditions occurs at similar rates, both in

the presence and absence of tertiary amine. These results also show the important role that amines play in decreasing the inhibiting effect of oxygen.

TABLE 12. A Comparative Study of the Effect of Oxygen Inhibition on the Rate of Cure of an Unsaturated Polyester Formulation.

IRRADIATED SAMPLE	CURE SPEED IN AIR		CURE SPEED NO AIR	
	⁻¹ mm	SECONDS	⁻¹ mm	SECONDS
TMBPO (no amine)	0.66	14.4	30	0.36
TMBPO with amine	4	2.4	32	0.32
DMPA (no amine)	0.66	14.4	30	0.36
DMPA with amine	4	2.4	30	0.36

In conclusion, the acylphosphine oxide TMBPO did not display any advantageous properties compared with the commercial photoinitiator DMPA in any of the systems tested. It can also be concluded that the acylphosphonates and the benzoylphosphonates can not be considered as useful photoinitiators for the production of surface coatings.

ACKNOWLEDGEMENTS

For the skills acquired in the application and testing of the surface coatings, special thanks must go to Leo Jansen. Similarly, special thanks are also due for Louis van Eersel, who was always available to repair temperamental instrumentation. I thank both men for their unlimited cooperation, support, patience and kindness. I also wish to thank Jeffrey Abrahams for the synthesis of the 1,3-dimorpholinopropane.

The resins used to prepare the formulations (all from Synthes B.V.) included a low molecular weight prepolymer, the epoxycyclohexane diacrylate of hexacure (A) (26.5% by wt.) in polyethylene glycol (100) diacrylate (11.4% by wt.) and hexacure (B) (17% by wt.) which is an unsaturated polyester (7% by wt.) in hexacure (A) (54% by wt.) and hexacure (B) (37% by wt.).

The UV curing was carried out using a Philips high-pressure Hg lamp, model HOK 4 (80 Watts/cm²), which was situated 15cm above a moving belt. The belt had a variable speed and had been calibrated so that the speed of flow of resin and the time of irradiation in seconds could be determined. The degree of cure for each film was assessed qualitatively by a finger rub test. The film surface was rubbed firmly by the forefinger wrapped in a thick linen cloth. When no visible deformation of the surface occurred, the film was considered cured. This test was repeated on a minimum of 5 samples.

EXPERIMENTAL

2,4,6-Trimethylbenzoyldiphenylphosphine oxide was synthesised as described previously in Chapter 2 [32]. 2,2-Dimethoxy-2-phenyl acetophenone was obtained from Ciba Geigy and recrystallised from petroleum ether (boiling range, 60-80 °C) and had a melting range of 65.4-65.7 °C. The synthesis of 1,3-dimorpholinopropane has been described [23]. The other amines, N-methyldiethanolamine, tribenzylamine, N-vinylcarbazole and ethyl-4-dimethylaminobenzoate (Janssen Chimica) were used as received.

The resins used to prepare the formulations (all from Synthese b.v.) included a low molecular weight prepolymer, the epoxydiacrylate of Setacure ^(R)AP 570 (26.6% by Wt.) in polyethyleneglycol (200) diacrylate (73.4% by Wt.) and Setacure ^(R)AP 571 which is an unsaturated polyester (53% by Wt.) in Setacure ^(R)AM 554 a polyethertriacyrylate, (47% by Wt.).

The UV curing was carried out using a Philips high-pressure Hg lamp, model HOK 6 (80 Watts/cm), which was situated 15cm above a moving belt. The belt had a variable speed and had been calibrated so that the speed of cure in m.min⁻¹ and the time of irradiation in seconds could be determined. The degree of cure for each film was measured arbitrarily by a finger rub test. The film surface was rubbed firmly by the forefinger wrapped in a thick linen cloth. When no visible deformation of the surface occurred, the film was considered cured. This test was repeated on a minimum of 5 samples.

The substrates used were satinised paper, blik (which is a coated tin plate) and cleaned glass thin layer chromatography plates (Merck). The substrates were coated using Erichsen rods, chosen to provide a wet film thickness in the region of 20-120 um. The Persoz hardness was determined using the Pendulum-Hardness test (Erichsen model 299 and 300). Between 12 and 18 samples per test were examined. The mean and standard deviation value for each test was subsequently calculated.

The polyethylene film used in the curing experiment to simulate the absence of air was "kitchen" cling film.

The absorbance spectra of the photoinitiators were recorded on a Hitachi 100-80A computerised spectrophotometer. The solvents, methanol and acetonitrile (Baker) were used directly from unopened bottles.

- [9] Van Landuyt, D. C., *J. Rad., Curing* 1984, 12 (3) 4-8.
- [10] Sumiyoshi T., Schnabel, W., Henne, A., Lechtken, F., *Polymer* 1985, 36 141-146.
- [11] *UV and EB Curing Formulations for Printing Inks, Coatings and Paints*. Edited by Holman, R., Site Technology, 1984.
- [12] Pappas, S. P., *Radiat. Phys. Chem.* 1983, 22, (4-6) 833-841.
- [13] *Photopolymerisation of Surface Coatings*, Ruffey, C. G., 1982, Wiley-Interscience.
- [14] Brann, B. L., *J. Rad., Curing* 1983, 22(27), 8-10.
- [15] Hoyle, C. E., *Kyu-Jun Kim, J. Rad., Curing* 1985, 12(1), 7-15.
- [16] Hoyle, C. E., *Kyu-Jun Kim, J. Appl. Polym. Sci.*, 1987, 22.

REFERENCES

- [1] Berner, G., Kirchmayr, R., Rist, G., J. Oil Col. Chem. Assoc., 1978, 61, 105-113.
- [2] Hageman, H.J., Progress in Org., Coatings, 1985, 13 123-150.
- [3] Jacobi, M., Henne, A., J. Rad. Curing 1983, 10 (4) 16-25.
- [4] Le(Ziem), D. D., J. Rad. Curing 1985, 12 (2) 2-8.
- [5] Hutchinson, J., Ledwith, A., Polymer 1973, 14 405-408.
- [6] Lissi, E.A., Zanocco, A., J. Polym. Science: Polym. Chem. Ed., 1983, 21, 2197-2202. J. Polym. Science: Polym. Letts. Ed., 1984, 22, 391-393.
- [7] Guthrie, J., Jeganathan, M. B., Otterburn, M. S., Woods, J., Polymer Bulletin 1986, 15, 51-58.
- [8] Clarke, S., Shanks, R. A., Polym. Photochem., 1981, 1 103-
.
- [9] Van Landuyt, D. C., J. Rad., Curing 1984, 11 (3) 4-8.
- [10] Sumiyoshi T., Schnabel, W., Henne, A., Lechtken, P., Polymer 1985, 26 141-146.
- [11] UV and EB Curing Formulations for Printing Inks Coatings and Paints. Edited by Holman, R., Sita Technology, 1984.
- [12] Pappas, S. P., Radiat. Phys. Chem. 1985, 25, (4-6) 633-641.
- [13] Photopolymerisation of Surface Coatings, Roffey, C. G., 1982, Wiley-Interscience.
- [14] Brann, B. L., J. Rad. Curing 1985, 12(3), 4-10.
- [15] Hoyle, C. E., Kyu-Jun Kim, J. Rad. Curing 1985, 12(4), 9-15.
- [16] Hoyle, C. E., Kyu-Jun Kim, J. Appl. Polym. Sci., 1987, 33,

2985-2996.

- [17] Hoyle, C. E., Kyu-Jun Kim, *Polymer*, 1988 29, 18-23.
- [18] *Textbook of Polymer Science*, Billmeyer, F. W., 1984, Wiley-Interscience.
- [19] Schirmann, P.J., Dexter, M., *Handbook of Coatings Additives*, Edited by Calbo, L.J., Chapter 8, 225-269, 1987 Marcel Dekker Inc.,
- [20] Kurumada, T., Ohsawa, H., *J. Polym. Sci., Polym. Chem. Ed.*, 1985, 23, 1477-1491.
- [21] Kurumada, T., Ohsawa, H., *J. Polym. Sci., Polym. Chem. Ed.*, 1985, 23, 2747-2756.
- [22] *UV Curing: Science and Technology*, Vol II, Pappas, S. P., 1985, Technology Marketing Corporation.
- [23] Davidson, R. S., Goodin, J. W., *Eur. Polym. J.*, 1985, 18, 597-606.
- [24] Berner, G., Puglisi, J., Kirchmayr, R., Rist, G., *J. Rad. Curing* 1979, 6, 2-9.
- [25] Osborn, C. L., *J. Rad. Curing* 1976 3, 2-11.
- [26] *UV Curing: Science and Technology*, Vol I, Pappas, S. P., 1978, Technology Marketing Corporation.
- [27] Sumiyoshi, T., Schnabel, W., Henne, A., *J. Photochem.*, 1985 30, 63-80.
- [28] Baxter, J. E., Davidson, R.S., Hageman, H. J., McLauchlan, K. A., Stevens, D.G., *J. Chem., Commun.*, 1987, (2) 73-75.
- [29] Sato, K., *Progress in Org., Coatings*, 1980, 8, 1-18.
- [30] Gaube, H. G., *Polym. Paint. Col. J.*, 1987, 177(4197), 582-590.
- [31] Chambers, S., Guthrie, J., Otterburn, M. S., Woods, J.,

Polym. Comm., 1986, 27, 209-211.

- [32] Baxter, J. E., Davidson, R. S., Hageman, H. J., Overeem, T., Makromol. Chemie Rapid Commun., 1987, 8, 311-314.

The
Photopolymerisation
of
Pigmented Films

Chapter 6

The Photopolymerisation of Pigmented Films

Chapter 6	The Photopolymerisation of Pigmented Films	
	Introduction	224
	Effects of Pigmentation on the UV Curing of Thin Films	226
	Competitive Absorption Effects	226
	Effect of Scattering by Pigment	227
	Titanium Dioxide as a Pigment	228
	Results and Discussion	230
	Acknowledgements	241
	Experimental	242
	References	244

INTRODUCTION

The use of UV light to polymerise low molecular weight materials of low volatility (100% solids) for the production of surface coatings has many advantages over conventional techniques, as described previously in Chapter 5. UV curable formulations for printing inks [1, 2], photoresists [3, 4-6], optical fibres [7, 8], adhesives [9] and metal coatings [10, 11] have been described recently in a number of publications. Many of these applications require that the surface coating formulation contains pigment. The addition of pigment to a UV curable surface coating will affect the photopolymerisation process in many ways. The principal effect will be on the curing process itself, however the physical properties of the film, and the storage stability will also be affected in some way [12]. Therefore, pigments cannot be considered as inert additives [13]. By virtue of their physical characteristics, pigments will compete with the photoinitiator for the incident radiation, thus reducing the photoinitiator efficiency. In particular, the strong absorption of UV radiation by titanium dioxide (TiO_2) limits the utility of conventional photoinitiators in pigmented coatings [14]. On account of their particulate nature, pigments such as TiO_2 will scatter, absorb, reflect and refract the UV radiation, and as a result, the natural transparency of the polymer is lost, thereby affecting the rate of cure [15]. Thus the development of suitable photoinitiators to efficiently polymerise pigmented UV curable coatings are required for the growing diversity of the many applications of this technique.

In this Chapter the photoinitiating efficiency of a thioxanthone derivative 2-chlorothioxanthone (CTX), developed specifically for the UV curing of pigmented coatings, has been compared with the acylphosphine oxide 2,4,6-trimethylbenzoyldi-phenylphosphine oxide (TMBPO). The acylphosphine oxides, as described in Chapter 5, are a "new, novel class of photoinitiators" [16]. Because of their absorbance characteristics, they have been claimed to be suitable photoinitiators for UV curable formulations containing certain pigments. The addition of tertiary amines as synergists with the thioxanthone derivatives was considered to be a drawback for the UV polymerisation of pigmented coatings [16], due to the potential of an amine to reduce the light fastness of the cured coatings. It appears that without amine however, acylphosphine oxides do not have any effect in pigmented acrylic resins [16]. It was also claimed that the thioxanthone-amine combination was unsuitable for curing unsaturated polyester resins in styrene, although the system was suitable for acrylic resins [16]. This may be due to styrene effectively quenching the triplet excited state of the thioxanthone [17]. The acylphosphine oxides were reported to be suitable for the polymerisation of unsaturated polyester resins containing styrene [16].

There are a large number of factors which affect the overall efficiency and properties of a UV cured coating (Chapter 5). The addition of a pigment to the UV curable formulation can reduce the photoinitiating efficiency by absorbing the incident

radiation and scattering the light. The pigment can also cause additional photodegradative effects, particularly in the case of TiO₂, as discussed below.

EFFECTS OF PIGMENTATION ON THE UV CURING OF THIN FILMS.

COMPETITIVE ABSORPTION EFFECTS.

When two or more UV absorbers (photoinitiators, photosensitisers or pigments) are present in a UV curable formulation, each species will absorb radiation. The total absorption, I_A , will be larger than that of either species alone, as shown in equation 1:-

$$I_A = I_0 (1 - \exp[-(E_1 C_1 + E_2 C_2 + E_3 C_3 + \dots + E_n C_n)l]) \quad (1)$$

where n is any number of absorbing components, l is the film thickness, I_0 the incident radiation and I_A is the total absorbed radiation. The fraction of light absorbed by compound 1 in the presence of compound 2 is related to the ratio of their optical densities. Consequently, the fraction of light absorbed by a component x is |-

$$I_{Ax} = I_A \frac{E_x C_x}{E_1 C_1 + E_2 C_2 + E_3 C_3 + \dots + E_x C_x} \quad (2)$$

Thus, when a pigment is dispersed in a UV curable formulation containing photoinitiator, the total absorption increases, but the amount absorbed by the photoinitiator decreases due to the competition by the pigment [12, 18]. Both the radiation intensity

and the extinction coefficients of the components in the formulation vary with wavelength, and therefore the fraction of radiation absorbed by each compound will also vary with wavelength. This can have profound affects upon the absorption of radiation by the photoinitiator in the bottom layers of the film. As described in Chapter 5, the absorption of UV light in the upper layers of the film [19-21] can be so strong that little radiation reaches the bottom of the film, and then only a fraction of that total radiation will be absorbed by the photoinitiator. The result of this poor absorption is often indicated by a loss of adhesion to the substrate and a poor through cure. As many pigments also absorb radiation in the UV range, they will compete with the photoinitiator for the incident radiation, particularly at the bottom of the film. Hence adhesion to the substrate and through cure are often much worse in pigmented films unless preventative measures (reduced cure speed) are taken. If too much radiation is absorbed at the film surface so that the surface of the film polymerises before the lower layers, wrinkling of the surface will result. This "puckering" of the surface is due to the differential forces that occur when the lower layers of the film shrink after the surface layer has polymerised. Although this phenomenon can occur with any type of coating, UV curable coatings containing pigments which scatter and absorb UV light are particularly susceptible [12, 18].

EFFECT OF SCATTERING BY PIGMENT

The presence of a pigment in a UV curable formulation will

also reflect i.e., scatter the incident radiation, hence diminishing the available radiation to the photoinitiator. The reflectance or scattering properties of a pigmented film depends upon the difference between the refractive index of the pigment and the vehicle, the particle size and the concentration of the pigment, and the wavelength of the radiation. These factors are all interrelated in their effect upon light scattering [12, 18]. The effect of scattering increases the effective path length of the radiation throughout the film. It will also increase the internal reflectance which, on a reflective substrate can be very pronounced in pigmented systems, and the diffusion of the radiation throughout the film.

Due to these scattering effects and the nature of the UV curable medium in which the pigment is dispersed, the calculation of the amount of radiation absorbed by a photoinitiator in the presence of a pigment is very complex, and cannot be solved by simple equations like (1) and (2).

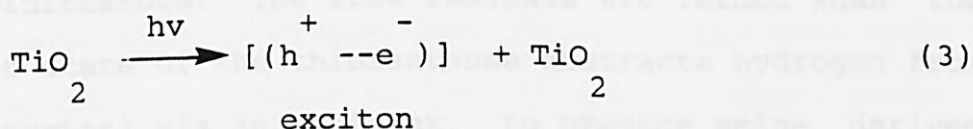
TITANIUM DIOXIDE AS A PIGMENT

Generally, white coatings are prepared using pigments which are effective in scattering visible light and absorb very little of it. TiO_2 is probably the most widely used white pigment due to its superior opacity at low pigment concentrations in thin films. There are two crystalline forms of TiO_2 , anatase and rutile, both of which are available as pigments commercially.

Titanium dioxide is transparent through the visible region of the spectrum but absorbs UV strongly at wavelengths below

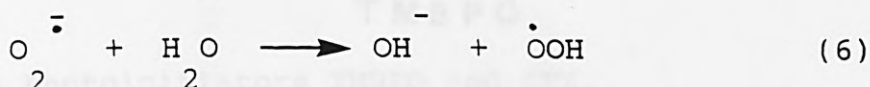
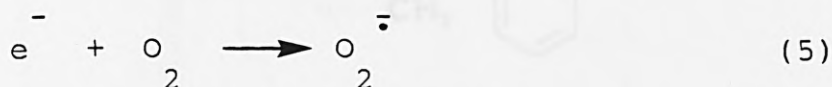
380nm [12, 14, 18]. The rutile and anatase forms start absorbing light at wavelengths below 425 nm and 400 nm respectively. As a result, coatings pigmented with the rutile form will have a slight yellow colouration compared to those pigmented with the anatase form. As the region 380-400nm represents a transition between the reflection and absorption of light, this 'window' can be used for sensitising photoinitiator systems such as the thioxanthone derivatives and the acylphosphine oxides which have absorbance maxima in the 380 nm region, and are therefore capable of absorbing the light in this 'window' region. Although the anatase form of TiO₂ provides a slightly larger window for UV transmission, the rutile form is generally preferred for UV curable formulations. The rutile form of TiO₂ has a higher refractive index than the anatase form which not only confers superior opacity, but also a greater refractive index difference between the pigment and the vehicle, thus scattering the incident radiation more efficiently [12, 14].

The photodecomposition of TiO₂ pigments by UV light in the presence of oxidisable organic compounds results in the undesirable film property commonly known as "chalking" [22]. Absorption of UV radiation by TiO₂ results in the promotion of electrons into the conduction band, thereby creating electron deficiencies or holes in the valence band (equation 3).



Interaction of the holes with hydroxide ions (equation 4), or the

electrons with oxygen (equation 5) and water (equation 6) can lead to the formation of free radicals at the surface of the TiO_2 particles. The radicals generated can bring about photopolymerisation and crosslinking [12, 15].



RESULTS and DISCUSSION.

The acylphosphine oxides are photoinitiators which function by a Norrish Type 1 photocleavage, producing initiating radical species via a short lived triplet excited state [16, 23, 24]. As a result of this there is little chance of the excited states of the photoinitiator being quenched by oxygen or monomer, and therefore the acylphosphine oxides should initiate the polymerisation of UV curable materials without the need to add synergists. It has been shown (Chapter 5 and [25]) however, that in order to effect an efficient cure speed, it is necessary to add tertiary amines as synergists to resin formulations containing acylphosphine oxides. The thioxanthone derivatives are also free radical photoinitiators. The free radicals are formed when the excited triplet state of the thioxanthone abstracts hydrogen from an amine (synergist) via an exciplex, to produce amine derived radicals capable of initiating polymerisation [17, 26]. It may be anticipated that as the thioxanthenes initiate polymerisation by

a bimolecular process they may well be less efficient than the acylphosphine oxides due to competitive quenching processes.

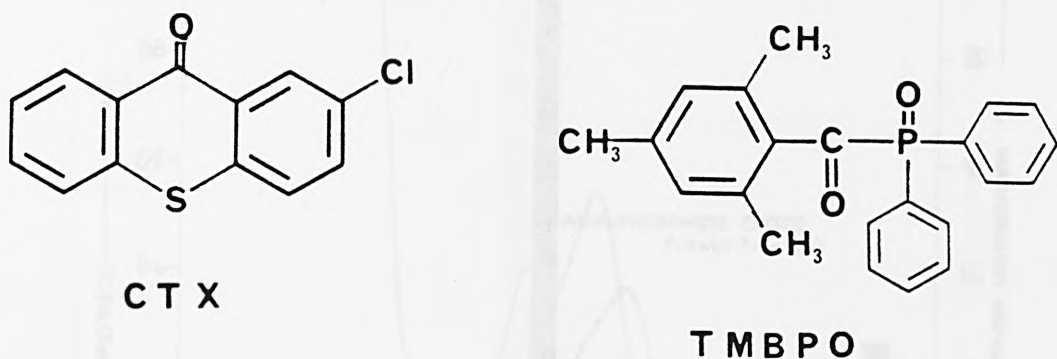


Figure 1. The Photoinitiators TMBPO and CTX.

Both the acylphosphine oxide 2,4,6-trimethylbenzoyl di-phenylphosphine oxide (TMBPO) and the thioxanthone, 2-chlorothioxanthone (CTX) possess strong absorption bands between 350 - 400 nm as shown in Figures 2 and 3. The Figures 2 and 3 compare the spectra of the photoinitiators with a histogram showing the relative spectral power distribution as a percentage of the lamp output, for the lamp used in the investigations. As a result of their intense absorption maximum around 380 nm, where pigments such as TiO₂ are relatively transparent [17], both photoinitiators are particularly useful for the UV curing of TiO₂ pigmented coating formulations. Both photoinitiators absorb in the wavelength region where the UV lamp used in these experiments has a particularly strong emission line (365 - 370 nm) as shown in Figures 2 and 3. From the spectral data provided, (Table 1 and Figure 3) it is reasonable to assume that CTX, with its much higher extinction coefficient, could be used at a much lower concentration than TMBPO.

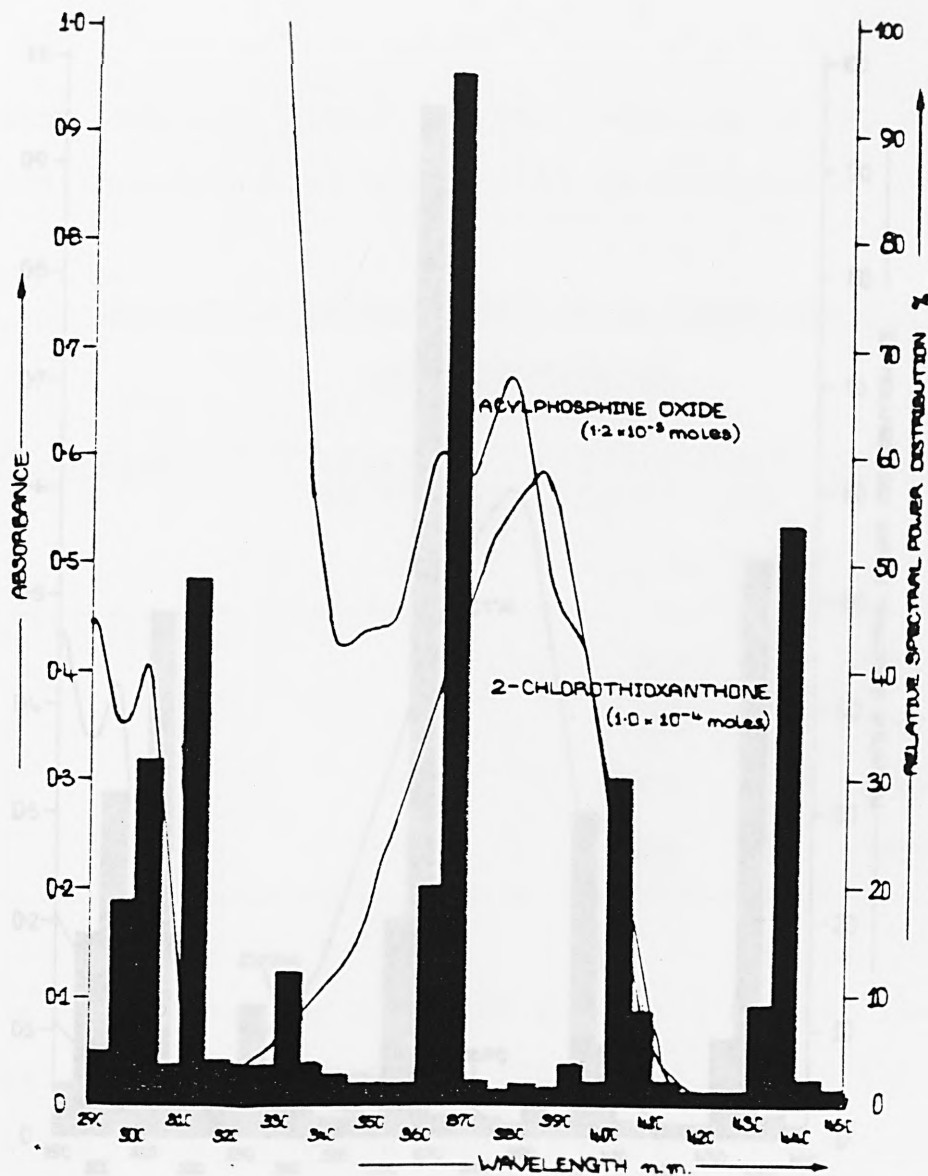


Figure 2 The Absorbance Spectra of TMBPO and CTX at Different Concentrations ($1.2 \cdot 10^{-3}$ moles and $1.0 \cdot 10^{-4}$ moles respectively).

The photoinitiators CTX and TMBPO were investigated in a TiO₂ pigmented epoxy-diacrylate formulation, containing N-methyl-diethanolamine as a synergist. During the experiments it was found that the acylphosphine oxide gave unacceptably low cure speeds in the absence of amine synergists. The most rapid cure speeds for both the CTX and the TMBPO formulations were determined over a range of variable amine and photoinitiator concentrations. The optimum concentration of the amine synergist and the photoinitiator was therefore determined, the results are shown in Table 2.

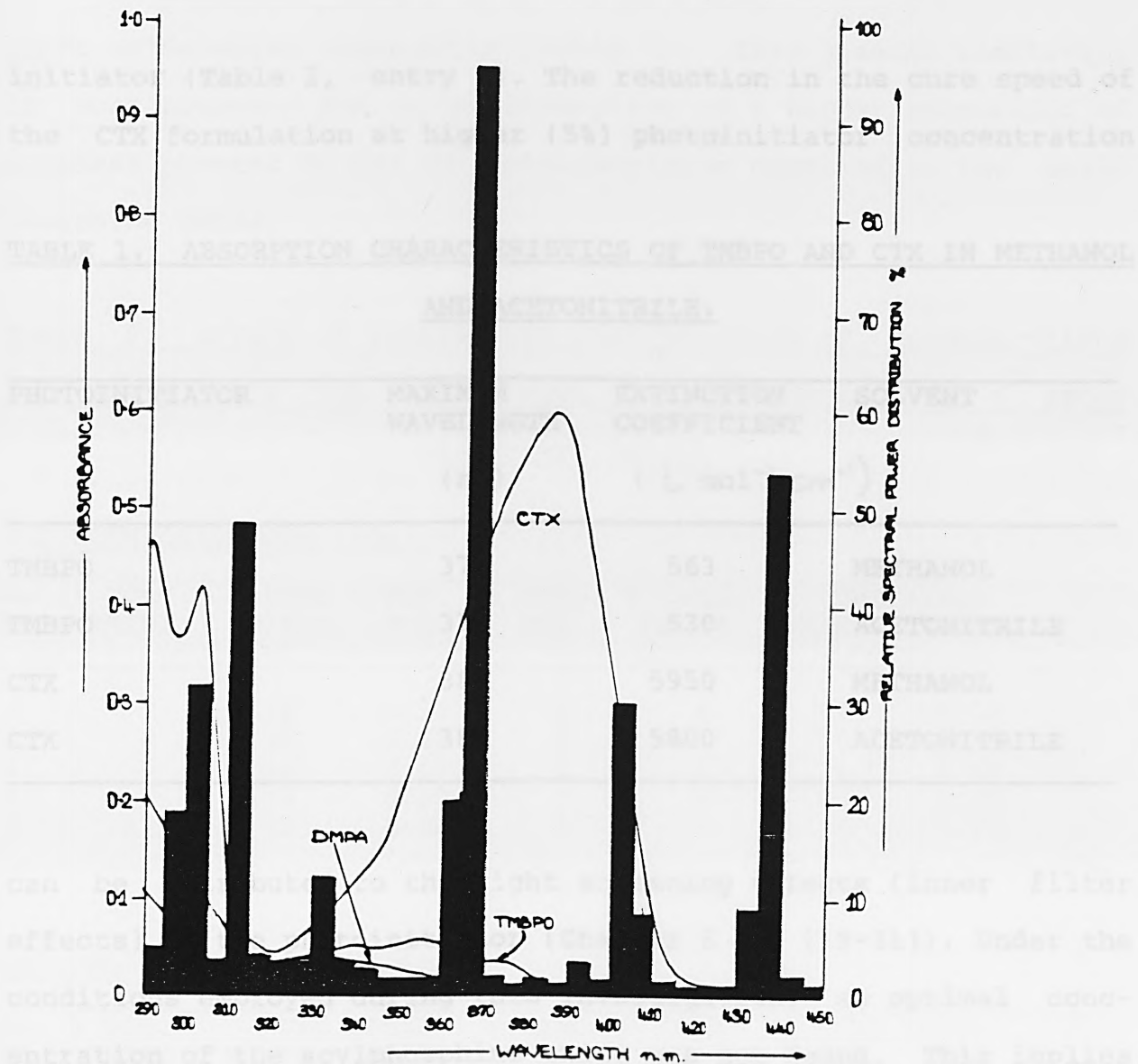


Figure 3 The absorbance Spectra of TMBPO and CTX at a Concentration of $1.0 \cdot 10^{-4}$ moles.

The synergistic effect of the amine is clearly shown in Table 2. The chlorothioxanthone formulations show a much faster cure speed than the acylphosphine oxide formulations for equivalent percentage concentrations of photoinitiator. This is particularly marked at the 1% photoinitiator level (Table 2 entries 1 and 6). An optimal amine concentration was observed (Table 2, entries 2 and 8), which suggests that the effect of amine is concentration dependent (see Chapter 5). Similarly, an optimal concentration was observed for the chlorothioxanthone photo-

initiator (Table 2, entry 4). The reduction in the cure speed of the CTX formulation at higher (5%) photoinitiator concentration

TABLE 1. ABSORPTION CHARACTERISTICS OF TMBPO AND CTX IN METHANOL AND ACETONITRILE.

PHOTOINITIATOR	MAXIMUM WAVELENGTH (nm)	EXTINCTION COEFFICIENT ($\text{L mol}^{-1} \text{cm}^{-1}$)	SOLVENT
TMBPO	377	563	METHANOL
TMBPO	378	530	ACETONITRILE
CTX	384	5950	METHANOL
CTX	384	5800	ACETONITRILE

can be attributed to the light screening effects (inner filter effects) of the photoinitiator (Chapter 5 and [19-21]). Under the conditions employed during this investigation, an optimal concentration of the acylphosphine oxide was not found. This implies that even at the highest (5%) concentration of photoinitiator used the light could still effectively penetrate the full thickness of the film.

A comparison of the rate of cure for the epoxy-diacrylate resin with and without pigment is shown in Table 2 (entries 8 and 11). At an optimum TMBPO and amine concentration the presence of pigment appeared to have very little effect upon the cure speed of the UV curable formulation. The chlorothioxanthone-amine combination resulted in much higher cure speeds than the acylphos-

phine oxide-amine combination (Table 2). This greater reactivity is most probably due to the absorption of a higher proportion of incident photons by the chlorothioxanthone compared to the acylphosphine oxide.

TABLE 2. EFFECT OF VARYING THE CONCENTRATION OF PHOTOINITIATOR AND AMINE UPON THE RATE OF CURE OF A PIGMENTED (TiO₂) EPOXY DIACRYLATE RESIN.

CHLOROTHIOXANTHONE (CTX).

	% Conc.		CURE SPEED		% Conc.		CURE SPEED	
	CTX	AMINE	M/MIN.	SECS.	CTX	AMINE	M/MIN.	SECS.
1)	3	2	18	0.54	1	4	18	0.54
2)	3	4	20	0.48	2	4	20	0.48
3)	3	6	14	0.68	3	4	20	0.48
4)	3	8	12	0.80	4	4	22	0.45
5)	3	10	12	0.80	5	4	16	0.60

ACYLPHOSPHINE OXIDE (TMBPO).

	% Conc.		CURE SPEED		% Conc.		CURE SPEED	
	TMBPO	AMINE	M/MIN.	SECS.	TMBPO	AMINE	M/MIN.	SECS.
6)	3	2	4	2.40	1	6	3 x 2	14.40
7)	3	4	8	1.20	2	6	8	1.20
8)	3	6	12	0.80	3	6	12	0.80
9)	3	8	10	0.96	4	6	14	0.68
10)	3	10	8	1.20	5	6	18	0.54
11)	3	6	12	0.80				

The photoinitiating efficiency of the two photoinitiators CTX and TMBPO were compared on different substrates. Using a combination of 3% (CTX)/4% amine and 3% (TMBPO)/6% amine on both glass and paper substrates, the degree of cure was assessed using

the Persoz Pendulum hardness test [27]. Pendulum hardness is related primarily to the cure response and the crosslinked density of the coating [28]. Infrared techniques have also established a good correlation between the pendulum hardness and the residual unsaturation within the film [29]. Therefore, the pendulum hardness values can be used as an approximate parameter for determining the degree of cure within a film. An optimum pendulum hardness value was determined for a 20 um film of the pigmented formulation on the glass substrate. This value was found to be 141.08 ± 4.27 seconds. The results in Table 3 show that a change of substrate caused very little difference in the

TABLE 3. EFFECT OF SUBSTRATE UPON THE RATE OF CURE OF A PIGMENTED (TiO₂) EPOXY RESIN AND THE EFFECT OF THE SUBSTRATE UPON FILM HARDNESS.

PHOTOINITIATOR	SUBSTRATE	CURE SPEED M/MIN.	SECS.	HARDNESS ** X ± σ ²	APPROX. % CURE.
CTX	PAPER	12	0.80	----	
	GLASS	10	0.96	35.89 ± 3.11	25.44
TMBPO	PAPER	10	0.96		
	GLASS	12	0.80	75.33 ± 7.59	53.0

** Optimum Hardness value : Glass 141.08 ± 4.27 .

cure speeds recorded for either photoinitiator. The hardness values obtained however are much lower than the optimum hardness value and are indicative of poor through cure. The acylphosphine oxide provided a much higher hardness value which suggests that more crosslinking occurred in the film cured with TMBPO than the

CTX. The coatings produced by both photoinitiators were very similar in their general appearance. The films were smooth, and glossy with a slight yellowish tinge. TMBPO was reported to impart little yellowing compared to CTX [16] although in this investigation both coatings appeared to exhibit about the same degree of yellowness. With prolonged exposure to UV irradiation, a similar degree of yellowness was observed.

The effectiveness of the two photoinitiators to polymerise various thicknesses of the pigmented epoxy-diacrylate formulation was investigated. The results obtained when the pigmented film thickness was increased differed considerably to those obtained with the non-pigmented films (Chapter 5 and [25]). Increasing the film thickness of the pigmented resin led to a marked decrease in the rate of cure, (Tables 4 and 5). The differences observed

TABLE 4. EFFECT OF FILM THICKNESS UPON THE RATE OF CURE OF A PIGMENTED (TiO₂) EPOXYDIACRYLATE RESIN AND EFFECT OF SUBSTRATE UPON THE FILM HARDNESS.

PHOTOINITIATOR	THICKNESS IN μ M	CURE SPEED IN M/MIN: SECS.				HARDNESS $\bar{x} \pm \sigma^2$
		PAPER		GLASS		
CTX	20	12	0.80	10	0.96	35.89 \pm 3.11
	40	10	0.96	6	1.60	36.67 \pm 2.36
	80	4	2.40	2	4.80	30.00 \pm 0.58
	120	2	4.80	2	4.80	34.67 \pm 3.04
TMBPO	20	10	0.96	12	0.80	75.33 \pm 7.59
	40	8	1.20	10	0.96	31.50 \pm 2.50
	80	4	2.40	4	2.40	33.67 \pm 0.94
	120	2	4.80	2	4.80	41.33 \pm 4.23

between these results and those obtained in Chapter 5 may be accounted for by the addition of TiO_2 . The increase in the film thickness not only resulted in slower cure speeds, but also poor absorption by the photoinitiator at the bottom of the film with the subsequent loss of adhesion (the films were very easily peeled away from the substrate), undesirable film properties (surface wrinkling and pigment migration) and a poor through cure, as shown by the low values obtained in the pendulum hardness determination (Table 4 and 5). In the case of thin films the absorption by the photoinitiator is increased with the addition of pigment [18]. This is due to the longer path length caused by scattering and the increased internal reflectance due to the diffusion of the radiation. An increase in the pigmented film thickness however, resulted in the absorption by the photoinitiator at the bottom of the film dropping precipitously, as shown by the ease with which the film could be removed from the substrate. Clearly, this result is due to the pigment reducing the effectiveness of penetration of the light through the film, with the consequence that the bottom portion of the film does not become fully cured. The occurrence of such an effect has important practical implications in that such films will exhibit poor adhesion to the substrate.

The physical appearance of the thicker TiO_2 pigmented films cured with each photoinitiator were very similar and generally poor. Surface wrinkling occurred, the effect becoming more pronounced as the film thickness increased. Despite this effect, the films had a glossy appearance. There were scattered areas in the

films which had a matt finish, due to the migration of pigment to the surface. This effect was observed at all thicknesses and with both photoinitiator formulations.

The investigation was continued using lower photoinitiator concentrations, but this did not lead to faster cure speeds or to a better through cure. In fact, reducing the concentration of the acylphosphine oxide to 1% resulted in no cure being obtained at all, for any thickness (Table 5). A 1% concentration of chlorothioxanthone however, resulted in reasonable cure speeds at all the thicknesses measured, and a better through cure (as determined by the Persoz hardness test) at a 1% concentration compared to a 3% concentration (Table 5). The film finishes obtained at the lower photoinitiator concentrations were glossy, with a degree of surface wrinkling and a little pigment migration to the surface with an increase in the film thickness. Nevertheless, the surface of the 20 um film at a 1% CTX concentration actually possessed the best physical appearance observed of all the coatings examined throughout the investigation.

The effect of oxygen upon the rate of cure was determined by applying the pigmented resin as a film to paper, covering this coating with polyethylene film and irradiating in the normal way. As noted during the investigation of the non-pigmented system (Chapter 5 and [25]), oxygen markedly inhibited the curing of the epoxy-diacrylate resin, (Table 6). Interestingly, the acylphosphine oxide initiated cure in the absence of amine when oxygen was also absent. This indicates that the photoinitiating properties of acylphosphine oxides are particularly sensitive to the

TABLE 5. EFFECT OF FILM THICKNESS UPON THE RATE OF CURE OF A PIGMENTED (TiO₂) EPOXYDIACRYLATE RESIN AND EFFECT OF SUBSTRATE UPON FILM HARDNESS.

CTX (1% CONCENTRATION)

THICKNESS μM	PAPER		GLASS		HARDNESS	
	M/MIN.	SECS.	M/MIN.	SECS.	$\bar{x} \pm$	
20	8	1.20	8	1.20	43.00 ±	2.45
40	8	1.20	8	1.20	38.33 ±	2.62
80	4	2.40	2	4.80	31.00 ±	1.41
120	2	4.80	1	9.6	37.33 ±	0.94

CTX (0.5% CONCENTRATION)

TMBPO (1% CONCENTRATION)

THICKNESS μM	PAPER		THICKNESS μM	PAPER	
	M/MIN.	SECS.		M/MIN.	SECS.
20	5 X 2	24.0	20	>10 X 2	>48.0
40	6 X 2	28.8	40	>10 X 2	>48.0
80	>10 X 2	>48.0	80	>10 X 2	>48.0
120	>10 X 2	>48.0	120	>10 X 2	>48.0

presence of oxygen. The ability of amine in mitigating the effect of oxygen is shown by the results in Table 6.

TABLE 6. A COMPARATIVE STUDY OF THE EFFECT OF OXYGEN INHIBITION ON THE RATE OF CURE OF A PIGMENTED RESIN.

IRRADIATED SAMPLE	CURE SPEED IN AIR		CURE SPEED NO AIR	
	M/MIN	SECONDS	M/MIN	SECONDS
TMBPO (no amine)	>0.2	>48.0	14.0	0.68
TMBPO with amine	10	0.96	14.0	0.68
CTX with amine	12	0.80	16.0	0.60

In conclusion, the acylphosphine oxide did not display any advantageous properties [16, 26] compared to the thioxanthone derivative when both photoinitiators were used in a pigmented UV curable formulation.

Chlorothioxanthone (CTX) and 2,2-bis[4-(dimethylamino)phenyl]propane (DABCO) were used as received.

The pigmented formulation was prepared from 24.00g of TiO₂ (Rutile, from Tiwhite International) and 22.00g of resin (Iron Synthes B.v.). The resin was a composite of a high molecular weight acrylic polyol (R1) dissolved in 40% xylene, Sotacure AP 544 an epoxydiacrylate oligomer, Sotacure AM 546, which is dianoldiacrylate (R2) and Sotacure AM 551 which is tri-propyleneglycol diacrylate (TPGDA) (R3) (xylene removed) and 2.25g of Sotacure AP 544 was combined together to disperse the pigment. This composition and 24.00g of TiO₂ were mixed together in a screw topped jar using a spatula. A further 10.00g of the Sotacure AM 544 and 10.00g of glass beads were added to the dispersed pigment mixture in the jar. This was then

ACKNOWLEDGEMENTS

I would like to thank Dr Roel Buter and his staff at Akzo Research Laboratories, Arnhem for their unlimited help and for sharing some of their expertise in the dispersion of pigments.

The UV curing experiments were carried out as described previously in Chapter 3 [25]. The substrates used were ordinary paper and cleaned glass thin layer chromatography plates (Merck). The substrates were coated using Eichel rods, selected to

EXPERIMENTAL

The synthesis of 2,4,6-trimethylbenzoyldiphenylphosphine oxide (TMBPO) has been described previously in Chapter 2 [30]. 2-Chlorothioxanthone (CTX) and N-methyldiethanolamine (Janssen Chimica) were used as received.

The pigmented formulation was prepared from 24.00g of TiO_2 (Rutile, from Tioxide International) and 32.00g of resin (from Synthese b.v.). The resin was a composite of a high molecular weight acrylic polyol Setalux 1151, dissolved in 49% xylene, Setacure AP 569 an epoxydiacrylate oligomer in Setacure AM 548, which is dianoldiacrylate LV, and Setacure AM 553 which is tri-propyleneglycoldiacrylate (TPGDA). 1.50g of Setalux 1151 (xylene removed) and 2.25g of Setacure AM 553 were combined together to disperse the pigment. This combination and 24.00g of TiO_2 were mixed together in a screw topped jar, using a spatula. A further 10.00g of the Setacure AM 553, and 50.00g of glass beads were added to the dispersed pigment mixture in the jar. This was then assembled into a Red Devil Shaker (from Erichsen GmbH) and shaken for 15 minutes. Following this operation, 4.53g of Setacure AM 553 and 13.42g of Setacure AP 569 were added and shaken on the Red Devil for another 15 minutes. The glass beads were filtered off using a fine mesh sieve.

The UV curing experiments were carried out as described previously in Chapter 5 [25]. The substrates used were satinised paper and cleaned glass thin layer chromatography plates (Merck). The substrates were coated using Erichsen rods, selected to

provide wet film thicknesses in the region of 20 - 120 μm . The Persoz pendulum hardness test and the UV curing experiments in the absence of air were previously described in Chapter 5.

The absorbance spectra of the photoinitiators were recorded at fixed concentrations on a Hitachi 100-80A computerised spectrophotometer in methanol and acetonitrile. Methanol and acetonitrile (Baker) were used directly from unopened bottles. The spectra obtained were compared with a histogram showing the relative spectral power distribution, as a percentage of the lamp output for the lamp used in the UV curing experiments, Figure 2. Figure 3 shows the spectra of CTX and TMBPO at different concentrations but at similar absorbances so that their maximum wavelength can be compared. The information shown in Table 1 was calculated using these spectra.

- [9] Woods, J., Radcove Conference Proc., PC83-414, May, 1983.
- [10] Hoebeke, J. H., Goffe, G. V., Desmarais, W., Dervalis, J. P., Radcove Conference Proc., PC83-443, May, 1983.
- [11] Turner, T. A., Radcove Conference Proc., PC83-268, May, 1983.
- [12] Wicks, Z. W., UV Curing, Science and Technology, Pappas, S. P., Ed., Chapter 4, Vol 1, Technology Marketing Corporation, 1978.
- [13] McQuinnan, V. B., ACS Symposium Series 33, Amer. Chem. Soc., 1978, 115-119; and ACS Coatings and Plastics Preprints, 1979, 25(1), 118-121.
- [14] Alaridgw, A. D., Frensch, P. D., Hutchinson, J., J. Pol.

REFERENCES.

- [1] Zylka, P., Radcure Conference Proc., FC83-251. May, 1983.
- [2] Roesch, K, F., Radcure Conference Proc., FC83-259, May, 1983.
- [3] Decker, C., Radcure Conference Proc., FC83-265, May, 1983.
- [4] Becker, L, A., Sopori, B, L., Chang, W, S, C., Applied Optics, 1978, 17, 1069-1071.
- [5] Loh, I, H., Martin, G, C., Kowel, S, T., Kornreich, P., Polymer Preprints, 1982, 23, 195-196.
- [6] Lacombat, M., Dubroeuq, G, M., Massin, J., Brevignon, M., Solid State Tech., 1980, 28(8), 115-121.
- [7] Newman, H, C., Radcure Conference Proc., FC83-267, May, 1983.
- [8] Lawson, K, R., Radcure Conference Proc., FC83-264, May, 1983.
- [9] Woods, J., Radcure Conference Proc., FC83-414, May, 1983.
- [10] Hoebeke, J, M., Loutz, J, M., Demarteau, W., Servais, J, P., Radcure Conference Proc., FC83-443, May, 1983.
- [11] Turner, T, A., Radcure Conference Proc., FC83-268, May, 1983.
- [12] Wicks, Z, W., UV Curing: Science and Technology, Pappas, S, P., Ed., Chapter 3, Vol I, Technology Marketing Corporation, 1978.
- [13] McGinniss, V, D., ACS Symposium Series 25, Amer. Chem. Soc., 1976, 134-149; and ACS Coatings and Plastics Preprints, 1975, 35(1), 118-123.
- [14] Aldridge, A, D., Francis, P, D., Hutchinson, J., J. Rad.

- Curing, 1984, 11(3), 10-17.
- [15] Schirmann, P. J., Dexter, M., Handbook of Coatings Additives, Ed., Calbo, J., Chapter 8, Marcel Dekker Inc., 1987, 225-269.
- [16] Jacobi, M., Henne, A., J. Rad. Curing 1983, 10 (4) 16-25.
- [17] Amirzadeh, G., Schnabel, W., Makromol. Chem. 1981, 182, 2821-2835.
- [18] Roffey, C. G., Photopolymerisation of Surface Coatings, Chapter 3, 110-117; Chapter 4, 178-180, Wiley-Inter., 1982.
- [19] Hutchison, J., Ledwith, A., 1973, Polymer 14 405-408.
- [20] Guthrie, J., Jeganathan, M. B., Otterburn, M. S., Woods, J., Polymer Bulletin 1986, 15 51-58.
- [21] Van Landuyt, D. C., J. Rad. Curing 1984, 11 (3) 4-8.
- [22] Pappas, S. P., Prog. in Org. Coatings, 1973/74, 2, 333-347.
- [23] Sumiyoshi, T., Schnabel, W., Henne, A., Lechtken, P., Polymer 1985, 26 141-146.
- [24] Baxter, J. E., Davidson, R. S., Hageman, H. J., McLauchlan, K. A., Stevens, D. G., J. Chem., Commun., 1987, (2) 73-75.
- [25] Baxter, J. E., Davidson, R. S., Hageman, H. J., Accepted for publication, Europ. Polym. J.,
- [26] Schnabel, W., J. Rad. Curing 1986, 13 (1) 26-34.
- [27] Sato, K., Progress in Org., Coatings, 1980, 8, 1-18.
- [28] Gaube, H. G., Polym. Paint. Col. J., 1987, 177 (4197), 582-590.
- [29] Berner, G., Kirchmayr, R., Rist, G., J. Oil Col. Chem. Assoc. 1978, 61, 105-113.
- [30] Baxter, J. E., Davidson, R. S., Hageman, H.J., Overeem, T., Makromol., Chemie Rapid Commun., 1987, 8, 311-314.

Chapter 7

Using FTIR Spectroscopy to Measure the Residual Unsaturation in Polymer Films

Chapter 7	Using FTIR Spectroscopy to Measure the Residual Unsaturation in Polymer Films	
	Introduction	246
	Background and Principles of Fourier Transform Infrared Spectroscopy	248
	Background	248
	Principles of Fourier Transform Infrared Spectroscopy	249
	Attenuated Total Reflectance Spectroscopy	253
	Quantitative Analysis using ATR	256
	Results and Discussion	258
	Acknowledgements	266
	Experimental	267
	Appendix A	275
	Appendix B	281
	References	284

INTRODUCTION

Following the conversion of a coating formulation from a liquid to the solid state using UV light, one needs to determine the extent to which the UV initiated polymerisation of the unsaturated compound has proceeded. This is normally determined by measuring the 'degree of cure'. The degree of cure is a widely used term which usually refers to the number of double bonds consumed during the photopolymerisation reaction. In practise, the degree of cure for surface coatings is mostly determined by empirical tests [1], such as solvent resistance, abrasion, pencil hardness and the thumb twist test. These tests provide at best, qualitative results because they are dependent upon the operator. Such physical methods also give an indication to the extent of crosslinking which has occurred with increasing irradiation, but not about the number of residual double bonds at the coating surface, substrate interface or throughout the bulk of the film. As this information would be of particular interest to the surface coatings industry, the earlier investigations [2] of Chapter 5 were extended to develop a means to examine the molecular changes quantitatively.

In order to study what changes occur at or near the coating's surface and at various depths in the film, the analytical technique of Fourier transform infrared spectroscopy (FTIR), in conjunction with transmission and ATR measurements, was applied. This technique offers many possibilities to study the amount of cure in surface coatings and is proving to be a unique analytical tool for the characterisation of coatings [3]. Amongst its

many advantages is the fact that as a non-destructive analytical technique it is able to measure glossy surface coatings providing information about the molecular changes which occur at the surface, substrate interface and throughout the bulk of the film. The spectrometer is coupled with a computer which controls all of the operations and collects the spectra in digital form, thus enabling many different techniques and manipulations to be used to enhance the spectral information. As a result, the FTIR technique can provide both qualitative and quantitative analysis with a high degree of accuracy.

The most common experimental techniques in FTIR used for both surface and interface spectroscopic studies are: external reflection or reflection absorption (RA); internal reflection or attenuated total reflectance (ATR); diffuse reflectance (DRF), photoacoustic (PA), emission (EM) and transmission (T). Each technique has limited applications which will ultimately restrict the choice of analytical method. In order to measure the degree of cure in a difunctional acrylate film following UV irradiation, thereby also studying the efficiencies of 2,2-dimethoxy-2-phenylacetophenone (DMPA) and the acylphosphine oxide, 2,4,6-trimethylbenzoyldiphenylphosphine oxide (TMBPO) as photoinitiators in the presence and absence of tertiary amine, FTIR/ATR was selected as the analytical technique. This technique is particularly useful for studying surface coatings and enables the degree of post cure, which occurs hours after the irradiation, to be measured. Variation of the ATR crystals, each possessing a different refractive index, enables one to depth profile a film in gradients. Therefore the possibility of a more detailed examination of the

degree of cure at the substrate interface and the extent to which oxygen inhibition occurs in the surface layers can be realised. ATR crystals can also be used to measure the transmission spectrum of the coating, thus providing information concerning the bulk composition of the sample under investigation.

BACKGROUND AND PRINCIPLES OF FOURIER TRANSFORM INFRARED SPECTROSCOPY

Background

FTIR spectroscopy is a classical example of the application of the uniqueness of Fourier's integral theorems, in which a complex wave function (interferogram) is transformed into an optical spectrum (signal versus frequency).

Fourier transform infrared spectrometers are based on the Michelson interferometer. Michelson invented the interferometer during the early 1890's so that the speed of light in a vacuum could be determined more accurately. Although Michelson apparently used a computer analog in this initial research, Fourier transformations were most probably beyond his capabilities. Subsequent refinements to interferometers occurred over the next 40 years, but the lack of electronic detectors confined interferometry applications to high-resolution spectroscopy. Jacquinot and Fellgett however, were able to point out two critical advantages of Michelson interferometers over conventional dispersive methods for the measurement of spectra, thus introducing Fourier transform spectroscopy. Fellgett was the first person

to perform a numerical Fourier transformation and calculate a spectrum. From his work in 1949, Fellgett proposed the multiplex advantage for Fourier spectroscopic methods, which is a statement of the improvement in the signal-to-noise ratio (S/N) gained by measuring frequencies simultaneously instead of sequentially. Additionally, if longer times are used for FTIR measurements, spectral S/N will improve as the square root of the measurement time increases. Jacquinot was able to show the throughput advantage of the Michelson interferometer from the increased spectral S/N which resulted from increased radiation at the detector. The FTIR spectrometer has no slits like the conventional dispersive infrared spectrometer, therefore radiation reaching the detector will be greater than that of a spectrometer with a monochromator.

Interferometry is the most accurate method known for the measurement of infrared frequencies. The mathematics involved to convert the acquired data to spectra is time consuming and can best be handled by high-speed digital computers.

Principles of Fourier Transform Infrared Spectroscopy

The Michelson interferometer is the principle, most commonly used component of a Fourier transform infrared spectrometer. This device, shown diagrammatically in Figure 1, essentially splits a beam of electromagnetic radiation into two beams, producing an interference pattern. The interferometer consists of a fixed mirror M_f , a movable mirror, M_m , and bisecting these two mirrors at an angle of 45° is a beam splitter, B_s , which ideally transmits half of the incoming radiation. The two beams are

reflected by M_f and M_m to B , where their amplitudes are combined before they exit from the interferometer on their way to the detector.

The nature of the interference between the two beams is determined by the distances each beam travels. If M_m and M_f are positioned at equal distances from B , the beams will be in phase and as a result will interfere constructively. If M_m is moved by one quarter of the incident light wavelength, the beams will be

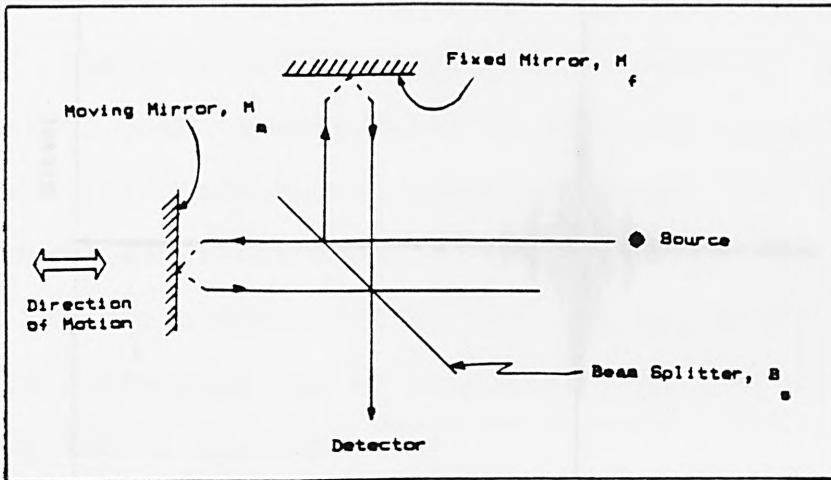


Figure 1. Diagram of a Michelson interferometer.

180° (half a wavelength) out of phase when they recombine at B because the beam has travelled to the moving mirror and then back again. At this point the two beams interfere destructively. The interferometer scan is obtained by translating the moving mirror away from the beam splitter at a constant velocity. During this motion the two beams interfere constructively and destructively at different points along the scan, resulting in the characteristic pattern of the light and dark brown of an interference pattern. For a monochromatic light source, the plot of the signal generated at the detector versus the displacement of M_m is a

where $I(x)$ is the interference as a function of mirror displacement

cosine function. When a polychromatic light source is used, the output is a complex cosine function which is the summation of all interferences caused by all simultaneous frequencies. The resulting signal is an interferogram (shown in Figure 2) which is

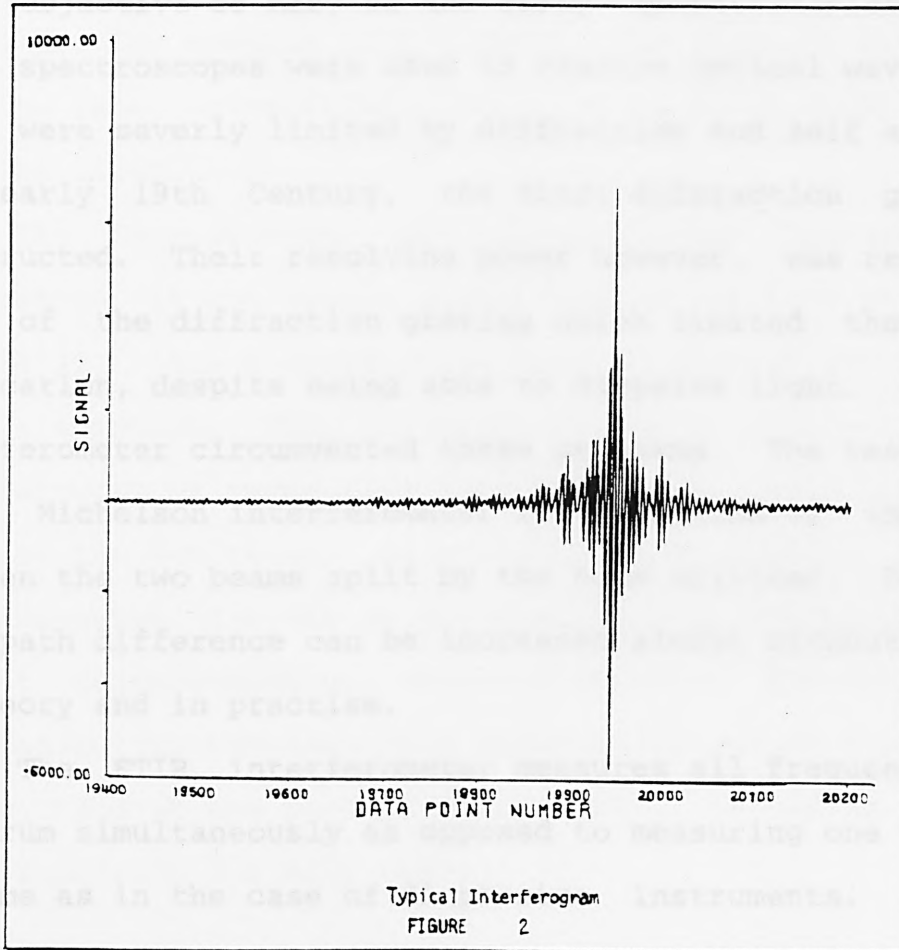


Figure 2. A typical interferogram.

related to the optical spectrum by the Fourier cosine transform:

$$I(x) = \int 2\pi \cos(2\theta x v) I(v) \cdot dv$$

and the inverse transform to obtain the spectrum:

$$I(v) = \int 2\pi \cos(2\theta x v) I(x) \cdot dx$$

where $I(x)$ is the interferogram as a function of mirror displace-

ment x and $I(\nu)$ is the intensity of the source with respect to the spectrum frequency ν [3].

The improvement of optical resolving power had been the prime objective of many of the early spectroscopists. Initially prism spectrosopes were used to resolve optical wavelengths, but these were severely limited by diffraction and self absorption. In the early 19th Century, the first diffraction gratings were constructed. Their resolving power however, was related to the size of the diffraction grating which limited their practical application, despite being able to disperse light. The use of an interferometer circumvented these problems. The resolving power of a Michelson interferometer is a function of the pathlength between the two beams split by the beam splitter, B (Figure 1). The path difference can be increased almost without limit, both in theory and in practise.

The FTIR interferometer measures all frequencies in the spectrum simultaneously as opposed to measuring one frequency at a time as in the case of dispersive instruments. Consequently, for the same output, FTIR is theoretically N (the number of elements in the spectrum) times faster than dispersive instruments. The use of mirrors in an interferometer, instead of the narrow slit used in a dispersive instrument, will not limit the energy throughput which depends only on the size of the mirrors used. In general, this results in an increase of 80-200 times the energy throughput, depending on the resolution, which in turn provides a higher sensitivity, allowing the detection of absorbance from lower concentrations of weakly absorbing species. For

equivalent measurement time and output, FTIR has a higher signal-to-noise ratio (S/N) than conventional IR because of the throughput (Jacquinot) and multiplex (Fellgett) advantages. FTIR has also been credited with having other advantages over conventional IR, for example high frequency calibration precision, fast scanning rate, significant reduction in stray light and multiple scanning capability.

The interferogram containing all the necessary spectral information is not easily identified in the form it is obtained (Figure 2), thus a computer is used to convert the interferogram into a spectrum. This manipulation can be performed on a single interferogram or successive interferograms, which are combined to increase the S/N ratio. As scan times are short (a few seconds) the increased S/N can be obtained quickly by signal averaging without using additional computation time. The ability to store and manipulate the data is a major advantage of computer interfacing, and at the present lower costs, is making FTIR spectroscopy available for many users.

Attenuated Total Reflectance Spectroscopy

Attenuated total reflectance (ATR) analysis is a simple and sensitive technique which can be used to study the surface and interface of thin polymer coatings using crystals of varying refractive index. Sample materials which are difficult to analyse by transmission measurements can often be characterised by ATR techniques. Unfortunately, certain limitations of the technique exist. High quality reproducible spectra will be achieved if the

samples are of a flexible nature or on a flexible substrate, so as to effect a good contact with the crystal. If the sample material does not allow a good contact to be maintained between itself and the crystal, then the spectral quality will be poor.

The ATR technique has been used successfully to analyse polymer films, fabrics, paper and rubber [4,5]. Variation of the angle of incident radiation should improve the spectral quality, change the penetration of the beam within the sample and the number of reflections, thus changing the total absorbance. The angle of incidence is measured from the normal to the reflecting surface. During analysis, infrared radiation is focussed onto the surface of the crystal at the entrance face at an angle of incidence greater than the critical angle, where it will undergo total internal reflection. The critical angle is defined as follows;

$$\sin \theta_c = n_1 / n_2 \quad (1)$$

where n_1 is the refractive of the sample material and n_2 is the refractive index of the crystal. Under such conditions, incident radiation will be internally reflected at each crystal - sample interface (Figure 3). The infrared beam however, will penetrate into the sample slightly. This penetration is known as an evanescent wave which will interact with sample molecules being either absorbed by the sample or reflected back to the crystal. After multiple internal reflections, the infrared radiation emerges from the crystal and is detected. The refractive index of the sample material varies in the region of an absorbance band, thus the critical angle will also change giving rise to a distorted

spectrum if it crosses over the angle of incidence. Increasing the angle of incidence will restore the total reflection condition eliminating the spectral distortion.

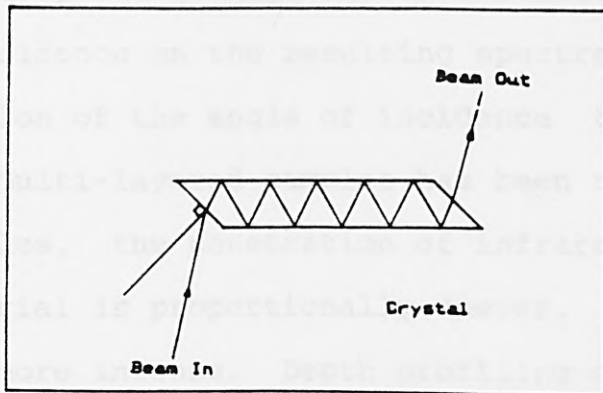


Figure 3. An illustration of total internal reflectance for a parallelogram ATR crystal.

The depth of penetration of the evanescent wave is dependent upon;

- 1) the refractive indices of the crystal and the sample,
- 2) the angle of incidence, and
- 3) the frequency of incident radiation.

This is shown below in Equation 2;

$$P = \frac{\lambda}{2\pi \left\{ \sin^2 \theta - \left(\frac{n_1}{n_2} \right)^2 \right\}^{0.5}} \quad (2)$$

where p is the depth of penetration, n_1 and n_2 are as identified in equation 1, and λ is the wavelength of the radiation.

From equation 2 it is possible to deduce that low frequency radiation will penetrate deeper into the coating sample than high frequency radiation. Similarly, for a given angle of incidence,

crystals composed of low refractive index materials will allow deeper penetration of infrared radiation into the coating sample than those composed of high refractive index. The effect of the angle of incidence on the resulting spectra [6] and the systematic variation of the angle of incidence to enable depth profiling of multi-layered samples has been reported [7,8]. With smaller angles, the penetration of infrared radiation into the sample material is proportionally deeper, thus the absorption bands are more intense. Depth profiling can also be achieved using different ATR crystals. Varying the crystals, each with a different refractive index, allows gradient trends within the film to be observed.

Quantitative Analysis using ATR

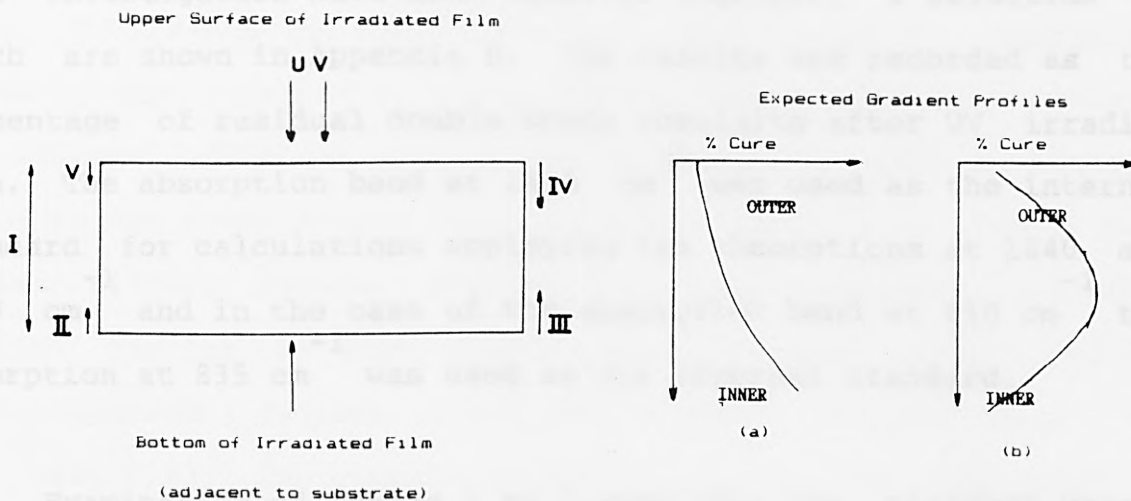
It is only recently that infrared spectroscopy has been used as a quantitative method of analysis. An important consideration to be made during quantitative analysis is that the infrared spectra does not only consist of an absorptive component but does in fact consist of a composite of the absorptive index and the refractive index. This property will cause deviations from the linearity of the concentration/intensity relationship, the Lambert-Beer law, and in the digital subtraction technique used extensively in FTIR analysis. In the case of transmission measurements however, the absorption property dominates the spectrum. The refractive loss is predominantly a surface and interface phenomenon, thus linearity will be maintained when measuring variable thicknesses of the sample as long as its

geometry remains the same. In the case of ATR measurements, the refractive property plays a significant role in the spectral appearance and it is for this reason why spectra obtained by different techniques and sampling geometries cannot be compared quantitatively [9]. Nevertheless, a recent report [4] has claimed that the ATR technique produced spectra which were very similar to transmission spectra. The quality and similarity of the spectra enabled comparisons to be made with reference spectra and real spectroscopic information to be extracted.

The intensity of the ATR spectrum, like the depth of penetration of the evanescent wave, is a function of the quantities previously described. These quantities are reproducible, enabling the comparison of different samples on different crystals. The optical contact between the ATR crystal and the sample however, is very difficult to reproduce, therefore making absolute intensity measurements less accurate. It is for this reason that the ATR results in this chapter should only be used to study the gradient trends within a film cured at one particular cure speed. Nevertheless, ATR can be used in a semi-quantitative fashion by comparing bands within a narrow frequency range.

Throughout this Chapter the convention that outer refers to the surface exposed to the light and inner refers to the surface furthest away from the light source has been adopted. As can be seen in Figure 4 examination of the films (1) with the outer surface in contact with the crystal and (2) with the inner surface in contact with the crystal, and using both of the cryst-

als, Ge and ZnSe, the degree of cure can be obtained at four levels in the film. Figure 4, profiles (a) and (b), show the type of profiling that could be obtained in this way.



- (I) Full depth probed using transmission spectroscopy.
- (II) Depth probed using Ge crystal in contact with the rear surface of irradiated film.
- (III) Depth probed using ZnSe crystal in contact with the rear surface of irradiated film.
- (IV) Depth probed using ZnSe crystal in contact with the irradiated surface.
- (V) Depth probed using Ge crystal in contact with the irradiated surface.

Figure 4. Illustration of the gradient profiles under investigation.

RESULTS AND DISCUSSION

The performance of the photoinitiators 2,4,6-trimethylbenzoyldiphenylphosphine oxide (TMBO) and 2,2-dimethoxy-2-phenylacetophenone (DMPA) was compared in the presence and absence of tertiary amine so that their curing potential could be assessed. Representative results showing the percentage cure at various depths in the film, the average amount of cure in the film, plus

an evaluation of the post curing effects measured are presented in Tables 1, 2 and 3. The other results that were obtained during this investigation have been compiled together, a selection of which are shown in Appendix B. The results are recorded as the percentage of residual double bonds remaining after UV irradiation. The absorption band at 1455 cm^{-1} was used as the internal standard for calculations employing the absorptions at 1640 cm^{-1} and 1620 cm^{-1} and in the case of the absorption band at 810 cm^{-1} the absorption at 835 cm^{-1} was used as the internal standard.

Examination of Tables 1 to 3 show that the residual unsaturation values obtained appear to depend upon whichever absorption band was selected for measurement. These values reflect the problems encountered with the selection of an appropriate baseline, because in many cases the peaks overlapped with each other. This made accurate measurement of peak areas difficult. Problems were encountered during the measurement of the peak at 810 cm^{-1} , because this peak and its internal standard were rather small, and in cases where spectra quality was poor, these peaks were indistinguishable. Nevertheless the trends observed at this frequency were similar to those found with the other two frequencies (1640 cm^{-1} , 1620 cm^{-1}). An accurate value of the percentage residual unsaturation could not be obtained from any of the spectra, although comparisons could be made between the differences in percentage residual unsaturation when the same absorption band was used throughout. Thus, clear trends were established.

2,4,6-Trimethylbenzoyldiphenylphosphine oxide (TMBPO), was

shown to be a less efficient photoinitiator for the photopolymerisation of clear coatings than 2,2-dimethoxy-2-phenylacetophenone (DMPA) (Chapter 5, [2,10]), although TMBPO decomposes faster under UV irradiation conditions when used at similar concentrations to DMPA (Chapter 8, [11]). It was established that in order to achieve efficient cure it was necessary to add a tertiary amine to the formulations as coinitiator (Chapter 5, [10]). Both photoinitiators undergo Norrish Type 1 photocleavage to produce radical species by short lived triplet excited states [12-14] with estimated lifetimes of < 1 ns for TMBPO [15] and about 1 ns for DMPA [14]. The results in Table 1 (entry (i)) show that the DMPA/amine combination has cured much more efficiently than the TMBPO/amine combination in terms of residual unsaturation. In the absence of amines however, (Table 2, entry (i)) DMPA showed slow, inefficient curing compared with TMBPO. Immediately following irradiation of the films containing amine it was noted that DMPA gave a dry tack free film surface, but that the TMBPO film surface remained tacky. This suggested that DMPA gave a faster cured film surface. The spectroscopic results support this inference and show that the through-cure was also better with DMPA compared to TMBPO. When the films were cured in the absence of amine it was not possible to distinguish the difference in cure between the DMPA and TMBPO irradiated films by subjective or arbitrary methods because both films appeared wet. Thus the results in Table 2 show the advantage of being able to quantify the degree of cure.

Table 1. The percentage residual unsaturation measured in a TPGDA film following UV irradiation at 4 m.min⁻¹ using TMBPO and DMPA in the presence of N-methyldiethanolamine.

Information obtained using FTIR-ATR Crystal	Order of measurement post irradiation	Percentage Residual Unsaturation measured at specified wavenumber.					
		TMBPO			DMPA		
		1640	1620	810	1640	1620	810
(i) Transmission, on ZnSe. (Bulk)	1	52	57	61	14	15	38
	2	55	60	59	16	16	29
	3	46	49	53	15	16	24
(ii) Inner Surface, on Ge. (ATR)	1	44	51	--	16	18	25
	2	39	44	--	17	18	41
	3	39	44	--	17	17	60
(iii) Inner Surface, on ZnSe. (ATR)	1	56	60	57	15	17	24
	2	55	61	55	16	18	26
	3	55	59	56	16	16	25
(iv) Outer Surface, on ZnSe. (ATR)	1	68	79	64	40	45	48
	2	72	82	64	37	44	51
	3	69	78	62	38	46	50
(v) Outer Surface, on Ge. (ATR)	1	74	80	--	34	38	--
	2	72	80	76	34	39	--
	3	69	79	--	37	40	--

* The time interval between each film measured as shown by the ordering 1,2,3 is about 2 hours.

The laser nephelometry studies of Chapter 4 [14] showed that the radical polymerisation reaction initiated by TMBPO had a much shorter induction period than that initiated by DMPA, and under these conditions was therefore less susceptible to the inhibiting effects of oxygen. It has been reported however, that TMBPO is more prone to oxygen inhibition than DMPA [10]. The fact that oxygen inhibition plays a significant role in the UV curing process is clearly shown in the results obtained during this

Table 2. The percentage residual unsaturation measured in TPGDA film following UV irradiation at 4 m.min using TMBPO and DMPA in the absence of amine.

Information obtained using FTIR-ATR Crystal	Order of measurement post irradiation	Percentage Residual Unsaturation measured at specified wavenumber.					
		TMBPO			DMPA		
		1640	1620	810	1640	1620	810
(i) Transmission, on ZnSe. (Bulk)	1	56	61	61	75	81	82
	2	68	78	56	(54)	(55)	66
	3	54	69	41	84	89	76
(ii) Inner Surface, on Ge. (ATR)	1	63	66	--	82	90	41
	2	64	68	--	77	82	--
	3	61	67	--	72	75	55
(iii) Inner Surface, on ZnSe. (ATR)	1	53	55	58	68	74	70
	2	55	61	62	64	67	72
	3	59	66	62	66	71	70
(iv) Outer Surface, on ZnSe. (ATR)	1	73	79	67	88	96	--
	2	77	87	58	91	--	--
	3	72	78	61	98	--	--
(v) Outer Surface, on Ge. (ATR)	1	69	74	--	86	93	--
	2	71	80	71	80	85	--
	3	84	93	61	90	97	78

* The time interval between each film measured as shown by the ordering 1,2,3 is about 2 hours.

investigation. The percentage of residual double bonds measured at the outer surface on both the Ge and ZnSe crystals (Figure 4, depths V and IV respectively) was much higher than that measured in the bulk (ZnSe crystal, Figure 4 depth I) or at the inner surface on both the Ge and ZnSe crystals (Figure 4, depths II and III respectively). When TPGDA was cured by DMPA in the presence of amine (Table 1 entries (iv) and (v)), the residual unsatura-

tion at the surface was twice that at the inner surface (Table 1 entries (ii) and (iii)). The FTIR results in both Tables 1 and 2 (entry (i)) show the presence of amine to have a less marked beneficial effect upon the degree of cure for films polymerised with TMBPO, compared with DMPA. The effect of amine upon the degree of cure for films photopolymerised with TMBPO was more marked as the irradiation time was increased. At 2m.min⁻¹ (4.8 seconds) in the absence of amine, 40 % of residual double bonds were found, whereas in the presence of amine 20 % of residual double were found [Appendix B].

Depth profiling coatings is a useful technique to gain an insight of the extent to which double bonds are consumed at different levels within the film. Especially since adhesion at the substrate-coating interface is recognised to be weak for UV cured films [16-20]. Using different crystals in the ATR accessory one might expect to observe either of the gradient patterns shown in Figure 4 (a or b). In the case of profile a, one would expect to observe slightly more residual unsaturation at the very outer surface layer, (depth V of Figure 4, Ge) where oxygen inhibits the radical reaction, than at the outer layer measured on the ZnSe crystal (depth IV of Figure 4). Below this surface layer, an increase in the amount of cure (decrease in the residual unsaturation) with increasing film depth would be expected, provided inner filter effects were insignificant. Inner filter effects would lead to undercure at the bottom of the film as shown by profile b of Figure 4. Transmission spectra should provide an average value of the extent of cure throughout the film as a whole. The results shown in Table 1 resemble the grad-

ient profile shown in Figure 4 a. In the case of Table 2, the absence of amine to prevent the inhibiting effects of oxygen have affected the gradient profile so that it resembles Figure 4 b more closely than Figure 4 a. Table 3 bears little resemblance to

Table 3. The percentage residual unsaturation measured in TPGDA film following UV irradiation at 8 m.min using DMPA in the presence of N-methyldiethanolamine.

Information obtained using FTIR-ATR Crystal	Order of measurement post irradiation	Percentage Residual Unsaturation measured at specified wavenumber		
		1640	1620	810
(i) Transmission, on ZnSe. (Bulk)	1	77	74	72
	2	67	67	80
	3	68	68	73
	4	67	67	74
(ii) Inner Surface, on Ge. (ATR)	1	55	55	73
	2	51	50	63
	3	51	52	68
	4	43	44	62
(iii) Inner Surface, on ZnSe. (ATR)	1	70	69	76
	2	74	74	77
	3	66	66	74
	4	66	67	78
(iv) Outer Surface, on ZnSe. (ATR)	1	59	63	93
	2	57	62	84
	3	56	60	87
	4	59	65	80
(v) Outer Surface, on Ge. (ATR)	1	55	57	--
	2	52	57	--
	3	57	63	--
	4	53	57	--

* The time interval between each film measured as shown by the ordering 1,2,3 and 4 is about 2 hours.

either profile. The uniformity of unsaturation throughout the

film might be explained by migration of unsaturated molecules through the partially polymerised coating.

Indications that polymerisation and crosslinking will continue in the film after irradiation are shown in Table 1 for TMBPO, at the inner (entries (ii), (iii)) and outer (entries (iv), (v)), surfaces and throughout the bulk generally (entry (i)) and in Table 3 for the bulk (entry (i)) measurement. A prerequisite for post-curing is the presence of residual unsaturation. In the case of TMBPO/amine, the post-curing effects recorded show clearly a reduction in the level of unsaturation which occurs with an increase in the post irradiation time. It is well known that carbon centred radicals have long lifetimes in films [21], therefore the post cure can be attributed to these radicals reacting with the residual unsaturation, thereby leading to further polymerisation.

In conclusion, FTIR/ATR spectroscopy has proved itself to be a useful analytical tool for probing the degree of cure as a function of depth in films produced by the photoinitiators TMBPO and DMPA. In addition, this technique and transmission spectroscopy provided evidence of post curing in thin films.

ACKNOWLEDGMENTS

I wish to acknowledge the help and support received in the FTIR department at Akzo Research laboratories, Arnhem. Special thanks go to Marieke de Boer who painstakingly ran and repeated many spectra, and helped with the tedious task of measuring peak heights many times over. I would also like to thank Pieter van Woerkom, who along with Marieke, gave many of their hours to this investigation, with useful discussions, examination of spectra and guidance to produce this chapter and a joint research paper.

Materials

The synthesis of 2,4,6-trimethylbenzoyl phenyl sulfone oxide was described in Chapter 1. 2,4,6-trimethylbenzoyl phenone (from Ciba Geigy) was recrystallized from petroleum ether (boiling range, 60-80 °C) and had a melting point range of 55.1-55.7 °C. N-methyldiethanolamine (Merck, distilled) was used as received.

The resins tested (all from Akzochem B.V.) included a low molecular weight prepolymer. The epoxy diacrylate of Setacure AP 570 (26.6% by wt) in polyethylene glycol (200) diacrylate (73.4% by wt), tripropylene glycol diacrylate (TPGDA) and hexane diol diacrylate (HEDA).

The substrates, either the APX crystals or satinised paper were coated using a 20 µm Ekichsen rod.

EXPERIMENTAL

Instruments

The Fourier transform infrared spectrometer used was a Digilab FTS-15E model with a MCT detector and 8 cm^{-1} resolution. The ATR crystals employed were ZnSe ($n = 2.4$) and Ge ($n = 4.0$). Each crystal measured $7 \text{ cm} \times 2 \text{ cm}$, with the 2 cm edge cut at an angle of 45° .

UV curing was carried out using a Philips high-pressure mercury-vapour lamp, model HOK 6 (80 Watts cm^{-1}), situated 15 cm above a moving belt with variable speed, which is calibrated in m.min^{-1} . As time of irradiation is inversely proportional to the speed of the moving belt, it can also be determined in seconds.

Materials

The synthesis of 2,4,6-trimethylbenzoyldiphenylphosphine oxide was described in Chapter 2. 2,2-Dimethoxy-2-phenylacetophenone (from Ciba Geigy) was recrystallised from petroleum ether (boiling range, $60\text{-}80^\circ \text{C}$) and had a melting point range of $65.4\text{-}65.7^\circ \text{C}$. N-methyldiethanolamine (Janssen Chimica) was used as received.

The resins tested (all from Synthese b.v.) included a low molecular weight prepolymer, the epoxy diacrylate of Setacure AP 570 (26.6% by Wt) in polyethyleneglycol (200) diacrylate (73.4% by Wt), tripropylene glycol diacrylate (TPGDA) and hexane diol diacrylate (HDDA).

The substrates, either the ATR crystals or satinised paper were coated using a 20 um Erichsen rod.

Selection of acrylate system to be examined

Initially, attempts were made to investigate the number of residual double bonds in an irradiated film comprising of Seta-cure AP 570 in PEGDA as used previously in Chapter 5. The resultant spectra however, were too complicated to observe any consistent trends because of the nature of the mixture, and to some extent the impurities present in the formulation [22]. Originally, the intention was to use the carbonyl peak at 1725 cm^{-1} as a reference peak and the peak at 810 cm^{-1} as the variable peak [23], in order to determine the residual unsaturation in the polymer film. The transmission spectra recorded by the FTIR technique however, showed the intensity of the carbonyl peak to be extremely high in comparison with the finger print region and, as a consequence, no suitable peak reflecting the degree of unsaturation could be found. Following this, extensive examinations of difunctional monomers were made which resulted in the selection of TPGDA as the most suitable monomer for further investigations, largely because of the quality of the spectra obtained.

The transmission spectra of both mono-TPGDA and polymerised TPGDA were recorded. From a close examination of these spectra the constant and variable peaks were identified for use in this investigation.

To measure the extent of cure at the film's inner surface, mono-TPGDA was applied to both ATR crystals using an Erichsen rod to give a wet film thickness of 20 μm . In the case

of the Ge crystal, the whole surface was covered, but for the ZnSe crystal only the central 2cm section was covered (see later). When coated, the crystals were placed upon a sheet of satinised paper and irradiated for a specific time as described in Chapter 5. The irradiated film on the ZnSe crystal was also used for transmission measurements. To determine the extent of cure at the external surface of the film, a sheet of satinised paper was coated with mono-TPGDA and irradiated for a specific time. Following irradiation, but prior to measurement, a section was cut from the paper and the coated surface was placed adjacent to the crystal. This enabled the spectrum of the coating's external surface to be recorded.

Shortly after their irradiation, the coated crystals and the irradiated film and crystals, were inserted individually into a standard ATR unit (Harrick, Type number TMP-220), placed in the spectrometer and their spectra recorded. When investigating the post curing effects, this procedure was repeated at approximately two hourly intervals. When all measurements had been completed, the crystals were cleaned and their individual spectra recorded. For the required quantitative analysis the spectra of the films were ratioed against that of the appropriate crystal.

Selection of the substrate for measuring the external surface

At the onset of the investigation glass was selected as the substrate to be used to measure the external surface of the irradiated film. The TPGDA was coated onto the glass and after irradiation, the coated surface was placed adjacent to the crys-

tal in the ATR attachment for scanning. Unfortunately a poor contact between the coating and the crystal ensued due to the rigid nature of the glass, and this led to a poor signal-to-noise ratio. An improvement was obtained using the flexible substrate satinised paper, which gave a much closer and a more uniform contact. Additionally, the use of this substrate mimics the general UV curing procedure more accurately and for this reason was used in the continuing investigations.

Measurement of the recorded spectra

The recorded spectra were plotted by the computer from an arbitrary baseline, the scale being automatically selected to show the relative peak heights. Because the scale varies with each recorded spectrum it is difficult to draw direct comparisons between these in absolute terms. Accordingly, as the recorded spectra are obtained by different techniques (ATR and transmission) they should not be compared with each other directly. The transmission spectra can be compared with each other if one considers relative peak heights with respect to an invariable peak (i.e., one whose intensity is not changed upon polymerisation) to correct for different film thicknesses etc,. The relative peak heights of the ATR-spectra serve to show gradient effects within each film. It is not advisable to compare the ATR-spectra recorded at different cure speeds and for different photoinitiators. This is because of probable variations in the effectiveness of contact between the crystal surface and the film, as well as the different effects which occur during the UV

polymerisation reaction (i.e., oxygen inhibition, migration of uncured acrylate through the film, etc).

The spectra recorded using both techniques are excellent, examples of which are shown in Appendix A. Following exposure to the UV radiation the number of double bonds remaining in the films are indicated by the intensity of the peaks at 1640 cm^{-1} , 1620 cm^{-1} and 810 cm^{-1} . The doublet occurring at 1640 cm^{-1} and 1620 cm^{-1} is relevant to the C=C stretching bond of vinyl groups, and the peak at 810 cm^{-1} is relevant to the CH deformation mode of the vinyl group i.e., $\text{CH}=\text{CH}$ [24]. Because the intensity of the spectra is determined by the effectiveness of the contact between the film and the crystal, any irregularities in the surface of the film such as wrinkling due to shrinkage, will affect the results. Therefore for quantitative work it is necessary to select a peak in the spectrum which will serve as an internal standard. Clearly the peak selected as internal standard must be associated with a bond which is not affected by polymerisation. For this reason the absorptions at 1455 cm^{-1} , relevant to the asymmetric bending vibration of $-\text{CH}_2$ [5, 24] and 835 cm^{-1} , relevant to the $-\text{CH}_2$ deformations and $\text{CH}_3-\text{O}-$ stretching [5, 24] were selected. Because the depth of penetration is inversely proportional to the frequency at which absorption occurs with ATR measurements, it is necessary to compare absorption bands reflecting the degree of cure with an internal standard which is in the same spectral region. Therefore the 1455 cm^{-1} absorption band was used as the reference peak, or internal standard, with the bands at 1640 cm^{-1} and 1620 cm^{-1} being used to measure the degree of cure. As a double check, the degree of cure was also assessed

by following the change in intensity of the 810 cm^{-1} band relative to the reference peak, or internal standard at 835 cm^{-1} .

When measuring the peak heights, a line was drawn at the base of each peak. From this baseline the peak height was measured using a mm ruler. Peak height ratio's were calculated from the spectra for the monomer sample and the samples irradiated at different cure speeds. From these values the number of residual double bonds associated with each variable peak were calculated.

Film Penetration

ATR was selected as an analytical technique in this investigation purposely to depth profile a film. As described earlier, the extent to which the infrared radiation, at a given frequency, will penetrate a film depends upon :-

- 1) the refractive indices of the film and the crystal used,
- 2) the angle of incidence, and
- 3) the quality of the contact between the film and the crystal.

Uncomplicated results were obtained for those samples where the film was applied and cured on the crystal, i.e., for the transmission and inner surface measurements. However, the outer surface measurements showed dissimilar absorbances which were attributed to differences in the contact between the film and the crystal.

When the film felt dry to touch, i.e., was completely poly-

merised, the contact between the film and the crystal was poor due to the uneven and rigid nature of the surface of the cured coating. This led therefore to a less effective penetration of the film by the infrared light, thus reducing the absorbance and, as a result, gave a low signal-to-noise ratio. With wetter, less cured films, the contact was much better, giving higher absorbance readings and a better signal-to-noise ratio. During this investigation, the external surface information obtained with the ZnSe crystal was much less affected by poor contact between the film and the crystal than that obtained with the Ge crystal. Generally the signal-to-noise ratio of the collected spectra was higher with the ZnSe crystal than with the Ge crystal because of a greater depth in penetration. Care was taken at all times to ensure that measurements were made under conditions where all the incident radiation passed through the films, thereby avoiding errors due to uncertainties in the 0% transmission level.

The FTIR detector measures infrared radiation as modulated by the instruments interferometer. Stray light by definition does not travel through the interferometer, but if present will be measured by the detector. However, stray light will not be modulated and will register as a D.C. offset signal. After Fourier transformation, D.C. measurements will be interpreted as zero frequency spectral information, and no matter what frequencies stray light is comprised of, all of the transformed information will be confined to zero frequency in the spectrum. As a result, stray light will not contribute to the infrared spectrum. However, it must be noted that stray light is measured by the detector and must be considered a problem if premature saturation

of the infrared detector is observed. It was for this reason that the amount of film covering the ZnSe crystal was reduced in order to compensate for the evanescent wave absorbing stray light.

The number of double bonds remaining in the films following irradiation are indicated by the intensity of the peaks at 1640 cm^{-1} , 1620 cm^{-1} and 910 cm^{-1} . The doublet appearing at 1640 cm^{-1} and 1620 cm^{-1} is related to the stretching mode of vinyl groups, and the peak at 910 cm^{-1} is related to the deformation mode of the vinyl group C-H.

On each figure above in the figures, the reference bands representing residual unsaturation are indicated and are indicated for ease of identification. They are as follows:

External Stretching

$\lambda = 1640 \text{ cm}^{-1}$

$\lambda = 1620 \text{ cm}^{-1}$

$\lambda = 910 \text{ cm}^{-1}$

Internal Stretching, Reference bands

$\lambda = 1640 \text{ cm}^{-1}$

$\lambda = 1620 \text{ cm}^{-1}$

APPENDIX A

The spectra recorded using the transmission and ATR techniques are excellent, as can be seen from the following examples. The number of double bonds remaining in the films following irradiation are indicated by the intensity of the peaks at 1640⁻¹ cm⁻¹, 1620⁻¹ cm⁻¹ and 810⁻¹ cm⁻¹. The doublet occurring at 1640⁻¹ cm⁻¹ and 1620⁻¹ cm⁻¹ is relevant to the C=C stretching bond of vinyl groups, and the peak at 810⁻¹ cm⁻¹ is relevant to the CH deformation mode of the vinyl group i.e., CH₂=CH [24,25].

On each figure shown in the Appendix the absorption bands representing residual unsaturation and the reference peaks are indicated for ease of identification. These are as follows:

Residual Unsaturation

- A = 1640⁻¹ cm⁻¹
- B = 1620⁻¹ cm⁻¹
- E = 810⁻¹ cm⁻¹

Internal Standard, Reference Peaks

- C = 1455⁻¹ cm⁻¹
- D = 835⁻¹ cm⁻¹

Figure I: Transmission Measurements of the film cured
-1
with DMPA/Amine at 8 m.min using a ZnSe crystal.

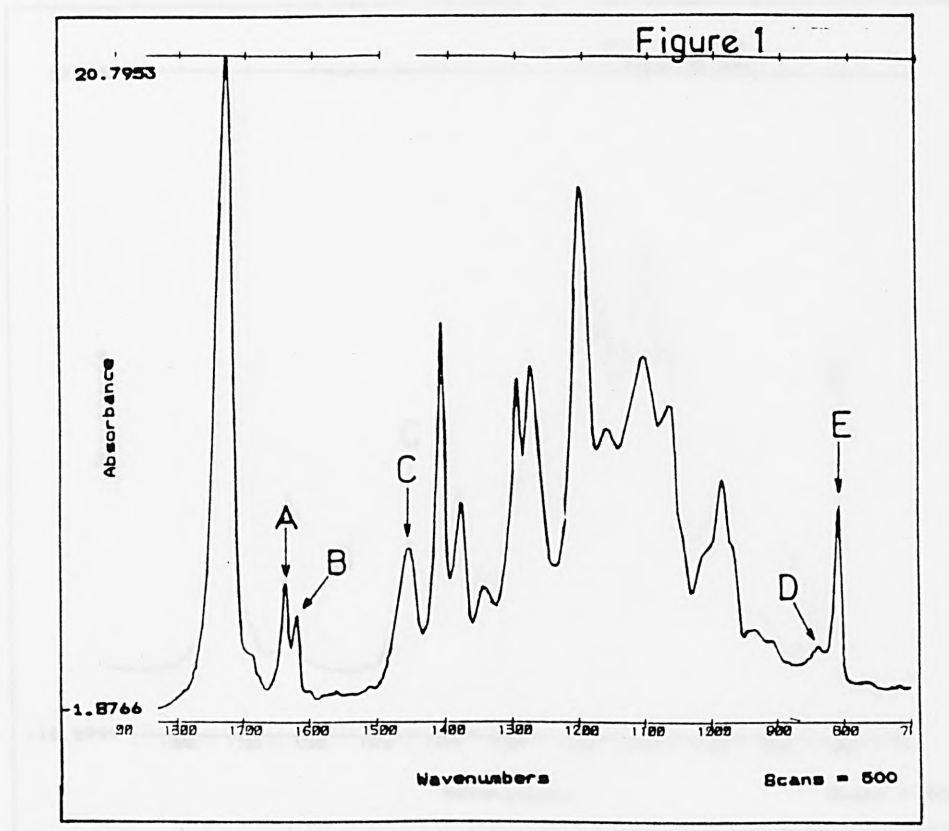


Figure II: ATR Measurements of the film's Inner Surface cured
-1
with DMPA/Amine at 8 m.min using a Ge crystal.

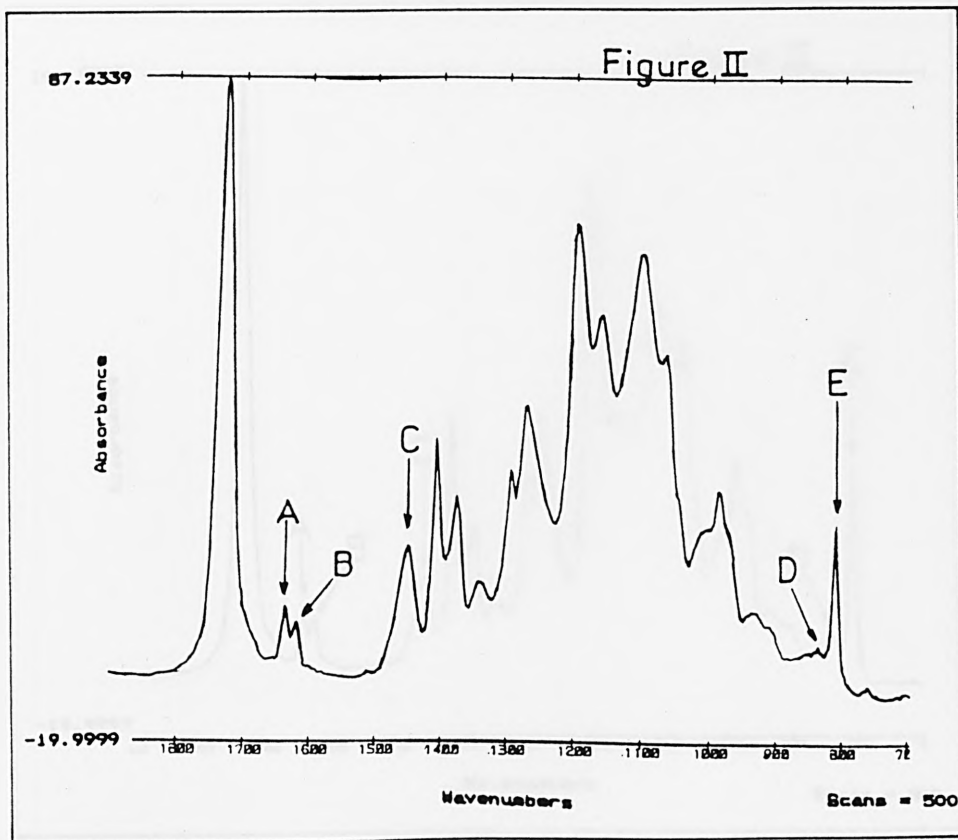


Figure III: ATR Measurements of the film's Inner Surface cured with DMPA/Amine at 8 m.min⁻¹ using a ZnSe crystal.

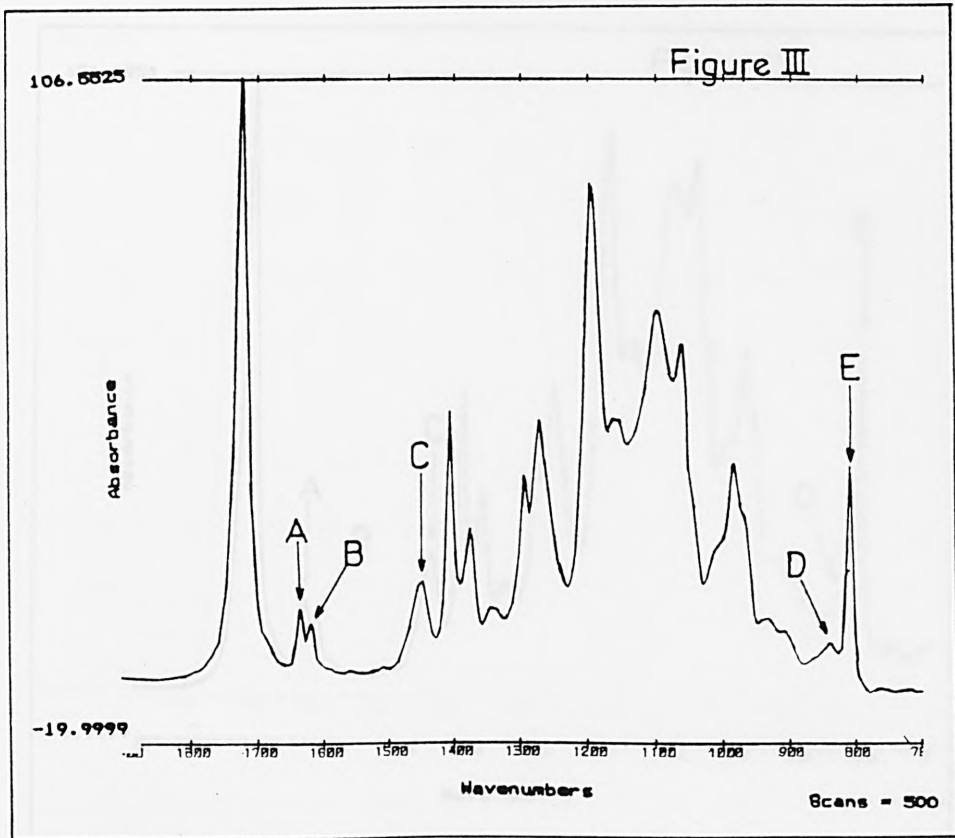


Figure IV: ATR Measurements of the film's Outer Surface cured
-1
with DMPA/Amine at 8 m.min using a ZnSe crystal.

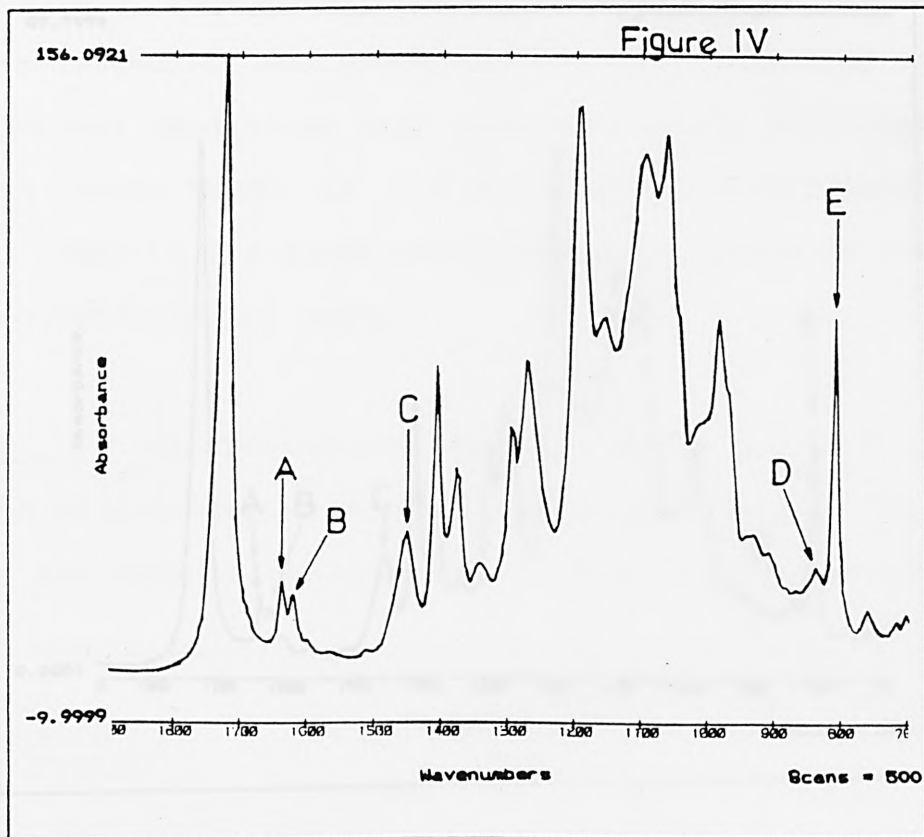
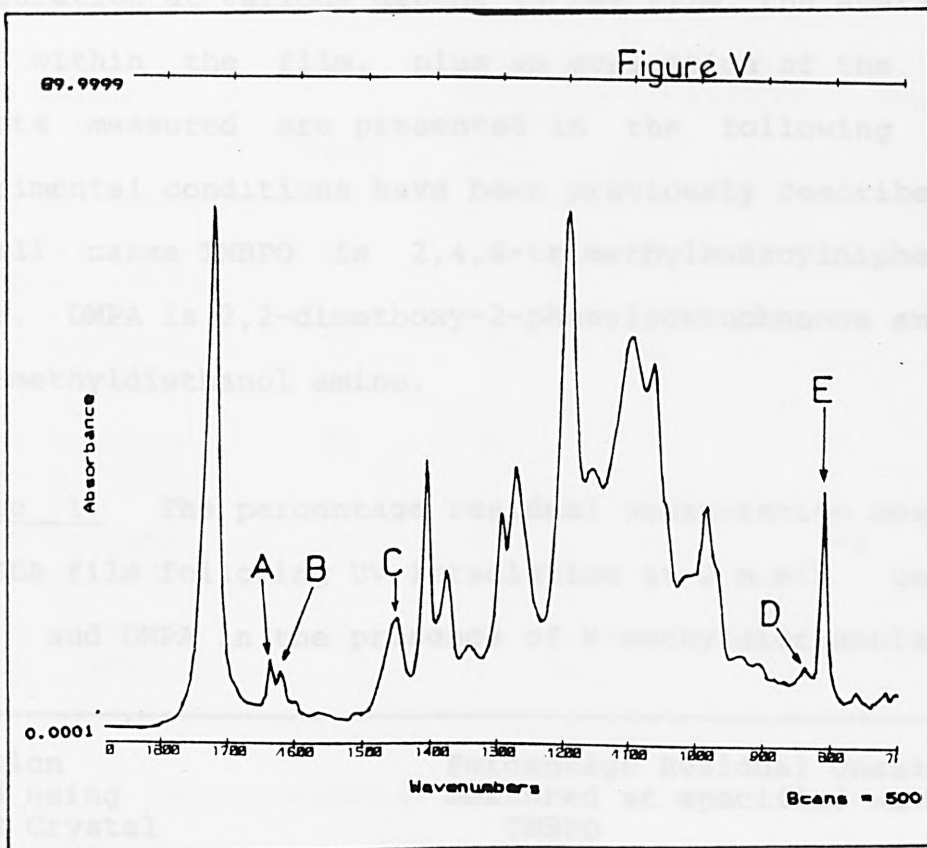


Figure V: ATR Measurements of the film's Outer Surface cured with DMPA/Amine at 8 m.min⁻¹ using a Ge crystal.



(i) Transmission, on ZnSe. (Bulk)	23	21	38	8	9	21
(ii) Inner Surface, on Ge. (ATR)	33	33	14	40	39	72
(iii) Inner Surface, on ZnSe. (ATR)	19	20	40	10	11	21
(iv) Outer Surface, on ZnSe. (ATR)	25	27	38	72	67	72
(v) Outer Surface, on Ge. (ATR)	23	26	29	41	41	48

APPENDIX B

Representative results showing the percentage residual unsaturation at various depths in the film, the average amount of cure within the film, plus an evaluation of the post curing effects measured are presented in the following tables. The experimental conditions have been previously described in detail. In all cases TMBPO is 2,4,6-trimethylbenzoyldiphenylphosphine oxide, DMPA is 2,2-dimethoxy-2-phenylacetophenone and the amine is N-methyldiethanol amine.

Table 1. The percentage residual unsaturation measured in a TPGDA film following UV irradiation at 2 m.min⁻¹ using TMBPO and DMPA in the presence of N-methyldiethanolamine.

Information obtained using FTIR-ATR Crystal	Percentage Residual Unsaturation measured at specified wavenumber.					
	TMBPO			DMPA		
	1640	1620	810	1640	1620	810
(i) Transmission, on ZnSe. (Bulk)	20	21	30	8	9	21
(ii) Inner Surface, on Ge. (ATR)	33	33	34	40	33	72
(iii) Inner Surface, on ZnSe. (ATR)	19	20	40	10	11	21
(iv) Outer Surface, on ZnSe. (ATR)	25	27	50	72	67	72
(v) Outer Surface, on Ge. (ATR)	23	26	29	41	41	49

Table 2. The percentage residual unsaturation measured in a
⁻¹
 TPGDA film following UV irradiation at 2 m.min using TMBPO and
 DMPA in the absence of N-methyldiethanolamine.

Information obtained using FTIR-ATR Crystal	Percentage Residual Unsaturation measured at specified wavenumber.					
	1640	TMBPO		DMPA		810
		1620	810	1640	1620	810
(i) Transmission, on ZnSe. (Bulk)	41	42	97	80	75	77
(ii) Inner Surface, on Ge. (ATR)	73	74	84	80	81	97
(iii) Inner Surface, on ZnSe. (ATR)	34	31	78	76	78	81
(iv) Outer Surface. on ZnSe. (ATR)	99	99	--	89	93	--
(v) Outer Surface, on Ge. (ATR)	89	85	92	81	76	--

Table 3. The percentage residual unsaturation measured in a
⁻¹
 TPGDA film following UV irradiation at 8 m.min using TMBPO and
 DMPA in the absence of N-methyldiethanolamine.

Information obtained using FTIR-ATR Crystal	Percentage Residual Unsaturation measured at specified wavenumber.					
	1640	TMBPO		DMPA		810
		1620	810	1640	1620	810
(i) Transmission, on ZnSe. (Bulk)	97	96	81	--	99	76
(iii) Inner Surface, on ZnSe. (ATR)	82	81	83	89	93	100
(iv) Outer Surface. on ZnSe. (ATR)	87	88	80	92	96	--
(v) Outer Surface, on Ge. (ATR)	83	85	97	96	96	99

Table 4. The percentage residual unsaturation measured in a TPGDA film following UV irradiation at 6 m.min⁻¹ using DMPA in the presence of N-methyldiethanolamine.

Information obtained using FTIR-ATR Crystal	Percentage Residual Unsaturation measured at specified wavenumber.		
	1640	DMPA 1620	810
(i) Transmission, on ZnSe. (Bulk)	36	41	53
(ii) Inner Surface, on Ge. (ATR)	31	33	58
(iii) Inner Surface, on ZnSe. (ATR)	46	51	53
(iv) Outer Surface, on ZnSe. (ATR)	48	55	62
(v) Outer Surface, on Ge. (ATR)	48	52	--

Table 5. The percentage residual unsaturation measured in a TPGDA film following UV irradiation at 10 m.min⁻¹ using DMPA in the presence of N-methyldiethanolamine.

Information obtained using FTIR-ATR Crystal	Percentage Residual Unsaturation measured at specified wavenumber.		
	1640	DMPA 1620	810
(i) Transmission, on ZnSe. (Bulk)	68	68	98
(ii) Inner Surface, on Ge. (ATR)	57	95	--
(iii) Inner Surface, on ZnSe. (ATR)	48	53	59
(iv) Outer Surface, on ZnSe. (ATR)	53	61	64
(v) Outer Surface, on Ge. (ATR)	50	60	--

REFERENCES

- [1] Brann, B.L., J. Rad. Curing 1985, 12 (4), 4-10.
- [2] Baxter, J.E., Davidson, R.S., Hageman, H.J., accepted for publication, European Polymer J.
- [3] Tinh Nguyen, Progress in Org. Coatings 1985, 13, 1-34.
- [4] Belton, P. S., Saffa, A. M., Wilson, R. H., Analyst 1987 112 1117-1120.
- [5] Hodson, J., Lander, J. A., Polymer 1987, 28 251-256.
- [6] Wilks, P. A., Appl. Spectrosc., 1968, 22, 782-784.
- [7] Hirschfeld, T., Appl. Spectrosc., 1977, 31, 289-292.
- [8] Tompkins, H. G., Appl. Spectrosc., 1974, 28, 334-341.
- [9] Ishida, H., Proc. Quant. Character. Plast and Rubber 1984, (6) 20-27.
- [10] Jacobi, M., Henne, A., J. Rad. Curing 1983, 10 (4), 16-25.
- [11] Baxter, J.E., Davidson, R.S., Hageman, H.J., Hakvoort, G.T.M., Overeem, T., to be published.
- [12] Baxter, J.E., Davidson, R.S., Hageman, H.J., Overeem. T., Makromol. Chem., Rapid Commun. 1987, 8, 311-314.
- [13] Baxter, J.E., Davidson, R.S., Hageman, H.J., McLauchlan, K.A., Stevens, D.G., J. Chem. Soc., Chem. Commun. 1987, (2) 73-75.
- [14] Hageman, H.J., Progress in Org. Coatings 1985, 13, 123-150.
- [15] Sumiyoshi, T., Schnabel, W., Henne, A., Lechtken, P., Polymer 1985, 26, 141-146.
- [16] Roffey, C. G., Photopolymerisation of Surface Coatings, Wiley, New York, 1982.
- [17] Holman, R., UV and EB Formulations for Printing Inks,

Coatings and Paints, Sita Technology, London, 1984.

- [18] Pappas, S. P., UV Curing: Science and Technology, Technology Marketing Corporation, Conn. Vol. I, 1978.
- [19] Pappas, S. P., UV Curing: Science and Technology, Technology Marketing Corporation, Conn. Vol. II, 1985.
- [20] Paul, S., Surface Coatings, Science and Technology, Wiley-Interscience, 1985.
- [21] Kloosterboer, J.G., Lijten, G.F.C.M., Greidanus, F.J.A.M., Polymer Commun., 1986, 27, 268-271. Kloosterboer, J.G., Lijten, G.F.C.M., Polymer Commun., 1987, 28, 2-5.
- [22] Hall, R.J., Van Der Maeden, F.P.B., Willemsen, A.C.C.M., Proceedings from Radcure Conference, Basel, 1985.
- [23] Davidson, R.S., Ellis, R.J., Wilkinson, S.A., Summersgill, C.A., Eur. Polym. J. 1987, 23 (2), 105-108.
- [24] George, W.O., Harris, W.C., Maddams, W.F., J.C.S. Perkin II 1987, 392-396; *ibid* 396-400.

Chapter 8

Investigation of the Photodecomposition Products of Photoinitiators and Proposed Mechanisms for their Formation

Chapter 8	Investigation of the Photodecomposition Products of Photoinitiators and Proposed Mechanisms for their Formation	
	Introduction	286
	Chromatography	288
	Liquid Chromatoraphy	289
	Gas Chromatography	291
	Gas Chromatography-Mass Spectrometer Systems	292
	Results and Discussion	293
	(1) Investigation of the Photodecomposition of TMBPO and DMPA	293
	The Mechanism of Photodecomposition	302
	(2) Decomposition of a TMBPO UV Curable Formulation	302
	Conclusion	307
	Acknowledgements	308
	Experimental	309
	Appendix A	319
	Appendix B	321
	Appendix C	323
	References	326

INTRODUCTION

When selecting photoinitiators for UV curable formulations it is important to consider the several criteria which will affect the overall efficiency of the formulation. Two of the more important criteria are the curing efficiency and shelf-life stability of the prepared formulation. The photoinitiators 2,4,6-trimethylbenzoyldiphenylphosphine oxide (TMBO) [1-3] and 2,2-dimethoxy-2-phenylacetophenone (DMPA) [4] undergo a Norrish Type 1 cleavage to produce initiating free radicals via an excited triplet state, as previously described in Chapter 1. On account of this property, they do not require amine synergists to effect the photopolymerisation of acrylates or other vinyl monomers. The addition of amines to UV curable formulations containing DMPA has however, been reported [5] to considerably enhance the surface cure of the film formed. Similarly, greater curing efficiency was obtained in the case of acylphosphine oxides when amines were added [6]. These findings are supported by earlier work (Chapter 5) where it was found that in order to achieve efficient cure speeds it was necessary to add a tertiary amine [7] to the formulations containing either photoinitiator. Recently it was reported [8], that the addition of amines to an acrylate formulation containing photoinitiators reacting by the Norrish Type 1 cleavage mechanism accelerated the rate of polymerisation because of the ability of the amines to scavenge the non-chain propagating oxygen-containing radicals. This report concurs with results obtained earlier [7] (Chapter 5), which also included photocuring in the absence of air, and led to the supposition that the role

of amine was predominantly one of an oxygen scavenger. Amines however, are effective hydrogen atom donors which will react readily with oxygen during the photopolymerisation process, resulting in the generation of efficient amine derived radicals via a hydroperoxy radical capable of initiating free radical polymerisation [9].

To verify the role of tertiary amines in UV curable formulations, the photodecomposition of the photoinitiators TMBPO and DMPA was investigated under normal UV curing conditions, both in the presence and absence of tertiary amine. To avoid the possibility of unreacted photoinitiator being trapped within the insoluble polymer matrix of the cured film, two different "model environments" were selected to simulate typical UV curing formulations. The model environments used were 1,5-pentanediol and dinonylphthalate, both of which are non-polymerisable viscous materials. The separation and examination of the photodecomposition products obtained from both photoinitiators in the presence and absence of the tertiary amines N-methyldiethanolamine (N-MDEA) and triethylamine (TEA) were achieved by liquid chromatography (HPLC), gas chromatography (GLC) and gas chromatography - mass spectrometry (GC-MS) techniques. It was necessary to use these analytical techniques to identify the photodecomposition products so that any reaction between the photogenerated radicals and the amine would be verified.

The same analytical techniques were subsequently used to investigate the shelf-life stability of TMBPO in an epoxydiacrylate | N-methyldiethanolamine UV curable formulation. Results had

been obtained in earlier investigations which indicated that TMBPO had a very short shelf-life. This finding contradicted that of earlier investigators who reported that TMBPO had adequate stability for practical purposes and was sufficiently stable towards amines used as coinitiators in UV cured lacquers [6]. The presence of chemically labile photoinitiator and some amines are known to reduce the shelf-life of UV curing formulations compared to those of EB formulations [10,11]. The possibility of amines causing considerable decreases in the shelf-life of acrylate based formulations, depending upon the level used, is well known [5]. UV curing formulations are highly reactive, thus selected photoinitiators need to be stable within these formulations for a period of some months, i.e., chemically inert under normal dark storage conditions.

CHROMATOGRAPHY

Chromatography includes various experimental techniques designed to separate mixtures of compounds so that it is possible to understand the composition of complex mixtures. The principle of the chromatographic process involves the separation of a mixture into pure compounds by their differential adsorption properties when distributed between a two phase system, one of which is stationary, the other mobile. Each adsorbent phase competes to adsorb the compounds being separated i.e., the stationary phase will retain the components which are the most easily adsorbed to varying extents, while the mobile phase carries them along with it, such that the mixture experiences two forces. It

is feasible to separate a mixture if the ratio between the amount of a particular component in each phase differs from that of another component. Thus separation is established because of a partitioning of the sample components between the moving and stationary phases [12,13].

Two chromatographic techniques have been used in this investigation and are discussed in more detail below

Liquid Chromatography

Of the different liquid chromatographic methods, which include liquid-liquid, liquid-solid, ion-exchange and size-exclusion chromatography, only liquid-liquid (LLC) and bonded phase chromatography (BPC) will be discussed in any detail because of their relevance to the work within this chapter. Liquid-liquid or partition chromatography involves a liquid stationary phase whose composition is different from that of the moving liquid phase, both being completely immiscible with each other. Sample molecules distribute between the mobile and stationary liquid phases, just as in liquid-liquid extraction within a separating funnel. The modification of LLC has led to an additional method, bonded-phase chromatography, which has become the most popular of the liquid chromatographic techniques [13]. BPC uses an organic stationary phase which is chemically bonded to a particle of high surface area, usually silica, in place of the mechanically held liquid phase in LLC. The polarity of the stationary phase can be changed to suit the separation to be effected by changing the

organic bonders. Conventionally the stationary phase is polar and the mobile phase is non-polar, however to separate components which are dissolved in water a reversed phase partition can be established. In this case, the mobile phase is polar and the stationary phase non-polar.

The separation of components occurs when the solvent or mobile phase flows through the column, resulting in the movement of sample molecules along the column. The separation of samples which contain early eluting bands exhibiting poor resolution, and late eluting bands, which are very often difficult to detect having unnecessarily long separation times, is a common problem in chromatography [12]. To avoid these elution problems HPLC instruments are fitted with a solvent programmer or gradient elution (GE) device [13]. Gradient elution will enable the separation of complex and difficult mixtures. A solvent programmer produces a systematic change in the composition of the mobile phase, and a mixture of two or more solvents are systematically varied to effect the desired separation. For example, a simple gradient is established when the solvency of the mobile phase is initially weak, thus slowing down the elution of the fast-eluting compounds and improving their resolution, becoming progressively stronger as the separation proceeds, thus speeding up the elution of slow-eluting compounds and improving their resolution. Detection of the eluting peaks can be effected by various techniques depending upon the nature of the property being measured (e.g., a bulk property such as refractive index, or a solute property such as UV absorption) [13]. The UV spectrophotometer is probably the most frequently used and versatile detector, because of the wide

selection of UV and visible wavelengths available for different operations.

Gas Chromatography

In gas-liquid chromatography, the stationary phase is a liquid held on a solid bead and the mobile phase is an inert gas. The sample is injected as a liquid and is then immediately volatilised. The components of the sample which are soluble in the stationary phase distribute themselves between it and the mobile phase according to the principles of equilibria. By forcing an inert carrier gas through the chromatographic column, elution is possible. The rate at which a component elutes depends upon its tendency to dissolve in the stationary phase. Components which are highly soluble in the stationary phase will elute later than those which are only slightly soluble [12].

Qualitative analysis of the sample depends upon the time each component peak elutes, whereas quantitative analysis of the sample is dependent upon the area under each eluting peak. Theoretically the retention time data should enable identification of a particular component. The procedure however, is limited by the existence of several variables which will reduce the reproducibility of the retention times. An eluting peak may be identified by comparison with an authentic sample if its composition is suspected, followed by spiking the sample under investigation with the authentic sample. If no additional peaks elute and the area under the unknown peak increases, there is a good chance that the two are identical and the compound has been identified.

Confirmation can be obtained by repeating the procedure using a different liquid phase.

Gas Chromatography-Mass Spectrometer Systems

The effluent from a gas chromatograph is usually a small quantity (10^{-12} to 10^{-3} g) of a pure compound or, less frequently, a simple mixture in the gas phase. This small amount of pure compound is ideal for direct transfer into a mass spectrometer source, providing the carrier gas (e.g., He) is largely removed first. The carrier gas is removed by separators which rely on either the faster diffusion of He, or preferential passage of the organic substrate through a membrane. The gas chromatograph is interfaced with the mass spectrometer. The spectrum of each component is obtained as it leaves the column. Identification of substances in very small quantities is possible (e.g., 10^{-9} to 10^{-12} g) by ionisation of the effluent vapour [15]. The molecular weight of each component can be measured from the mass to charge ratio (m/z values) of the molecular ion formed. If no molecular ion is detected however, its structure, and hence the molecular weight can be deduced from the charged fragments (identified by their m/z values) emitted following the breakdown of the molecular ion. By way of contrast, Table I shows that there is

RESULTS AND DISCUSSION

1) Investigation of the Photodecomposition of TMBPO and DMPA;

The photocuring efficiency of 2,4,6-trimethylbenzoyldi-phenylphosphine oxide (TMBPO) has been shown to be less efficient than that exhibited by 2,2-dimethoxy-2-phenylacetophenone (DMPA) in clear coatings [6]. This observation is supported by earlier experimental results (Chapter 5) [7]. In both cases it was found necessary to add tertiary amines to the formulations to increase the cure speeds of the thin films. The increases in cure speeds were quite dramatic, indicating that tertiary amines play a significant role in the photopolymerisation process. To establish the function of each component in these UV curing formulations the rate of photodecomposition of both TMBPO and DMPA photoinitiators were investigated in the presence and absence of tertiary amine. This investigation was conducted in a model environment selected to mimic a clear UV curable coating. Table 1 shows that the addition of an amine does not accelerate the photodecomposition of DMPA.

DMPA undergoes a Norrish Type 1 cleavage process via a very short lived triplet state [4], thus it is not surprising that the excited photoinitiator does not react with the amine in a bimolecular reaction. By way of contrast, Table 2 shows that there is an effect of added amine upon the photodecomposition of TMBPO.

The addition of amine led to a much faster rate of decomposition of TMBPO at the higher belt speeds (30 - 60 m.min⁻¹), which decreased to approximately the same rate as the samples without amine at the slower belt speeds (8 - 20 m.min⁻¹). It is

Table 1. The percentage photodecomposition of DMPA in Dinonyl-phthalate in the presence and absence of N-methyldiethanolamine, under UV curing conditions.

	CURE SPEED IN M/MIN	% RESIDUAL DMPA	
		NO AMINE	WITH AMINE
(1)	60	74.14	78.50
(2)	50	71.02	73.27
(3)	40	66.49	69.40
(4)	30	59.54	62.13
(5)	20	39.52	48.39
(6)	10	12.84	20.73
(7)	8	11.73	13.49
(8)	6	6.48	10.14
(9)	4	4.86	2.76
(10)	2	0.00	0.00

unlikely that the effect of added amine influences the Norrish Type I cleavage process of TMBPO when one considers the short triplet lifetime of the acylphosphine oxide [1]. The increase in the rate observed could be attributed to non-photochemical processes which involve nucleophilic attack by photoproducts, such as hydroperoxides, upon the acylphosphine oxide, or alternatively, a decomposition mechanism via an S₂ reaction in which the photo-produced radicals e.g., peroxy radicals, induce the decomposition of the oxide. From a comparison of the rate of decomposition of the two photoinitiators one would conclude that the faster

Table 2. The percentage photodecomposition of TMBPO in Dinonylphthalate in the presence and absence of N-methyldiethanolamine, under UV curing conditions.

	CURE SPEED IN M/MIN	% RESIDUAL TMBPO NO AMINE	WITH AMINE
(1)	60	71.01	54.21
(2)	50	63.21	52.42
(3)	40	53.01	44.28
(4)	30	37.48	29.81
(5)	20	18.23	19.86
(6)	10	3.17	5.10
(7)	8	2.34	2.68
(8)	6	2.74	0.00
(9)	4	0.00	0.00
(10)	2	0.00	0.00

decomposition rate of the acylphosphine oxide should make it the more efficient photoinitiator for the polymerisation of acrylates. These experiments however, were conducted purely on a weight to weight basis and the fact that their absorption properties in the 300-400 nm wavelength region are different [7] was ignored. In reality, DMPA is the more efficient photoinitiator despite its poorer light absorption characteristics.

The results obtained suggest that despite the rapid photodecomposition of TMBPO under UV curing conditions, not all the photogenerated radicals participate in the initiation of polymer-

isation. It is conceivable that the phosphorus centred radicals are rapidly scavenged by oxygen thus reducing their potential to initiate polymerisation. This reasoning is supported by earlier experimental work (Chapter 6) [7], whereby the acylphosphine oxides were found to be good photoinitiators for the curing of acrylate resins in the absence of oxygen. Similarly, a recent investigation of the effect of amine

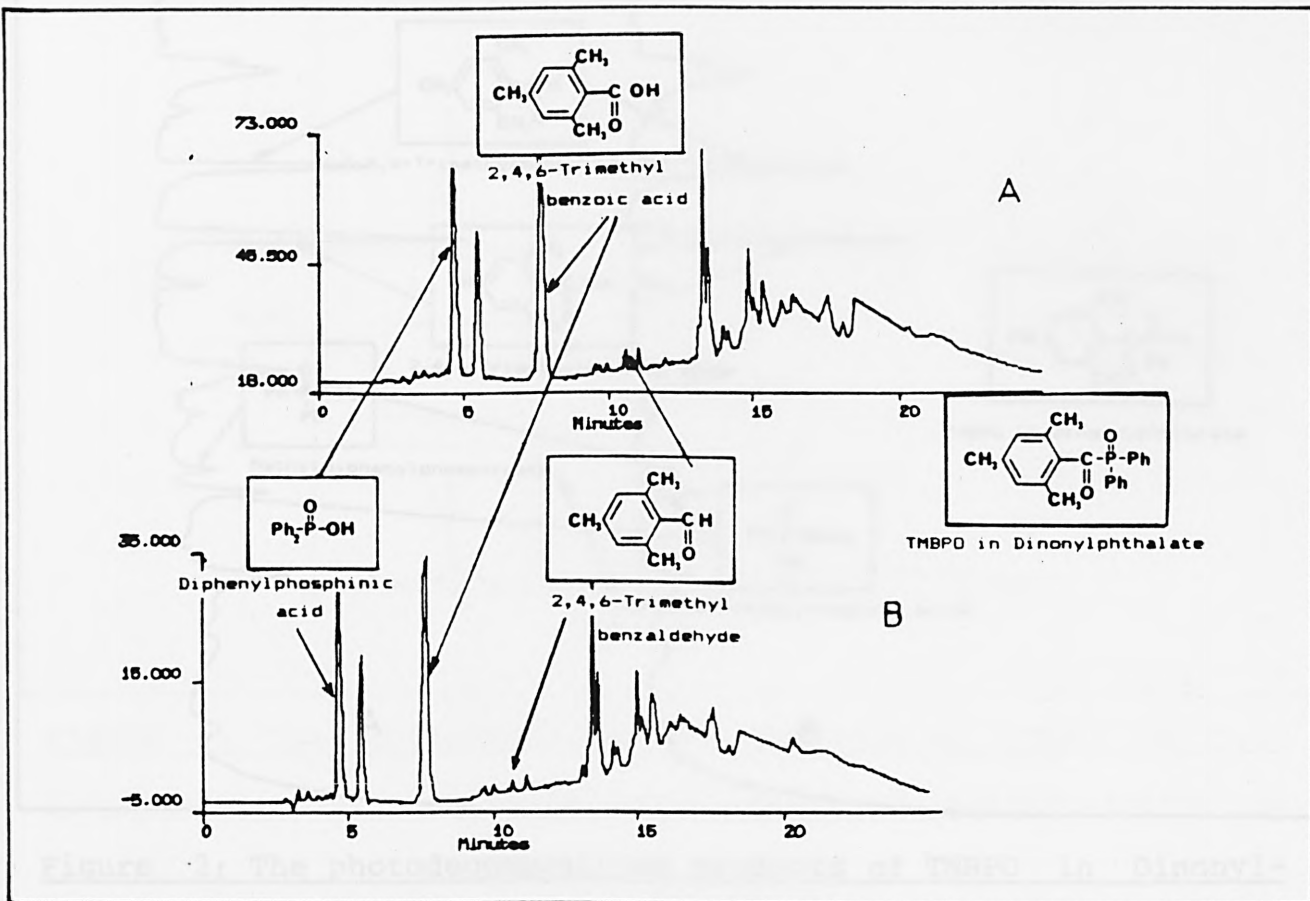


Figure 1; The photodecomposition products of TMBPO in Dinonylphthalate, in the presence and absence of triethylamine, as identified by HPLC.

synergists on the photoinitiated polymerisation of an air saturated diacrylate resin supported the supposition that certain

amines are capable of sustaining a radical chain process for oxygen scavenging [8].

Following the photodecomposition of the acylphosphine oxide TMBPO in the model environment dinonylphthalate both in the presence and absence of triethylamine, identification of the reaction products was performed. By comparison with authentic

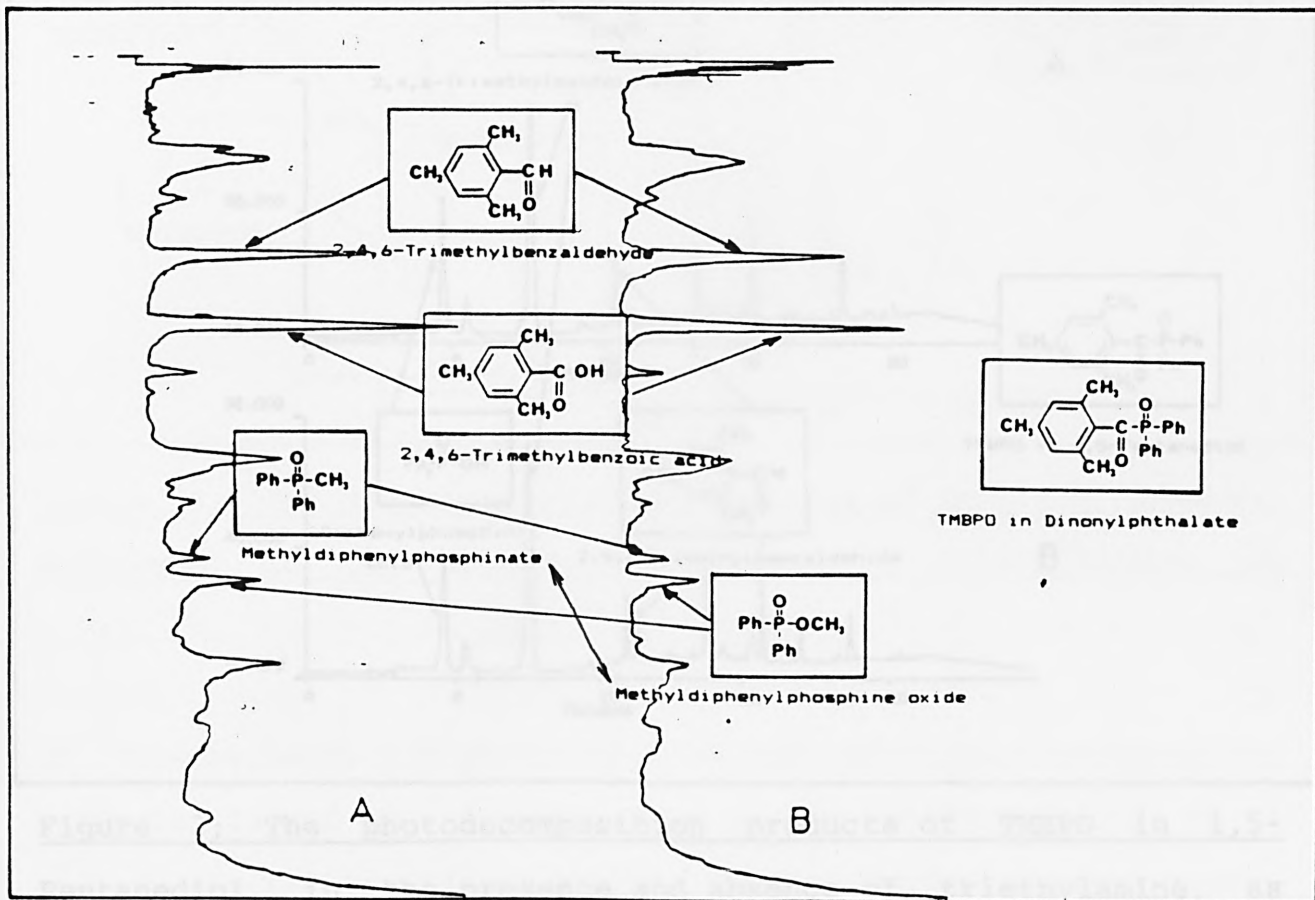


Figure 2; The photodecomposition products of TMBPO in Dinonylphthalate, in the presence and absence of triethylamine, as identified by GLC and Mass Spectrometry.

samples (as judged by HPLC and GLC analysis) and by an examination of the GC-MS fragmentation patterns, identical reaction products were formed in the presence (Figures 1A and 2A) and

absence (Figure 1B and 2B) of triethylamine. Similarly, the photodecomposition products of TMBPO formed in the model environment 1,5-pentenediol (Figure 3A and 3B) were identified to be identical in the presence and absence of triethylamine.

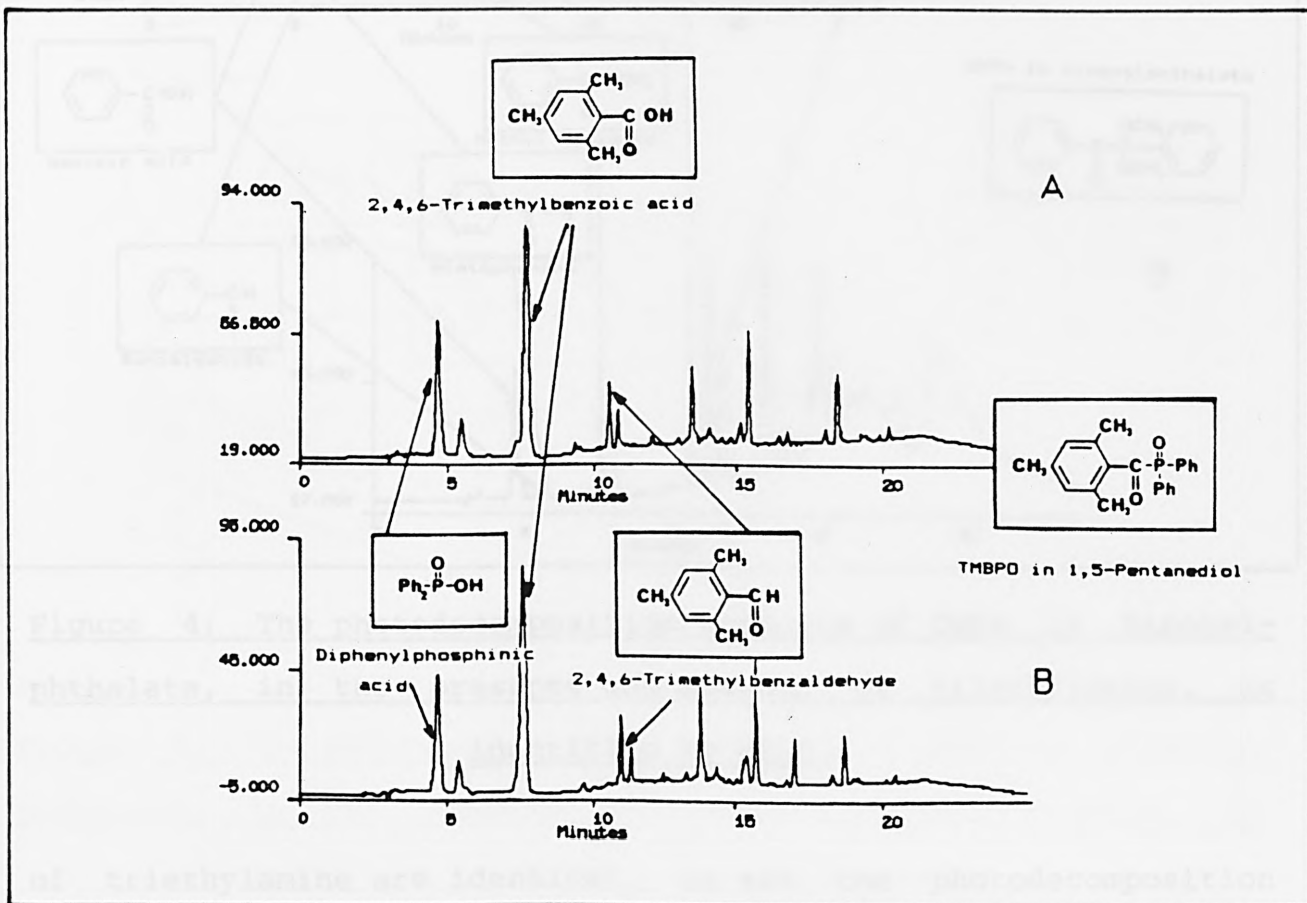


Figure 3; The photodecomposition products of TMBPO in 1,5-Pentenediol, in the presence and absence of triethylamine, as identified by HPLC.

Similar trends were observed when the photodecomposition products of DMPA were examined. The chromatograms showing the photodecomposition products formed in dinonylphthalate, both in the presence (Figures 4A and 5A) and absence (Figures 4B and 5B)

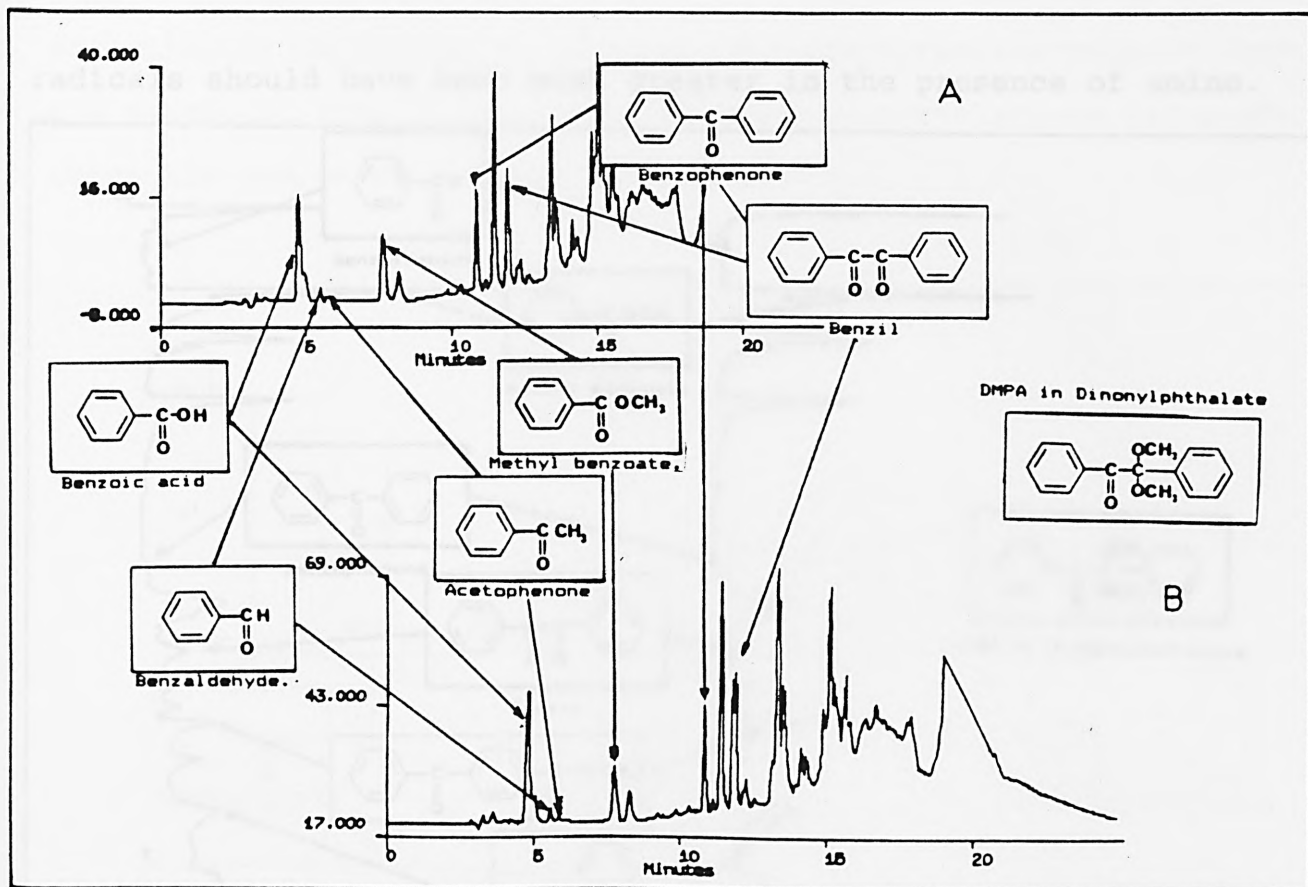


Figure 4; The photodecomposition products of DMPA in Dinonylphthalate, in the presence and absence of triethylamine, as identified by HPLC.

of triethylamine are identical, as are the photodecomposition products formed in 1,5-pentandiol in the presence (Figure 6A) and absence (Figure 6B) of triethylamine. Supporting mass spectral data for the products formed upon the photodecomposition of both TMBPO and DMPA are show in part in Appendices A and B respectively.

These results clearly indicate that the photoinitiators do not interact with the amine and also that the photogenerated initiator radicals are not scavenged by the amine. If this had been the case the yield of aldehydes derived from the aroyl

radicals should have been much greater in the presence of amine.

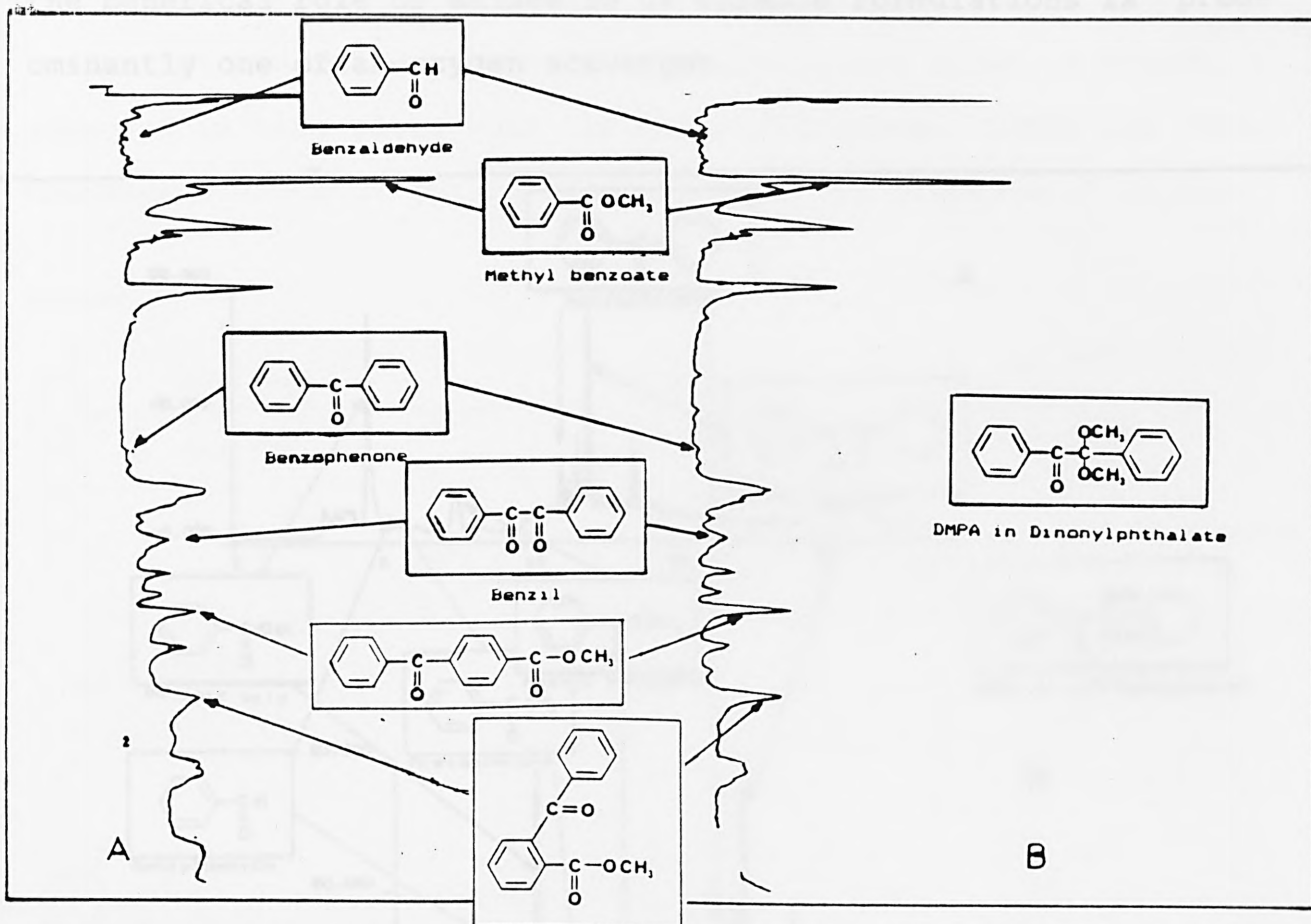


Figure 5; The photodecomposition products of DMPA in Dinonylphthalate, in the presence and absence of triethylamine, as identified by GLC and Mass Spectrometry.

Considering these results, showing identical reaction products in the presence and absence of amine, and those from earlier investigations [7] where UV curing was performed in the absence of air, the possibility of an α -aminoalkyl radical generated via the reaction of primary radicals with the triethylamine being solely responsible for improving the curing efficiency so

dramatically is unlikely. Thus the combined results suggest that the beneficial role of amines in UV curable formulations is predominantly one of an oxygen scavenger.

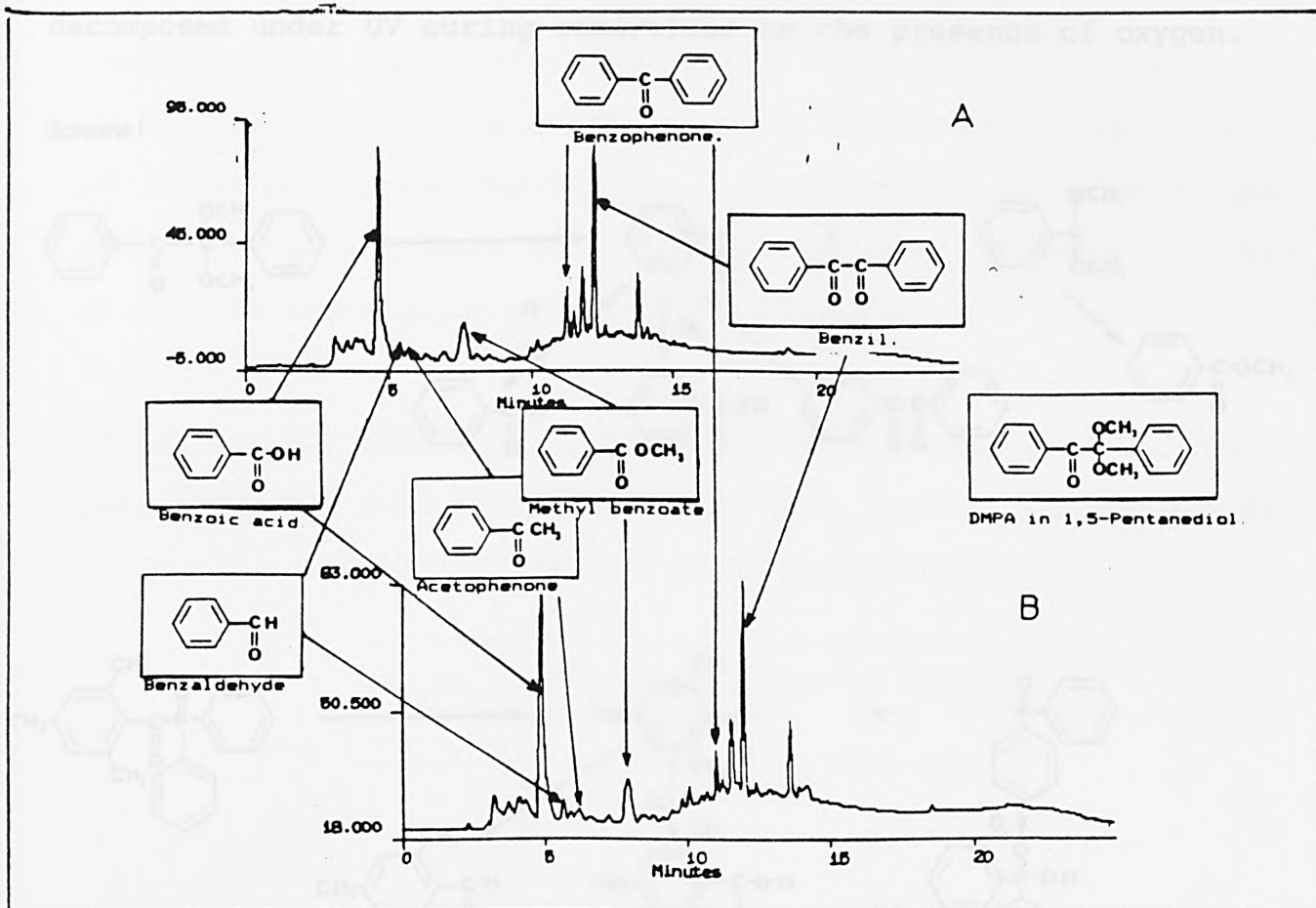


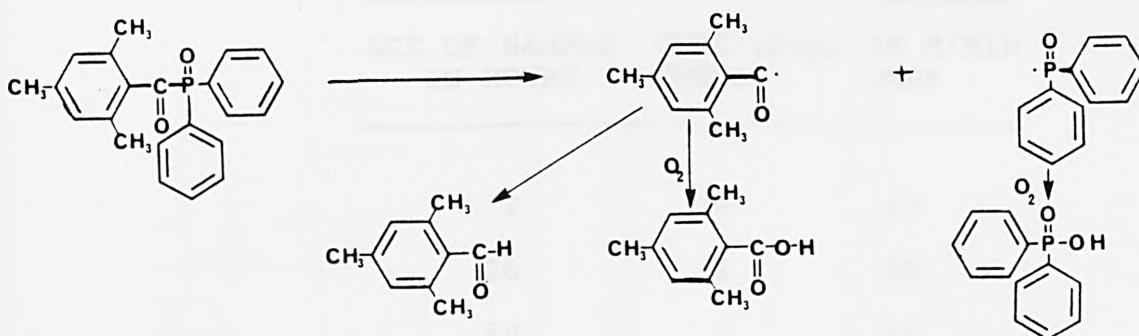
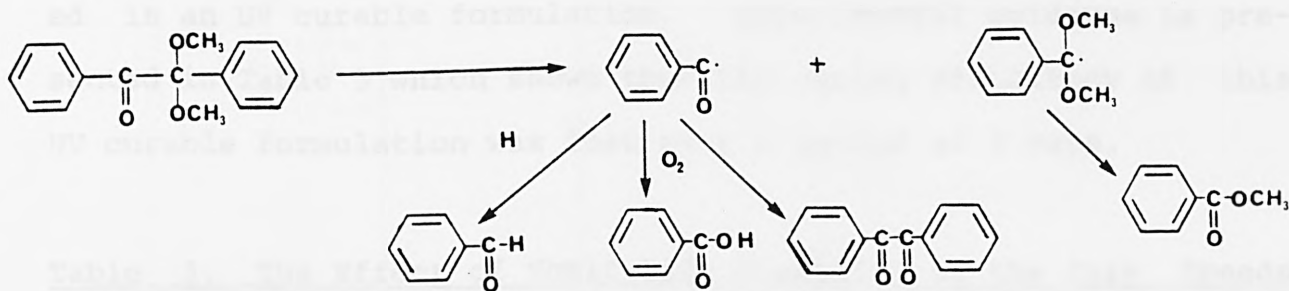
Figure 6; The photodecomposition products of DMPA in 1,5-Pentandiol, in the presence and absence of triethylamine, as identified by HPLC.

During the selection of components which constitute a UV curable formulation, the storage stability or shelf-life of the prepared formulation is one of the main criteria to be considered. The storage stability will be greatly reduced by contaminants present in the resin following manufacture, or already present in the storage container being used. Similarly, heat and

The Mechanism of Photodecomposition.

From product identification (Appendices A and B) under the analytical conditions employed, the processes shown in Scheme 1 appeared to take place when the photoinitiators, TMBPO and DMPA, decomposed under UV curing conditions in the presence of oxygen.

Scheme 1



2) Decomposition of a TMBPO UV Curable Formulation.

During the selection of components which constitute a UV curable formulation, the storage stability or shelf-life of the prepared formulation is one of the main criteria to be considered. The storage stability will be greatly reduced by contaminants present in the resin following manufacture, or already present in the storage container being used. Similarly, heat and

light, chemically labile photoinitiators, added amines or alcohols may also contributed towards a reduction of the stability of the formulation [5,10,11].

A series of investigations were performed in order to ascertain the shelf-life stability of TMBPO as a photoinitiator in the presence of N-methyldiethanolamine when both were contained in an UV curable formulation. Experimental evidence is presented in Table 3 which shows that the curing efficiency of this UV curable formulation was lost over a period of 3 days.

Table 3. The Effect of Shelf-Life Stability on the Cure Speeds for TMBPO and DMPA Photoinitiators in a N-methyldiethanolamine-epoxydiacrylate UV Curable Formulation.

AGE OF SAMPLE IN HOURS	CURE SPEED TMBPO	IN M/MIN DMPA
2	20	20
26	16	20
50	1	20

A freshly prepared TMBPO UV curable formulation was monitored and compared with a DMPA UV curable formulation. Both were stored under the same conditions. Within 50 hours the cure speed had dropped from 20 m.min⁻¹ to 1 m.min⁻¹ compared with little or no change in the DMPA formulation. Chromatographic analysis of this mixture led to the results presented in the chromatogram

(figure 7) which shows the 4 decomposition products generated in

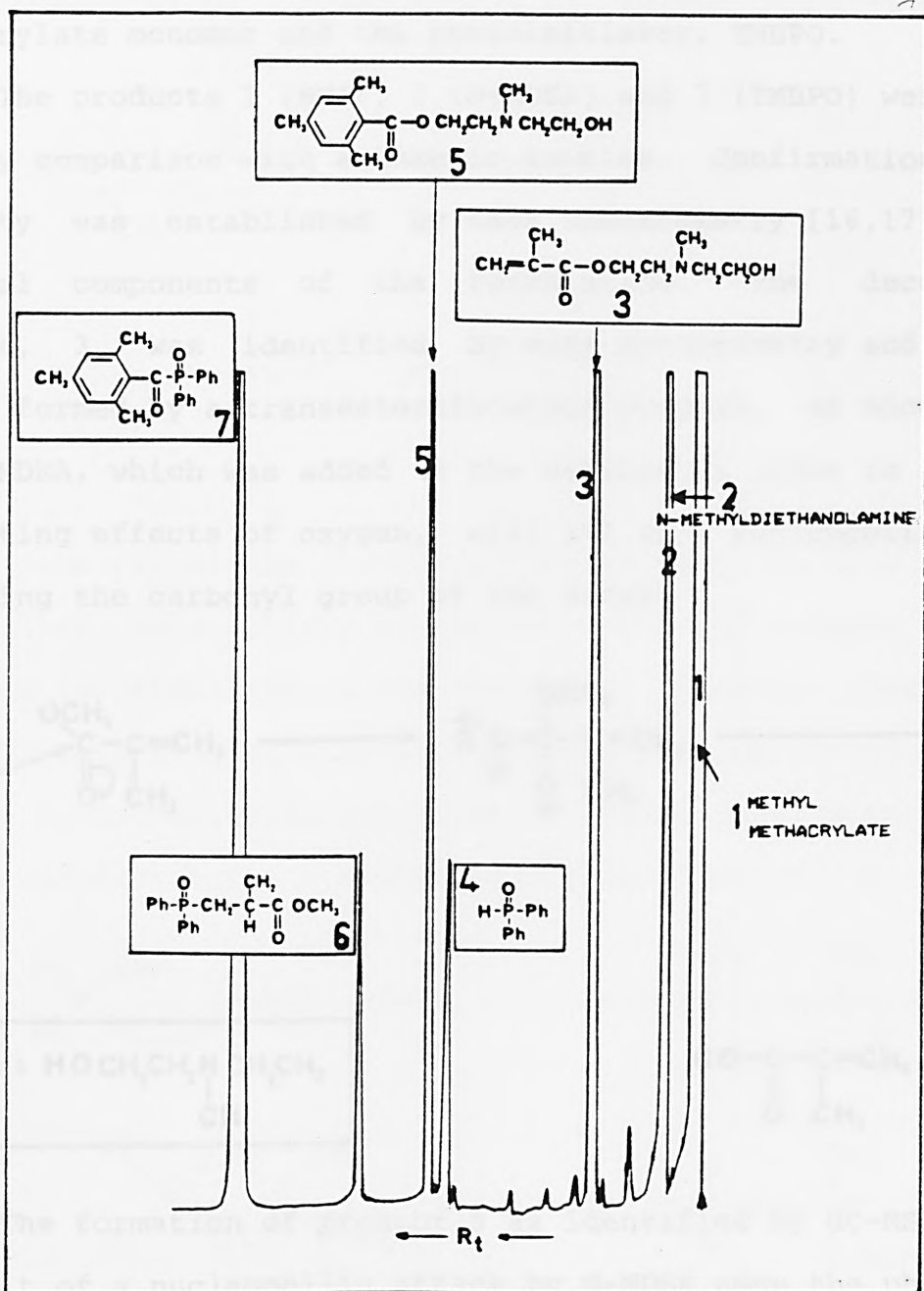
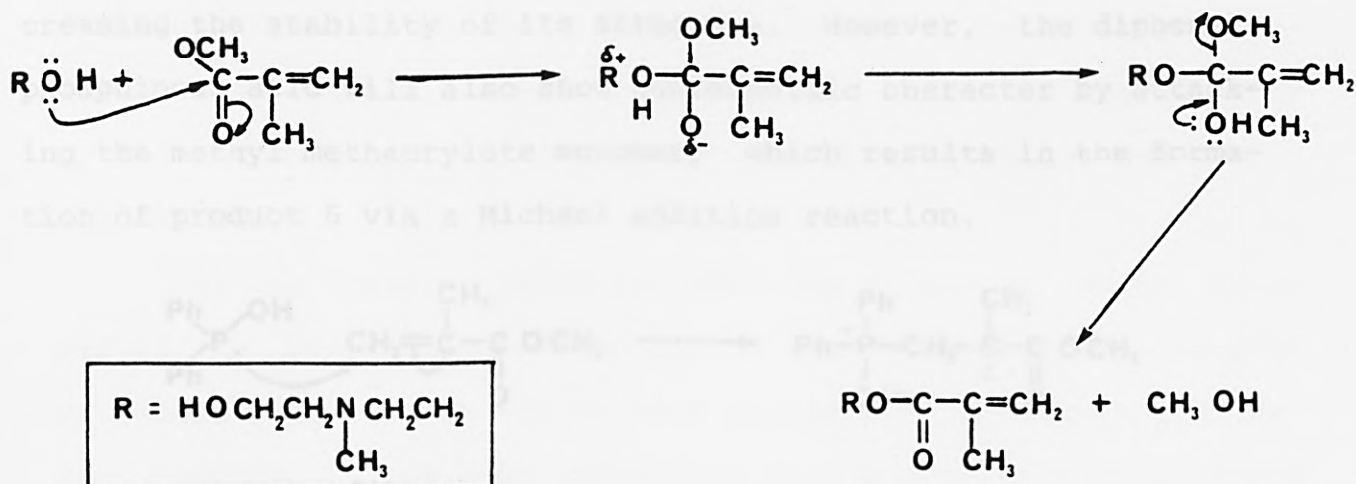


Figure 7; The decomposition products of TMBPO in methyl methacrylate monomer containing N-methyldiethanolamine as identified by GLC and Mass Spectrometry.

the prepared formulation. Subsequent identification by GLC analysis and mass spectroscopy showed the products to be the result of

direct and indirect nucleophilic attack by N-MDEA upon the methyl methacrylate monomer and the photoinitiator, TMBPO.

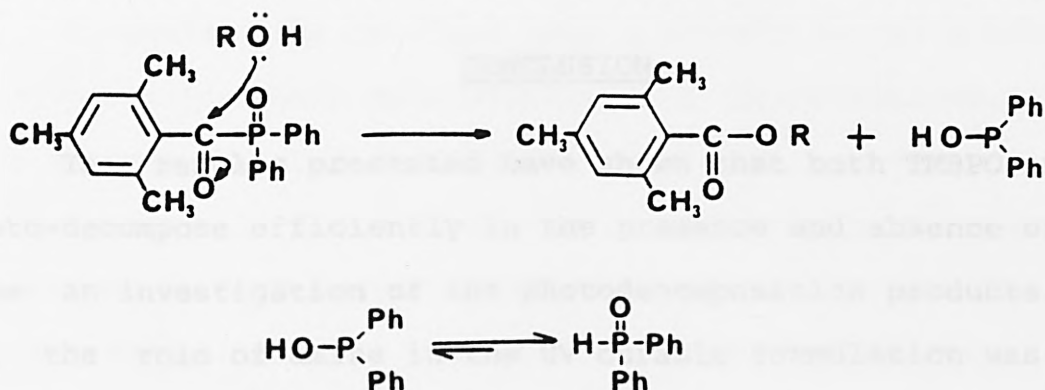
The products 1 (MMA), 2 (N-MDEA) and 7 (TMBPO) were identified by comparison with authentic samples. Confirmation of their identity was established by mass spectrometry [16,17] as the original components of the formulation. The decomposition product, 3, was identified by mass spectrometry and was most likely formed by a transesterification process, as shown below. The N-MDEA, which was added to the mixture in order to reduce the inhibiting effects of oxygen, will act as a nucleophilic reagent attacking the carbonyl group of the ester.



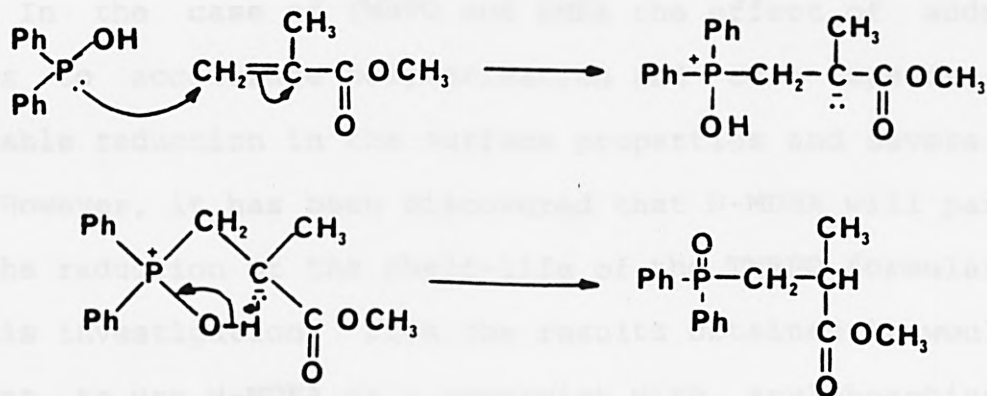
The formation of product 5 as identified by GC-MS arises as a result of a nucleophilic attack by N-MDEA upon the photoinitiator, TMBPO itself. The electron deficient carbonyl group of the photoinitiator is attacked by the aminoalcohol, which yields product 5 and diphenylphosphinous acid, as shown below.

The diphenylphosphinous acid formed as shown above will readily tautomerise to give product 4 (diphenylphosphine oxide)

with the position of equilibrium lying towards the formation of the phosphine oxide, shown below. The predominance of the penta-



valent form (4) of the diphenylphosphine oxide is expected on the account of it's ability to undergo $d\pi--p\pi$ bonding thus increasing the stability of its structure. However, the diphenylphosphinous acid will also show nucleophilic character by attacking the methyl methacrylate monomer, which results in the formation of product 6 via a Michael addition reaction.



These product studies demonstrated the deleterious effect of including an aminoalcohol in UV curable formulations containing the acylphosphine oxide TMBPO. A schematic representation of the fragmentation patterns of the phosphinyl radical is shown in Appendix C together with the mass spectra for each of the unknown

products (3-6), [16,17].

CONCLUSION

The results presented have shown that both TMBPO and DMPA photo-decompose efficiently in the presence and absence of amine. From an investigation of the photodecomposition products obtained, the role of amine in the UV curable formulation was identified as predominantly one of an oxygen scavenger. Earlier experimental evidence has shown (Chapter 5) [7] that in the absence of amines the curing efficiency of both photoinitiators is poor. An additional problem came to light when the shelf-life stability of TMBPO was found to be short in an UV curable formulation containing N-MDEA. This was found to be a result of the nucleophilicity of the aminoalcohol, which attacked the photoinitiator and acrylate monomer.

In the case of TMBPO and DMPA the effect of added amine serves to accelerate polymerisation and cure speeds, without noticeable reduction in the surface properties and severe yellowing. However, it has been discovered that N-MDEA will participate in the reduction of the shelf-life of the TMBPO formulation used in this investigation. From the results obtained it would appear prudent to use N-MDEA as a synergist with acylphosphine oxides with due care and the use of unsubstituted tertiary amines may be preferable to overcome the side reactions associated with the reactivity of the hydroxyl groups.

ACKNOWLEDGEMENTS

I would like to thank most sincerely Gerard Hakvoort and Ton Overeem for their many experimental contributions, patience and the many helpful discussions about the results and the work in progress. I would also like to thank the mass spectroscopy department at Akzo Research Laboratories, Arnhem, for their significant contribution to this work and their helpfulness.

performed on a 15 μ fused silica column (internal diameter 4.6 mm) containing DB-5 (95% dimethyl- and 5% phenylmethylsiloxane); the carrier gas used was nitrogen.

HPLC analysis was performed on a Waters Modular Liquid Chromatography System which was equipped with Model 8000 A pumps and the Wisp 710 B Automatic Sample Processor. System control, quantification and reporting was carried out by the Waters 840 Chromatography Station. A Waters model 797 UV-absorbance detector ($\lambda = 254$ nm) was used. All separations were carried out on a Beharbond C8 column.

The Gas Liquid Chromatography (GLC) experiments were performed on a Varian 3700 GC Chromatograph with a Flame Ionization Detector, using a temperature programmed range 40-210 $^{\circ}$ C at a rate of 10 $^{\circ}$ C min⁻¹. The analyses were performed on a 15 μ fused silica column (internal diameter 4.6 mm) containing DB-5, with nitrogen as the carrier gas.

The UV curing experiments were carried out as described previously (Chapter 1) [1]. As the rate of irradiation is inver-

EXPERIMENTAL

Instrumentation:

The mass spectra were recorded on a Finnegan MAT 212 (EI) mass spectrometer (mass range 10-900, scan rate 1.1 sec per dec, resolution 800) which was interfaced with a Varian 3700 gas chromatograph. A temperature programme was used for the separations (range 70-230 °C at a rate of 10 °C min⁻¹) which were performed on a 15 m fused silica column (wide bore 1.5 µm) containing DB-5 (95 % dimethyl-, 5 % diphenyl-, polysiloxane); the carrier gas used was Helium.

HPLC analysis was performed on a Waters Modular Liquid Chromatography System which was equipped with Model 6000 A pumps and the Wisp 710 B Automatic Sample Processor. System control, quantification and reporting was carried out by the Waters 840 Chromatography Station. A Kratos Spectroflow 757 UV-absorbance detector ($\lambda = 254$ nm) was used. All separations were carried out on a Bakerbond C4 column.

The Gas Liquid Chromatography (GLC) experiments were performed on a Varian 3700 Gas Chromatograph with a Flame Ionisation Detector, using a temperature programme (range 60-230 °C at a rate of 10 °C min⁻¹). The separations were performed on a 15 m fused silica column (internal diameter 0.32 mm) containing DB-5, with nitrogen as the carrier gas.

The UV curing experiments were carried out as described previously (Chapter 5) [7]. As the time of irradiation is inver-

sely proportional to the cure speed (speed of the moving belt), recorded in m.min⁻¹, it can be recorded in seconds.

Materials:

Mesitaldehyde, 2,4,6-trimethylbenzoic acid, diphenylphosphinic acid, benzaldehyde, acetophenone, methyl benzoate, benzoic acid, biphenyl, benzophenone, benzil, triethylamine and N-methyldiethanolamine [N-MDEA] (all from Janssen Chimica) were used as received. Dinonylphthalate (from Merck), methyl methacrylate and 1,5-pentanediol (from Aldrich) were also used as received.

2,2-Dimethoxy-2-phenylacetophenone (from Ciba Geigy) was recrystallised from petroleum ether (boiling range, 60-80 °C) and had a melting point range of 65.4-65.7 °C. 2,4,6-trimethylbenzoyl diphenylphosphine oxide was synthesised as described previously in Chapter 2.

A low molecular weight prepolymer, the epoxydiacrylate of Setacure[®] AP 570 (26.6% by Wt.) in polyethyleneglycol (200) diacrylate (PEGDA) (73.4% by Wt.). was the resin used (from Synthese b.v.). Satinised paper was the substrate used in all irradiations. The coatings were applied to the substrate using an Erichsen rod to give a wet film thickness of 20 µm.

1) Examination of the Photodecomposition of TMBPO in Dinonylphthalate.

A solution of TMBPO in dinonylphthalate was prepared by dissolving 1.20g (3% by Wt.) of the photoinitiator in 40.00g of dinonylphthalate. 20 µm thick films of the solution were applied

to satinised paper using an Erichsen rod. The coated papers were passed through the UV curing apparatus at specific belt speeds. The control and variation of the belt speeds enabled the extent of decomposition to be examined over a variety of known irradiation times. After curing, the coating was scraped from the substrate and analysed. All of the experiments were carried out in duplicate using freshly prepared solutions which were analysed directly after the irradiation.

i) Primary HPLC Analysis.

The irradiated samples (of known weight) were dissolved in methanol (HPLC grade), and separated by a gradient elution programme. The gradients were established between two degassed eluents, eluent A consisted of acetonitrile/water (vol. ratio 70:30) and eluent B consisted of acetonitrile/water (vol. ratio 90:10). A linear gradient was established from 100% of A to 100% of B over a period of 5 minutes. The flow rate was 1 ml.min⁻¹.

From this analysis the extent to which the photoinitiator had decomposed was determined and thereby the amount of TMBPO which had decomposed was assessed as a function of irradiation time. The results are shown in Table 2.

In order to identify the reaction products, another sample was prepared as before and cured at a speed of 2 m.min⁻¹. This was then analysed as follows.

ii) Secondary HPLC Analysis.

The analytical equipment used was described previously under the instrumentation heading. The irradiated sample was

dissolved in methanol (HPLC grade) and applied to the column. Once again gradients were established between two degassed eluents, eluent A consisted of acetonitrile/water/phosphoric acid (vol. ratio 30:70:0.1) and eluent B consisted of acetonitrile/water/phosphoric acid (vol. ratio 90:10:0.1). This time the linear gradient was established from 100% of A to 100% of B over a period of 15 minutes. The flow rate was 1 ml.min⁻¹.

A representative chromatogram is shown in Figure 1 (A). In order to identify the products detected, the retention times of a number of possible products (authentic samples) were determined. Where a match between the retention time of one of these authentic samples and a product was obtained a chromatogram was run in which the reaction mixture was spiked with the authentic sample. The observation of simultaneous elution of the authentic sample and product was taken as indicative evidence for the identity of the product. Further confirmation of these assignments was sought using other analytical methods as described below.

iii) GLC Analysis.

The reaction mixture was applied to a 15 m fused silica column assembled within the GLC apparatus described earlier in the instrumentation section. Elution was facilitated by the use of temperature programming. A representative chromatogram is shown in Figure 2 (A).

Identification of products was carried out in a similar manner to that described for the HPLC analysis. Retention times were matched to those of authentic samples.

iv) GC-Mass Spectrometry.

The reaction mixture was applied to the same column as used in the GLC analysis which was installed within a GC instrument which was interfaced with a mass spectrometer. The significant peaks in the GC-MS trace were examined in detail i.e., the fragmentation patterns were recorded. These breakdown patterns are shown in part in Appendix A.

2) Examination of the Photodecomposition of TMBPO in Dinonylphthalate in the Presence of an Amine.

A solution of TMBPO in dinonylphthalate was prepared by dissolving 1.20g (3% by Wt.) of the photoinitiator and 2.40g (6% by weight) of N-methyldiethanolamine (N-MDEA) in 40.00g of dinonylphthalate. The examination of this freshly prepared solution, was made in order to determine the extent to which the photoinitiator had decomposed under the conditions described in Experiment 1. The amount of TMBPO decomposed (in the presence of amine) was assessed as a function of irradiation time as soon as the irradiations were completed. The results are shown in Table 2.

In order to identify the reaction products, another sample was prepared. This sample consisted of 1.20g (3% by weight) of TMBPO photoinitiator, 2.40g (6% by weight) of triethylamine (TEA) dissolved in 40.00g of dinonylphthalate. Examination and analysis of the photodecomposition products was made under similar conditions and methods to those employed in Experiment 1. Representative chromatograms are shown in Figures 1 (B) and 2 (B), and the

mass spectral breakdown patterns are shown in part in Appendix A.

3) Examination of the Photodecomposition of DMPA in Dinonylphthalate.

A solution of DMPA in dinonylphthalate was prepared by dissolving 1.20g (3% by Wt.) of the photoinitiator in 40.00g of dinonylphthalate. An examination of the extent to which the photoinitiator decomposed was determined under the experimental conditions previously described in Experiment 1. The amount of DMPA decomposed was assessed as a function of irradiation time; the results are shown in Table 1.

In order to identify the reaction products, another sample was prepared as described before. Examination and analysis of the photodecomposition products was made under similar conditions and methods to those employed in Experiment 1. Representative chromatograms are shown in Figures 4 (B) and 5 (A), and the mass spectral breakdown patterns are shown in part in Appendix B.

4) Examination of the Photodecomposition of DMPA in Dinonylphthalate in the Presence of an Amine.

A solution of DMPA in dinonylphthalate was prepared by dissolving 1.20g (3% by Wt.) of the photoinitiator and 2.40g (6% by weight) of N-MDEA in 40.00g of dinonylphthalate. An examination of the extent to which the photoinitiator decomposed under the experimental conditions described in Experiment 1 was determined. The amount of DMPA decomposed (in the presence of amine) was assessed as a function of irradiation time. The results are

shown in Table 1.

In order to identify the reaction products, another sample was prepared as described in Experiment 2, except the photoinitiator in this case was DMPA. Examination and analysis of the photodecomposition products was performed under similar conditions and methods to those employed in Experiment 1. Representative chromatograms are shown in Figures 4 (A) and 5 (B), and the mass spectral breakdown patterns are shown in part in Appendix B.

5) Examination of the Photodecomposition of TMBPO in
1,5-Pentanediol.

A solution of TMBPO in 1,5-Pentanediol was prepared by dissolving 1.20g (3% by Wt.) of the photoinitiator in 40.00g of 1,5-pentanediol. The photodecomposition of the initiator TMBPO was investigated in detail in order to identify the photodecomposition products yielded. Analysis was performed under the same conditions, using the same methods and instrumentation as described in Experiment 1, section (ii). A representative chromatogram is shown in Figure 3 (A).

6) Examination of the Photodecomposition of TMBPO in
1,5-Pentanediol in the Presence of Amine.

A solution of TMBPO in 1,5-Pentanediol was prepared by dissolving 1.20g (3% by Wt.) of the photoinitiator and 2.40g (6% by weight) of TEA in 40.00g of 1,5-pentanediol. This solution was investigated as described above in Experiment 5. A representative

chromatogram is shown in Figure 3 (B).

7) Examination of the Photodecomposition of DMPA in
1,5-Pentenediol.

A solution of DMPA in 1,5-Pentenediol was prepared by dissolving 1.20g (3% by Wt.) of the photoinitiator in 40.00g of 1,5-pentenediol. This solution was investigated as described above in Experiment 5. A representative chromatogram is shown in Figure 6 (B).

8) Examination of the Photodecomposition of DMPA in
1,5-Pentenediol in the Presence of Amine.

A solution of DMPA in 1,5-Pentenediol was prepared by dissolving 1.20g (3% by Wt.) of the photoinitiator and 2.40g (6% by weight) of TEA in 40.00g of 1,5-pentenediol. This solution was investigated as described above in Experiment 5. A representative chromatogram is shown in Figure 6 (A).

9) Examination of the Shelf-life of Epoxydiacrylate
Formulations containing TMBPO.

During preliminary investigations of the curing efficiency of both TMBPO and DMPA in the presence and absence of N-methyldiethanolamine in an epoxydiacrylate formulation (Chapter 5) [7] it was clearly apparent that the cure speed of the TMBPO/N-methyldiethanolamine formulation deteriorated after 24 hours. A detailed investigation of the shelf-life stability of TMBPO was

performed. Formulations were prepared by dissolving 0.30g (3% by Wt.) of TMBPO and 0.60g (6% by Wt.) N-MDEA in 10.00g of Setacure^(R) AP 570/PEGDA (200) resin which were stored in brown glass bottles in a box at room (20 c) temperature. An examination of how the cure speed deteriorated with the increasing age of the prepared formulation was determined and the results are shown in Table 3. The UV curing efficiency of the TMBPO formulation was determined by the usual method over a number of days. On day 5 the TMBPO formulation was analysed by GLC for starting materials and decomposition products, using the analytical conditions, instrumentation, column and methods previously described in Experiment 1, sections (iii) and (iv). GLC analysis of the decomposing mixture was unable to provide any conclusive information because the chromatograms obtained were too complicated to allow the identification of products or starting materials.

10) Examination of the Shelf-life of Epoxydiacrylate

Formulations containing DMPA.

A detailed investigation of the shelf-life stability of DMPA was also performed as described in Experiment 9. The formulations were prepared by dissolving 0.30g (3% by Wt.) of DMPA and 0.60g (6% by Wt.) N-MDEA in 10.00g of Setacure^(R) AP 570/PEGDA (200) resin which were stored as described in Experiment 9. Examination of the cure speed (by the usual curing methods) as the age of the prepared formulation increased, was determined; the results are shown in Table 3. As the curing efficiency remained constant over a period of days, further analysis was not

considered necessary.

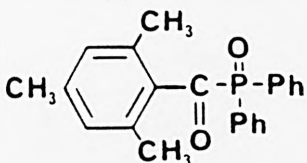
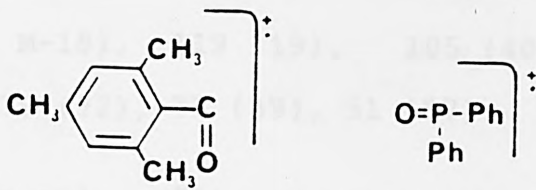
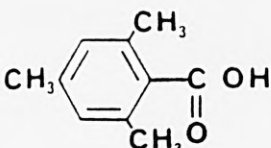
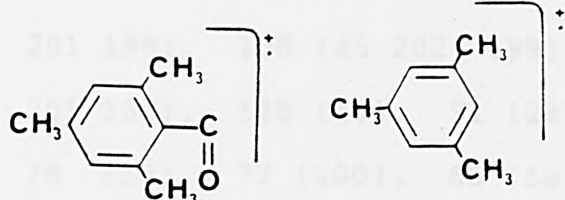
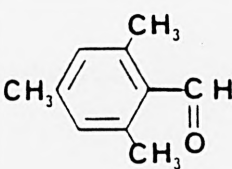
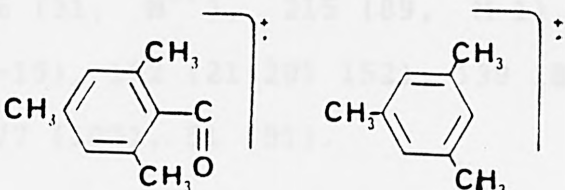
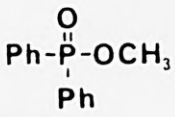
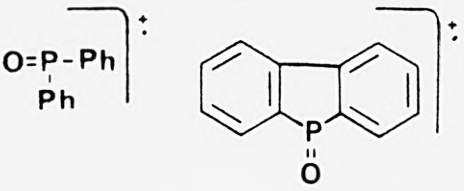
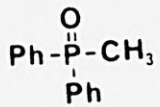
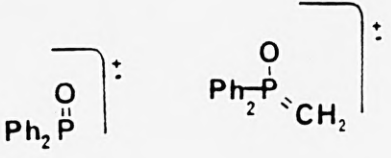
11) Examination of the Stability of TMBPO in a mixture of Methyl Methacrylate and N-methyldiethanolamine.

The UV curing formulation described in Experiment 9 was replaced by one containing methyl methacrylate monomer (MMA), to enable identification of the decomposition products. The TMBPO formulation was prepared as described previously in Experiment 9, using MMA instead of the epoxydiacrylate resin. This was stored in a brown glass bottle, in a box at room temperature, maintaining a dark environment continually. The decomposition of the photoinitiator in the dark environment was followed daily by GLC analysis, as described in Experiment 9, the products being identified by comparison with authentic samples. At this point, only the starting materials MMA, N-MDEA and TMBPO could be identified by comparison. A representative chromatogram is shown in Figure 7.

After a period of 10 days, the decomposition mixture was analysed by GC-MS. Figure 7 shows the structures of the products 3 to 6, identified by mass spectrometry; Appendix C shows in part the mass spectral breakdown patterns of these products.

APPENDIX A

Selected mass Spectral Data for the Products Formed upon the
Photodecomposition of Photoinitiators TMBPO and DMPA.

Compounds	Molecular Ion	Significant Fragmentation Ions
<p>TMBPO</p> 	<p>348 (I = 0.3)</p>	
<p>2,4,6-trimethylbenzoic acid</p> 	<p>164 (I = 36)</p>	
<p>2,4,6-trimethylbenzaldehyde</p> 	<p>148 (I = 52)</p>	
<p>Methyldiphenylphosphinate</p> 	<p>232 (I = 30)</p>	
<p>Methyldiphenylphosphine Oxide</p> 	<p>216 (I = 31)</p>	

Products from the photodecomposition of TMBPO in the presence and absence of triethylamine, in dinonylphthalate.

MS (70 eV), m/z (int): [2] 148 (52, $M^{+\bullet}$), 147 (95, M-1), 119 (100, M-29), 105 (33), 91 (75), 77 (53), 65 (33), 51 (23).

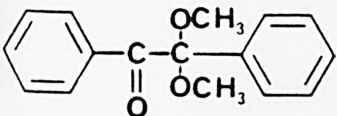
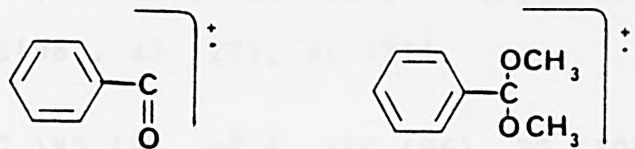
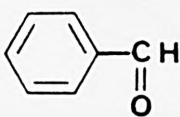
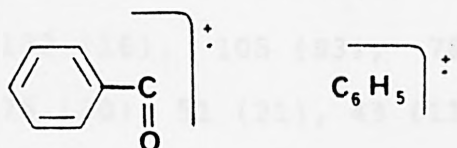
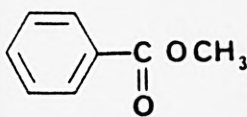
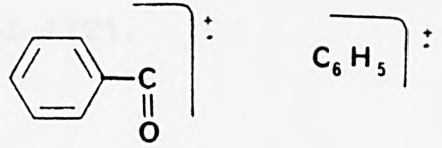
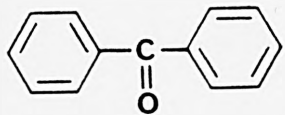
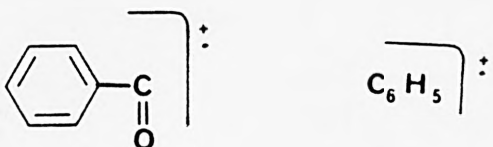
[4] 164 (36, $M^{+\bullet}$), 147 (89, M-17), 146 (100, M-18), 119 (19), 105 (40), 91 (72), 79 (32), 77 (39), 51 (57).

[6] 232 (30, $M^{+\bullet}$), 231 (81, M-1), 216 (4, M-16), 202 (14), 201 (14, M-31), 199 (51, 201 199), 155 (45 202 199), 152 (25, 201 152), 125 (10), 91 (28), 79 (6), 78 (17), 77 (100), 65 (10), 51 (59).

[7] 216 (31, $M^{+\bullet}$), 215 (89, M-1), 201 (76, M-15), 152 (21, 201 152), 139 18, 91 (21), 77 (100), 51 (91).

APPENDIX B

Selected mass Spectral Data for the Products Formed upon the Photodecomposition of Photoinitiators TMBPO and DMPA.

Compounds	Molecular Ion	Significant Fragmentation Ions
<p>DMPA</p> 	<p>256 (I = 2)</p>	
<p>Benzaldehyde</p> 	<p>106 (I = 68)</p>	
<p>Methyl Benzoate</p> 	<p>136 (I = 100)</p>	
<p>Benzophenone</p> 	<p>182 (I = 21)</p>	

products from the photodecomposition of DMPA in the presence and absence of triethylamine in dinonylphthalate.

MS (70 eV), m/z (int): [8] 106 (68, m^{\ddagger}), 105 (84, M-1), 77 (100), 51 (46).

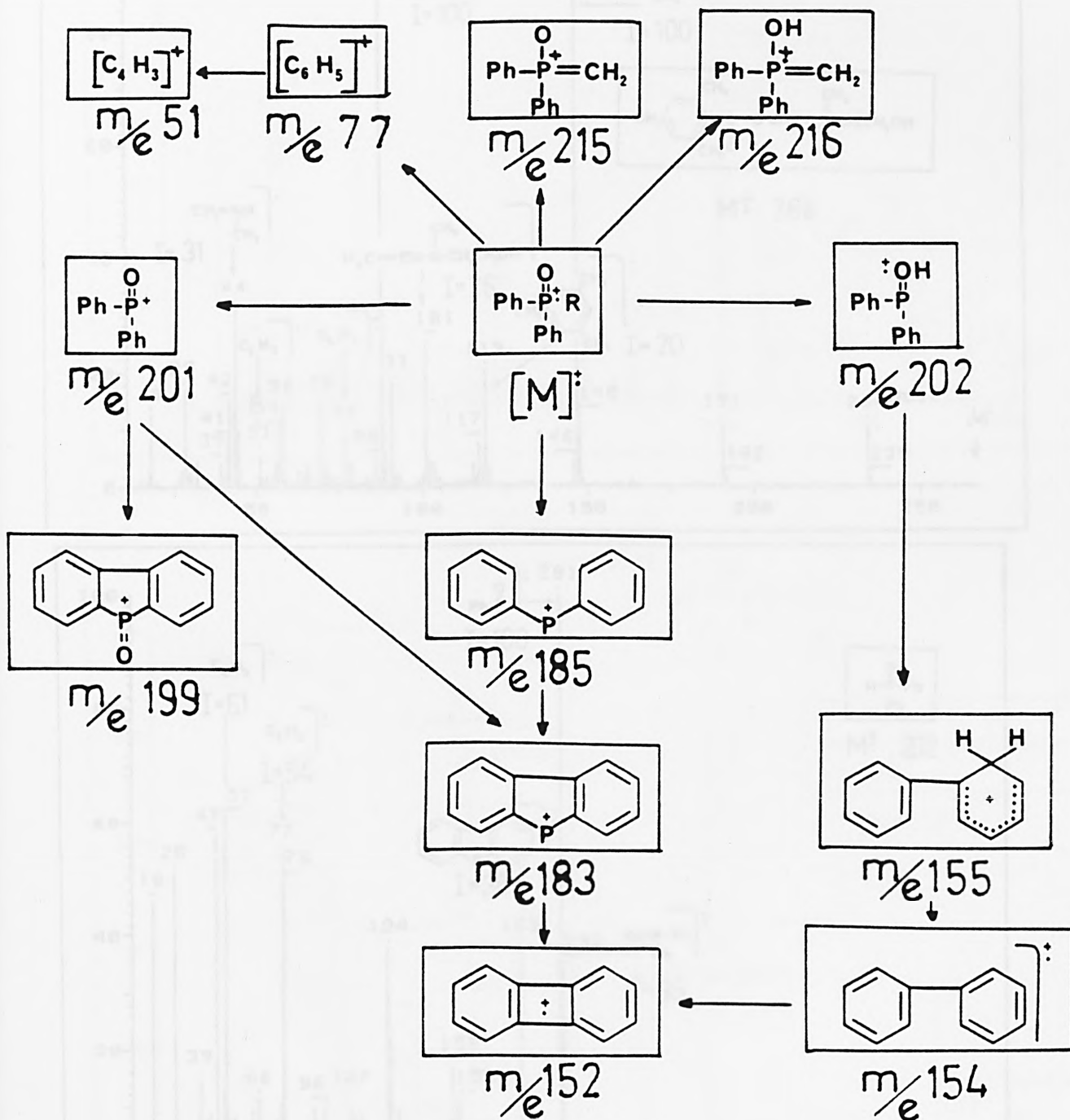
[9] 136 (100, M^{\ddagger}), 135 (24, M-1), 105 (99, M-15), 92 (51), 77 (98), 57 (99), 51(98), 43 (17), 41 (31).

12 182 (21, m^{\ddagger}), 105 (86), 77 (100), 51 (28).

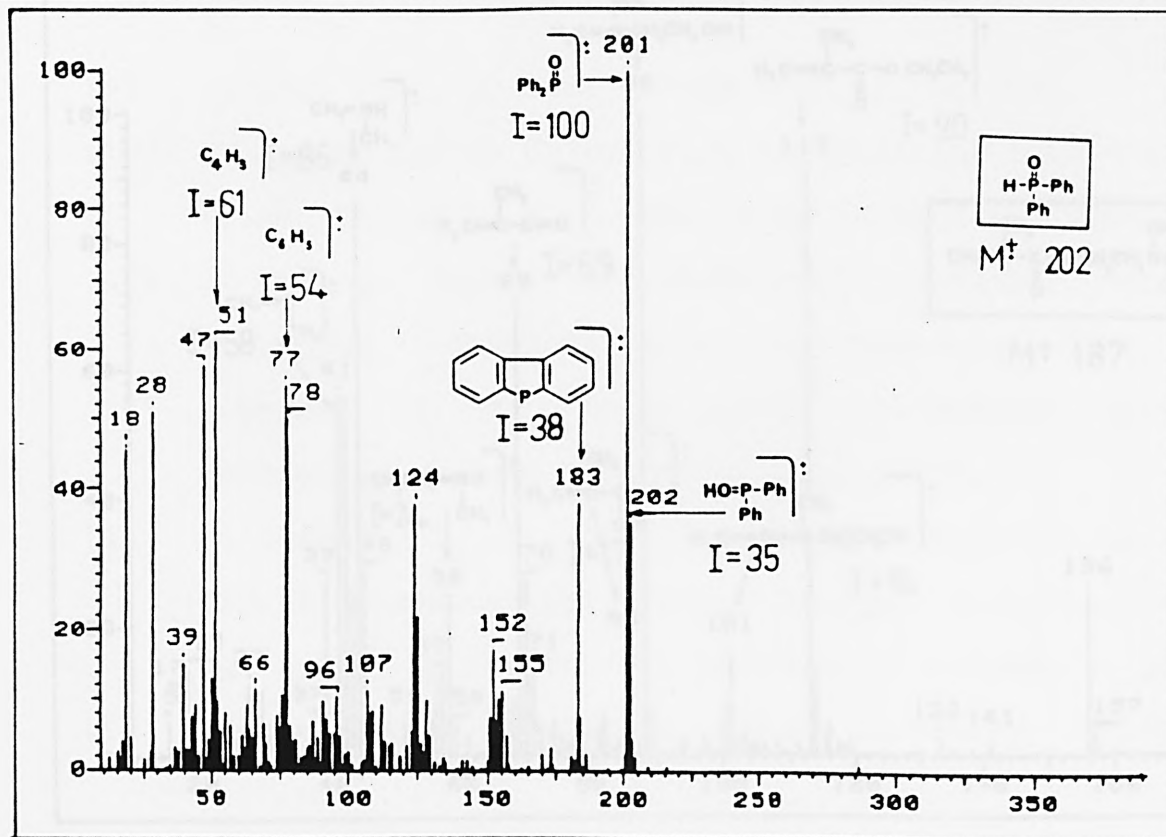
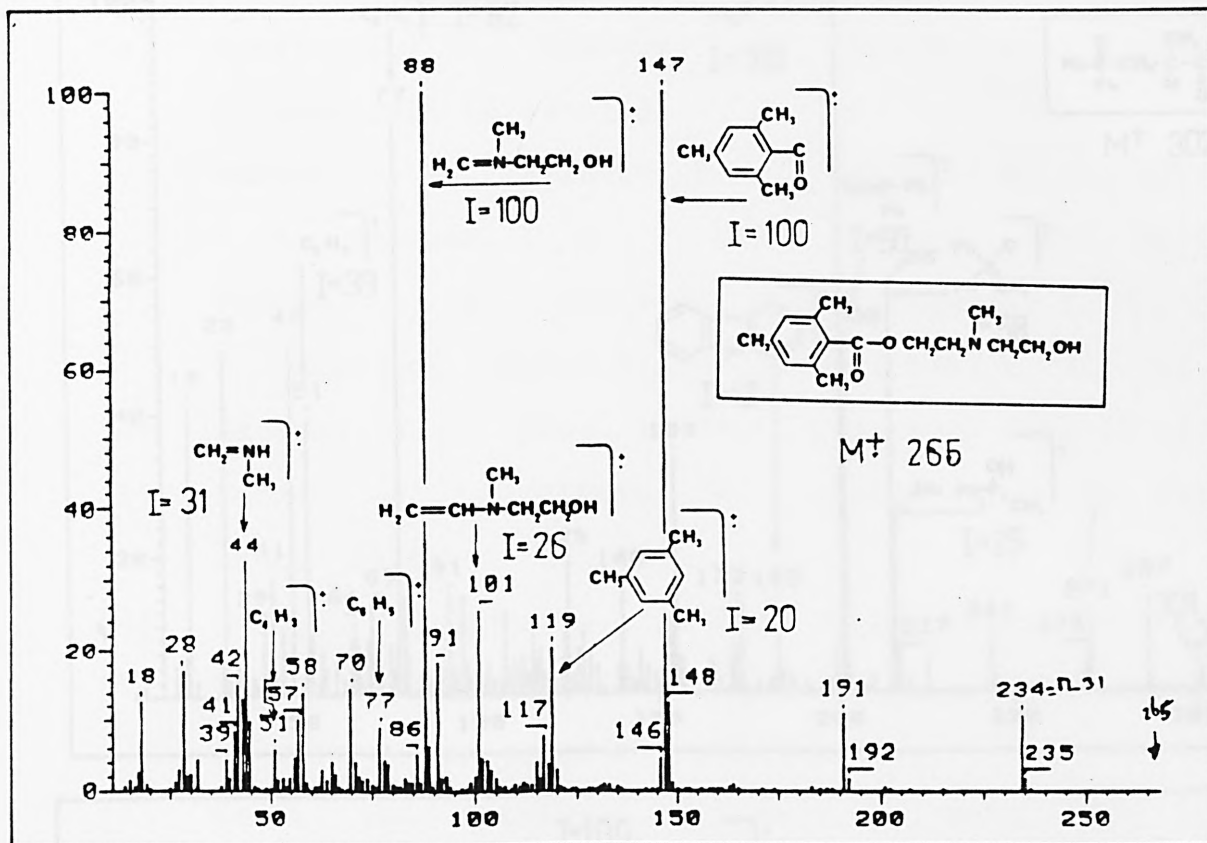
[15] 240 (13, M^{\ddagger}), 225 (1, M-15), 209 (14, M-31), 181 (14, M-59), 163 (100, M-77), 133 (16), 105 (83), 78 (9), 77 (86), 76 (30), 51 (21), 43 (11), 41 (9).

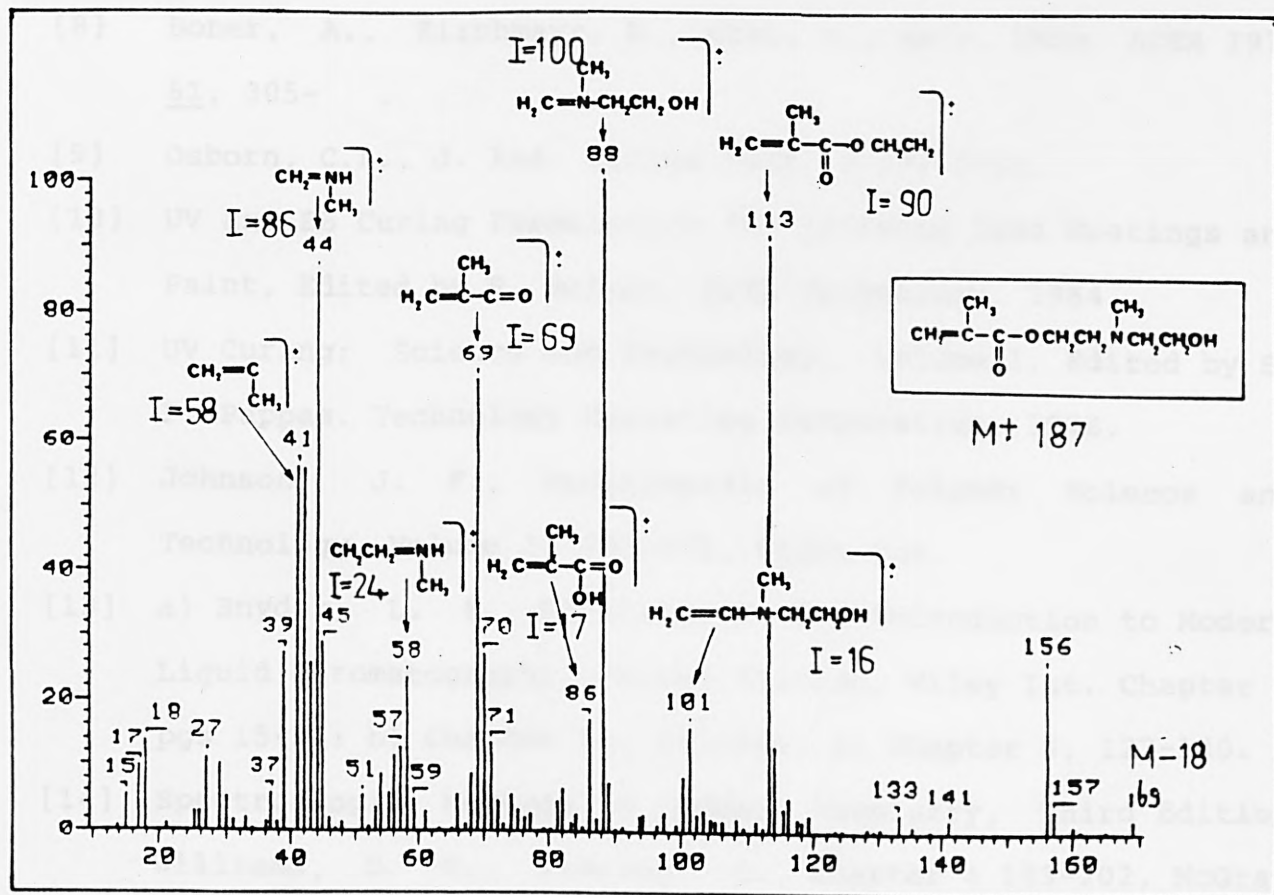
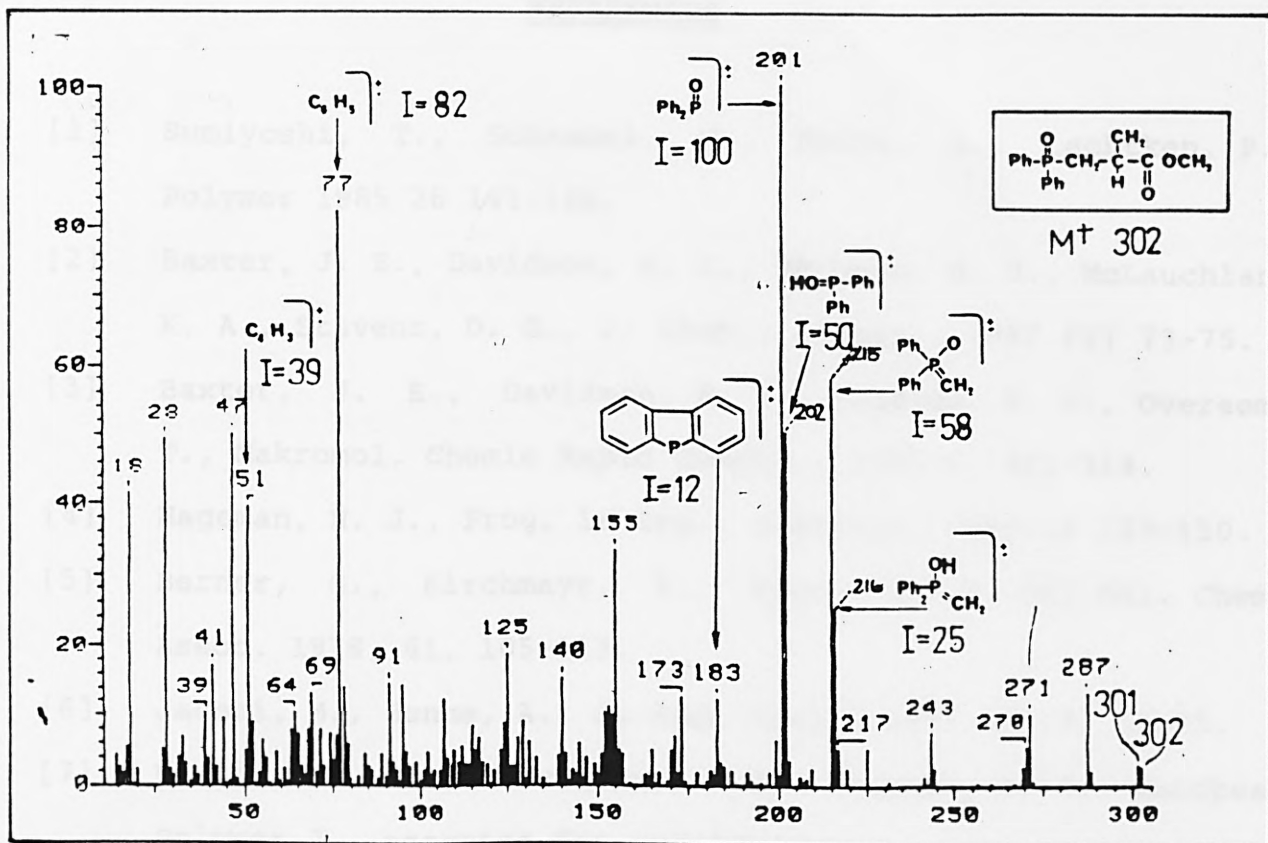
[15] 240 (18, M^{\ddagger}), 225 (1, M-15), 209 (11, M-31), 181 (14, M-59), 163 (40, M-77), 135 (11), 105 (100), 78 (3), 77 (60), 51 (22).

Schematic Representation of the Fragmentation Patterns of the Phosphinyl Radical [16,17].



The Mass Spectra for the Products Formed upon the Decomposition of the Photoinitiator TMBPO.





REFERENCES

- [1] Sumiyoshi, T., Schnabel, W., Henne, A., Lechtken, P., Polymer 1985 26 141-146.
- [2] Baxter, J. E., Davidson, R. S., Hageman, H. J., McLauchlan, K. A., Stevens, D. G., J. Chem., Commun., 1987 (2) 73-75.
- [3] Baxter, J. E., Davidson, R. S., Hageman, H. J., Overeem, T., Makromol. Chemie Rapid Commun., 1987 8, 311-314.
- [4] Hageman, H. J., Prog. in Org., Coatings, 1985 13 123-150.
- [5] Berner, G., Kirchmayr, R., Rist, G., J. Oil Col. Chem. Assoc. 1978, 61, 105-113.
- [6] Jacobi, M., Henne, A., J. Rad. Curing 1983 10 (4) 16-25.
- [7] Baxter, J. E., Davidson, R.S, Hageman, H. J., European Polymer J., accepted for publication.
- [8] Boner, A., Kirchmayr, R., Rist, G., Helv. Chim. ACTA 1978 61, 305- .
- [9] Osborn, C.L., J. Rad. Curing 1976, 3 (3) 2-11.
- [10] UV and EB Curing Formulation for Printing Inks Coatings and Paint, Edited by R. Holman, SITA Technology. 1984.
- [11] UV Curing: Science and Technology, Volume 1. Edited by S. P. Pappas. Technology Marketing Corporation. 1978.
- [12] Johnson, J. F., Encyclopedia of Polymer Science and Technology. Volume 3, 491-531, Wiley Int.
- [13] a) Snyder, L. R., Kirkland, J. J., Introduction to Modern Liquid Chromatography, Second Edition, Wiley Int. Chapter 2 pgs 15-22; b) Chapter 16, 663-668; c) Chapter 4, 127-140.
- [14] Spectroscopic Methods in Organic Chemistry, Third Edition Williams, D. H., Fleming, I., Chapter 4 153-202, McGraw

Hill.

- [15] Hoyle, C. E., Kyu-Jun Kim, J. Rad. Curing 1985 12 (4) 9-15.
J. Appl., Polym. Science 1987 33, 2985-2996.
- [16] Goff, S. D., Jelus, L., Schweizer, E. E., Org. Mass Spec.
1977, 12 (1) 33-36.
- [17] Berndt, K. G., Gloyna, D., Henning, H. G., J. f. Prakt.
Chemie. 1981, 3 445-450.